BC Geological Survey
Assessment Report
31728

Airborne Geophysical Interpretation

of the

Porphyry Creek Survey

Omineca Mining Division, British Columbia

NTS Map Sheet 93M/04

for

DUNCASTLE GOLD CORP.

by

Intrepid GEOPHYSICS LTD.

Christopher Campbell, P. Geo.
October 30, 2010 (revised Jan 31, 2011)

4505 Cove Cliff Road
North Vancouver, BC
Canada V7G 1H7

Project no.10-218-DUN

Summary

A helicopter-borne electromagnetic, magnetic and radiometric survey was flown by Fugro Airborne Surveys in July 2010 over the Porphyry Creek property of Duncastle Gold Corp.; this survey comprised 495 line-kilometres of data acquired on a grid pattern of 200 m spaced east–west traverses controlled by 1,000 m spaced north–south tie lines. The survey was completed without incident in 13 flights spread over 4 days of actual production; although very poor weather severely impacted this production, no days were lost to equipment or safety issues.

Analogies to mineralization surrounding (e.g., Porphyry Creek North, Black Pilot as well as Sultana and Red Rose) suggest that any mineralization on the Porphyry Creek block typically consists of polymetallic veins which may be related to the emplacement of feldspar porphyritic intrusive rocks of the so-called Rocher Deboule intrusion (itself part of the Bulkley Plutonic Suite) into coarse clastic sedimentary rocks (siltstone and argillite) of the Skeena Group - Red Rose Formation. Comparison of the MINFILE occurrences in the general area reveals a significant degree of correlation to magnetic highs.

The known mineralization of this region is not expected to provide particularly strong conductive responses due to the relatively thin and discontinuous nature of the vein and stockwork systems as well as the perhaps dissemination of the associated sulphides. Nonetheless, the magnetic intensity images and derived derivatives serve to delineate the contacts of both magnetic and non-magnetic units. The latter could reflect felsic intrusions or siliceous breccias that might host auriferous mineralization. Arguably the strongest airborne electromagnetic response lays on the eastern half of the Porphyry claim block, ~1 km east of Tina, wherein a moderately strong bedrock conductor occurs. A total of 6 anomalous conductive zones are identified and mapped by this interpretation; 2 singularly magnetic high zones, and 9 potentially-enhanced K% 'target zones' were additionally identified as 'areas of interest' for follow-up in 2010.

A conclusion from this analysis and interpretation is that the magnetic data may be more revealing in identifying zones of complexity and possible alteration (specifically, magnetite destruction) on the Porphyry Creek property; in contrast, direct detection of significant sulphides through the (presumed) associated electromagnetic response may be much more problematic. Enhancement filters applied to the magnetic grid have highlighted a number of dominant structural orientations and trends. A major northwest-southeast magnetic fabric is identified which cuts through and breaks the NNW–SSE pattern of the known geology; a minor NE-SW trend is also mapped by the multiscale edge analysis in the northern portion of the study. Both these trends provide potential for significant fracturing and mobilization of mineralized fluids. The gamma-ray spectrometer data (specifically, increased K% suggesting anomalous K-alteration) correlates to several of the known showings, principally on the eastern flanks of the Rocher Deboule range, and in conjunction with the magnetics appears to be supporting the targeting of specific areas interpreted to include high fracture densities and inferred, potassic alteration.

Table of Contents

List of Tables

List of Figures

1. Introduction

The Porphyry Creek project includes 41 claims (13,097 hectares) and is located within the Omineca Mining Division of northwest British Columbia. The property lays approximately 10 kilometres south of New Hazelton, itself laying on Highway 16 between Smithers and Terrace.

The Porphyry Creek area has a long history of exploration and development from high-grade vein systems, dating back to at least 1910. The area saw substantial production between 1915 and 1954 from the nearby Rocher Deboule and Red Rose mines, as well as lesser production from the Victoria, Cap and Highland Boy mines. Exploration has been intermittent since the closure of these mines, with the most substantial work occurring in the 1980s on the Rocher Deboule, Victoria, Red Rose and Killarney/Jones prospects. Duncastle Gold has consolidated claims in the area, compiling numerous showings and prospects into a larger geologic model to enable the first modern, systematic exploration of the area. No significant exploration work has been done to investigate the potential for porphyry-related deposits on the property prior to the current project.

An airborne electromagnetic, magnetic and radiometric survey was conceived and designed to cover the property and aid in the design of the 2010 exploration program. Overarching objectives of this survey were two-fold:

- provide high resolution electromagnetic, magnetic and radiometric data for the direct detection and delineation of sulphide-associated gold-silver occurrences
- facilitate the mapping of bedrock lithologies and structure which in turn influence the emplacement or hosting of economic mineralization.

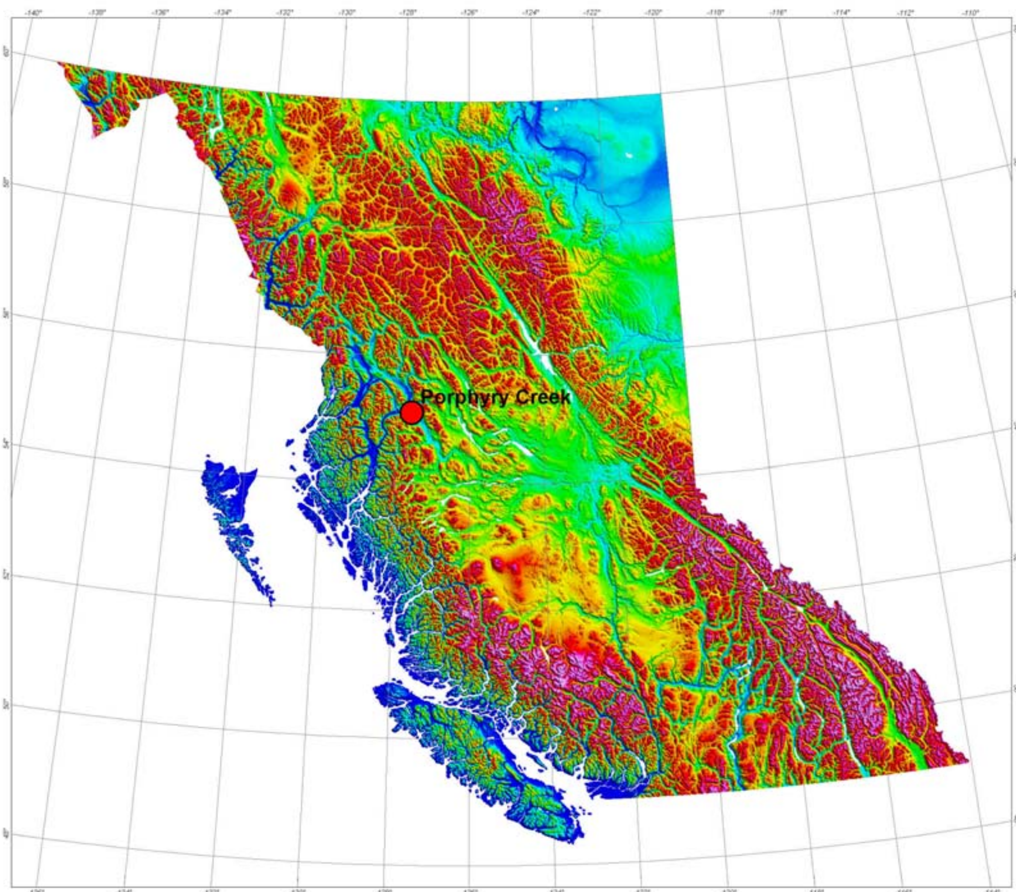

Figure 1. Project Location (highlighted in red)

Fugro Airborne Surveys was subsequently contracted in May 2010 by Duncastle Gold Corp. to fly a helicopter-borne electromagnetic/magnetic/radiometric survey over its Porphyry Creek property in northwestern British Columbia.

1.1. Location and Access

The property lies within NTS map sheets 93M/04 with its geographic center at approximately Longitude 127°35'04" West, Latitude 55°06'37" North. It is located 10 km south of New Hazelton, and ~45 km northwest of Smithers, which was used as a base of operations by the airborne contractor in June–July 2010.

The Porphyry Creek property is located along the rugged Rocher Deboule Mountain Range, south of New Hazelton. Direct road access into the area is limited, but services are readily available within a few kilometres of the property in New Hazelton and Smithers. Parts of the property have limited ground access via poorly maintained 4WD roads and rough trails, but much of the area is only accessible by helicopter. Past producing mines in the area are at high elevation, and glaciers or permanent ice fields cover some of the peaks.

The main road accessing the property is the old Rocher Deboule mine road, with branches accessing the Red Rose Mine and Armagosa workings. This road follows Juniper Creek northeast from Skeena Crossing on the Yellowhead highway about 10 km south of New Hazelton. This road is presently washed out in several locations, and is only passable by 4WD for about five kilometres beyond the highway intersection; beyond that, it is seasonally passable by All-Terrain Vehicle. A newer, active forestry road accesses the southeast side of Juniper Creek and touches the extreme southwest corner of the property.

1.2. Claims

	Tenure No.	Claim Name	Expiry	Area
1	532096	BRUNSWICK	2011-06-30	314.5
2	532103	ARMAGOSA	2011-06-30	166.4
3	532105	SLATER	2011-06-30	92.5
4	535639	OHIO EAST	2011-06-30	369.7
5	542244	PORPHYRY	2011-06-30	462.2
6	542246	TINA	2011-06-30	462.4
7	542247	RIDGE	2011-06-30	462.5
8	542254	JUPITER	2011-06-30	462.7
9	547139	TILTUSHA	2011-06-30	185.1
10	549610	PORPHYRY WEST	2011-06-30	258.8
11	556426	BRIAN BORU	2011-06-30	333.3
12	567326	SLATE CREEK	2011-06-30	444.3
13	567334	BORU EAST	2011-06-30	463.0
14	574185	KILLARNEY	2011-06-30	259.3
15	577335	PORPHYRY EAST	2011-06-30	425.4
16	577338	BORU GLACIER	2011-06-30	462.8
17	577340	SLATER	2011-06-30	462.8
18	577343	SOUTH CAP	2011-06-30	203.8
19	577348	RIDGE	2011-06-30	462.7
20	577353	SOUTH RIDGE	2011-06-30	203.7
21	581191	SW1	2011-06-30	111.1
22	606970	RED ROSE	2011-06-30	203.4
23	622463	SULTANA	2011-06-30	370.2
24	622466	SULTANA NORTH	2011-06-30	166.5
25	622503	MT	2011-06-30	277.7
26	659243	SE FRINGE	2011-06-30	222.1
27	705527	MT SW	2011-06-30	333.3
28	705528	MT SE	2011-06-30	314.8

29	705529	SULTANA SE	2011-06-30	111.1
30	764883	CENTER WEST	2011-06-30	444.1
31	764942	CENTER WEST 2	2011-06-30	111.0
32	785882	CHINA CREEK 1	2011-06-30	443.3
33	785902	CHINA PORPHYRY N	2011-06-30	443.4
34	785922	CHINA PORPHYRY 2	2011-06-30	443.5
35	785942	CHINA PORPHYRY 3	2011-06-30	443.6
36	785962	PORPHYRY CREEK TIE	2011-06-30	184.9
37	831318	PORPHYRY EAST	2011-08-11	295.9
38	833726	NE 1	2011-09-16	332.7
39	833727	NE 2	2011-09-16	332.5
40	833728	NE 3	2011-09-16	332.4
41	833729	NE 4	2011-09-16	221.6
			Total	**13,097.0**

Table 1: Summary of Mineral Claims

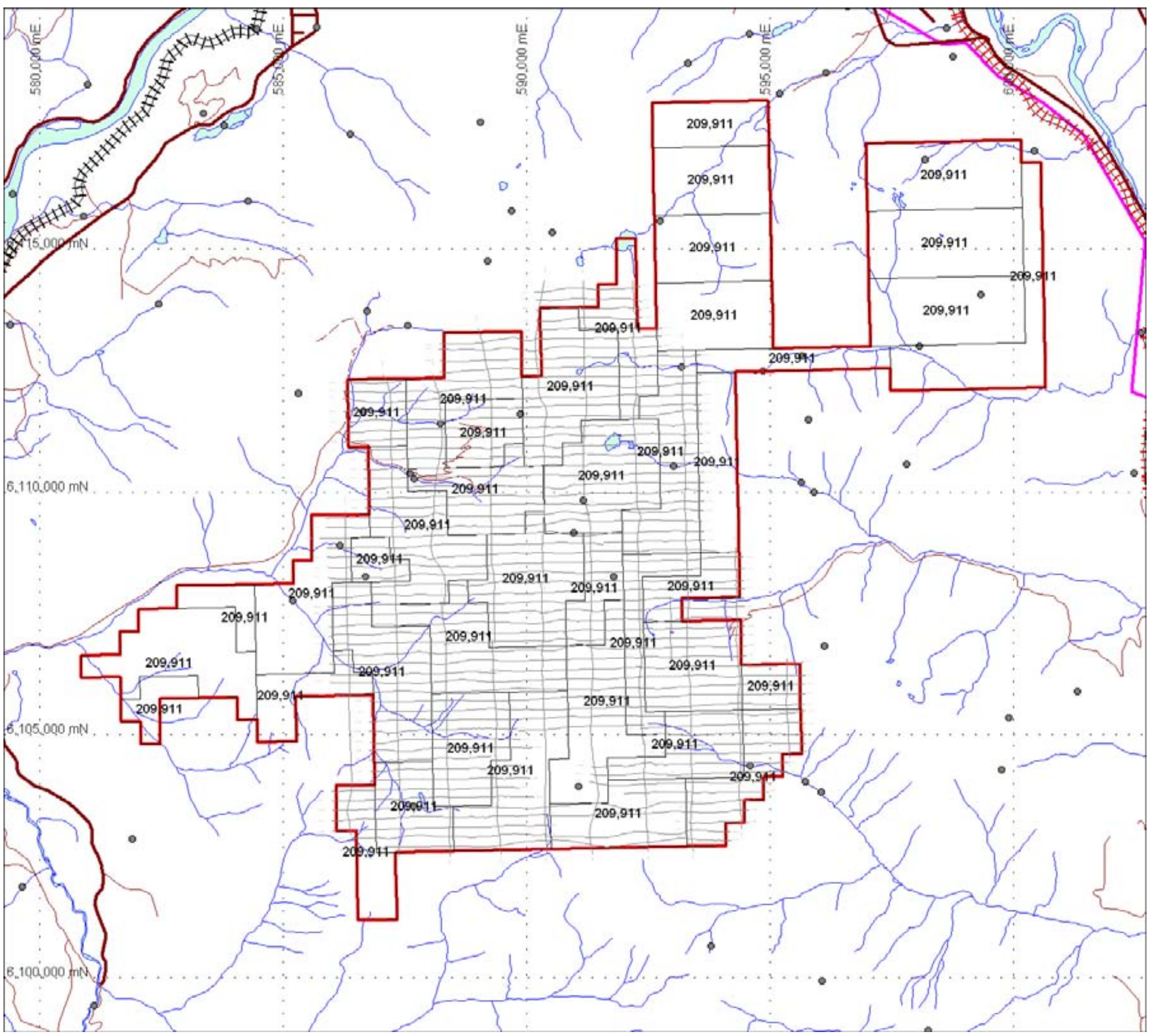

Figure 2. Claim Map with airborne geophysical flight path shown.

1.3. Climate and Physiography

The property includes many high elevation peaks, steep ridges and talus slopes that are free of forest cover; valleys and lower slopes are generally heavily forested. Elevations range from below 900 m to almost 2,400 m above sea level.

The Rocher Deboule Range is located on the eastern edge of the much larger Coast Mountain Range resulting in a mix of coastal and interior British Columbia weather patterns. Climate in the Hazelton area is reported as semi-arid and annual precipitation is less than 51 centimetres per year. However, the core of the Porphyry Creek property is significantly higher, and correspondingly experiences far more dramatic and inclement weather patterns. Since there are heavy snow accumulations in winter, the recommended exploration work season for high elevations is between July and September. Lower elevation zones can be explored from May through October. It should be noted that accumulation of deep snow at higher elevations could result in a heavy spring runoff. With the onset of summer, snow melting is rapid and by July most of the property is snow free, apart from isolated areas of permanent snowfield. The summer months tend to be dry and hot, though Pacific coastal storms do occasionally reach inland.

2. Geology

2.1. Regional Geology

British Columbia can be subdivided into five belts running roughly parallel with the north-westerly grain of the Cordillera. These five belts, from west to east, today are called the Insular, Coast, Intermontane, Omineca and Foreland belts accreted to North America (Figure 3). The most easterly of these, the Foreland Belt, is the youngest, being formed when Proterozoic and Paleozoic sedimentary rocks were thrust up onto the continental margin to form the Rocky Mountains. The Omineca Belt is composed primarily of Devonian-Mississippian magmatic island arc sequences formed on the edge of North America. The intermontane belt is a complex assemblage of Carboniferous to early Jurassic aged rocks which are largely arc-related. Younger arc-related magmatic activity continued into the Tertiary. The Coastal Belt which is composed of plutonic and metamorphic rocks forms the suture zone between the Intermontane Belt and the exotically derived Insular Belt.

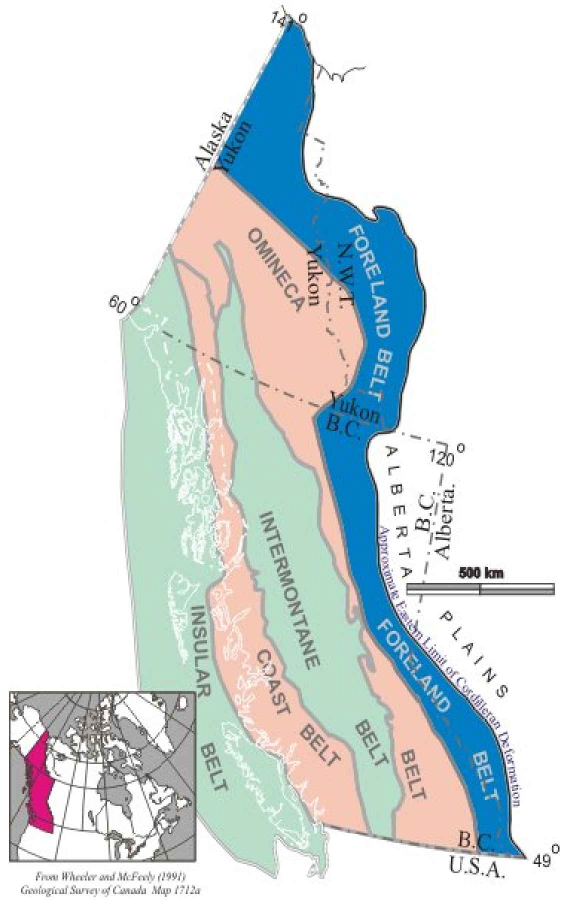

Figure 3. Five Belt Framework of the Canadian Cordillera (Geological Survey of Canada)

The Omineca Belt (in which the Porphyry Creek property lays) is the region of overlap between the volcanic and sedimentary strata in the Intermontane Belt to the west, and sedimentary rocks of the Foreland Belt to the east. The nature of the rocks and their chemistry suggests that the Omineca Belt contains the boundary between new continental crust and rocks eroded from the old continent.

Warkentin and Young[1] report that the western part of the project area is underlain by the Lower Cretaceous Skeena Group - Red Rose Formation clastic sediments, and the Cretaceous Kasalka Group - Brian Boru Formation andesitic volcanics, while the eastern portion is underlain by Late Cretaceous Bulkley intrusives (the Rocher Deboule stock), which forms a massive, prominently jointed body of porphyritic (biotite and K-Spar phenocrysts) granodiorite. Alpite, pegmatite, porphyritic andesite, felsite, lamprophyre and granitoid dykes/sills are common throughout the pluton and extend into the surrounding country rock. NNW trending steeply dipping joint structures are prominent in the contact zone of the Cretaceous pluton and Jurassic volcanics/sediments. This NNW trending joint set parallels the contact, and there is a subsidiary set of joints perpendicular to the contact, which roughly traces the main mineral trend (i.e., 070° strike, moderate to steep N dip) of some of the historical deposits in the area.

Several prominent faults traverse the area, including the N–S trending Cap and Chicago Creek Faults. The east side of the Chicago Creek fault has been uplifted and displaced several hundred meters to the south. There is also at least one prominent cross fault, the Mill Fault, which lies to the south of the Red Rose Mine on the east side of the Chicago Creek Fault and likely follows Red Rose Creek on the west side.

The regional geology of the claim area is below below on Figure 4.

[1] Warkentin, D. and Young, C., 2008. Porphyry Creek Project: West Side of Rocher Deboule Range - Stream and Rock Geochemistry Report; December 15, 2008 (internal report submitted to Duncastle Gold Corp.), 26 p.

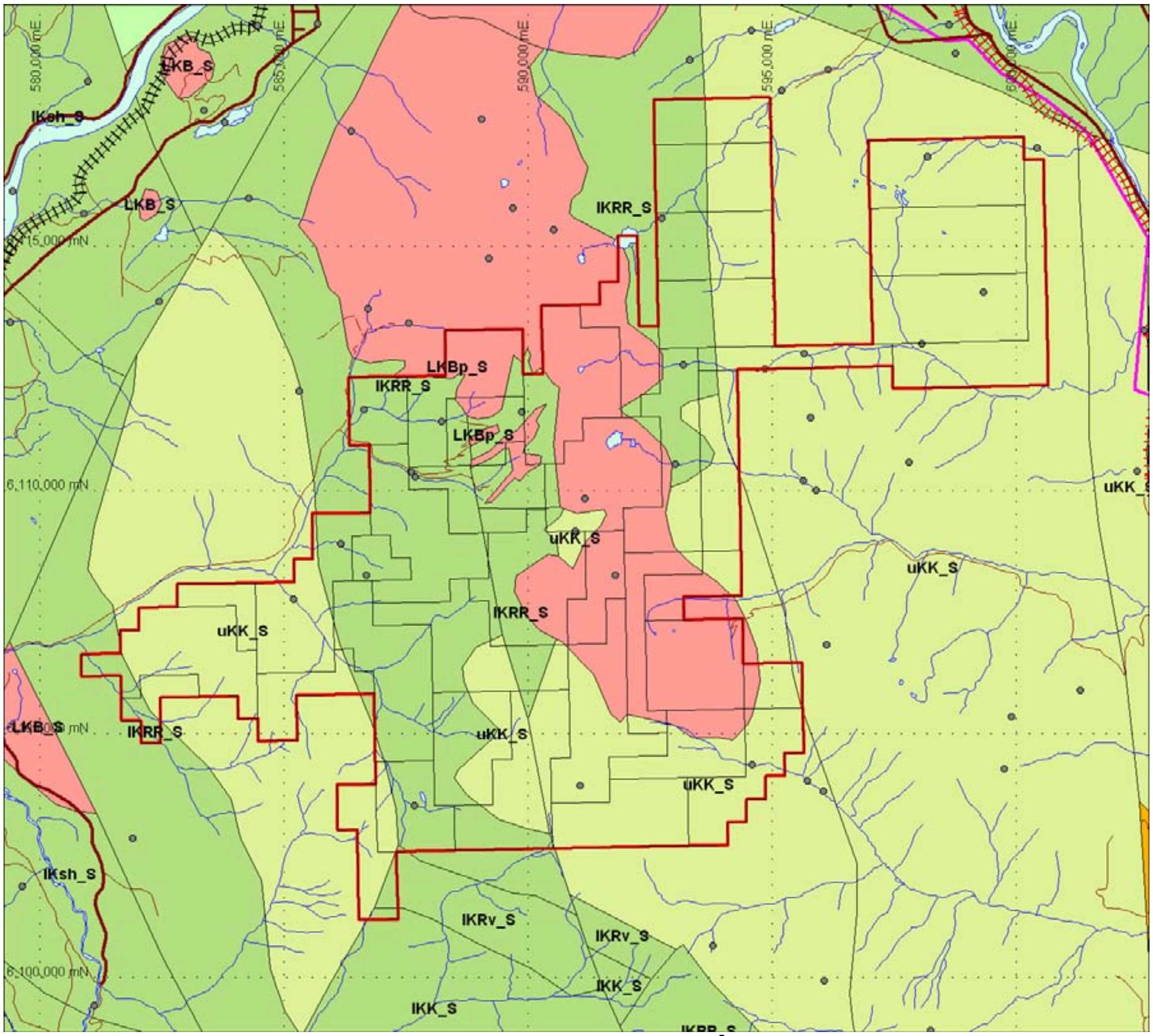

Figure 4. Regional Geology[2]

2.2. **Local Geology** (Warkentin and Young, 2008)

The Porphyry Creek project area is primarily underlain by argillites and greywacke of the Red Rose Formation, and by andesitic volcanics of the Kasalka Group. The Red Rose sediments strike northeast and dip 45° southeast and have been altered to hornfels in the vicinity of the porphyrytic intrusives (Rocher Deboule stock) that form the east-central part of the project area. In the Brunswick prospect area, some intrusive dioritic features are evident.

Several major faults cross the area, two of which appear to intersect west of the Brunswick prospect. The Chicago Creek Fault is a major north-south normal fault with an estimated displacement of 600 to 900 meters. It has been traced over a total length of nearly 35 kilometres. The Mill Fault trends east-southeast, following Red Rose Creek. It appears to have been displaced several hundred meters to the south by the Chicago Creek Fault. The Cap fault, which is another major north-south fault, crosses the western part of the main project area, as well as the smaller claim block adjacent to the Cap mine. In the vicinity of the Cap mine, this fault appears to be displaced by another major (unnamed) northeast striking fault.

[2] Digital Geology Map of British Columbia: Tile NN8-9 North Coast and Queen Charlotte Islands/Haida Gwaii, N.W.D. Massey, D.G. MacIntyre, J.W. Haggart, P.J. Desjardins, C.L. Wagner and R.T. Cooney; B.C. Ministry of Energy and Mines, Geofile 2005-5.

A fault zone known as the Red Rose Shear runs roughly parallel to, and is likely subsidiary to, the Chicago Creek Fault in the area around the Red Rose Mine. The Red Rose tungsten vein occurs where this shear passes through an intrusive tongue of diorite. Outside the diorite the shear is mainly a narrow seam. The full extent of this shear is unknown, but its trend projects towards additional diorite tongues to the south of the mine. The diorite is distinct from the much larger granodiorite intrusive and significant bodies have only been mapped at the Red Rose Mine and around the headwaters of Red Rose Creek.

Known mineralization in the area occurs as base and precious metal values in quartz vein structures located along fractures and shears related to localized northeast or northwest trending fault sets. Most of the known mineral occurrences (aside from the southern Jones-Killarney-Brian Boru showings) lie within 1000 meters of the contact of the Rocher Deboule intrusive stock with the surrounding country rock. Past production in the area has principally been for copper and tungsten, but values in gold, silver, cobalt, molybdenum, lead and zinc are also found.

Veins can vary widely in their mineralization. At the Red Rose mine the upper part of the vein contained mainly scheelite with minor amounts of chalcopyrite. At lower levels, chalcopyrite was much more abundant and there were values in gold and molybdenite. At the Rocher Deboule mine, just outside the project boundary to the north, chalcopyrite was the principal economic mineral, with significant gold and silver values. At the Victoria mine, as short distance to the north, mineralization is primarily cobalt sulpharsenides with high gold values and minor molybdenite. At the Brunswick mine the quartz veins are mineralised mainly with galena, sphalerite and tetrahedrite, with lesser amounts of chalcopyrite.

In the Brian Boru Creek area, besides narrow veins containing base metal sulphides, there is also reportedly semi-massive to massive sulphide mineralization occurring at or near the contact between andesitic and rhyolitic volcanics. Mineralization is primarily massive sphalerite and pyrrhotite, with significant amounts of galena and chalcopyrite in some of the smaller veins.

2.3. Exploration Model

The concept target on the Porphyry Creek property is a porphyry system, inferred as several kilometres in scale. The property includes multiple high-grade gold, silver and base metal showings and previous workings (which may be epithermal veins above the sought porphyry system?) on both sides of a well defined (Natural Resources Canada regional aeromagnetics) 10 km long magnetic anomaly itself closely coincident with the axis of the Rocher Deboule range and underlying granodiorite intrusion.

An excellent review of the relationships between the geological model and exploration techniques for porphyry Cu ± Au deposits is provided by Holliday and Cooke[3] in their 2007 paper "…Copper ± gold ± molybdenum porphyry deposits are large tonnage, low-grade hypogene resources. The deposit class is unified by a close spatial, temporal and genetic association between subvolcanic porphyritic intrusive complexes (the 'porphyry') and hypogene mineralization and hydrothermal alteration mineral assemblages that occur in and around them."

A very concise description of possible porphyry systems is further provided by Rogers[4] "…fracture-controlled quartz-sulphide veinlets and veins, and sulphide disseminations in fractures hosted by, or proximal to, high-level, calc-alkaline, intermediate to felsic, porphyritic intrusions. There may be a spatial and genetic relationship to high-level (epizonal), calc-alkaline, intermediate to felsic stocks, dykes, sills, and breccia pipes, with porphyritic phases, that are

[3] Holliday, J. R. and Cooke, D. R., 2007. Advances in Geological Models and Exploration Methods for Copper ± Gold Porphyry Deposits; **in** "Proceedings of Exploration 07: Fifth Decennial International Conference on Mineral Exploration" edited by B. Milkereit, 2007, p. 791–809.

[4] Rogers, M., 2010. Model No. 28, Calc-Alkaline Porphyry Copper-Molybdenum-Gold-Tungsten. Saskatchewan Mineral Deposit Models, Geological Services and Mineral Resource Information.

intrusive into volcanic and sedimentary rocks. These commonly occur as subvolcanic intrusions to volcanic complexes. The porphyritic intrusions and/or the surrounding country rocks may host the mineralization. Multiple intrusive phases and brecciation are common. Typical general associations are: quartz monzonite to alkali feldspar granite: Mo-W; granodiorite to quartz monzonite: Cu-Mo; and diorite-quartz diorite-tonalite: Cu-Au-(Mo)."

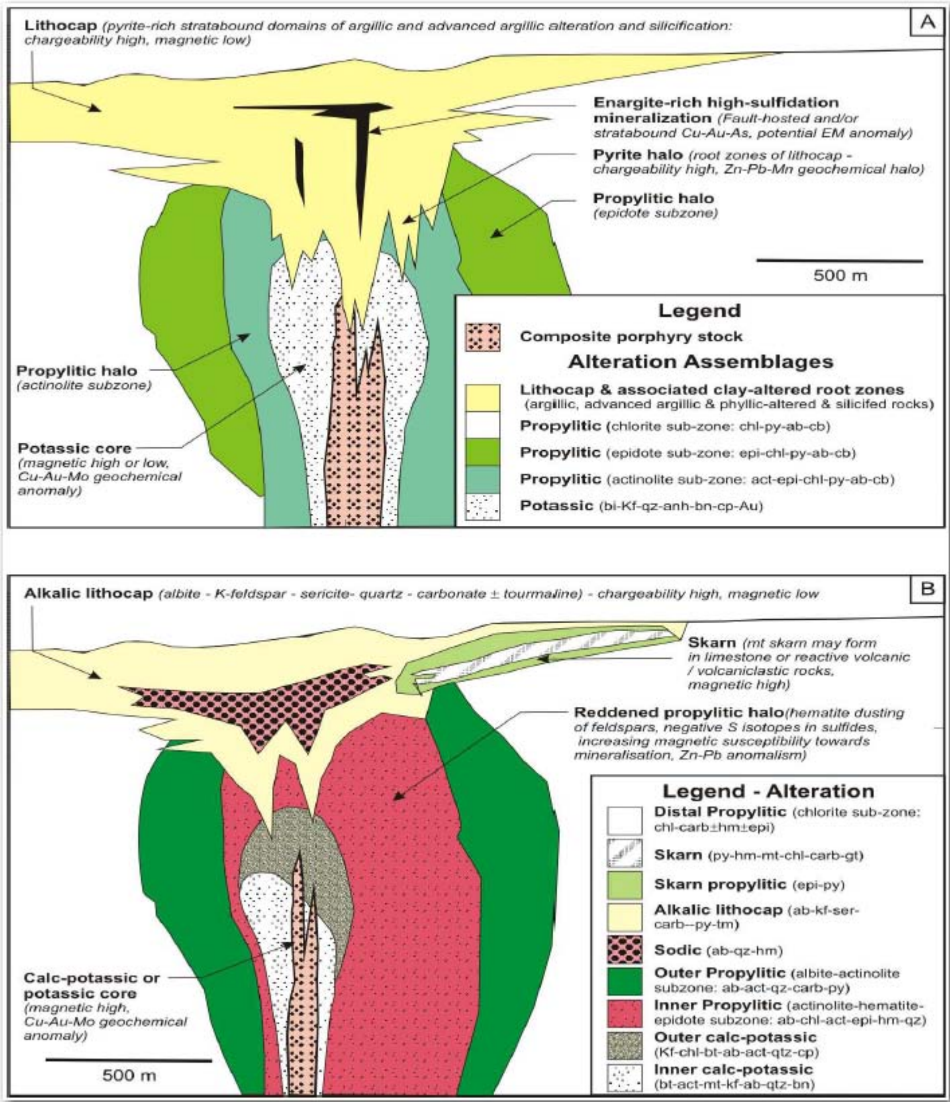

Figure 5. Schematic illustration of alteration zoning and overprinting relationships in a calc-alkalic porphyry system (from Holliday and Cooke, 2007)

3. Airborne Geophysics

3.1. Exploration Criteria

As pointed out by Hodges and Amine[5], gold mineralization presents a challenge for geophysical surveys. First, because the gold mineralization itself does not provide a contrast with the host geology that is detectable by any of the geophysical parameters, and second, because economic deposits can be quite small, with complex geology and structure. Discovery of gold deposits

[5] Hodges, G. and Amine, D., 2010. Exploration for Gold Deposits with Airborne Geophysics. KEGS PDAC Symposium 2010

requires geophysical surveys that can detect subtle structures that control deposition, and directly detect the weak anomalies created by alteration and deposition processes. Exploration for gold is therefore commonly a mapping exercise. Magnetic and electromagnetic and gamma-ray spectrometric surveys can all be valuable mapping tools, depending on the terrain, the regolith and geomorphology, and the target.

Geophysical signatures may include all or some of the following:

- airborne and ground magnetic surveys to detect magnetite-rich zones and as an aid to mapping;
- induced polarization/resistivity surveys to outline disseminated sulphides;
- resistivity surveys to help map alteration zones;
- airborne and ground radiometric surveys to help delineate K-rich alteration zones;
- audio-frequency magnetotelluric surveys to define the limits of the porphyry systems; and
- short-wave infrared spectroscopy for clay alteration identification in the field.

The low mineral concentrations of porphyry-related deposits generally do not provide direct-targeting for any EM system, unless there is significant supergene enrichment. Exploration for these deposits does benefit from using airborne geophysics, however, including electromagnetic, magnetic and radiometric applications for mapping geology, structure and alteration. Based on these characteristics and through extrapolations to the known and suspected mineralization on the Porphyry Creek property, an airborne geophysical survey of combined electromagnetic (broadband, frequency-domain Dighem), magnetics and gamma-ray spectrometry was chosen as the first pass method of mapping and hopefully delineating controlling structures, possible sulphide mineralization, and pronounced potassium alteration.

3.2. Operations

Fugro Airborne Surveys was contracted by Duncastle Gold in May 2010 to fly a helicopter-borne aeromagnetic/electromagnetic/radiometric survey over the Porphyry Creek property in northwestern British Columbia. The technical objectives of the survey were two-fold as stated in the introduction and in the preceding sections; to provide high resolution electromagnetic, magnetic and radiometric data for the direct detection and delineation of sulphide-associated gold-silver occurrences, and to facilitate the mapping of bedrock lithologies and structure which in turn influence the emplacement or hosting of economic mineralization.

Survey coverage consisted of approximately 495 line-km, including tie lines. Flight lines were flown east-west (090°–270°) with a line separation of 200 m. Tie lines were flown orthogonal to the traverse lines (000°–180°) at intervals of 1 km. Survey operations took place June 22 – July 19, 2010; bad weather consisting of wind, rain and persistent low cloud cover over the central portion of the property (mountain tops) severely affected production. A total of 13 production flights only were achieved in 4 days (July 7–8th and 18–19th, respectively) during this period. A total of 21 days were put down as weather days (chargeable standby); no days were lost to equipment or safety issues.

The survey employed the DIGHEM$^{V\text{-}DSP}$ electromagnetic system. Ancillary equipment consisted of a magnetometer, radar and barometric altimeters, a digital video camera, a digital recorder, a 256-channel spectrometer, and an electronic navigation system. The instrumentation was installed in an AS350-B3 turbine helicopter (Registration C-FIDA) that was provided by Great Slave Helicopters Ltd. The helicopter flew at an average airspeed of 100 km/h with a nominal EM sensor height of approximately 40 metres. The spectrometer crystal package was housed within the helicopter, with a nominal terrain clearance of 68 metres.

In several portions of the survey area, steep topography forced the pilot to exceed normal terrain clearance for reasons of safety. It is possible that some valid anomalous features may have escaped detection in areas where the bird height exceeded 120 m. There are several gaps in the resistivity grids, where high flying precluded the calculation of valid resistivities. Several lines had to be flown in segments, in an attempt to obtain more coverage. In difficult areas where near-vertical climbs were necessary, the forward speed of the helicopter was reduced to a level that permitted excessive bird swinging. This problem, combined with the severe stresses to which the bird was subjected, gave rise to aerodynamic noise levels that are slightly higher than normal on some lines. Where warranted, reflights were carried out to minimize these adverse effects.

A complete description of the field program is provided by the contractor's logistical report[6], attached to this report as Appendix A.

Electromagnetics

The Dighem electromagnetic system utilizes a multi-coil coaxial/coplanar technique to energize conductors in different directions. The coaxial coils are vertical with their axes in the flight direction. The coplanar coils are horizontal. The secondary fields are sensed simultaneously by means of receiver coils that are maximum-coupled to their respective transmitter coils. The system yields an in-phase and a quadrature channel from each transmitter-receiver coil-pair. In HEM, the coplanar coils lie in the horizontal plane with their axes vertical, and parallel. These coils are most sensitive to massive conductive bodies, horizontal layers, and the halfspace. Coaxial coils in an HEM system are in the vertical plane, with their axes horizontal and collinear in the flight direction. These are most sensitive to vertical conductive objects in the ground, such as thin, steeply dipping conductors perpendicular to the flight direction. Coaxial coils generally give the sharpest anomalies over localized conductors.

- in-phase: that component of the measured secondary field that has the same phase as the transmitter and the primary field. The in-phase component is stronger than the quadrature phase over relatively higher conductivity.
- quadrature: that component of the measured secondary field that is phase-shifted 90? from the primary field. The quadrature component tends to be stronger than the in-phase over relatively weaker conductivity.

Radiometrics:

Radioactivity maps have proven highly useful for environmental studies, geological mapping, and mineral exploration, often indicating features not seen by other techniques. Radiation, specifically gamma-rays, is released through the spontaneous decay of radioactive elements. The 3 most common naturally occurring radioactive elements are potassium, uranium and thorium. These elements are found at some concentration in most rock-forming minerals. Potassium, for example, occurs mainly in the mineral feldspar which is an abundant and widespread mineral in the earth's crust, and a prominent component of granitic rock. Uranium and thorium are generally present in low concentrations (measured in parts per million (ppm) in a wide range of minerals. Where uranium occurs at high concentrations, it represents a target of economic interest. The concentrations of potassium, uranium and thorium may thus be quickly mapped through the use of airborne surveys using the distinctive gamma ray spectra from these 3 radioactive elements.

Magnetics:

Modern high-resolution aeromagnetic data provides a clearer view of completely obscured rocks, allowing much finer divisions of provinces regionally, and units locally. As magnetic field compilations extend to greater scales, they may be used to tie existing isolated interpretations or maps together through continuous data coverage, provide continent-scale perspectives on geologic structure and evolution, and extend geological mapping of exposed (particularly

[6] Fugro Airborne Surveys, 2010. DIGHEM$^{V\text{-}DSP}$ survey for Duncastle Gold Corp. Porphyry Creek property, New Hazelton, BC. Report no. 10037, September 9, 2010, 112 p.

Precambrian basement) regions into sediment-covered areas. A fundamental building block in these interpretations is the geophysical domain, distinguished on the basis of anomaly trend, texture, and amplitude. Where basement is exposed, these domains often coincide with lithotectonic domains, geologic provinces, or cratons, depending on the scale of investigation. Delineating areas of magnetic anomalies having similar characteristics is intended, therefore, to isolate areas of crust having similar lithological, metamorphic, and structural character, and possibly, history. Anomaly trends may indicate the type of deformation undergone: for example, sets of parallel, narrow curvilinear anomalies may attest to penetrative deformation whereas broad ovoid anomalies might suggest relatively undeformed plutons. The average anomaly amplitude within a domain reflects its bulk physical properties. For example, calc-alkaline magmatic arcs generally are marked by belts of high-amplitude positive magnetic anomalies while greenstone terranes commonly are associated with subdued magnetic fields. Additionally, where anomaly trends show abrupt changes in direction at domain boundaries, the relative age of the adjacent domains may also be inferred.

3.3. Data Presentation

The airborne geophysical interpretation is based on an integrated analysis using a combination of GEOSOFT's integrated editors (spreadsheet and flight path), INTREPID's advanced Fourier filtering and multiscale edge detection, ER MAPPER's image enhancements and MAPINFO's GIS capability. All the final data is also presented as a series of digital maps and images generated at scale of 1:50,000. The airborne geophysical gridded data was analyzed using the following enhanced images:

- Total Magnetic Intensity; pseudocolour and colourdrape images
- Calculated Vertical Derivative; greyscale shaded-relief and colourdrape images
- Total Horizontal Derivative; colourdrape images
- Analytic Signal (total gradient); colourdrape images
- Tilt derivative; colourdrape images
- Total horizontal derivative of the tilt derivative; colourdrape images
- corrected potassium (i.e., K^{40}) as equivalent ground concentration by weight in percent (%K); pseudocolour images
- corrected uranium (the spectrometer directly measures Bi^{214} which is an indirect measure of uranium) as equivalent ground concentration by weight in parts per million (eU ppm); pseudocolour images
- corrected thorium (the spectrometer directly measures Tl^{208} which is an indirect measure of thorium) as equivalent ground concentration by weight in parts per million (eTh ppm); pseudocolour images
- Natural Air Absorbed Dose Rate computed from the K (%), eU (ppm), eTh (ppm) concentrations [Absorbed Dose Rate = 13.08 K + 5.43 eU + 2.69 eTh (nGy/h) 'Natural Air Absorbed Dose Rate' is different from the traditional 'Total Count', in that it excludes radiation from man-made contaminants]
- Ternary K-Th-U images fused with magnetics; pseudocolour and colourdrape images
- Apparent resistivities based on 900, 7200 and 56,000 Hz coplanar coils; pseudocolour images
- Mulitplots of magnetics, radiometrics and electromagnetics.

Projection Specifications:

Map projection	NUTM09
Datum	NAD83
Central meridian	129° West
False Easting	500000 m
False Northing	0 m
Scale Factor	0.9996 m

In addition, the analysis and interpretation included a methodical review of the underlying profile data via both the contractor-supplied multiplots and an interactive review via GEOSOFT's integrated editors; example shown below in Figure 6.

The subsequent analysis depends in part at least on the processing, visualization, mapping, and integration capabilities provided by specialized geophysical software. Discrete features and trends are checked on a profile by profile basis, linked to a variety of images and GIS layers, before final decisions as to interpretation and recommendations for ground follow-up are made.

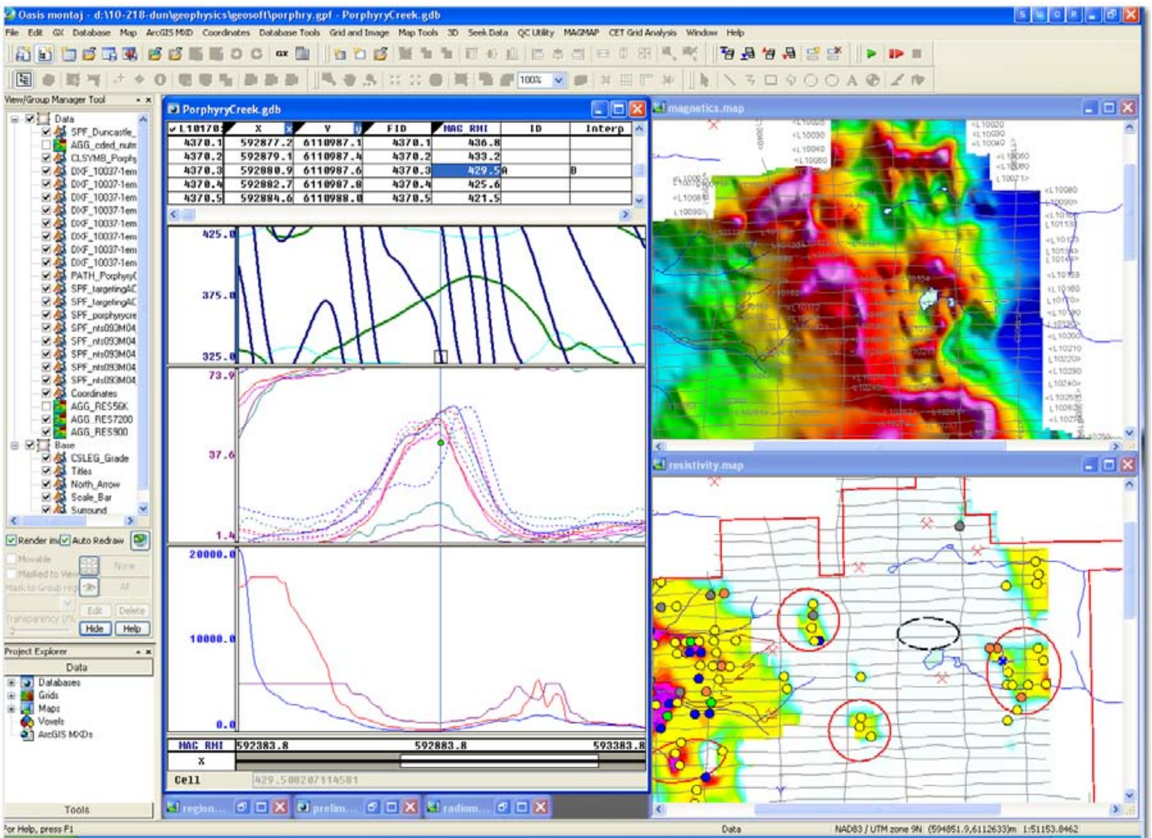

Figure 6. Interactive review of profiles and images

One of the by-products from the airborne geophysics program is a digital elevation model, derived from the GPS height and radar altimeter. Although not as accurate as a terrestrial geodetic survey, it remains a relatively inexpensive and accurate model of the topography of the study area. The errors contained in these sorts of DEMs are of the order of approximately 10 metres; the main contributions being from the radar altimeter data (1–2 metres) and the GPS height data (5–10 metres). When height comparisons are made in areas of flat terrain to elevations obtained during the course of third order gravity traverses and/or the elevations of geodetic stations, the errors are on the order of approximately 2 metres.

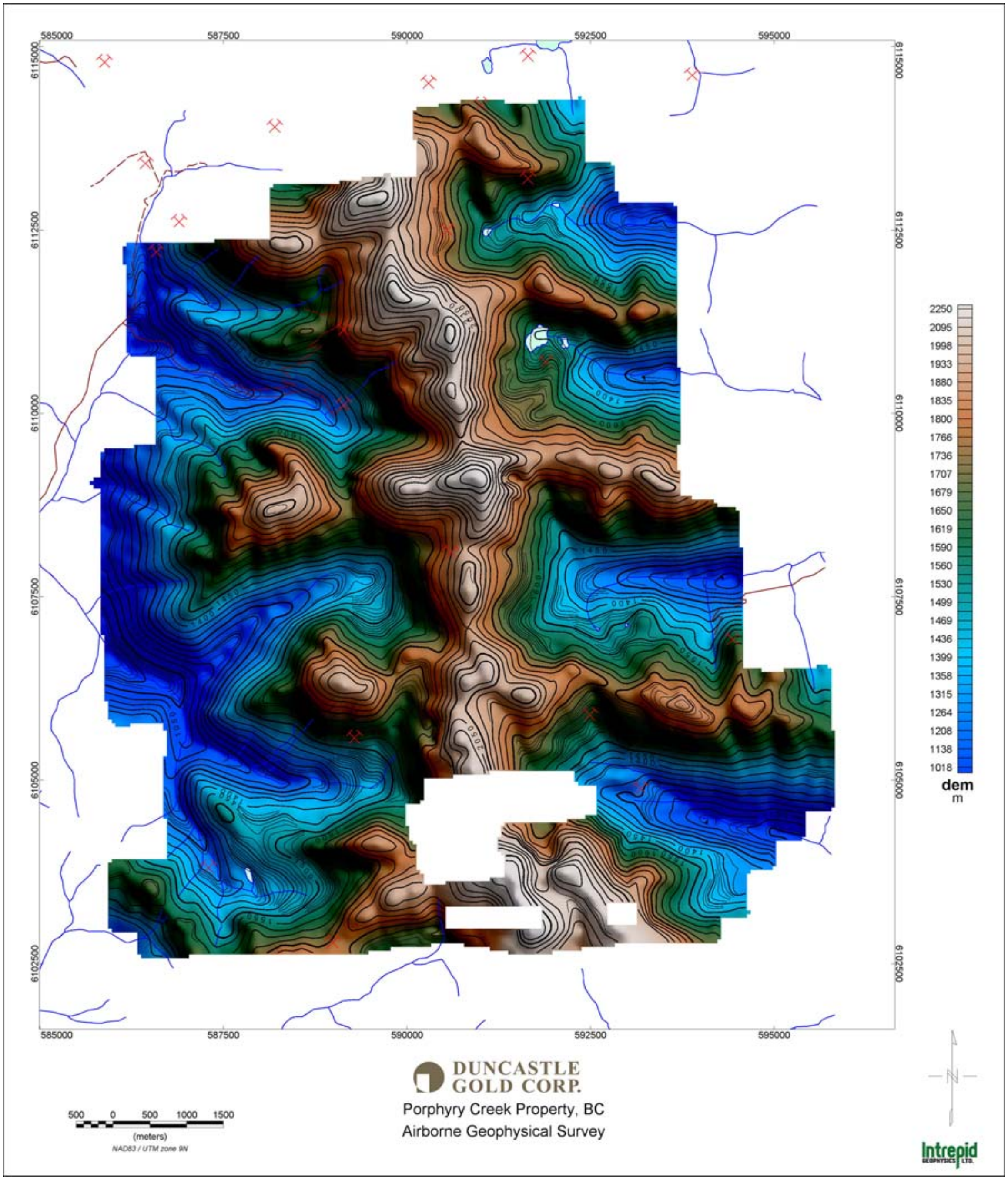

Figure 7. Digital Elevation Model, derived from airborne geophysics (10 m contours shown).

The final residual magnetic intensity (Figure 8, below) has been corrected for parallax and diurnal, and a spike-removal filter applied. Additionally, the data was edited for abrupt elevation shifts which did cause some associated jumps or spikes. The data was then tie-line levelled and gridded using a bi-directional grid technique using a 50 m cell size, one-quarter of the nominal traverse line spacing. A correction for the regional reference field (IGRF) was applied in order to arrive at the final residual magnetic intensity.

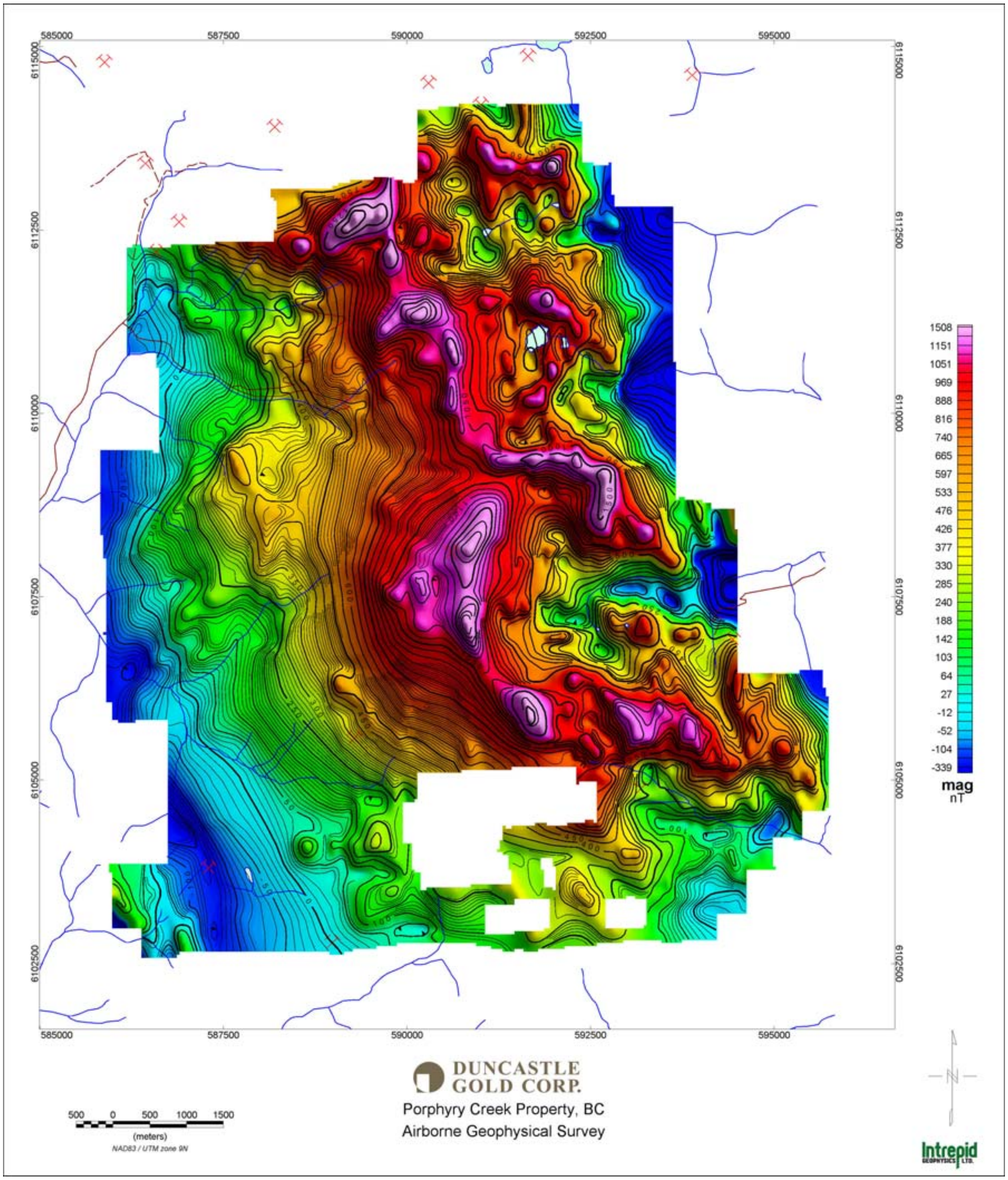

Figure 8. Residual Magnetic Intensity (10 nT contours shown).

A 'Ternary Radioelement Map' (K, eU, eTh) (Figure 9, below) is a special product that provides a unique view of the composite data set; the industry 'standard' (albeit with variations particularly across national boundaries) for radiometrics RGB or CMY displays is K for red-cyan, Th for green-magenta and U for blue-yellow. The least important data, which is generally taken to be uranium as it's least occurring, is sent to the blue-yellow gun as this is the colour to which the eye is least sensitive. The ternary map below, however, adopts the NRCAN [Airborne Geophysics Section (Grant[7])] protocol wherein a CMY colour model for eU, K and eTh respectively, is used

[7] Grant, J.A., 1998 "Ten things the textbooks don't tell you about processing and archiving airborne gamma ray spectrometric data," *in* Current Research 1998 D. Geological Survey of Canada, Ottawa, 83-87.

for a printed map because the information is more readily visible. The objective here is to show in a single colour image the relative concentrations of eU (cyan), K (magenta) and eTh (yellow). Variations in total radiation are shown by colour intensity, pale shades indicate low radioactivity. The ternary map emphasizes subtle distinctions in the relative concentrations of the radioelements, thereby 'fingerprinting' formations, either individually or collectively. Several of the geological units which underlay the study area appear to possess distinctive radioelement signatures, shown by the colour contrasts of the ternary map.

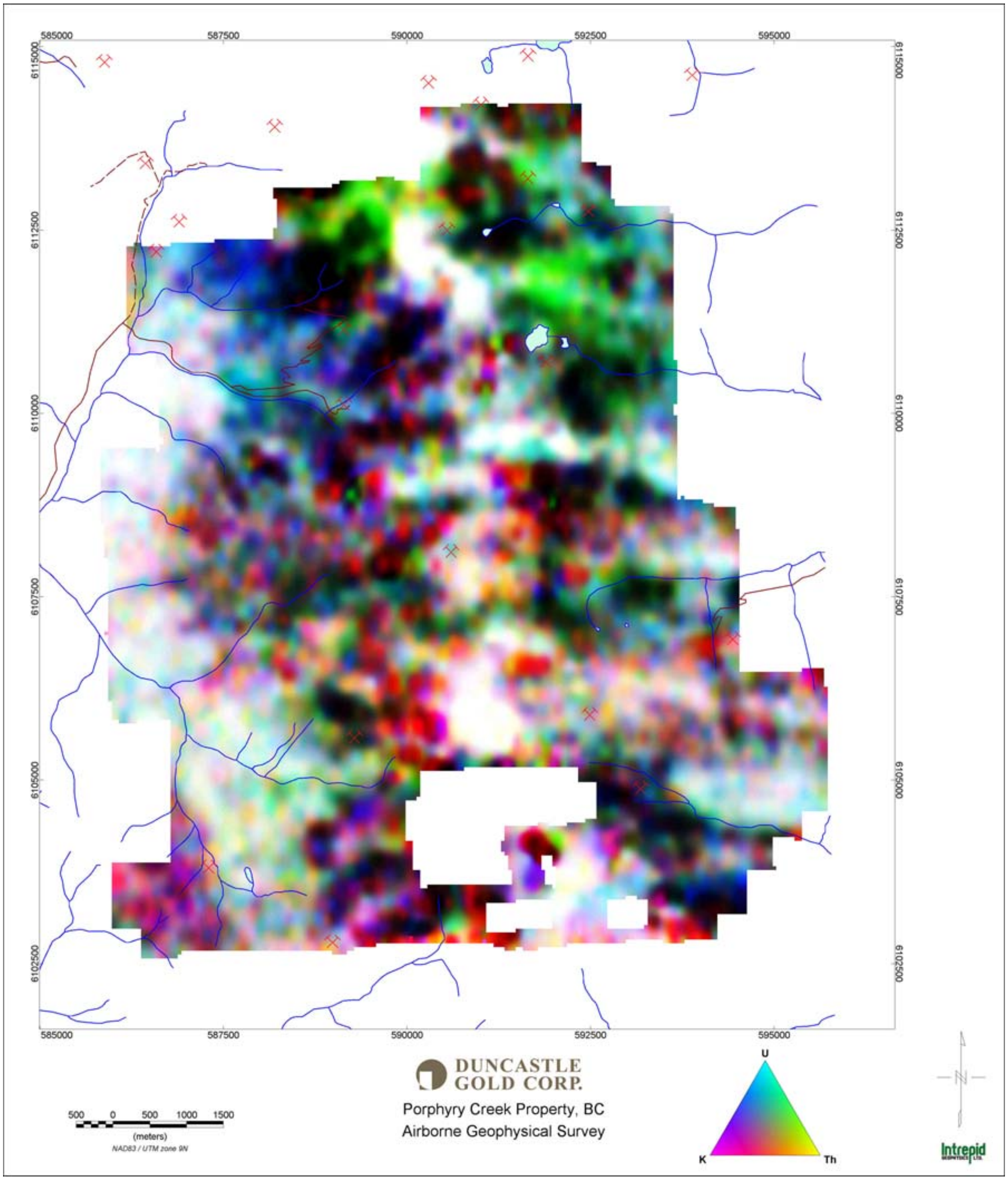

Figure 9. Ternary CMY (eU-K-eTh)

Figure 9 above is shown with the lakes and rivers in solid colour, overprinting the geophysics. Airborne gamma-ray spectrometry measures only the top 30 cm (or less) of the earth's surface.

There is essentially, no 'penetration' and any noticeable body of water therefore masks the effective response.

Apparent resistivity grids, which display the conductive properties of the survey area, were produced by the contractor from the 900 Hz, 7200 Hz, and 56,000 Hz coplanar data; these images are presented in the following figures.

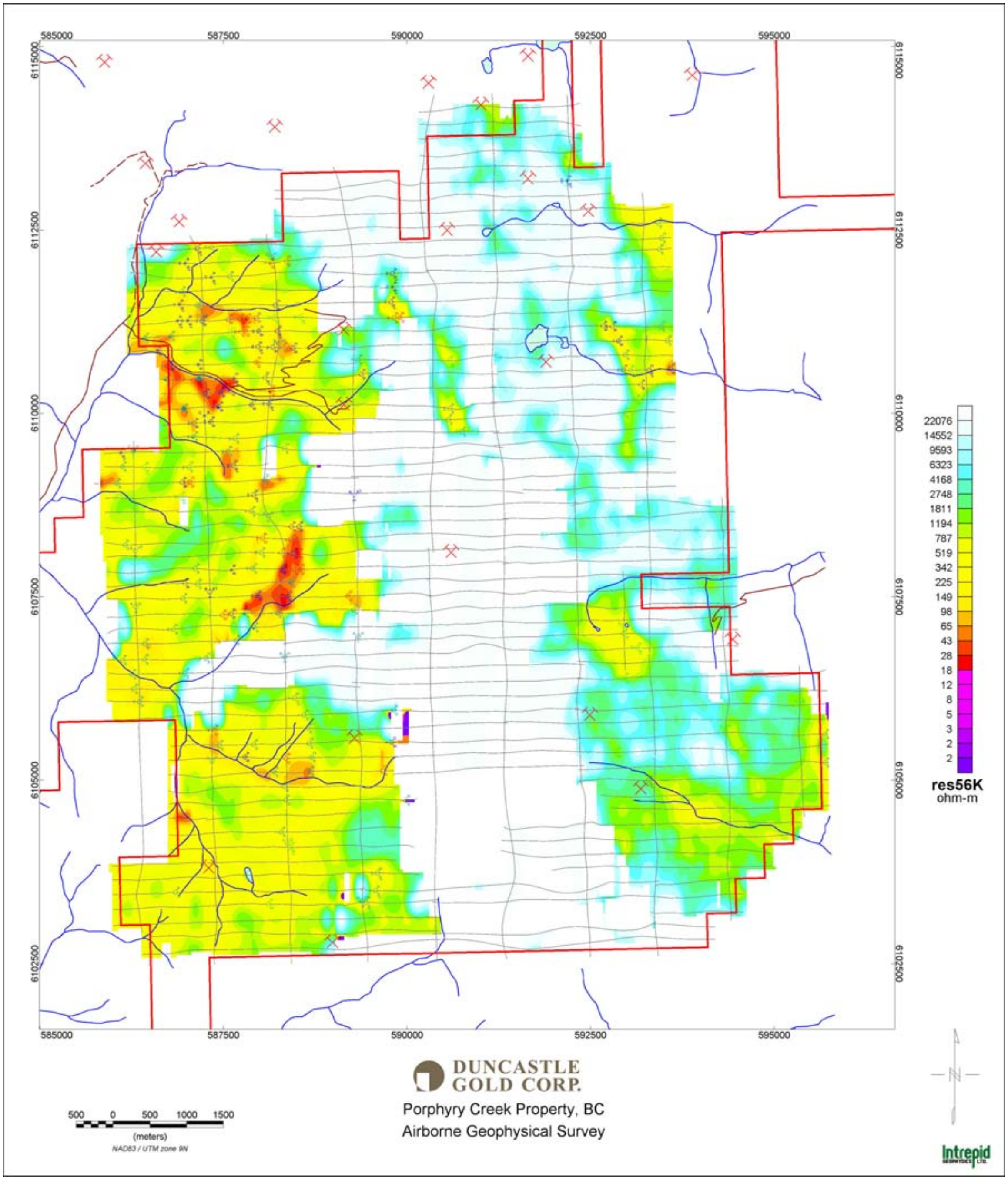

Figure 10. Apparent Resistivity calculated from 56,000 Hz coplanar in-phase and quadrature channels.

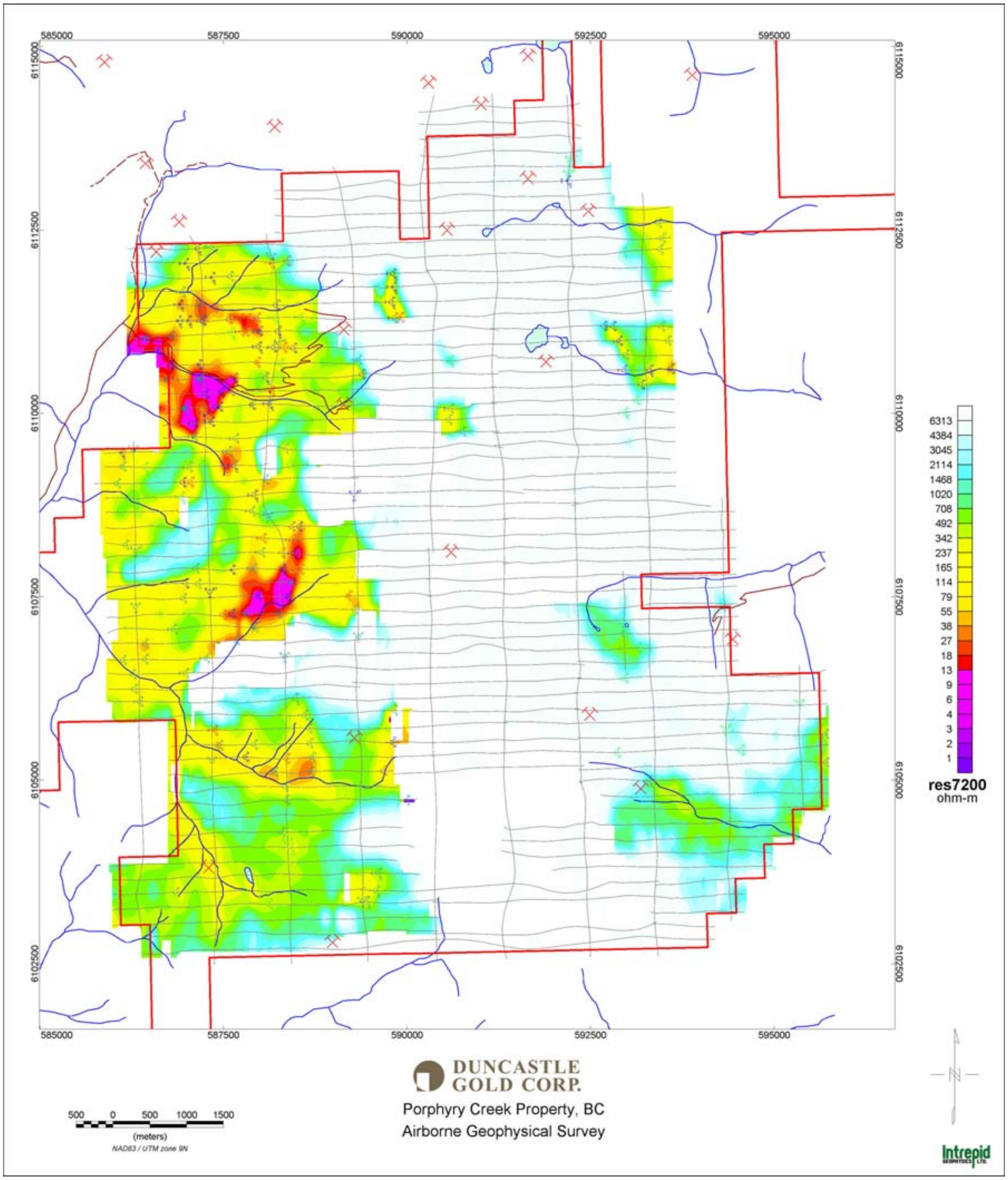

Figure 11. Apparent Resistivity calculated from 7,200 Hz coplanar in-phase and quadrature channels.

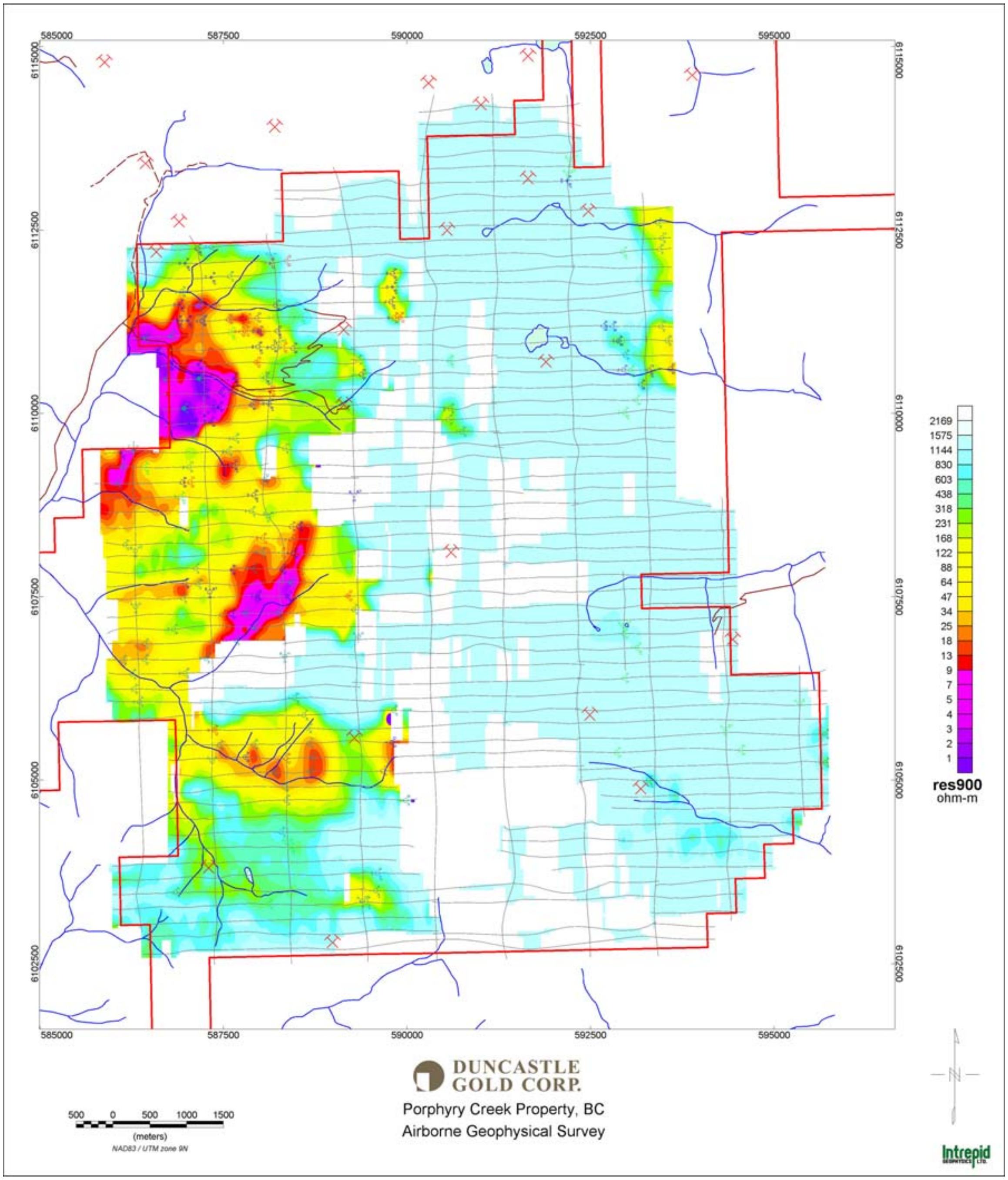

Figure 12. Apparent Resistivity calculated from900 Hz coplanar in-phase and quadrature channels.

The maximum resistivity values, which are calculated for each frequency, are 1,300, 8,400, and 30,000 ohm-m respectively. These cut-offs eliminate the erratic higher resistivities that would result from unstable ratios of very small EM amplitudes. There are several gaps in coverage evident on the resistivity maps. These are due to a combination of flight path breaks and/or high flying over areas of severe topography for reasons of safety. The EM system is out of ground effect above 150 m, so no resistivities are calculated above this height, as evidenced by the blank areas in the central and south areas. Some of these gaps could be minimized by relaxing the interline gridding limits, but it is believed better to leave the gaps in, to indicate where there is no valid coverage.

4. Data Interpretation

4.1. Overview — Magnetics/Radiometrics/Electromagnetics

Normally, a comparison of the airborne geophysical response to the known showings on the property is carried out, and then parallels to these sought and identified throughout the survey as a whole. Analogies to mineralization surrounding (e.g., Porphyry Creek North, Black Pilot as well as Sultana and Red Rose) suggest that any mineralization on the Porphyry Creek block typically consists of polymetallic veins which may be related to the emplacement of feldspar porphyritic intrusive rocks of the so-called Rocher Deboule intrusion (itself part of the Bulkley Plutonic Suite) into coarse clastic sedimentary rocks (siltstone and argillite) of the Skeena Group - Red Rose Formation. Comparison of the MINFILE occurrences in the general area reveals a significant degree of correlation to magnetic highs, but little to no correlation to the electromagnetics and/or radiometrics.

The mineralization of this region was not expected to provide particularly strong conductive responses due to the relatively thin and discontinuous nature of the vein and stockwork systems as well as the perhaps dissemination of the associated sulphides. Nonetheless, the magnetic intensity images and derived derivatives serve to delineate the contacts of both magnetic and non-magnetic units. The latter could reflect felsic intrusions or siliceous breccias that might host auriferous mineralization). The combined magnetic and resistivity parameters have also outlined a few interesting magnetic lows and resistivity highs that could in turn reflect alteration zones or siliceous caps.

Overall, there occur many deeply-buried, flat-dipping highly conductive sources in the west and NE quadrant, as well as a few near-vertical thin sources particularly in the eastern half of the surveyed block; the significance of these remains to be established. The current focus of exploration by Duncastle Gold is either along the crest of the topographic ridge (Roche Deboule Mountains) or on the eastern half of the property. If the location of the Sultana deposit is accurate (Line 10380; fiducial 2173.8) it appears to lie within a broad, moderately conductive zone of surficial conductivity, near an E–W break along the south contact of a magnetic unit. The AEM response itself is classed as very weak with an apparent conductance of ~1 mS. Big Thing (porphyry Cu +/- Mo +/- Au laying southwest of Sultana) has virtually no AEM response, although MT (southeast of Big Thing) is coincident with a very weak surficial anomaly.

Northward, Balsam (porphyry Cu +/- Mo +/- Au), Black Pilot and Porphyry Creek North (both porphyry Mo) have no correlation to the AEM. Blue Lake at the very northern edge of the survey does appear to correlate, however, to a very weak and probably surficial response (albeit only partially resolved by this survey). Tina (another porphyry Mo) similarly shows some correlation to a very weak, surficial-type response.

Arguably the best AEM response on the eastern half of the Porphyry claim block occurs ~1 km east of Tina, wherein a moderately strong bedrock conductor plots at 592880.9 mE, 6110987.6 mN. A series of what are believed to be surficial anomalies occur to both the south and north; a low-resistivity zone is mapped as elongated NW–SE and which lays along the eastern flank of a magnetically positive ‘spur.’ While the magnetic gradient is dominantly NNW–SSE at 345°–350° NE cross-linear or structure is suggested by the magnetic analysis.

Enhancement filters applied to the magnetic grid have highlighted a number of dominant structural orientations and trends. Interpretation these data has identified regionally significant structures that define the gross structural architecture of the area. Geological mapping taken from the available regional geology sheets has been incorporated with the structural interpretation for improved geological context. A sophisticated suite of filter enhancements were applied to the gridded magnetic data. From these, the total horizontal derivative (THD) and the tilt derivative (TILT) were found to be the most informative, and are referenced further in the report[8].

A combination of the total horizontal and tilt derivative are highly suitable for mapping shallow basement structure and mineral exploration targets; they have distinct advantages over many conventional derivatives. The total horizontal derivative provides an effective alternative to the vertical derivative to map continuity of structures and enhance magnetic fabric. The advantages of the tilt derivative are its abilities to normalize a magnetic field image and to discriminate between signal and noise.

Additionally, a suite of filters known as the 'ZS' filters[9] (after Zhiqun Shi, the primary author of this development) were employed and are depicted in summary form on Figure 13 below. Two types of filters have been developed for the purpose of enhancing weak magnetic anomalies from near-surface sources while simultaneously enhancing low-amplitude, long-wavelength magnetic anomalies from deep-seated or regional sources. The Edge filter group highlights edges surrounding both shallow and deeper magnetic sources. The results are used to infer the location of the boundaries of magnetised lithologies. The Block filter group has the effect of transforming the data into "zones" which, similar to image classification systems, segregate anomalous zones into apparent lithological categories. Both filter groups change the textural character of a dataset and thereby facilitate interpretation of geological structures.

Figure 13 following illustrates several advantages of the ZS filters; the 1vd, tilt and analytic signal derivatives will typically not provide easily interpreted edges when the sources are weakly magnetized or deeply buried, whereas the Edge and EdgeZone filter are designed to overcome that limitation. The two Edge filters appear to provide a very sharp delineation of geologic units and at the same time, provides a relatively clear indication of structural breaks, such as at Sultana and in the northwest portion of the study where a northeast-trending element is mapped. The Block filters (Area, Block and Plateau) appear to map the central magnetic core of the Rocher Deboule intrusion.

[8] Verduzco, B., Fairhead, J. D., and MacKenzie, C., 2004, "New insights into magnetic derivatives for structural mapping," The Leading Edge, February 2004, pp. 116–119.

[9] Shi, Z. and Butt, G., 2004, New enhancement filters for geological mapping, Extended Abstracts, ASEG 17th Geophysical Conference and Exhibition, Sydney 2004.

MINFILE no.	Name	Xnad83	Ynad83	Principal Minerals	Deposit Type	Airborne Geophysics
093M 068	Armagosa	586608	6112204	Cu, W	Flood Basalt-Associated Ni-Cu, I12:W veins	no mag, nor AEM (edge of survey, poorly resolved)
093M 059	Balsam	590555	6112494	Cu	Porphyry Cu +/- Mo +/- Au	no AEM nor GRS; direct assoc. w/ mag high
093M 062	Big Thing	592477	6105888	Mo, Cu	Porphyry Cu +/- Mo +/- Au	no AEM nor GRS; occurs in circular mag. Low
093M 115	Black Pilot	592462	6112756	Zn	Polymetallic veins Ag-Pb-Zn+/-Au	no AEM; strong K anomaly, occurs off flank of mag high
093M 064	Brian Boru	589291	6105578	Ag, Zn, Pb	Polymetallic veins Ag-Pb-Zn+/-Au	occurs off western flank NW-magnetic high; no direct AEM nor GRS
093M 066	Brunswick	589136	6110117	Ag, Zn, Pb, Au, Cu	Polymetallic veins Ag-Pb-Zn+/-Au	no direct mag nor AEM; occurs on N-flank K-alteration?
093M 154	Jones	588963	6102789	Cu, Zn	Polymetallic veins Ag-Pb-Zn+/-Au	no geophysical assoc.
093M 065	Jupiter	590580	6108109	Mo, Cu	Porphyry Cu +/- Mo +/- Au	western flank strong mag. high; no AEM nor GRS
093M 114	Killarney	587283	6103802	Ag, Zn, Pb, Sn	Polymetallic veins Ag-Pb-Zn+/-Au	indirect elongated mag low, weak AEM (surficial response only?); no GRS
093M 054	Lone Star	593889	6114612	Fe	*:Unknown	(off survey)
093M 063	MT	593200	6104879	Cu, Mo	Porphyry Cu +/- Mo +/- Au	weak surficial AEM; may coincide with mag. low; lays on N-flank K-anomaly
093M 058	Porphyry Creek N	591624	6113195	Mo	Porphyry Mo (Low F- type)	no AEM; lays on N-flank K-anomaly; indirect assoc. w/ mag high.
093M 067	Red Rose	589116	6111140	W, Cu, Au, Ag, Mo, U	W veins	western flank strong mag. high; no AEM nor GRS
093M 061	Sultana *	593137	6106853	Ag, Cu, Mo, Au	Polymetallic veins Ag-Pb-Zn+/-Au, L04:Porphyry Cu +/- Mo +/- Au	moderate AEM response on S-flank local mag. high; indirect GRS
093M 060	Tina	591867	6110695	Mo	Porphyry Mo (Low F- type)	weak (surficial?) AEM

* Sultana coordinates taken from trench just north of dyke.

Table 2. MINFILE occurrences and Dighem^{V} magnetic, radiometric response indicated.

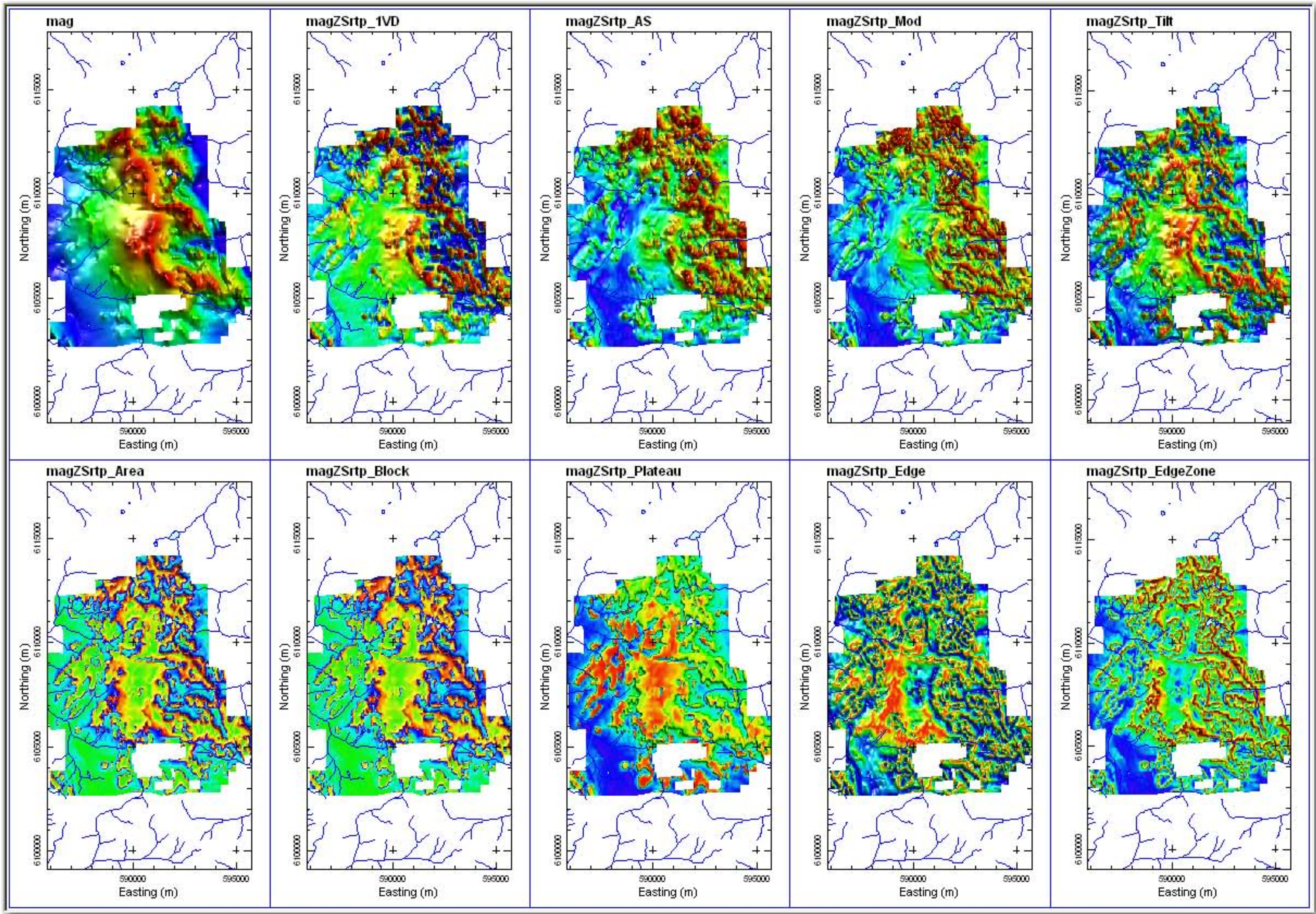

Figure 13. ZS Filters applied to total magnetic intensity (reduced-to-pole)

4.2. Multiscale edge analysis

The analysis of lineaments is of fundamental importance to understanding geological structures and the stress regimes in which they are produced. Automatic analysis of lineaments has previously been done with information mapped from remotely sensed data, using either satellite-based imagery or aerial photographs. Potential field data may also be analyzed in terms of their lineament content. Edge detection and automatic trend analysis using gradients in such data are methods for producing unbiased estimates of sharp lateral changes in physical properties of rocks. The assumption is made that the position of the maxima in the horizontal gradient of gravity or magnetic data represents the edges of the source bodies, although this should be used with caution. Such maxima can be detected and mapped as points, providing the interpreter with an unbiased estimate of their positions. The process of mapping maxima as points can be extended to many different levels of upward continuation, thus providing sets of points that can be displayed in three dimensions, using the height of upward continuation as the z-dimension. There have been recent developments and use of this method for interpretation of potential field data (e.g. Archibald *et al,* 1999[10] and Hornby *et al,* 1999[11]).

Archibald *et al* refer to this process as "multiscale edge analysis." Milligan[12] more recently discusses the spatial and directional analysis of potential field gradients and in particular, new methods to help solve and display three-dimensional crustal architecture using a proprietary system of Eüler deconvolution 'worms.'

In multiscale edge analysis the assumption is made that lower levels of upward continuation map near-surface sources while higher levels of continuation map deeper sources. This assumption is generally true but must be treated with caution, due to the non-uniqueness of potential field solutions. The INTREPID software's unique implementation of multiscale edge analysis includes the use of Eüler 'worms' which provide a view of structural geology obtained directly from potential field geophysical data. The method is based on Fourier techniques for continuation, reduction to pole and total horizontal derivatives coupled with automatic edge detection.

This 'fabric analysis' determines the preferred orientation of basement or at least, magnetic linears within the Homestake property. A number of statistical analytical methods of analyzing fabrics have been devised, with perhaps the simplest way of presenting and analyzing the data being diagrammatically via a rose diagram, shown on a following figure.

A preferred NNW–SSE strike mimicking topography is clearly shown by this data, albeit with a significant population of cross-cutting structural fabric. A further analysis and correlation to geology and the possible impact on economic mineralization is currently underway in conjunction with staff of Duncastle Gold. Nonetheless, a number of dominant structural orientations and key features in the data have been identified on the basis of the magnetic data. These include:

- A major system striking NW–SE is observed in all datasets; magnetic, radiometric and AEM as well as to some extent, the digital elevation. Significant structural disturbance is felt reasonable and indeed is observed in the magnetic derivatives.
- Later (?) and minor NE-SW cross-cutting structures and lineaments are apparent to some degree, and are especially emphasized by the multiscale edge analysis.

[10] Archibald, N., Gow, P. and Boschetti, F., 1999, Multiscale edge analysis of potential field data: Exploration Geophysics, 30, 38-44.

[11] Hornby, P., Boschetti, F. and Horowitz, F.G., 1999, Analysis of potential field data in the wavelet domain: Geophysical Journal International, 137, 175-196.

[12] Milligan, P. R., Lyons, P. and Direen, N. G., 2003, Spatial and directional analysis of potential field gradients—new methods to help solve and display three-dimensional crustal architecture: Australian Society of Exploration Geophysicists' 16th Geophysical Conference and Exhibition, February 2003, Adelaide, Extended Abstracts.

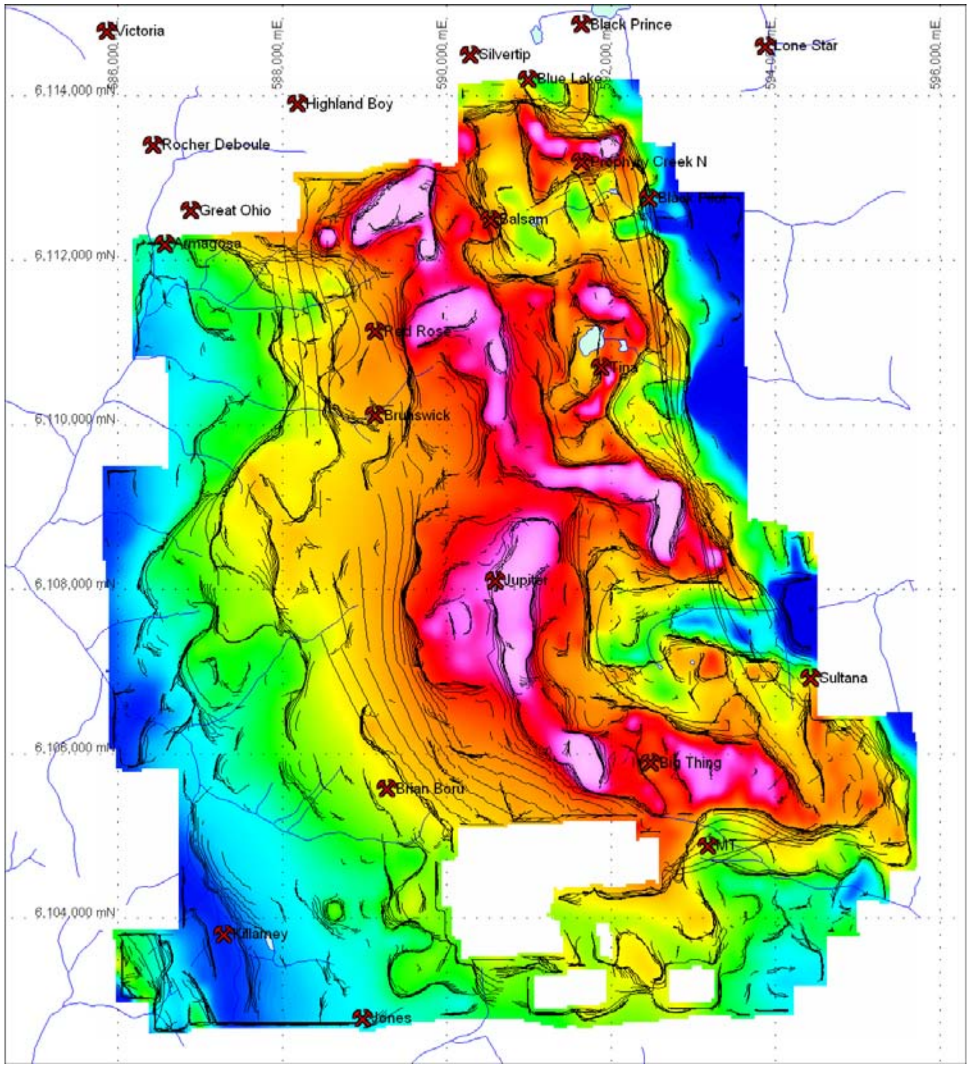

Figure 14. Multiscale Edge Analysis superimposed upon Residual Magnetic Intensity image

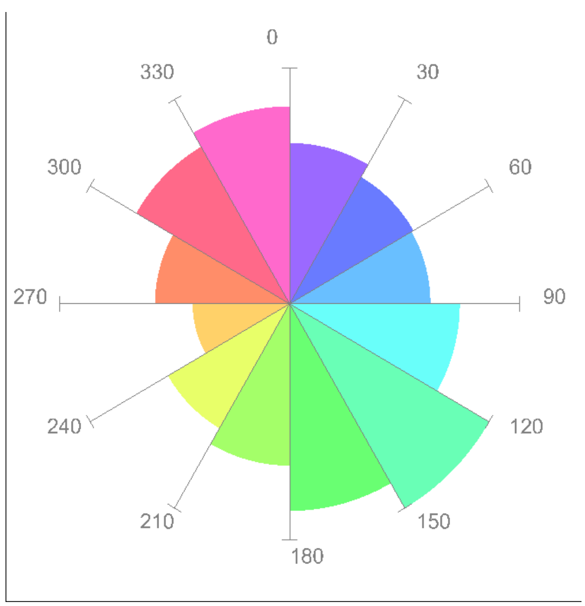

Figure 15. Rose Diagram – Magnetic Strikes

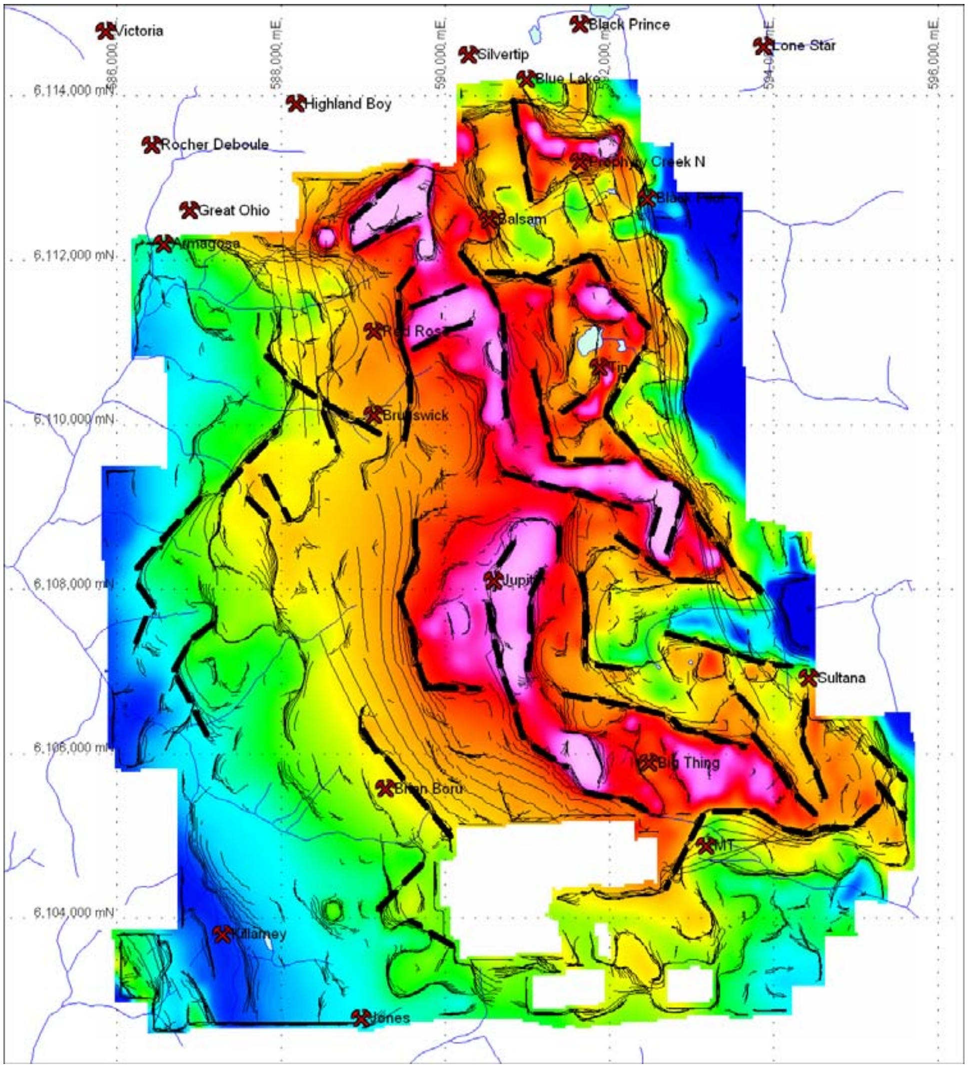

Figure 16. Residual Magnetic Intensity with major inferred structural breaks/contacts superimposed.

The Centre for Exploration Targeting (CET) based at the University of Western Australia has developed algorithms for Texture Analysis, Phase Analysis, and Structure Detection of potential field data sets. These are versatile algorithms useful for grid texture analysis, lineament detection, edge detection, and thresholding; this technology was utilized on the Porphyry Creek claim group. Gold mineralisation is known to occur near major crustal breaks manifesting as large-scale shear zones, which act as conduits for mineralising fluids. Mineralisation occurs in regions of structural complexity adjacent to the shear zones. Progressing towards the automatic detection of such regions, the proposed system finds firstly regions of magnetic discontinuity that correspond to both lithological boundaries and shear zones using a combination of texture analysis and symmetry feature detection techniques. Secondly, it examines the data using fractal analysis to find areas nearby with a complex magnetic expression (zones of structural complexity). The most prospective areas are those where inferred structural complexity occurs adjacent to the regions of magnetic discontinuity.[13] Arising out of this analysis are the following images:

[13] Holden, E-J., Dentith, M. and Kovesi, P., “Towards the automatic analysis of regional aeromagnetic data to identify regions prospective for gold deposits”, Computers & Geosciences, Volume 34, Number 11, pp. 1505–1513, 2008.

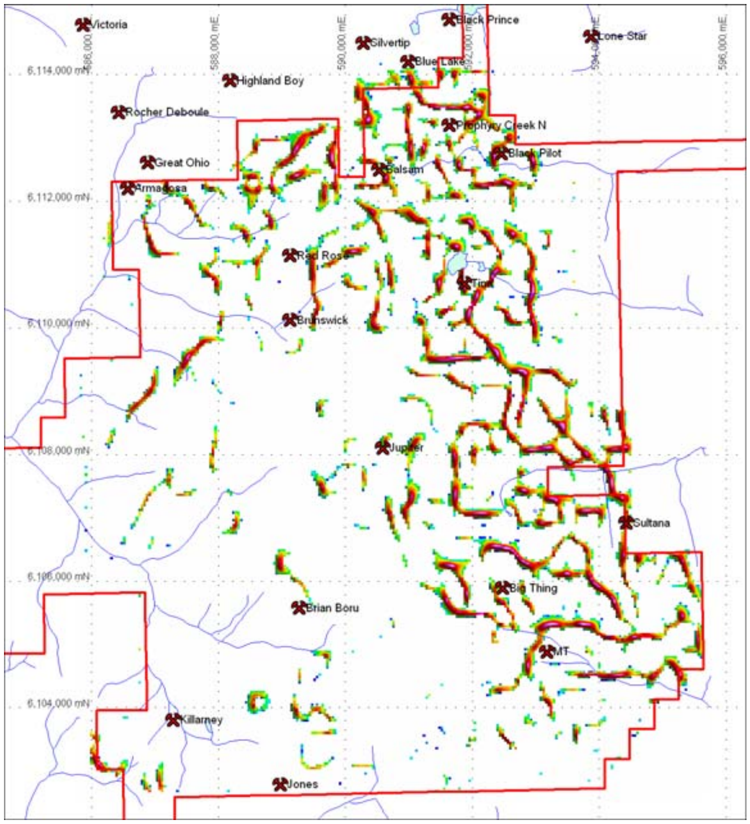

Figure 17a. Phase Symmetry, positive polarity axes indicated

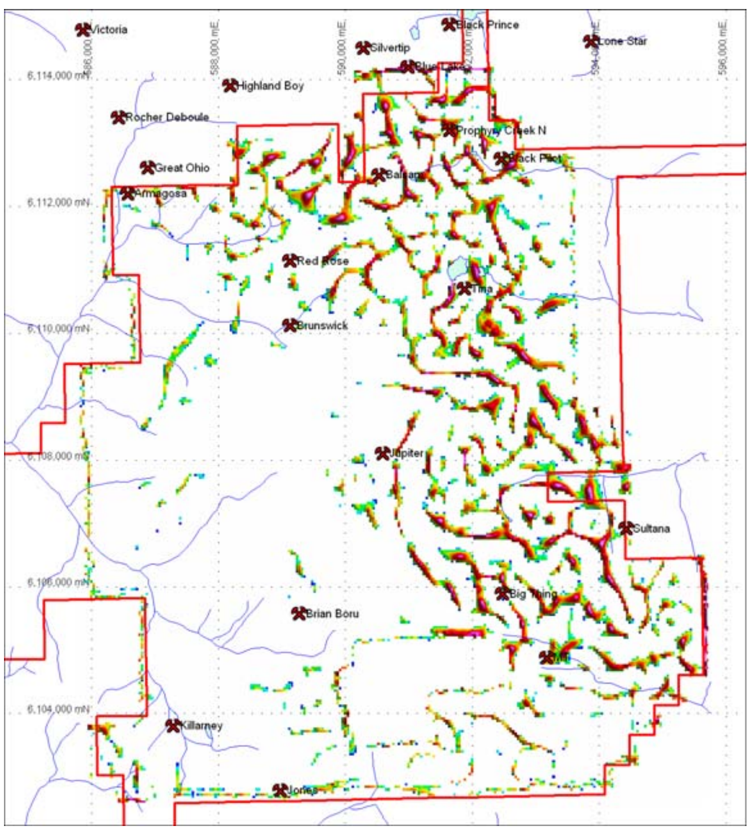

Figure 17b. Phase Symmetry, negative polarity axes indicated

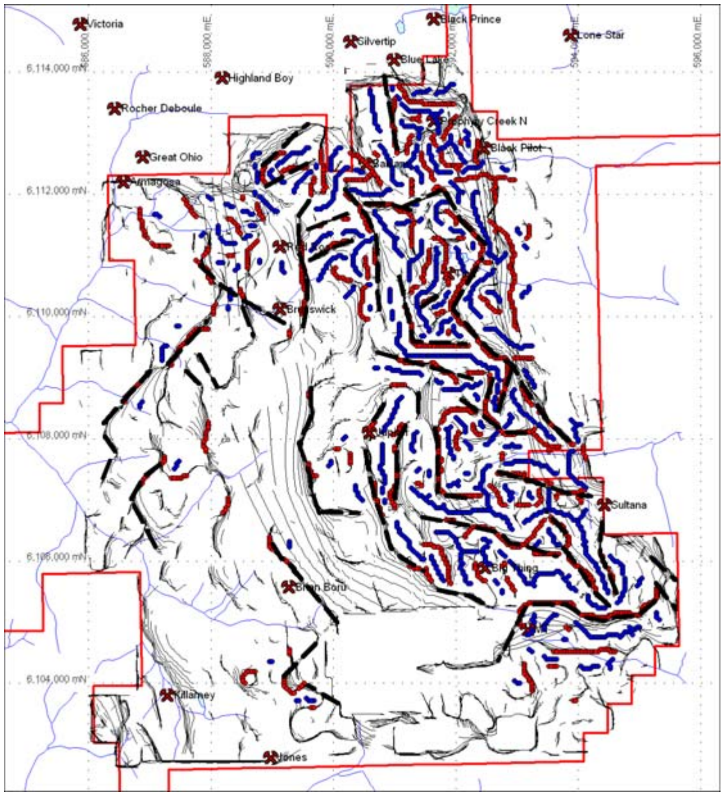

Figure 18. Cumulative magnetic linears indicating structure and contacts
(blue indicates negative phase symmetry, red indicates positive phase symmetry)

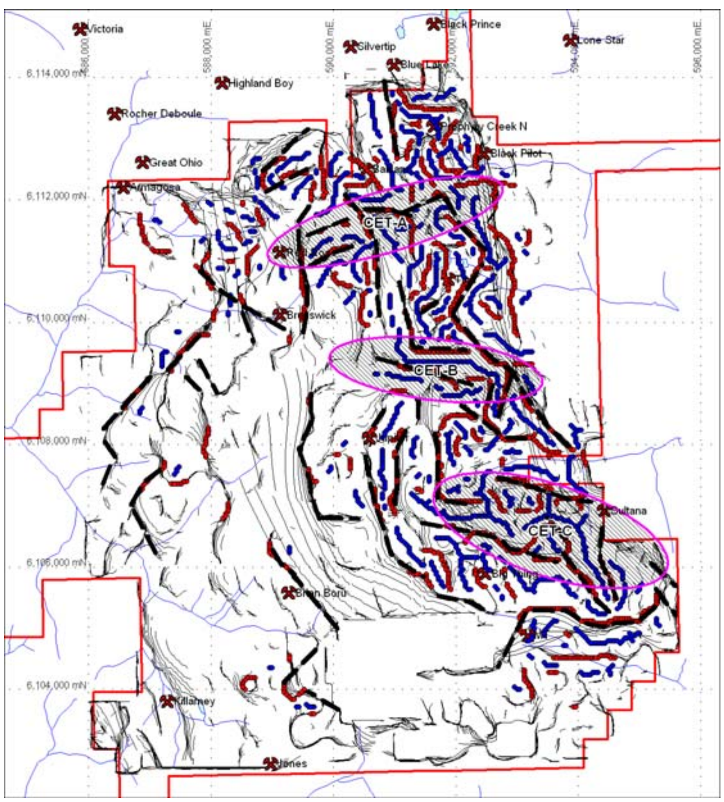

Figure 19. Phase symmetry and multiscale edge detection with identified zones of magnetic discontinuity adjacent to shear zones / lithologic boundaries. Possible zones of complexity marked as CET-A – C.

4.3. Electromagnetics

The Coaxial 5500 Hz responses and the mid-frequency difference channels are used as two of the main picking criteria on the Porphyry Creek project. The 7200 Hz coplanar results were also weighted to provide picks over wider or flat-dipping sources. Most anomalies in the area are of moderate amplitude, and yield moderately low conductance, generally less than 10 Siemens.

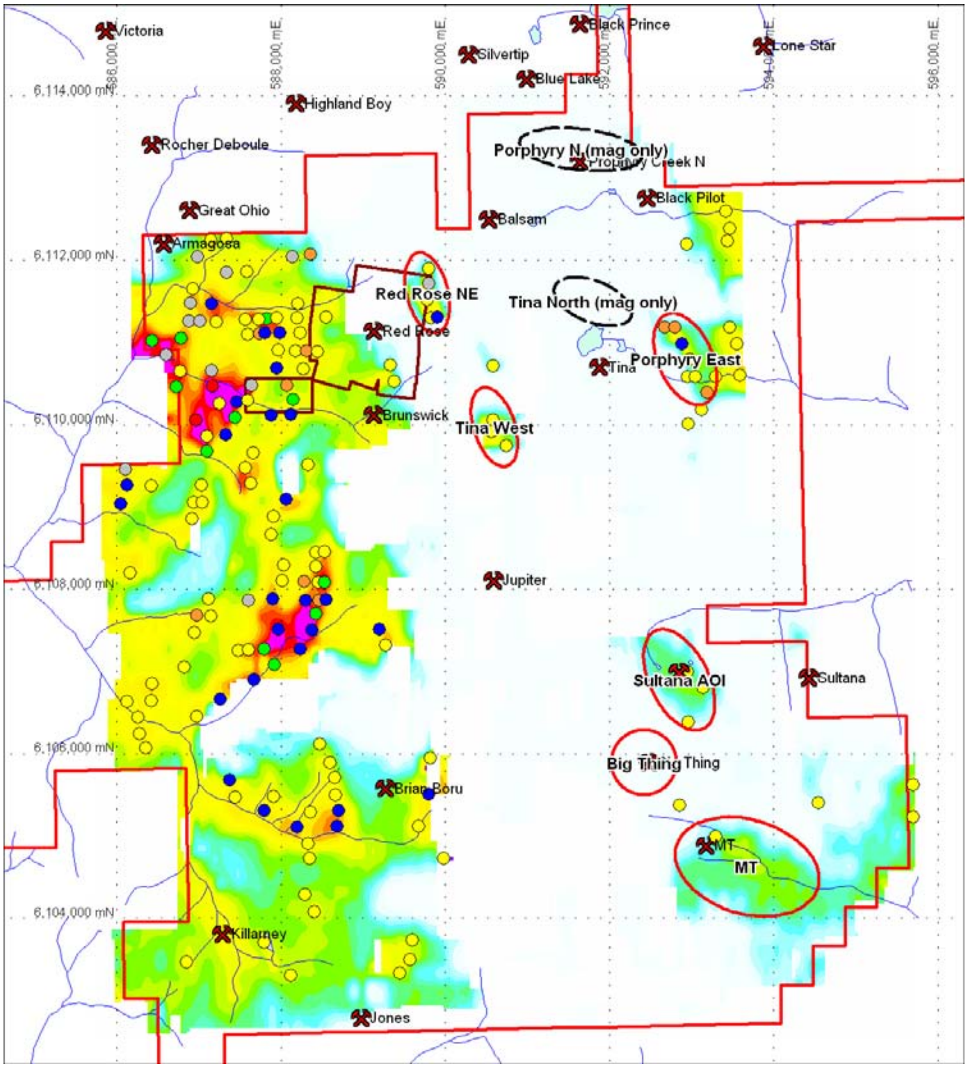

Figure 20. Apparent Resistivity (7200 KHz) with AEM anomalies and target areas indicated.

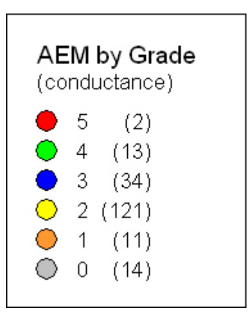

Many of these in turn are felt to be due to conductive overburden or flat-lying conductive layer (less than 100 ohm-m) associated with one of the three main zones of lower resistivity on the western slopes of the Hazelton Mountains. Other anomalies yield more discrete characteristics, and often coincide with magnetic linears that could reflect contacts, faults, or shears. These inferred contacts and structural breaks are considered to be of particular interest as they may have influenced or controlled mineral deposition within the survey area.

4.4. Radiometrics

The radiometric (airborne gamma-ray spectrometry) 'areas of interest' circled below denote elevated counts per second across the full decay window; additional processing to extract radioelement ratios is currently being carried out by Fugro Airborne Surveys. Nevertheless, these AOIs suggest some degree of correlation between anomalous resistivity and magnetics as previously discussed.

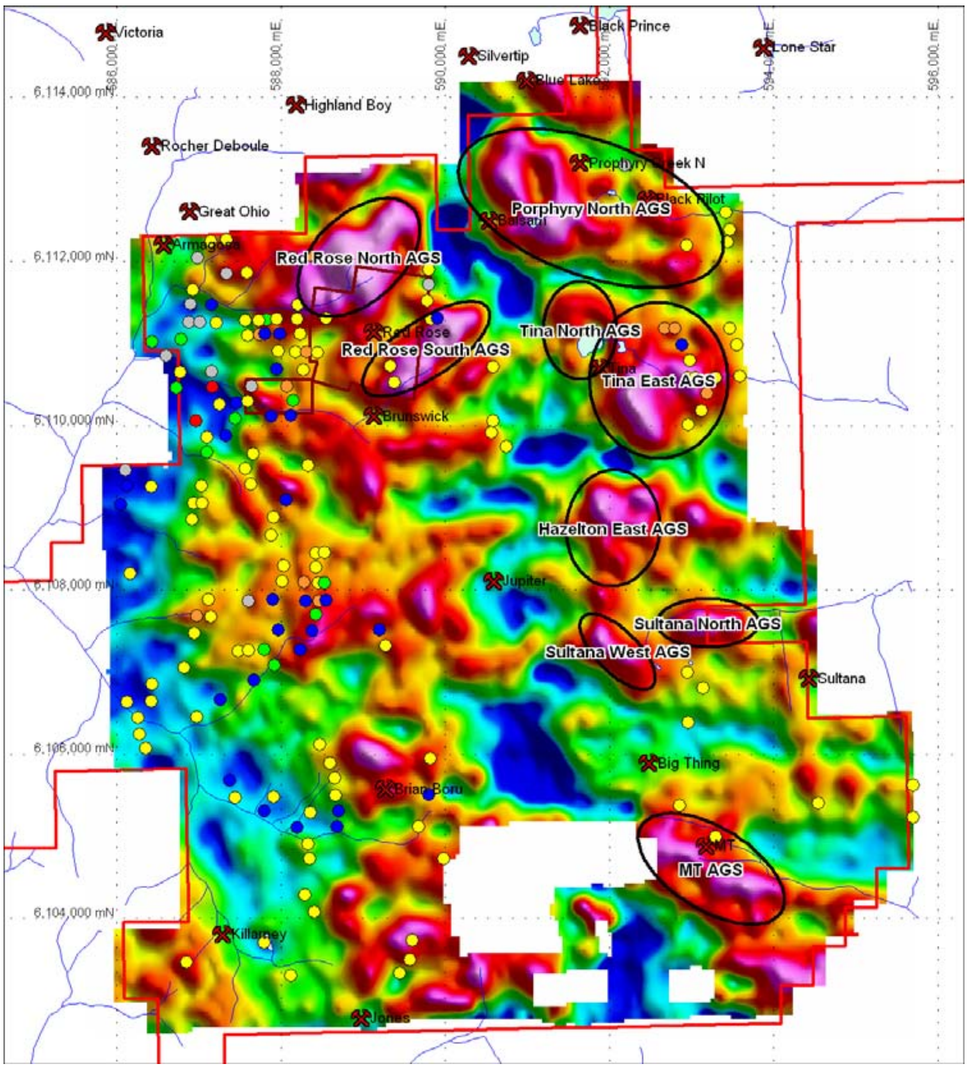

Figure 21. Airborne Gamma Ray Spectrometry: Total Counts (corrected) with Areas of Interest circled

Ore zones in porphyry systems are generally associated (Rogers, 2010; Holliday and Cooke, 2007) with areas of high fracture densities and potassic alteration. The areas of interest indicated above should contain both these pathfinders, assuming that structural disturbances and complexities are reflected by the magnetic patterns previously discussed.

5. Conclusions and Recommendations

A helicopter-borne electromagnetic, magnetic and radiometric survey was flown by Fugro Airborne Surveys in July 2010 over the Porphyry Creek property of Duncastle Gold Corp.; this survey comprises 495 line-kilometres of data acquired on a grid pattern of 200 m spaced east–west traverses controlled by 1,000 m spaced north–south tie lines. The survey was completed without incident in 13 flights spread over 4 days of actual production; although very poor weather severely impacted this production, no days were lost to equipment or safety issues.

Products obtained from this airborne geophysical survey include the residual magnetic intensity and various derivative grids, multi-channel gamma-ray spectrometer grids of potassium, thorium and uranium from which ratios may be further determined, as well as both inphase and quadrature components of the three coplanar and two coaxial channels comprising the airborne electromagnetics. The latter led in turn to apparent resistivity grids which were subsequently imaged and integrated with the magnetic and radiometric grids in order to arrive at a final interpretation.

The original objectives of this survey were two-fold:

- provide high resolution electromagnetic, magnetic and radiometric data for the direct detection and delineation of sulphide-associated gold-silver occurrences
- facilitate the mapping of bedrock lithologies and structure which in turn influence the emplacement or hosting of economic mineralization.

These objective have been or are being met via this interpretation; the data has enabled both the mapping and delineation of controlling structures, and identification of pronounced potassium alteration. A comparison of the known mineral occurrences within the survey boundaries was undertaken and results tabulated. From this analysis, the known mineralized occurrences or showings typically do not possess an electromagnetic signature, but are typically associated, at the least indirectly, with magnetic positive anomalies. The spectrometer data (specifically, increased K% suggesting anomalous K-alteration) also appears to correlate to several of the showings, principally on the eastern flanks of the Rocher Deboule range.

A conclusion from this analysis and interpretation is that the magnetic data may be more revealing in identifying zones of complexity and possible alteration (specifically, magnetite destruction); in contrast, direct detection of significant sulphides through the (presumed) associated electromagnetic response may be much more problematic. Nevertheless, a few bedrock conductors are identified which should be further investigated on the ground as reflecting anomalous sulphide mineralization, and 2–3 magnetic highs spatially associated with significant, inferred structural disturbances and at least proximal to resistive lows may represent mineralized systems.

A methodical profile by profile review of the Dighem^{V} data was carried out; several airborne electromagnetic (AEM) responses have been identified as possibly significant and marked for ground follow-up and further investigation. The AEM anomalies so mapped do not, however, typically suggest significant or characteristic zones of conductivity that might be related to basement conductors such as sulphide-enriched mineralization/alteration features; i.e., most of the AEM responses do not possess direct magnetic correlation typical of economic sulphide mineralization. An exception to this observation occurs with the AEM anomalies marking both the Sultana and Tina mineral showings.

A total of 6 anomalous conductive zones are identified and mapped by this interpretation; 2 singularly magnetic high zones, and 9 potentially-enhanced K% 'target zones' were additionally identified as 'areas of interest' for follow-up. All zones are located precisely by the differential GPS coordinates inherent to the airborne geophysical survey. The targets are all felt worthy of ground follow-up in the remaining summer-autumn field season as time and weather/logistical conditions permit; further investigation is believed warranted in future programs as budgets and time allows.

Enhancement filters applied to the magnetic grid have highlighted a number of dominant structural orientations and trends. A major northwest-southeast magnetic fabric is identified which cuts through and breaks the NNW–SSE pattern of the known geology; a minor NE-SW trend is also mapped by the multiscale edge analysis in the northern portion of the study. Both these trends provide potential for significant fracturing and mobilization of mineralized fluids.

All targets, and zones or areas of interest are supplied separately to Duncastle Gold as mapinfo *.tab files with accompanying annotation and georeferencing.

A recommendation is herein made to include a careful integration of these geophysical data with the summary geologic and eventual drilling results obtained from the remaining 2010 field season in order to both assess the true significance of the geophysics in the overall exploration of this property, and to prioritize targets or zones for field investigations in 2011.

6. Certificate of Professional Qualifications

I, Christopher J. Campbell, with business address of 4505 Cove Cliff Road, North Vancouver British Columbia V7G 1H7, hereby certify that:

- I am a graduate (1972) of the University of British Columbia, with a Bachelor of Science degree in Geophysics.
- I am a graduate (1986) of the University of Denver, with a Masters of Business Administration.
- I am a registered member in good standing of the Association of Professional Engineers and Geoscientists of British Columbia.
- I have practiced my profession for approximately thirty-five years in Canada (British Columbia, Alberta, Saskatchewan, Manitoba, Ontario, Quebec, Newfoundland/Labrador, Yukon and Northwest Territories / Nunavut), United States of America, Australia, Russia, and Africa.
- I have no interest, direct or indirect, in the properties or securities of Duncastle Gold Corp., or in any of their related companies or joint venture partners anywhere in Canada.

Dated this day October 30, 2010 in North Vancouver, British Columbia.

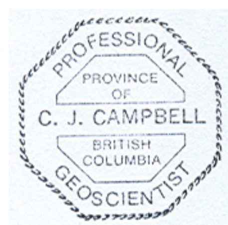

Christopher J. Campbell, P. Geo.

7. Statement of Costs

<u>Contractors</u>

Fugro Airborne Surveys Corp Invoiced total (pre-tax) *495 line-km survey, data preparation, Fugro report*	$165,480
Intrepid Geophysics Ltd 9.5 days @ $1,000/day *Program management, quality control, data analysis, final reporting*	$9,500
TOTAL COST	**$174,980**

Appendix A.

Fugro Airborne Surveys

DIGHEM$^{V\text{-}DSP}$ Survey

For

Duncastle Gold Corp.

Porphyry Creek Property
New Hazelton, BC

Report #10037

September 9, 2010

Report #10037

DIGHEM$^{V\text{-}DSP}$ SURVEY
FOR
DUNCASTLE GOLD CORP.
PORPHYRY CREEK PROPERTY
NEW HAZLETON, B.C.

NTS: 93M/4

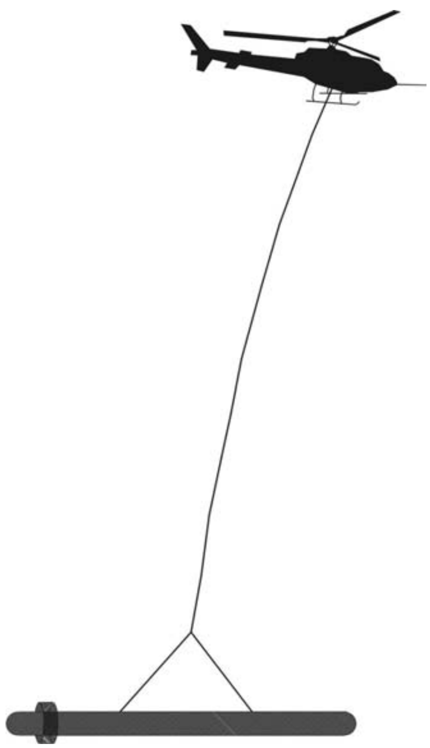

Fugro Airborne Surveys Corp.
Mississauga, Ontario

September 9, 2010

Fugro Airborne Surveys, 2505 Meadowvale Boulevard, Mississauga, Ontario, Canada, L5N 5S2
Phone: 1 905 812 0212, Fax: 1 905 812 1504

SUMMARY

This report describes the logistics, data acquisition, processing and presentation of results of a DIGHEM^{V} airborne geophysical survey carried out for Duncastle Gold Corp., over a property located south of New Hazleton, B.C. Total coverage of the survey block amounted to 495 km. The survey was flown from July 7 to July 19, 2010

The purpose of the survey was to provide information that could be used to map the geology and structure of the survey area, to locate any resistive zones that might reflect polymetallic quartz-vein systems, and to detect any conductive zones that could be due to sulphide/oxide mineralization. This was accomplished by using a DIGHEM^{V-DSP} multi-coil, multi-frequency electromagnetic system, supplemented by a high-sensitivity cesium magnetometer and a 256-channel spectrometer. The information from these sensors was processed to produce maps that display the magnetic, radiometric, and conductive properties of the survey area. A GPS electronic navigation system ensured accurate positioning of the geophysical data with respect to the base maps.

The survey data were processed and compiled in the Fugro Airborne Surveys Toronto office. Map products and digital data were provided in accordance with the scales and formats specified in the Survey Agreement.

The survey property several anomalous features, some of which are considered to be of moderate to high priority as exploration targets. Although quartz-rich auriferous targets are likely to be associated with resistive units, there are several strong bedrock conductors that could reflect sulphide type targets. Some of these warrant further investigation using appropriate surface exploration techniques. Areas of interest may be assigned priorities on the basis of supporting geophysical, geochemical and/or geological information. After initial investigations have been carried out, it may be necessary to re-evaluate the remaining anomalies based on information acquired from the follow-up program.

CONTENTS

APPENDICES

1. INTRODUCTION

A DIGHEM^{V-DSP} electromagnetic/resistivity/magnetic/radiometric survey was flown for Duncastle Gold Corp., from July 7 to July 19, 2010, over a survey block located approximately 10 km south of New Hazleton, B.C. The survey area can be located on map sheet 93 M/4. (Figure 1).

Survey coverage consisted of approximately 495 line-km, including tie lines. Flight lines were flown east-west (90°-270°) with a line separation of 200 m. Tie lines were flown orthogonal to the traverse lines (N-S) at intervals of 1 km.

The survey employed the DIGHEM^{V-DSP} electromagnetic system. Ancillary equipment consisted of a magnetometer, radar and barometric altimeters, a digital video camera, a digital recorder, a 256-channel spectrometer, and an electronic navigation system. The instrumentation was installed in an AS350-B3 turbine helicopter (Registration C-FIDA) that was provided by Great Slave Helicopters Ltd.. The helicopter flew at an average airspeed of 100 km/h with an EM sensor height of approximately 40 metres. The spectrometer crystal package was housed within the helicopter, with a nominal terrain clearance of 68m.

In several portions of the survey area, steep topography forced the pilot to exceed normal terrain clearance for reasons of safety. It is possible that some valid anomalous features may have escaped detection in areas where the bird height exceeded 120 m. There are several gaps in the resistivity grids, where high flying precluded the calculation of valid resistivities. Several lines had to be flown in segments, in an attempt to obtain more coverage.

In difficult areas where near-vertical climbs were necessary, the forward speed of the helicopter was reduced to a level that permitted excessive bird swinging. This problem, combined with the severe stresses to which the bird was subjected, gave rise to aerodynamic noise levels that are slightly higher than normal on some lines. Where warranted, reflights were carried out to minimize these adverse effects.

Fugro Airborne Surveys DIGHEM^{V} EM bird with AS350-B3

2. SURVEY AREA

The base of operations for the survey was established at Smithers, B.C.. Table 2-1 lists the corner coordinates of the survey area in WGS 84, UTM Zone 9N, central meridian 129°W.

Table 2-1

NAD83 UTM Zone 9N

Block	Corners	X-UTM (E)	Y-UTM (N)
10037-1	1	586319	6112306
Porphyry	2	588310	6112345
Creek	3	588292	6113273
Property	4	590282	6113313
	5	590263	6114240
	6	592254	6114281
	7	592273	6113354
	8	592672	6113362
	9	592681	6112898
	10	593478	6112915
	11	593566	6108742
	12	594364	6108758
	13	594413	6106440
	14	595610	6106466
	15	595650	6104611
	16	595251	6104602
	17	595261	6104139
	18	594862	6104130
	19	594871	6103667
	20	594472	6103658
	21	594482	6103195
	22	594083	6103186
	23	594093	6102723
	24	586508	6102569
	25	586499	6103033

Block	Corner s	X-UTM (E)	Y-UTM (N)
10037-1	27	586082	6103953
	28	586880	6103968
	29	586844	6105822
	30	586046	6105807
	31	585974	6109516
	32	586772	6109532
	33	586744	6110923
	34	586346	6110915

The survey specifications were as follows:

Parameter	Specifications
Traverse line direction	East-West
Traverse line spacing	200 m
Tie line direction	North-South
Tie line spacing	1km
Sample interval	10 Hz, 2.77 m @ 100 km/hr
Aircraft mean terrain clearance	68 m
Spectrometer (in Aircraft)	68m
EM sensor mean terrain clearance	40
Mag sensor mean terrain clearance	40 m
Average speed	100 km/h
Navigation (guidance)	±5 m, Real-time GPS
Post-survey flight path	±2 m, Differential GPS

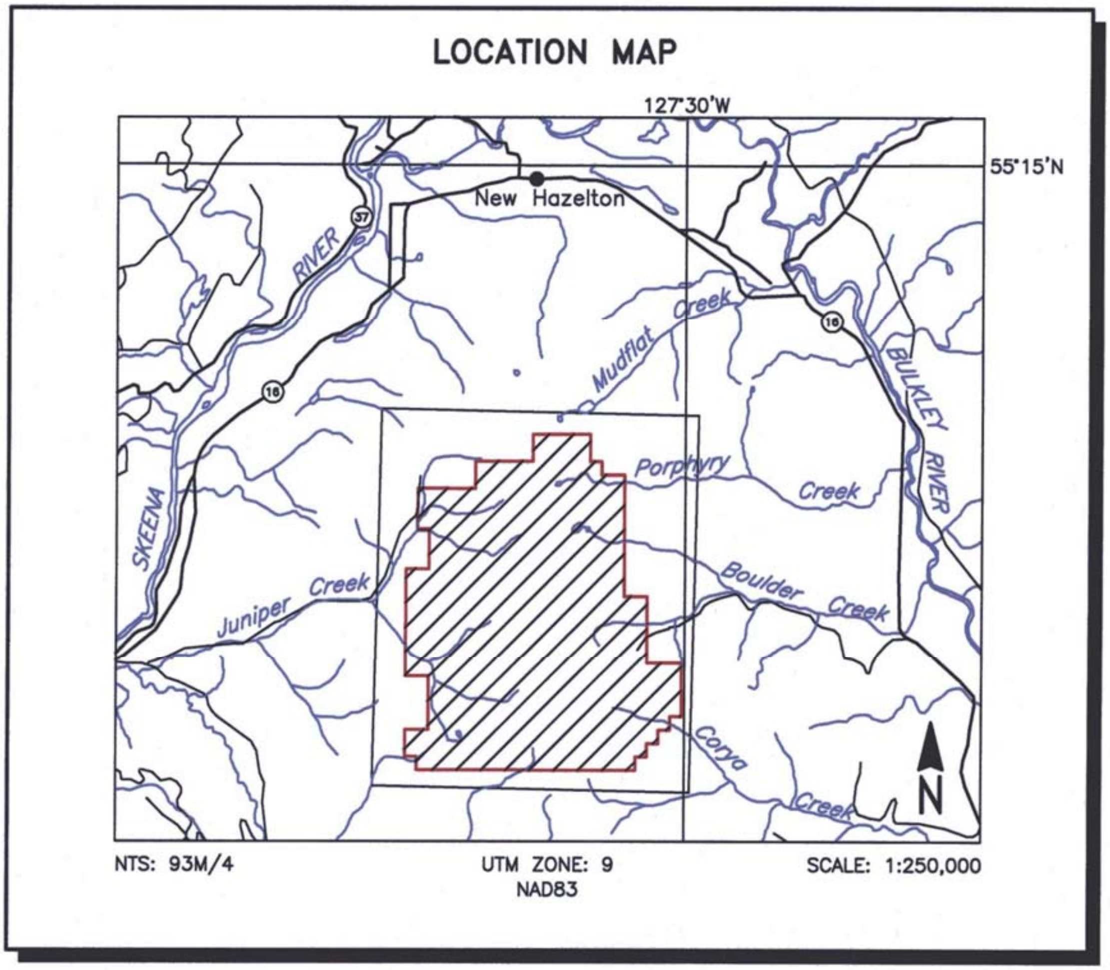

Figure 1
Location Map and Sheet Layout
Porphyry Creek Property
Job # 10037

3. SURVEY EQUIPMENT

This section provides a brief description of the geophysical instruments used to acquire the survey data and the calibration procedures employed. The geophysical equipment was installed in an AS350-B3 helicopter. This aircraft provides a safe and efficient platform for surveys of this type.

Electromagnetic System

Model: DIGHEM$^{V\text{-}DSP}$ BKS 54

Type: Towed bird, symmetric dipole configuration operated at a nominal survey altitude of 35 m. Coil separation is 8 m for 900 Hz, 1000 Hz, 5500 Hz and 7200 Hz, and 6.3 m for the 56,000 Hz coil-pair.

Coil orientations, frequencies and dipole moments

Atm^2	orientation		nominal	actual
211	coaxial	/	1000 Hz	1067 Hz
211	coplanar	/	900 Hz	923 Hz
67	coaxial	/	5500 Hz	5491 Hz
56	coplanar	/	7200 Hz	7093 Hz
15	coplanar	/	56,000 Hz	55600 Hz

Channels recorded: 5 in-phase channels
5 quadrature channels
2 monitor channels

Sensitivity: 0.06 ppm at 1000 Hz Cx
0.12 ppm at 900 Hz Cp
0.12 ppm at 5,500 Hz Cx
0.24 ppm at 7,200 Hz Cp
0.60 ppm at 56,000 Hz Cp

Sample rate: 10 per second, equivalent to 1 sample every 2.77 m, at a survey speed of 100 km/h.

The electromagnetic system utilizes a multi-coil coaxial/coplanar technique to energize conductors in different directions. The coaxial coils are vertical with their axes in the flight direction. The coplanar coils are horizontal. The secondary fields are sensed simultaneously by means of receiver coils that are maximum coupled to their respective transmitter coils. The system yields an in-phase and a quadrature channel from each transmitter-receiver coil-pair.

EM System Calibration

The initial calibration procedure at the factory involves three stages; primary field bucking, phase calibration and gain calibration. In the first stage, the primary field at each receiver coil is cancelled, or "bucked out", by precise positioning of five bucking coils.

The initial phase calibration adjusts the phase angle of the receiver to match that of the transmitter. A ferrite bar, which produces a purely in-phase anomaly, is positioned near each receiver coil. The bar is rotated from minimum to maximum field coupling and the responses for the in-phase and quadrature components for each coil pair/frequency are measured. The phase of the response is adjusted at the console to return an in-phase only response for each coil-pair.

The initial gain calibration uses external coils designed to produce an equal response on in-phase and quadrature components for each frequency/coil-pair. The coil parameters and distances are designed to produce pre-determined responses at the receiver, when the calibration coil is activated. The gain at the console is adjusted to yield secondary responses of exactly 100 ppm and 200 ppm on the coaxial and coplanar channels respectively. Gain calibrations on the ground are carried out at the beginning and end of the survey, or whenever key components are replaced.

The phase and gain calibrations each measure a relative change in the secondary field, rather than an absolute value. This removes any dependency of the calibration procedure on the secondary field due to the ground, except under circumstances of extreme ground conductivity.

Subsequent calibrations of the gain, phase and the system zero level are performed in the air. These internal calibrations are carried out before, after, and at regular intervals during each flight. The system is flown to an altitude high enough to be out of range of any secondary field from the earth (the altitude is dependent on ground resistivity) at which point the zero, or base level of the system is established.

Calibration coils in the bird are activated for each frequency by closing a switch to form a closed circuit through the coil. The transmitter induces a current in this loop, which creates a secondary field in the receiver of precisely known phase and amplitude. Linear system drift is automatically removed by re-establishing zero levels between the internal calibrations. Any phase and gain changes in the system are recorded by the digital receiver to allow post-flight corrections. (The Fugro AutoCal process automatically resets the phase and gain to the correct, pre-determined value.)

Using real-time Fast Fourier Transforms and the calibration procedures outlined above, the data are processed in real-time, from the measured total field to inphase and quadrature components, at a rate of 10 samples per second.

Airborne Magnetometer

Model:	Fugro D1344 processor with Scintrex CS-3 sensor
Type:	Optically pumped cesium vapour
Sensitivity:	0.01 nT
Sample rate:	10 per second

The magnetometer sensor is housed in the tail of the EM bird, 28 m below the helicopter.

Magnetic Base Station

<u>Primary</u>

Model:	Fugro CF1 base station with timing provided by integrated GPS	
Sensor type:	Scintrex CS-3	
Counter specifications:	Accuracy:	±0.1 nT
	Resolution:	0.01 nT
	Sample rate	1 Hz
GPS specifications:	Model:	Marconi Allstar
	Type:	Code and carrier tracking of L1 band, 12-channel, C/A code at 1575.42 MHz
	Sensitivity:	-90 dBm, 1.0 second update
	Accuracy:	Manufacturer's stated accuracy for differential corrected GPS is 2 m.

Environmental Monitor specifications:

Temperature:
- Accuracy: ±1.5ºC max
- Resolution: 0.0305ºC
- Sample rate: 1 Hz
- Range: -40ºC to +75ºC

Barometric pressure:
- Model: Motorola MPXA4115A
- Accuracy: ±3.0º kPa max (-20ºC to 105ºC temp. ranges)
- Resolution: 0.013 kPa
- Sample rate: 1 Hz
- Range: 55 kPa to 108 kPa

<u>Backup</u>

Model:	GEM Systems GSM-19T
Type:	Digital recording proton precession
Sensitivity:	0.10 nT
Sample rate:	3 second intervals

A digital recorder is operated in conjunction with the base station magnetometer to record the diurnal variations of the earth's magnetic field. The clock of the base station is synchronized with that of the airborne system, using GPS time, to permit subsequent removal of diurnal drift. The Fugro CF1 magnetic base station was located at Latitude 54° 49’ 10.7099” N, Longitude 127° 11’ 32.21652” W, at an elevation of 423.11 m (WGS84-UTM Zone 9N)

Navigation (Global Positioning System)

Airborne Receiver for Real-time Navigation & Guidance

Model:	Novatel OEM4/V (WAAS) with PNAV 2100 interface
Type:	Code and carrier tracking of L1-C/A code at 1575.42 MHz and L2-P code at 1227.0 MHz. Dual frequency, 24-channel.
Sensitivity:	-132 dBm, 10 Hz update
Accuracy:	Manufacturer’s stated accuracy is better than 5 metres real-time
Antenna:	Aero AT1675 Mounted on tail of aircraft

Primary Base Station for Post-Survey Differential Correction

Model:	NovAtel OEM4/V
Type:	Code and carrier tracking of L1-C/A code at 1575.42 MHz and L2-P code at 1227.0 MHz. Dual frequency, 24-channel.
Sample rate:	10 Hz update.
Accuracy:	Better than 1 metre in differential mode.

The Wide Area Augmentation System (WAAS enabled) NovAtel OEM/V is a line of sight, satellite navigation system that utilizes time-coded signals from at least four of forty-eight available satellites. Both GLONASS and NAVSTAR satellite constellations are used to calculate the position and to provide real time guidance to the helicopter. For flight path processing, a similar NovAtel system was used as the primary base station receiver. The mobile and base station raw XYZ data were recorded, thereby permitting post-survey differential corrections for theoretical accuracies of better than 2 metres. A Marconi Allstar GPS unit, part of the CF-1, was used as a secondary (back-up) base station.

Each base station receiver is able to calculate its own latitude and longitude. For this survey, the primary GPS station was located in Smithers, at the same coordinates given previously for the CF-1 magnetic base station. The GPS records data relative to the WGS84 ellipsoid. Conversion software is used to transform the WGS84 coordinates to the UTM Zone 9N system displayed on the maps.

Radar Altimeter

Manufacturer:	Honeywell/Sperry
Model:	AA300
Type:	Short pulse modulation, 4.3 GHz
Sensitivity:	0.3 m. (Accuracy of ± 5%)
Sample rate:	10 per second

The radar altimeter measures the vertical distance between the helicopter and the ground. This information is used in the processing algorithm that determines conductor depth.

Laser Altimeter

Manufacturer:	Optech
Model:	ADMGPA100.
Type:	Fixed pulse repetition rate of 2 kHz
Sensitivity:	±5 cm from 10ºC to 30ºC
	±10 cm from -20ºC to +50ºC

The laser altimeter is housed in the EM bird, and measures the distance from the EM bird to ground, except in areas of dense tree cover.

Barometric Pressure and Temperature Sensors

Model:	DIGHEM D-1300	
Type:	Motorola MPX4115AP analog pressure sensor. AD592AN high-impedance remote temperature sensors.	
Sensitivity:	Pressure:	150 mV/kPa
	Temperature:	100 mV/°C or 10 mV/°C (selectable)
Sample rate:	10 per second	

The D-1300 circuit is used in conjunction with one barometric sensor and up to three temperature sensors. Two sensors (baro and temp) are installed in the EM console in the aircraft, to monitor pressure (1KPA) and internal operating temperatures (TEMP_INT). A third sensor (TEMP_EXT) is used to record the external temperature during flight.

Digital Data Acquisition System

Manufacturer:	Fugro
Model:	HeliDAS– Integrated Data Acquisition System
Recorder:	San Disk compact flash card (PCMCIA)

The stored data are downloaded to the field workstation PC at the survey base, for verification, backup and preparation of in-field products.

Video Flight Path Recording System

Type:	Axis 2420 Digital Network Camera
Recorder:	Axis 241S Video Server + Tablet Computer
Format:	BDX/BIN

Fiducial numbers are recorded continuously and are displayed on the margin of each image. This procedure ensures accurate correlation of data with respect to visible features on the ground.

Spectrometer

Manufacturer:	Radiation Solutions
Model:	RS 500 - Console ID#5522
Type:	256 Multichannel, Potassium stabilized. NaI detector crystals
Accuracy:	1 count/sec.
Update:	1 integrated sample/sec.

The RS 500 Airborne Spectrometer employs four downward looking crystals (16.8 L or 1024 cu.in.) and one upward looking crystal (4.2 L or 256 cu.in.). The downward crystal records the radiometric spectrum from 410 KeV to 3 MeV over 256 discrete energy windows, as well as a cosmic ray channel that detects photons with energy levels above 3.0 MeV. From these 256 channels, the standard Total Count, Potassium, Uranium and Thorium channels are extracted. The upward crystal is used to measure and correct for Radon.

The shock-protected Sodium Iodide (Thallium) crystal package is unheated, and is automatically stabilized with respect to the Potassium peak. The RS 500 provides raw or Compton stripped data that has been automatically corrected for gain, base level, ADC offset, and dead time.

The system is calibrated on-site, using three accurately positioned hand-held sources. Additionally, fixed-site hover tests or repeat test lines are flown to determine if there are any differences in background. This procedure allows corrections to be applied to each survey flight, to eliminate any differences that might result from changes in temperature or humidity.

4. QUALITY CONTROL

Digital data for each flight were transferred to the field workstation, in order to verify data quality and completeness. A database was created and updated using Geosoft Oasis Montaj and proprietary Fugro Atlas software. This allowed the field personnel to calculate, display and verify both the positional (flight path) and geophysical data on a screen or printer. Records were examined as a preliminary assessment of the data acquired for each flight.

In-field processing of Fugro survey data consists of differential corrections to the airborne GPS data, verification of EM calibrations, drift correction of the raw airborne EM data, spike rejection and filtering of all geophysical and ancillary data, verification of flight videos, calculation of preliminary resistivity data, diurnal correction, and preliminary leveling of magnetic data.

All data, including base station records, were checked on a daily basis, to ensure compliance with the survey contract specifications. Reflights were required if any of the following specifications were not met.

Navigation - Positional (x,y) accuracy of better than 10 m, with a CEP (circular error of probability) of 95%.

Flight Path - No lines to exceed a departure of more than ±25% from the planned line spacing over a continuous distance of more than 1 km, except for reasons of safety.

Clearance - Mean terrain sensor clearance of 35 m, ±10 m, except where precluded by safety considerations, e.g., restricted or populated areas, severe topography, obstructions, tree canopy, aerodynamic limitations, etc.

Airborne Mag The non-normalized 4th difference will not exceed 1.6 nT over a continuous distance of 1 kilometre, excluding areas where this specification is exceeded due to natural anomalies. Aerodynamic magnetometer noise envelope not to exceed 0.5 nT over a distance of more than 1 km.

Base Mag - Diurnal variations not to exceed 10 nT over a straight-line time chord of 1 minute.

EM - Non-linear drift not to exceed 3 x normal noise limits between internal (in-flight) calibrations. Spheric pulses may occur having strong peaks but narrow widths. The EM data area considered acceptable when their occurrence is less than 10 spheric events exceeding the stated noise specification for a given frequency per 100 samples continuously over a distance of 2,000 metres.

Frequency	**Coil Orientation**	**Peak to Peak Noise Envelope (ppm)**
1000Hz	vertical coaxial	5.0
900 Hz	horizontal coplanar	10.0
5500 Hz	vertical coaxial	10.0
7200 Hz	horizontal coplanar	20.0
56,000 Hz	horizontal coplanar	40.0

5. DATA PROCESSING

Flight Path Recovery

The raw range data from at least four satellites are simultaneously recorded by both the base and mobile GPS units. The geographic positions of both units, relative to the model ellipsoid, are calculated from this information. Differential corrections, which are obtained from the base station, are applied to the mobile unit data to provide a post-flight track of the aircraft, accurate to within 2 m. Speed checks of the flight path are also carried out to determine if there are any spikes or gaps in the data.

The corrected WGS84 latitude/longitude coordinates are transformed to the UTM coordinate system used on the final maps. Images or plots are then created to provide a visual check of the flight path.

Electromagnetic Data

EM data are processed at the recorded sample rate of 10 samples/second. If necessary, appropriate spheric rejection filters are applied to reduce noise to acceptable levels. EM test profiles are then created to allow the interpreter to select the most appropriate EM anomaly picking controls for a given survey area. The EM picking parameters depend on several factors but are primarily based on the dynamic range of the resistivities within the survey area, and the types and expected geophysical responses of the targets being sought.

Anomalous electromagnetic responses are selected and analysed by computer to provide a preliminary electromagnetic anomaly map. The automatic selection algorithm is intentionally oversensitive to assure that no meaningful responses are missed. Using the preliminary map in conjunction with the multi-parameter stacked profiles, the interpreter then classifies the anomalies according to their source and eliminates those that are not substantiated by the data. The final EM anomaly map includes bedrock, surficial and cultural conductors. A map containing only bedrock conductors can be generated, if desired.

Apparent Resistivity

The apparent resistivity in ohm-m can be generated from the in-phase and quadrature EM components for any of the frequencies, using a pseudo-layer half-space model. The inputs to the resistivity algorithm are the inphase and quadrature amplitudes of the secondary field. The algorithm calculates the apparent resistivity in ohm-m, and the apparent height of the bird above the conductive source. The upper (pseudo) layer is merely an artifice to allow for the difference between the computed sensor-source distance and the measured sensor height, as determined by the radar or laser altimeter. Any errors in the altimeter reading, caused by heavy tree cover, are included in the pseudo-layer and do not affect the resistivity calculation. The apparent depth estimates, however, will reflect the altimeter errors.

In areas where the effects of magnetic permeability or dielectric permittivity have suppressed the inphase responses, the calculated resistivities will be erroneously high. Various algorithms and inversion techniques can be used to partially correct for the effects of permeability and permittivity.

Apparent resistivity maps portray all of the information for a given frequency over the entire survey area. This full coverage contrasts with the electromagnetic anomaly map, which provides information only over interpreted conductors. The large dynamic range afforded by the multiple frequencies makes the apparent resistivity parameter an excellent mapping tool.

The preliminary apparent resistivity maps and images are carefully inspected to identify any lines or line segments that might require base level adjustments. Subtle changes between in-flight calibrations of the system can result in line-to-line differences that are more recognizable in resistive (low signal amplitude) areas. If required, manual level adjustments are carried out to eliminate or minimize resistivity differences that can be attributed, in part, to changes in operating temperatures. These leveling adjustments are usually very subtle, and do not result in the degradation of discrete anomalies.

After the manual leveling process is complete, revised resistivity grids are created. The resulting grids can be subjected to a microleveling technique in order to smooth the data for contouring. The coplanar resistivity parameter has a broad 'footprint' that requires very little filtering.

The calculated resistivities for the 900 Hz, 7200 Hz and 56kHz coplanar frequencies are included in the XYZ and grid archives. Values are in ohm-metres on all final products.

Resistivity-depth Sections (optional)

The apparent resistivities for all frequencies can be displayed simultaneously as coloured resistivity-depth sections. Usually, only the coplanar data are displayed as the close frequency separation between the coplanar and adjacent coaxial data tends to distort the section. The sections can be plotted using the topographic elevation profile as the surface. The digital terrain values, in metres a.m.s.l., can be calculated from the GPS Z-value or barometric altimeter, minus the aircraft radar altimeter. The resistivity sections can also be "sliced" to provide resistivity plan maps at various depths.

Resistivity-depth sections can be generated in three formats:

(1) Sengpiel resistivity sections, where the apparent resistivity for each frequency is plotted at the depth of the centroid of the in-phase current flow[1]; and,

(2) Differential resistivity sections, where the differential resistivity is plotted at the differential depth[2].

(3) Occam[3] or Multi-layer[4] inversion.

Both the Sengpiel and differential methods are derived from the pseudo-layer half-space model. Both yield a coloured resistivity-depth section that attempts to portray a smoothed approximation of the true resistivity distribution with depth. Resistivity-depth sections are most useful in conductive layered situations, but may be unreliable in areas of moderate to high resistivity where signal amplitudes are weak. In areas where in-phase responses have been suppressed by the effects of magnetite, or adversely affected by cultural features, the computed resistivities may be unreliable.

Both the Occam and multi-layer inversions compute the layered earth resistivity model that would best match the measured EM data. The Occam inversion uses a series of thin, fixed layers (usually 20 x 5m and 10 x 10m layers) and computes resistivities to fit the EM data. The multi-layer inversion computes the resistivity and thickness for each of a defined number of layers (typically 3-5 layers) to best fit the data.

Residual Magnetic Intensity

A fourth difference editing routine was applied to the total magnetic field data to remove any spikes. The aeromagnetic data were then corrected for diurnal variation using the magnetic base station data. The results were then inspected using tie-traverse line intercepts. Manual adjustments were applied to any lines that required leveling, as indicated by the tie-traverse differences, or by shadowed images of the gridded magnetic data.

---

1 Sengpiel, K.P., 1988, Approximate Inversion of Airborne EM Data from Multilayered Ground: Geophysical Prospecting 36, 446-459.

2 Huang, H. and Fraser, D.C., 1993, Differential Resistivity Method for Multi-frequency Airborne EM Sounding: presented at Intern. Airb. EM Workshop, Tucson, Ariz.

3 Constable et al, 1987, Occam's inversion: a practical algorithm for generating smooth models from electromagnetic sounding data: Geophysics, 52, 289-300.

4 Huang H., and Palacky, G.J., 1991, Damped least-squares inversion of time domain airborne EM data based on singular value decomposition: Geophysical Prospecting, 39, 827-844.

The residual magnetic intensity (RMI) is derived from the total magnetic field (TMF), the diurnal variation, and the regional magnetic field (IGRF). The total magnetic intensity was measured in the aircraft, the diurnal was measured from the ground station, and the regional magnetic field was calculated from the updated IGRF. (International Geo-magnetic Reference Field) The IGRF, calculated for the specific location, altitude and the time of the survey, was then removed from the resultant total magnetic intensity to yield the residual magnetic intensity. The manually leveled data were then subjected to a microleveling filter.

Calculated Vertical Magnetic Gradient

The diurnally-corrected total magnetic field data were subjected to a processing algorithm that enhances the response of magnetic bodies in the upper 500 m and attenuates the response of deeper bodies. The resulting vertical gradient map provides better definition and resolution of near-surface magnetic units. It also identifies weak magnetic features that may not be evident on the total field map. However, regional magnetic variations and changes in lithology may be better defined on the total magnetic field parameter.

EM Magnetite (optional)

The apparent percent magnetite by weight is computed wherever magnetite produces a negative in-phase EM response. This calculation is more meaningful in resistive areas.

Magnetic Derivatives (optional)

The total magnetic field data can be subjected to a variety of filtering techniques to yield maps or images of the following:

enhanced magnetics
second vertical derivative

reduction to the pole/equator

magnetic susceptibility with reduction to the pole

upward/downward continuations

analytic signal

All of these filtering techniques improve the recognition of near-surface magnetic bodies, with the exception of upward continuation. Any of these parameters can be produced on request.

Digital Elevation (optional)

The radar altimeter values (ALTR – aircraft to ground clearance) are subtracted from the differentially corrected and de-spiked GPS-Z values to produce profiles of the topography along the survey lines. .The calculated digital terrain data are then tie-line leveled and can be adjusted to any known benchmarks in the survey area. Any remaining subtle line-to-line discrepancies are then removed manually. After the manual corrections are applied, the digital terrain data are filtered with a microleveling algorithm. These values are gridded to produce contour maps or images showing approximate elevations within the survey area

The accuracy of the elevation calculation is directly dependent on the accuracy of the two input parameters, ALTR and GPS-Z. The ALTR value may be erroneous in areas of heavy tree cover, where the altimeter reflects the distance to the tree canopy rather than the ground. The GPS-Z value is primarily dependent on the number of available satellites. Although post-processing of GPS data will yield X and Y accuracies in the order of 1-2 metres, the accuracy of the Z value is usually much less, sometimes in the ±10 metre range. Further inaccuracies may be introduced during the interpolation and gridding process.

Because of the inherent inaccuracies of this method, no guarantee is made or implied that the information displayed is a true representation of the height above sea level.

Although this product may be of some use as a general reference, THIS PRODUCT MUST NOT BE USED FOR NAVIGATION PURPOSES.

Contour, Colour and Shadow Map Displays

The geophysical data are interpolated onto a regular grid using a modified Akima spline technique. The resulting grid is suitable for image processing and generation of contour maps. The grid cell size is normally 20% of the line interval for magnetic and resistivity grids, but 25% of the line interval for the radiometric grids .

Colour maps are produced by interpolating the grid down to the pixel size. The parameter is then incremented with respect to specific amplitude ranges to provide colour "contour" maps.

Monochromatic shadow maps or images are generated by employing an artificial sun to cast shadows on a surface defined by the geophysical grid. There are many variations in the shadowing technique. These techniques can be applied to total field or enhanced magnetic data, magnetic derivatives, resistivity, etc. The shadowing technique is also used as a quality control method to detect subtle changes between lines.

Multi-channel Stacked Profiles (Optional)

Distance-based profiles of the digitally recorded geophysical data can be generated and plotted at an appropriate scale. These profiles also contain the calculated parameters that are used in the interpretation process. These are produced as worksheets prior to interpretation, and can also be presented in the final corrected form after interpretation as paper prints or digital PDF files. The profiles display electromagnetic anomalies with their respective interpretive symbols.

Radiometric Data

All radiometric data reductions performed by Fugro rigorously follow the procedures described in the IAEA Technical Report 323[5].

All processing of radiometric data was undertaken at the natural sampling rate of the spectrometer, i.e., one second. The data were not interpolated to match the fundamental 0.1 second interval of the EM and magnetic data.

The following sections describe each step in the process.

Dead Time Correction

After the raw data have been checked and edited to remove any spikes or gaps, the first step in the reduction sequence for AGS data is dead-time correction. This is carried out using electronically measured dead-time data. Dead-time correction is made to each window using the expression:

$$N = \frac{n}{1 - Tr} \qquad (4.1)$$

where:

n is the corrected count in each second

Tr is the recorded dead-time, the time taken to process all pulses reaching the detector in one second.

Dead-time correction is applied to each window in the downward-looking detector, (including the cosmic and total count windows), but not to the upward-looking data, as these are processed by different circuits.

Intermediate Filtering for Background Corrections

Digital filters are applied to radar altimeter data to smooth sudden jumps that can arise when flying over steep terrain which cause problems when height correcting the data. A 5 point filter is used. The spectrometer cosmic channel is also filtered to reduce statistical noise. In this case, an 11 to 21 point filter would be used. To calculate radon background from the upward-looking detector data, heavily filtered uranium upward, uranium downward, and thorium downward data are needed as described below. Original data will also be preserved.

- Radar altimeter is smoothed with a 5-point Hanning filter
- The Cosmic window is smoothed with a 21-point Hanning filter

Aircraft and Cosmic Background

The determination of the cosmic and aircraft background expressions for each spectral window has been described in chapter 4 of IAEA Technical Report 323. These expressions are of the form:

$$N = a + bC \qquad (4.2)$$

where: N is the combined cosmic and aircraft background in each spectral window,
a is the aircraft background in the window,
C is the cosmic channel count and
b is the cosmic stripping factor for the window.

The expressions are evaluated for each window at each data point using the filtered cosmic channel data and the results subtracted from the data.

Radon Background

---

[5] Exploranium, I.A.E.A. Report, Airborne Gamma-Ray Spectrometer Surveying, Technical Report No. 323, 1991.

Determination of the constants necessary for the correction of background due to radon using upward detectors requires several steps. The procedure outlined in IAEA 323 is generally correct, but more recent studies have refined the process. The first step, determining the contributions of atmospheric radon to the various spectrometry windows is best achieved through a series of test flights, usually over water. The method of least squares allows the constants in equations 4.9 to 4.12 (IAEA 323) to be determined. The next step is to determine the response of the upward looking detector to radiation from the ground (equation 4.13 IAEA 323). The procedure recommended by Grasty and Hovgaard (1996) summarized below, is more reliable than that in IAEA 323.

In view of the high correlation between radiation in the uranium and thorium windows, it is better to assume that the upward response originating from the ground can be correlated to either counts in the thorium window or to counts in the uranium window. This is equivalent to assuming that either a1 or a2 is equal to 0. Solving for a1 or a2 is accomplished by subtracting measurements for the upward channel and the uranium channel (or thorium channel) at approximately 30s intervals to find a set of differences. The total count channel will be used to determine whether the radioactivity is increasing or decreasing. It is necessary to first subtract the counts in the uranium channel (or thorium channel) from the total count, to reduce bias of the final result. If the total count channel indicates that the radioactivity is decreasing, the sign of both the upward and downward differences must be reversed. The value of the constant is then simply the ratio of the sum of the adjusted differences in the upward channel divided by the sum of the adjusted differences in the downward channel.

The expression for the radon component in the downward uranium window is given by:

$$Ur = \frac{u - a1U - a2T + a2bT - bu}{3au - a1 - a2aT} \qquad (4.3)$$

where: Ur is the radon background detected in the downward U window
u is the measured count in the upward uranium window
U is the measured count in the downward uranium window
T is the measured count in the downward thorium window
a1, a2, au and aT are proportionality factors and

bu and bT are constants determined experimentally.

Using the values for a1 or a2 determined above in this equation will result in a reasonable estimate of Ur, which will permit the other channels to be corrected for radon.

The measured count rates u, U and T used in equation (4.6) must first be corrected for cosmic and aircraft background. The radon counts in the total count, potassium, and thorium windows, can be calculated from Ur using equations (4.10), (4.11) and (4.12) from IAEA Report 323.

Because of the low count rate in the upward uranium window, this window must be filtered considerably to reduce statistical noise. For a system with two upward-looking detectors of volume 8.4 L, a 200 point running average should be suitable. In areas of unusually high radioactivity pulse pile-up can occur and errors will arise in the calculated value of Ur. In these areas the radon background component should not be calculated but interpolated from adjacent sections of line.

A test line was established in the survey area. Tests were carried out at the start and end of each day, and at the end of each flight. Data were acquired over a four-minute period at the nominal survey altitude (68 m). The data were then corrected for dead-time, aircraft background and cosmic activity.

The survey altitude test data were used to monitor atmospheric background and to calibrate the upward and downward looking detector systems. Variations in the uranium window can be partly due to radon but also due to soil moisture variations, or small changes in the flying height or flight path. Variations due to soil moisture and flight path errors can largely be overcome by a simple normalization procedure based on the count in the thorium window. The procedure assumes a given percentage change in thorium count from the ground will correspond to the same percentage change in the uranium counts from the ground. First, the average thorium count rate for the tests during the entire survey period is found. Then, for each test, the uranium count rate is multiplied by the average thorium count, divided by the thorium count for that flight.

Changes from flight to flight in the resulting normalized uranium count are then due to variations in radon and corrections can be determined for each flight. This procedure is described more fully in IAEA Technical Report 323.

Calculation of Effective Height AGL

The filtered radar altimeter data will be used in adjusting the stripping ratios for altitude and to carry out attenuation corrections. They are then converted to effective height (h e) at STP by the expression: (4.4)

$$he = \frac{h * 273.15}{T + 273.15} * \frac{P}{1013} \qquad (4.4)$$

where: h is the observed radar altitude
T is the measured air temperature in degrees C
P is the barometric pressure in millibars

If necessary, the pressure can be estimated from the barometric (or GPS) altitude using the expression: (4.5)

$$P = Poe^{-H/8581} \qquad (4.5)$$

where: H is the barometric (or GPS) altitude in metres
Po is the barometric pressure (at sea level) in millibars

Stripping

The stripping ratios α, β, γ, a, b and g are determined over calibration pads as described in Chapter 4 of Report 323. The principal ratios a, β and g vary with STP altitude above the ground and should be adjusted before stripping is carried out. Using the six stripping ratios, the background corrected count rates in the three windows can be stripped to give the counts in the potassium, uranium and thorium windows that originate solely from potassium, uranium and thorium. These stripped count rates are given by equations (4.44) to (4.47) in the Report.

Attenuation Correction

The background corrected total count and stripped count rates vary exponentially with aircraft altitude. Consequently, the measured count rate is related to the count rate at the nominal survey altitude by the equation: (4.6)

$$Ns = Nme^{u(ho-h)} \qquad (4.6)$$

Where: Ns is the count rate normalized to the nominal survey altitude, ho,
Nm is the background corrected, stripped count rate at STP equivalent height h,
m is the attenuation coefficient for that window.

Conversion to Apparent Radioelement Concentrations

The fully corrected count rate data is used to estimate the concentrations in the ground of each of the three radioelements, potassium, uranium and thorium. The procedure determines the concentrations that would give the observed count rates, if uniformly distributed in an infinite horizontal slab source. Because the U and Th windows actually measure ^{214}Bi and ^{208}Tl respectively, the calculation implicitly assumes radioactive equilibrium in the U and Th decay series. The U and Th concentrations are therefore expressed as equivalent concentrations, eU and eTh. The calculated potassium, uranium and thorium concentrations are determined using the expression:

$$C = N / S \qquad (4.7)$$

where: C is the concentration of element (K%, eU ppm or eTh ppm)
S is he broad source sensitivity for the window, and
N is the count rate for each window, after dead-time, background, stripping and attenuation correction.

An estimate of the air absorbed dose rate from geological sources will be made from the apparent concentrations, K%, eU ppm and eTh ppm, using the expression:

$$E = 13.1 * K + 5.67 * eU + 2.49 * eTh \qquad (4.8)$$

expressed as $nGyh^{-1}$ (nanoGray/hour)

Calculation of Radioelement Ratios

The ratios of the three radioelements (eU/eTh, eU/K and eTh/K) are frequently plotted as profiles. Due to statistical uncertainties in the individual radioelement measurements, some care must be taken in the calculation of these ratios. A common method of determining ratios is as follows:

1. Neglect any data points where the potassium concentration is less than 0.25% as these measurements are likely to be over water.

2. Progressively sum the element concentrations of adjacent points on either side of the data point until the total accumulated concentration exceeds a threshold value. This threshold is normally set to be equivalent to at least 100 counts for both the numerator and denominator.

3. Calculate the ratios using the accumulated sums. With this method, the errors associated with the calculated ratios will be similar for all data points. For contouring, the ratios can be produced directly from the gridded concentration data by ring searching to ensure both numerator and denominator exceeds the 100 count threshold as above.

Gridding

Most map products require the data to be interpolated onto a regular grid. Many of the standard gridding algorithms are unsuited to AGS data, because of the inherent statistical variations. A suitable gridding algorithm was used; one that takes the average of all data points lying within a circular or elliptical area, inversely weighted for distance from the grid point.

6. PRODUCTS

This section lists the final maps and products that have been provided under the terms of the survey agreement. Other products can be prepared from the existing dataset, if requested. These include magnetic enhancements or derivatives, digital elevation, resistivity-depth sections, inversions, or depth slices. These parameters can be displayed as colour maps or images.

Base Maps

Base maps of the survey area were produced by scanning published topographic maps to a bitmap (.bmp) format. This process provides a relatively accurate, distortion-free base that facilitates correlation of the navigation data to the map coordinate system. The topographic files were combined with geophysical data for plotting the final maps. All maps were created using the following parameters:

Projection Description:

Datum:	NAD 83		
Ellipsoid:	GRS80		
Projection:	UTM (Zone9N)		
Central Meridian:	129°W		
False Northing:	0		
False Easting:	500000		
Scale Factor:	0.9996		
WGS84 to Local Conversion:	Molodensky		
Datum Shifts:	DX: 0	DY: 0	DZ: 0

Final Products

Two sets of the following colour maps were produced on a single map sheet at a scale of 1:20,000. Flight lines and topography are shown on all map products. Digital (PDF) versions have also been included on the Final Data Archive. Preliminary and intermediate products, including digital products sent to the Consultant, are not listed.

Parameters	Blackline	Colour
EM Anomalies		2
Residual Magnetic Intensity		2
Calculated Vertical Magnetic Gradient		2
Apparent Resistivity 7200 Hz		2
Apparent Resistivity 56,000 Hz		2
Radiometrics - Air Absorbed Dose Rate		2
- %Potassium		2
- Equivalent Uranium (ppm)		2
- Equivalent Thorium (ppm)		2
eU/eTh Ratio (Digital Grids Only)		
eU/K Ratio (Digital Grids Only)		
eTh/K Ratio (Digital Grids Only)		

Additional Products

Digital Archive (see Archive Description)	1 DVD
Survey Report (+ digital PDF version)	2 copies
Flight Path Video (BIN/BDX format) with viewer	4 DVDs

7. SURVEY RESULTS

General Discussion

Table 7-1 summarizes the EM responses in the survey area, with respect to conductance grade and interpretation. For “discrete” conductors (B, D, or T), the apparent conductance and depth values shown in the EM Anomaly list appended to this report have been calculated from “local” in-phase and quadrature amplitudes of the Coaxial 5500 Hz frequency, using a near-vertical, half plane model. Conductance values for the broader (S, H, or E) types have been calculated from absolute amplitudes using a half-space model.

Wide bedrock conductors or flat-lying conductive units, (S, H, or E) whether from surficial or bedrock sources, may give rise to very broad anomalous responses on the EM profiles. These may not appear on the electromagnetic anomaly map if they have a regional character rather than a locally anomalous character. These broad conductors, which more closely approximate a half-space model, will be maximum coupled to the horizontal (coplanar) coil-pair and should be more evident on the resistivity parameters. Resistivity maps, therefore, may be more valuable than the electromagnetic anomaly maps, in areas where broad or flat-lying conductors are considered to be of importance. Contoured resistivity maps, based on the 7200 Hz and 56 kHz coplanar data, are included with this report. Resistivity grids for all three coplanar frequencies are also included on the final data archive.

The picking and interpretation procedure relies on several parameters and calculated functions. For this survey, the Coaxial 5500 Hz responses and the mid-frequency difference channels were used as two of the main picking criteria. The 7200 Hz coplanar results were also weighted to provide picks over wider or flat-dipping sources. The quadrature channels provided picks in any areas where the in-phase responses might have been suppressed by magnetite.

TABLE 7-1 EM ANOMALY STATISTICS

Porphyry Creek Property

CONDUCTOR GRADE	CONDUCTANCE RANGE SIEMENS (MHOS)	NUMBER OF RESPONSES
7	>100	0
6	50 - 100	0
5	20 - 50	2
4	10 - 20	12
3	5 - 10	31
2	1 - 5	118
1	<1	11
*	INDETERMINATE	14
TOTAL		188

CONDUCTOR MODEL	MOST LIKELY SOURCE	NUMBER OF RESPONSES
D	DISCRETE BEDROCK CONDUCTOR	22
B	DISCRETE BEDROCK CONDUCTOR	53
S	CONDUCTIVE COVER	25
H	ROCK UNIT OR THICK COVER	82
E	EDGE OF WIDE CONDUCTOR	6
L	CULTURE	0
TOTAL		188

(SEE EM MAP LEGEND FOR EXPLANATIONS)

Excellent resolution and discrimination of conductors was accomplished by using a fast sampling rate of 0.1 sec and by employing a “common” frequency (5500/7200 Hz) on two orthogonal coil-pairs (coaxial and coplanar). The resulting difference channel parameters often permit differentiation of bedrock and surficial conductors, even though they may exhibit similar conductance values. Because of the poorly conductive nature of the expected mineralization in the area, the difference calculations were based on the mid frequencies rather than the low frequencies. The lower frequencies tend to “see deeper” in conductive environments, but the higher frequencies respond better to weaker conductors and resistive units, and are probably better suited to this specific target.

Anomalies that occur near the ends of the survey lines (i.e., outside the survey area), should be viewed with caution. Some of the weaker anomalies could be due to aerodynamic noise, i.e., bird bending, which is created by abnormal stresses to which the bird is subjected during the climb and turn of the aircraft between lines. Such aerodynamic noise is usually manifested by an anomaly on the coaxial in-phase channel only, although severe stresses can affect the coplanar in-phase channels as well.

Magnetic Results

A Fugro CF-1 magnetic base station, with a Scintrex CS-3 cesium vapour sensor, was operated at the survey base to record diurnal variations of the earth's magnetic field. The clock of the base station was synchronized with that of the airborne system to permit subsequent removal of diurnal drift. A GEM Systems GSM-19T proton precession magnetometer was also operated as a backup unit

The residual magnetic field data (IGRF removed) have been presented as contours on the base map using a contour interval of 10nT where gradients permit. The map shows the magnetic properties of the rock units underlying the survey area.

The total magnetic field data have been subjected to a processing algorithm to produce maps of the calculated vertical gradient. This procedure enhances near-surface magnetic units and suppresses regional gradients. It also provides better definition and resolution of magnetic units and displays weak magnetic features that may not be clearly evident on the total field maps.

There is some evidence on the magnetic maps that suggests that the survey area has been subjected to deformation and/or alteration. These structural complexities are evident on the contour maps as variations in magnetic intensity, irregular patterns, and as offsets or changes in strike direction.

Magnetic relief over the property is moderately high, yielding a dynamic range of about 2840 nT. The local magnetic strike is generally NNW (340° ±20°) with at least two east-trending units and a prominent NE- striking linear low in the NW quadrant of the property. It is interesting to note the close correlation between the magnetic highs and the N-trending ridge of high ground that dominates the central portion of the block. This suggests that the units comprising the higher ground exhibit higher magnetic susceptibilities. These units are also more resistive than those in the valleys, but this is to be expected over areas where the magnetite contribution is greater, and/or where overburden cover is thinner. Alluvial material in the creek beds is generally more conductive. A broad, buried, non-magnetic conductive unit in the western portion of the property, yields resistivities of less than 50 ohm-m.

Several other contacts, faults, and both magnetic and non-magnetic linear trends can be inferred from the calculated vertical gradient data. Some of these lows are nearly parallel to the primary NNW magnetic strike, while others appear to intrude or intersect the regional trend. Four of the more prominent features are the inferred linear lows near anomaly 10182C (320°), west of 10232B (35°), through 10450B (338°), and possibly line 10134 at fiducial 4288 (355°). There are several other more subtle breaks or contacts that can be inferred from the CVG data. Although some of these are quite weak and of limited strike extent, they are also considered to be of potential interest as they may have influenced or controlled mineral deposition in the area.

If specific magnetic intensities can be assigned to the rock types that are believed to host the target mineralization, it may be possible to select areas of higher priority on the basis of the magnetic data. This is based on the assumption that the magnetite content of the host rocks will give rise to a limited range of contour values that will permit differentiation of various lithological units.

The magnetic results, in conjunction with the other geophysical parameters, have provided valuable information that can be used to help map the geology and structure in the survey area.

Radiometric Data

The radiometric data are self-explanatory. Although the results do not appear to be attenuated by overburden cover the lower elevations in the west, there are a few local weak Potassium or Uranium zones that appear to be mapping distinct rock types or zones of alteration, particularly on the flanks of the main topographic ridge. There is no direct correlation between resistivity/conductivity and radioelement concentrations. Nor does there appear to be any consistent relationship between the radiometric and magnetic patterns. All three parameters appear to be responding to different causative sources, or different depths of exploration. The spectrometer is restricted to the upper half-metre, the resistivity to the upper 90m or so, and the magnetic data responding primarily to the deeper basement units.

There are a few exceptions, however, particularly in the eastern 70% of the block that is dominated by higher resistivities. Most of the radioelement highs occur in this area. Some of these features could be partially due to inaccurate altitude corrections in areas of steep topography. Fault-controlled valleys can also yield higher counts that are coincident with linear magnetic lows. Some silica-rich alluvial deposits can yield (thorium) highs. Younger sediments within the valleys will be more closely related to the rock types from which they were derived.

Apparent Resistivity

Apparent resistivity grids, which display the conductive properties of the survey area, were produced from the 900 Hz, 7200 Hz, and 56,000 Hz coplanar data. The maximum resistivity values, which are calculated for each frequency, are 1,300, 8,400, and 30,000 ohm-m respectively. These cut-offs eliminate the erratic higher resistivities that would result from unstable ratios of very small EM amplitudes.

There are several gaps in coverage evident on the resistivity maps. These are due to a combination of flight path breaks and/or high flying over areas of severe topography for reasons of safety.. The EM system is out of ground effect above 150 m, so no resistivities are calculated above this height, as evidenced by the blank areas in the central and south areas. Some of these gaps could be minimized by relaxing the interline gridding limits, but it is better to leave the gaps in, to indicate where there is no valid coverage.

In general, the resistivity patterns show moderately good correlation with topography and poor agreement with magnetic trends. This suggests that some of the resistivity lows are probably related to conductive alluvial cover, rather than bedrock features, and that the magnetic parameter is responding to changes in the bedrock structure and lithology. A few of the resistivity highs are at least partially due to the effects of magnetite suppression.

The changes in the composition of the upper layers are more evident on the higher frequencies, and the 56 kHz resistivity parameter should therefore help to map resistive quartz-rich units near surface, unless they are masked by conductive cover. Narrow resistivity highs on the 56 kHz maps should be investigated, as they could reflect quartz-vein type intrusions that could host polymetallic or auriferous mineralization. The broader resistivity highs that are evident on many of the profiles, could be due to siliceous caps, large porphyritic intrusions, or frozen ground, but could also reflect an absence of overburden cover.

There are other resistivity lows in the area, many of which appear to be stronger on the (deeper) 900 Hz frequency. Note the highly conductive units that dominate the western portion of the property. This suggests the presence of a second layer that is often more conductive than the weathered upper layer(s). This second layer is quite extensive and is probably not an exploration target, unless it can be determined that this buried unit could also host economic mineralization. However, attention may be focused on areas where this zone appears to be faulted or folded, or where anomaly characteristics differ along strike. These highly conductive units are generally non-magnetic, and could therefore represent conductive (graphitic) shales. The more conductive portions have been outlined on the EM Anomaly Map as Zones A through I. The zone outlines approximate the 100 ohm-m contour from the 7200 Hz resistivity parameter.

Electromagnetic Anomalies

It is highly unlikely that auriferous quartz-rich units would show as discrete conductors in this environment, unless they were associated with highly-altered, porous shears or faults, or were associated with appreciable amounts of conductive clays, graphite or sulphides. However, EM anomalies were picked and interpreted for this survey area, in an attempt to locate some of the controlling shears or faults that might be conductive enough to yield discrete responses, and to detect any conductive polymetallic zones or sulphide mineralization that might exist on the property.

The EM anomalies resulting from this survey appear to fall within one of three general categories. The first type consists of discrete, well-defined anomalies that yield marked inflections on the difference channels. These anomalies are usually attributed to conductive sulphides or graphite and are generally given a "B", "T" or "D" interpretive symbol, denoting a bedrock source. Roughly 40% of the anomalous EM responses fall into this category.

The second class of anomalies comprises moderately broad responses that exhibit the characteristics of a half-space and do not yield well-defined inflections on the difference channels. This group comprises approximately 60% of the anomalies detected by the survey. Anomalies in this category are usually given an "S" or "H" interpretive symbol. The “S” denotes a conductive layer at surface while the “H” indicates a conductive half-space or a buried half-space beneath more resistive cover.

The lack of a difference channel response usually implies a broad or flat-lying conductive source such as overburden, clays, or buried flat-dipping bedrock units.. Some of these anomalies could reflect zones of deep weathering or alteration plugs, both of which can yield “non-discrete” signatures. Although these flat-dipping sources may not yield “discrete” EM anomalies, they are maximum-coupled to the coplanar coils, and will be clearly displayed on the resistivity parameters.

The effects of conductive overburden are evident over portions of the survey area, particularly in the west. Although the difference channels (DIFI and DIFQ) are extremely valuable in detecting bedrock conductors that are partially masked by conductive overburden, sharp undulations in the terrain, or in the bedrock/overburden interface, can yield anomalies in the difference channels that may be interpreted as possible bedrock conductors. Such anomalies usually fall into the "S?" or "B?" classification but may also be given an "E" interpretive symbol, denoting a resistivity contrast at the edge of a conductive unit.

The "?" symbol does not question the validity of an anomaly, but instead indicates some degree of uncertainty as to which is the most appropriate EM source model. This ambiguity results from the combination of effects from two or more conductive sources, such as overburden and bedrock, gradational changes, moderately shallow dips or suspected contributions from culture. The presence of a conductive upper layer has a tendency to mask or alter the characteristics of bedrock conductors, making interpretation difficult. This problem is further exacerbated in the presence of magnetite.

Magnetite can cause suppression or polarity reversals of the in-phase components, particularly at the lower frequencies in resistive areas. The effects of magnetite-rich rock units are usually evident on the multi-parameter geophysical data profiles as negative excursions of the lower frequency in-phase channels. Magnetite effects occur on several lines, particularly in the magnetic/resistive central portion. Line 10081 is one such example, where the 900 Hz in-phase is negative.

In areas where EM responses are evident primarily on the quadrature components, zones of poor conductivity are indicated. Where these responses are coincident with magnetic anomalies, it is possible that the in-phase component amplitudes have been suppressed by the effects of magnetite. Poorly conductive magnetic features can give rise to resistivity anomalies that are only slightly below or slightly above background. If it is expected that poorly-conductive economic mineralization could be associated with magnetite-rich units, most of these weakly anomalous features will be of interest. In areas where magnetite causes the in-phase components to become negative, the apparent conductance and depth of EM anomalies will be unreliable. Magnetite effects usually give rise to overstated (higher) resistivity values and understated (shallow) depth calculations.

The electromagnetic anomaly maps show the anomaly locations with the interpreted conductor type, dip, conductance and depth being indicated by symbols. Direct magnetic correlation is also shown if it exists. An attempt has been made to show the strike direction and length of the (possible bedrock) conductors on the EM Anomaly map, only where the anomalies can be correlated from line to line with a reasonable degree of confidence. These conductors are the most likely to be caused by increases in sulphide content.

Potential Targets in the Survey Area

Previous work has confirmed the presence of polymetallic mineralization on the property, in addition to two past producers in the area. Potential targets within the area are expected to be associated with non-conductive quartz-rich vein systems that are probably non-magnetic. It is impractical, therefore, to assess the relative merits of EM anomalies on the basis of conductance. As is common with many gold or polymetallic exploration projects, an "indirect" approach, using the magnetic/resistivity/radiometric data to define zones of favourable structure, will likely yield more meaningful results. The geophysical data should be carefully analysed to locate the more favourable areas for further investigation on the ground.

The Sultana occurrence is reportedly located near UTM 593130 E, 6106855 N. If these coordinates are accurate, that would place it close to fiducial 2174 on survey line 10380. An attempt to determine the geophysical "signature" over the known Sultana mineralization shows a weak, poorly defined EM anomaly (10380A) that has been attributed to a near surface conductor. The EM anomaly is part of moderately broad, weakly conductive (<600 ohm-m) zone at surface, which is approximately 500 m x 1.1 km. This conductive unit is flanked on the ENE by an oblate resistivity high (>15,000 ohm-m). The Sultana occurrence also appears to lie in close proximity to a (faulted) magnetic contact that strikes 93°, along the southern edge of three small blocks of magnetic material. Immediately west of this location, there is a second linear break that can be inferred from the CVG data, striking 343° through fiducial 2177, almost parallel to tie line 19075.

The inferred structure derived from the vertical magnetic gradient should help to define other similarly zones that are structurally controlled. The presence of the broad, moderately conductive zone could also be significant, if it can be directly related to the rock unit (fractured granodiorite?) that hosts the Sultana mineralization. There is no clearly defined radioelement signature, but there is a moderate total count high about 800 m to the north and northwest. If the line/fiducial location for this zone is accurate, the data suggest that it yields a subtle EM response in a broad, moderate resistivity low, near an inferred faulted magnetic contact. These characteristics may be distinctive enough to allow them to be used as criteria to directly locate other similarly mineralized zones on the property, or at least to help identify some of the more favourable areas for exploration.

Conversely, narrow resistive units seen primarily on the 56 kHz frequency could reflect intrusive dykes, while larger, circular highs, could possibly represent porphyritic units. These “non-conductive” areas are also considered to be of interest, particularly around their perimeter or where they appear to be structurally deformed..

The EM Anomaly map shows several sources of bedrock conductivity that are considered to be of interest if the property has the potential to host sulphide deposits. The possible “discrete” bedrock conductors have been colour-coded on the EM Anomaly map, with thin sources (<5 m) shown in Red. and possible bedrock conductors in dark Blue. Surficial (S) and buried half-space layers (H) are in light Green, while Edge effects (E) are light Grey. The colour scheme permits quick identification of the more interesting bedrock type responses detected in the area. As mentioned previously, many of these apparent bedrock anomalies could be due to broad, flat-dipping conductive (shale) units that might be formational in nature. If any of these responses occur in areas of favourable geology or geochemistry, it is recommended that they be given a higher priority.

The following table lists just a few of the possible bedrock sources that might reflect near vertical shears, conductive clays or shales, or sources of possible sulphide-type mineralization. These are considered to be the more attractive geophysical responses, based on favourable structure, magnetic association, conductance, length, or depth extent.

Anomaly	Type	Mag	Comments

Anomaly	Type	Mag	Comments
10110B 10110C	D D	7 -	These two thin sources occur near the south contact of a moderate magnetic high. They are located on a south-facing slope, near the eastern limb of a moderate resistivity low. Anomaly 10110C suggests a possible westerly dip, while 10110B is nearly vertical. The latter exhibits a very weak magnetic correlation.
10124A 10154A 10154B	B? D D	85 46 -	Anomaly 10124A occurs at the northern end of a 600 m-long, south-trending conductor, that extends to 10154B. This strong, thin, west-dipping conductor is associated with a S-trending magnetic unit, and is likely due to conductive magnetic sulphides such as pyrrhotite. This attractive (sulphide) target occurs along the ridge of Red Rose Peak. Anomalies 10154A and 10154B, at the south end, could reflect two thin sources, or the edges of a single (80 m) thick source. The significance of this conductor is enhanced by its proximity to the old Red Rose mine, about 600 m to the west. Further investigation is recommended is this has not already been done.
10140C 10162B 10162D 10162E 10162F 10172D 10182C 10202C 10212B 10222A	B H D D B D D D B B	- - 23 8 23 - - - 12 10	With the possible exception of 10202D, all of the anomalies in this group are associated with a large resistivity low shown on the EM map as Zone A. A few of these anomalies yield weak magnetic correlation, while others, such as 10162B, suggest a broad, buried, highly conductive, non-magnetic half-space. At the north end, there are at least four separate, south-striking conductors of moderately short strike length through anpmalies 10162D-G. The strong thin responses at 10162D, 10182C, and 10202C, all suggest steep easterly dips that occur near a magnetic contact, The latter anomaly (10202C) is located near the intersection of two inferred faults or non-magnetic dyke-like intrusions that strike NE and NW. Anomalies 10212B and 10222A, in the southwest, are also magnetic. The magnetic sources in Zone A may be of interest, in addition to those that are related to faults or contacts. Zone A remains open to the west.
10160A 10160B 10170A 10190D	B B B B	- 28 77 -	The anomalies in this group occur in the northeast quadrant, north of Boulder Creek. The first three anomalies form a 600 m-long SSE-trending (157°) resistivity low, near the eastern flank of a magnetic high. Anomalies 10190C and D, about 800 m to the ESE, are in the Boulder Creek valley, which gives rise to a separate, larger resistivity low that is open to the east.

Anomaly	Type	Mag	Comments
10250A	H	-	This broad response is in Zone B, a highly conductive, non-magnetic buried unit that is open to the west. Low priority.
10243B 10250D	H B?	168 169	Zone C is a circular resistivity low that coincides with an interesting magnetic high. The north end of this moderately broad SSE-trending magnetic conductor abuts a prominent dyke-like magnetic low that strikes NE. Additional work may be required to check the causative source of this zone.
10260B 10260C	B D	- 28	These two anomalies comprise Zone D, which abuts the same dyke-like magnetic low that strikes SW from Zone C. Anomaly 10260C suggests a possible thin source that is contact related. A 400 m dextral offset can be inferred from the CVG data through fiducial 3564 on line 10260C.
10260D 10271B	H B?	- 28	These two anomalies are associated with Zone E, a small oblate resistivity low. The northern anomaly coincides with a subtle magnetic low, while the southern response is on a relative magnetic high. The two EM anomalies are probably due to different causative sources.
10301B 10301C 10311B 10311D 10350A 10340B 10340C	D D D D D B B	55 11 - - - 13 -	Zone F is a large, highly conductive unit that hosts several discrete sources. The four S-trending conductors in the north are nearly parallel. The unit is generally non-magnetic, except in the north, near 10301B, where a lobe of magnetic material strikes south to line 10330. At least seven strong responses have been attributed to thin bedrock sources, with 10301C indicating a probable dip to the east. Anomalies 10340B and C both yield very strong resistivity lows of less than 2 ohm-m. High flying has precluded resistivity calculations to the SE, so the limits of Zone F are not defined in this area. The zone remains open at depth, beyond the west end of line 10370.
10340D	D	-	Zone G is a small incomplete resistivity low that hosts a thin source at 10340D. The anomaly is located in a S-trending magnetic low, just west of a magnetic contact.
10403			Not a conductor, but there is a very small magnetic high on a topographic high at fiducial 2465 on this line.
10430A 10455A 10455B	D B D	15 - -	These three anomalies are located near the north edge of Zone H, part of a non-magnetic resistivity low that follows the ESE-trending Brian Boru Creek valley.

Anomaly	Type	Mag	Comments
10444D	B	8	This anomaly at the end of line 10440 is incomplete, and yields a partial resistivity shown as Zone I. It is part of the same SSE-trending magnetic feature observed on line 10403.

The foregoing text describes some of the anomalous responses that are representative of possible and probable bedrock conductors in the survey area. There are many other conductive responses in the survey block that have not been discussed. Most have been attributed to overburden or large, buried conductive layers that are considered to be of little interest unless they are related to structural breaks, alteration zones, or areas of favourable geology.

In the search for quartz-vein hosted polymetallic or auriferous mineralization, the value of EM conductors may be of little importance, unless the mineralization is associated with conductive material such as sulphides, conductive shears or faults, alteration products, or magnetite-rich zones. Although several attractive, highly conductive sources have been detected by the survey , resistive zones may actually be of greater significance in this area,, particularly if the host rocks are siliceous. On the Porphyry Creek property, the magnetic parameter appears to have been an effective tool in delineating rock units and zones of structural deformation. However, the causative sources of the numerous conductive and resistive units should also be checked.

8. CONCLUSIONS AND RECOMMENDATIONS

This report provides a very brief description of the survey results and describes the equipment, data processing procedures and logistics of the Porphyry Creek Property survey.

The various maps included with this report display the magnetic, radiometric, and conductive properties of the survey area. It is recommended that a complete assessment and detailed evaluation of the survey results be carried out, in conjunction with all available geophysical, geological and geochemical information.

There are 188 EM anomalies in the survey block, many of which are typical of sulphide or graphite responses. Many of these may warrant additional work but some of the larger flat-dipping zones in the west are not considered to be attractive exploration targets unless it can be demonstrated that mineralization in this area is associated with appreciable amounts of conductive sulphides. The resistivity maps have defined several zones that appear to reflect variations in both the near-surface layers and in the deeper underlying units. More significant, perhaps, are the many resistive units on the property that could represent possible siliceous intrusions or quartz-vein type mineralization. Both resistive and conductive responses could prove to be potential targets in this area, even though they may be weak or poorly defined.

Most anomalies in the area are moderately broad and often poorly defined. Some have been attributed to conductive overburden or deep weathering, although several are associated with buried conductive rock units. Others coincide with magnetic gradients that may reflect contacts, faults or shears. Such structural breaks are considered to be of particular interest as they may have influenced or controlled mineral deposition within the survey area.

The EM and resistivity data have been seriously affected by severe topographic variations that have led to several gaps in resistivity coverage. Excessively high flying over some of the steeper ravines has yielded secondary EM fields that are of insufficient amplitudes to yield reliable resistivity calculations. Although the magnetic data are relatively immune to changes in flying height, the radiometric data may also be adversely affected by erroneous altitude corrections.

If the location is correct, the survey lines over the Sultana occurrence (reportedly near Line 10380 at fiducial 2172) have yielded subtle signatures that might be used to help locate other similarly mineralized zones on the Porphyry Creek Property. The moderately weak EM response is near the eastern edge of a broad resistivity low that has been attributed primarily to surficial conductivity, but which could reflect the fractured granodiorite host unit. The mineralization appears to be located near the southern (faulted) contact of a small magnetic unit. The magnetic results, therefore, might be more useful than the EM/resistivity parameter, to locate the more favourable structures, contacts, and geological units that are more likely to host the quartz-vein type mineralization.

The resistive anomalies, as well as the interpreted bedrock conductors defined by the survey, should be subjected to further investigation, using appropriate surface exploration techniques. Anomalies that are currently considered to be of moderately low priority may require upgrading if follow-up results are favourable.

The radioelement ratio grids are considered to be more valuable than the equivalent radioelement parameters, because they tend to minimize amplitude changes due to variations in overburden thickness and flying heights. Ratios can also help to enhance or isolate the contributions from one element relative to the others, in areas of higher background concentrations.

Respectfully submitted,

FUGRO AIRBORNE SURVEYS CORP.

R_10037

APPENDIX A

LIST OF PERSONNEL

The following personnel were involved in the acquisition, processing, interpretation and presentation of data, relating to a DIGHEM^{V} airborne geophysical survey carried out for Duncastle Gold Corp., over the Porphyry Creek Property, near New Hazleton, B.C. The survey consisted of 495 km of coverage, flown from July 9 to July 19, 2010.

Aaron Rampersand	Geophysical Equipment Operator
Henry She	Geophysical Equipment Operator
Amir Soltanzadeh	Data Processor/ Crew Leader
Richardo White	Geophysical Data Processor
Lyn Vanderstarren	Drafting Supervisor
Greg Charbonneau	Pilot (Great Slave Helicopters Ltd.)

All personnel are employees of Fugro Airborne Surveys, except for the pilot who is an employee of Great Slave Helicopters Ltd.

APPENDIX B

Processing Flow Chart - Electromagnetic Data

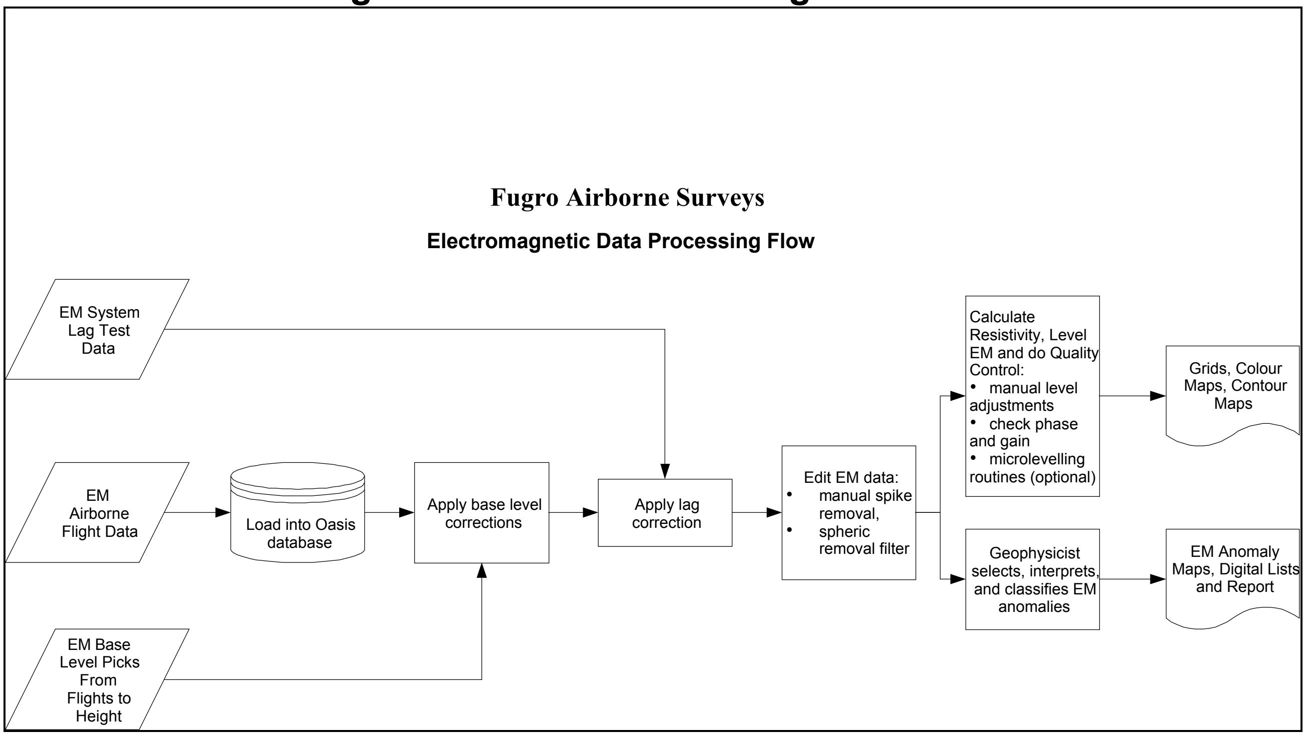

Processing Flow Chart - Magnetic Data

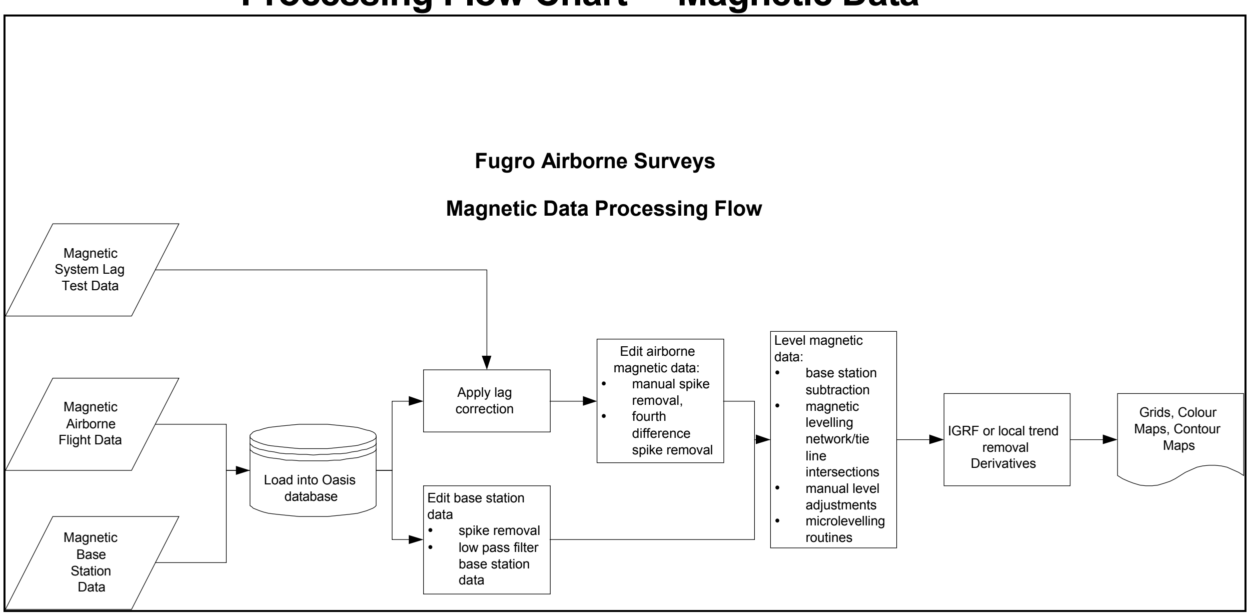

BACKGROUND INFORMATION

Electromagnetics

Fugro electromagnetic responses fall into two general classes, discrete and broad. The discrete class consists of sharp, well-defined anomalies from discrete conductors such as sulphide lenses and steeply dipping sheets of graphite and sulphides. The broad class consists of wide anomalies from conductors having a large horizontal surface such as flatly dipping graphite or sulphide sheets, saline water-saturated sedimentary formations, conductive overburden and rock, kimberlite pipes and geothermal zones. A vertical conductive slab with a width of 200 m would straddle these two classes.

The vertical sheet (half plane) is the most common model used for the analysis of discrete conductors. The following section entitled **Discrete Conductor Analysis** describes this model in detail, including the effect of using it on anomalies caused by broad conductors such as conductive overburden.

The conductive earth (half-space) model is more suitable for broad conductors that carry an S, H, or E type interpretation symbol. Conductance values for these anomalous responses are based on the absolute amplitudes of the selected coplanar channels. Resistivity maps result from the use of this model. A later section entitled **Resistivity Mapping** describes the method further.

Geometric Interpretation

The geophysical interpreter attempts to determine the geometric shape and dip of the conductor. Figure C-1 shows typical HEM anomaly shapes, which are used to guide the geometric interpretation.

Discrete Conductor Analysis

The EM anomalies appearing on the electromagnetic map are analyzed by computer to give the conductance (i.e., conductivity-thickness product) in siemens (mhos). The B, D, and T type calculations are based on a vertical sheet model or a horizontal sheet model, depending on the interpreted anomaly symbol. This is not an unreasonable procedure, because the computed conductance increases as the electrical quality of the conductor increases, regardless of its true shape. HEM anomalies are divided into seven grades of conductance, as shown in Table C-1. The conductance in siemens (mhos) is the reciprocal of resistance in ohms.

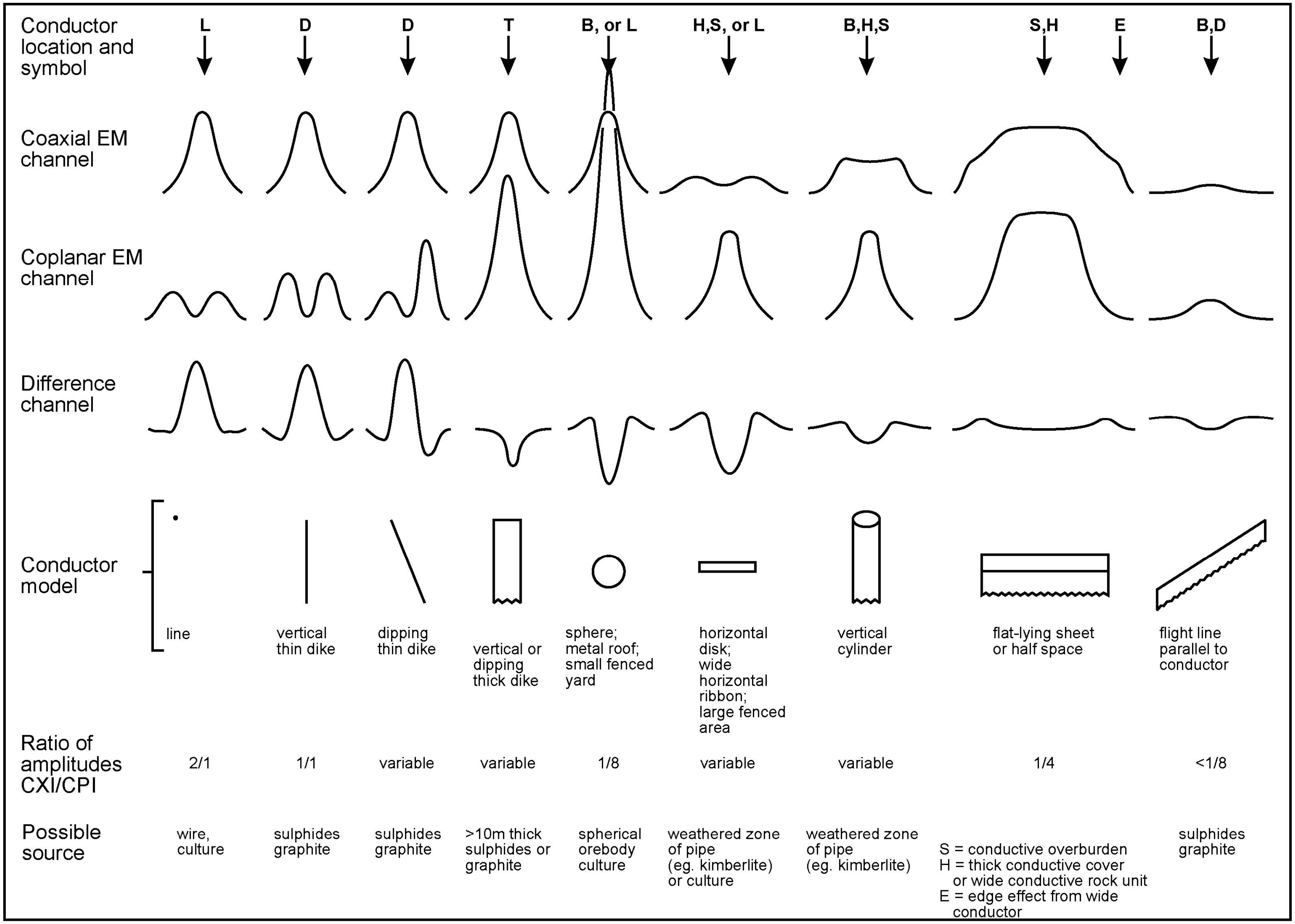

Typical HEM anomaly shapes
Figure C-1

The conductance value is a geological parameter because it is a characteristic of the conductor alone. It generally is independent of frequency, flying height or depth of burial, apart from the averaging over a greater portion of the conductor as height increases. Small anomalies from deeply buried strong conductors are not confused with small anomalies from shallow weak conductors because the former will have larger conductance values.

Table C-1. EM Anomaly Grades

Anomaly Grade	Siemens
7	> 100
6	50 - 100
5	20 - 50
4	10 - 20
3	5 - 10
2	1 - 5
1	< 1

Conductive overburden generally produces broad EM responses which may not be shown as anomalies on the geophysical maps. However, patchy conductive overburden in otherwise resistive areas can yield discrete anomalies with a conductance grade (cf. Table C-1) of 1, 2 or even 3 for conducting clays which have resistivities as low as 50 ohm-m. In areas where ground resistivities are below 10 ohm-m, anomalies caused by weathering variations and similar causes can have any conductance grade. The anomaly shapes from the multiple coils often allow such conductors to be recognized, and these are indicated by the letters S, H, and sometimes E on the geophysical maps (see EM legend on maps).

For bedrock conductors, the higher anomaly grades indicate increasingly higher conductances. Examples: the New Insco copper discovery (Noranda, Canada) yielded a grade 5 anomaly, as did the neighbouring copper-zinc Magusi River ore body; Mattabi (copper-zinc, Sturgeon Lake, Canada) and Whistle (nickel, Sudbury, Canada) gave grade 6; and the Montcalm nickel-copper discovery (Timmins, Canada) yielded a grade 7 anomaly. Graphite and sulphides can span all grades but, in any particular survey area, field work may show that the different grades indicate different types of conductors.

Strong conductors (i.e., grades 6 and 7) are characteristic of massive sulphides or graphite. Moderate conductors (grades 4 and 5) typically reflect graphite or sulphides of a less massive character, while weak bedrock conductors (grades 1 to 3) can signify poorly connected graphite or heavily disseminated sulphides. Grades 1 and 2 conductors may not respond to ground EM equipment using frequencies less than 2000 Hz.

The presence of sphalerite or gangue can result in ore deposits having weak to moderate conductances. As an example, the three million ton lead-zinc deposit of Restigouche Mining Corporation near Bathurst, Canada, yielded a well-defined grade 2 conductor. The 10 percent by volume of sphalerite occurs as a coating around the fine grained massive pyrite, thereby inhibiting electrical conduction. Faults, fractures and shear zones may produce anomalies that typically have low conductances (e.g., grades 1 to 3). Conductive rock formations can yield anomalies of any conductance grade. The conductive materials in such rock formations can be salt water, weathered products such as clays, original depositional clays, and carbonaceous material.

For each interpreted electromagnetic anomaly on the geophysical maps, a letter identifier and an interpretive symbol are plotted beside the EM grade symbol. The EM grade symbols will usually be discernible, but any obliterated information can be obtained from the anomaly listing appended to this report.

The conductance measurement is considered more reliable than the depth estimate. There are a number of factors that can produce an error in the depth estimate, including the averaging of topographic variations by the altimeter, overlying conductive overburden, and the location and attitude of the conductor relative to the flight line. Conductor location and attitude can provide an erroneous depth estimate because the stronger part of the conductor may be deeper or to one side of the flight line, or because it has a shallow dip. A heavy tree cover can also produce errors in depth estimates. This is because the depth estimate is computed as the distance of bird from conductor, minus the altimeter reading. The altimeter can lock onto the top of a dense forest canopy. This situation yields an erroneously large depth estimate but does not affect the conductance estimate.

Dip symbols are used to indicate the direction of dip of conductors. These symbols are used only when the anomaly shapes are unambiguous, which usually requires a fairly resistive environment.

A further interpretation is presented on the EM map by means of the line-to-line correlation of bedrock anomalies, which is based on a comparison of anomaly shapes on adjacent lines. This provides conductor axes that may define the geological structure over portions of the survey area. The absence of conductor axes in an area implies that anomalies could not be correlated from line to line with reasonable confidence.

The electromagnetic anomalies are designed to provide a correct impression of conductor quality by means of the conductance grade symbols. The symbols can stand alone with geology when planning a follow-up program. The actual conductance values are printed in the attached anomaly list for those who wish quantitative data. The EM map provides an interpretation of conductors in terms of length, strike and dip, geometric shape, conductance, and thickness. The accuracy is comparable to an interpretation from a high quality ground EM survey having the same line spacing.

The appended EM anomaly list provides a tabulation of anomalies in ppm, conductance, and depth for the vertical sheet or horizontal sheet models. The vertical sheet model (B, D, and T types) uses the local coaxial amplitudes for the calculation. Values for the horizontal sheet model (S, H, and E types) are calculated from the absolute amplitudes of the selected coplanar channels. No conductance or depth estimates are shown for weak anomalous responses that are not of sufficient amplitude to yield reliable calculations, or where magnetite effects have caused negative in-phase responses.

Questionable Anomalies

The EM maps may contain anomalous responses that are displayed as asterisks (*). These responses denote weak anomalies of indeterminate conductance, which may reflect one of the following: a weak conductor near the surface, a strong conductor at depth (e.g., 100 to 120 m below surface) or to one side of the flight line, or aerodynamic noise. Those responses that have the appearance of valid bedrock anomalies on the flight profiles are indicated by appropriate interpretive symbols (see EM legend on maps). The others probably do not warrant further investigation unless their locations are of considerable geological interest.

The Thickness Parameter

A comparison of coaxial and coplanar shapes can provide an indication of the thickness of a steeply dipping conductor. The amplitude of the coplanar anomaly (e.g., CPI channel) increases relative to the coaxial anomaly (e.g., CXI) as the apparent thickness increases, i.e., the thickness in the horizontal plane. (The thickness is equal to the conductor width if the conductor dips at 90 degrees and strikes at right angles to the flight line.) This report refers to a conductor as thin when the thickness is likely to be less than 5 m, and thick when in excess of 10 m. Thick conductors are indicated on the EM map by parentheses "( )". For base metal exploration in steeply dipping geology, thick conductors can be high priority targets because many massive sulphide ore bodies are thick. The system cannot sense the thickness when the strike of the conductor is subparallel to the flight line, when the conductor has a shallow dip, when the anomaly amplitudes are small, or when the resistivity of the environment is below 100 ohm-m.

Resistivity Mapping

Resistivity mapping is useful in areas where broad or flat lying conductive units are of interest. One example of this is the clay alteration which is associated with Carlin-type deposits in the south west United States. The resistivity parameter was able to identify the clay alteration zone over the Cove deposit. The alteration zone appeared as a strong resistivity low on the 900 Hz resistivity parameter. The 7,200 Hz and 56,000 Hz resistivities showed more detail in the covering sediments, and delineated a range front fault. This is typical in many areas of the south west United States, where conductive near surface sediments, which may sometimes be alkalic, attenuate the higher frequencies.

Resistivity mapping has proven successful for locating diatremes in diamond exploration. Weathering products from relatively soft kimberlite pipes produce a resistivity contrast with the unaltered host rock. In many cases weathered kimberlite pipes were associated with thick conductive layers that contrasted with overlying or adjacent relatively thin layers of lake bottom sediments or overburden.

Areas of widespread conductivity are commonly encountered during surveys. These conductive zones may reflect alteration zones, shallow-dipping sulphide or graphite-rich units, saline ground water, or conductive overburden. In such areas, EM amplitude changes can be generated by decreases of only 5 m in survey altitude, as well as by increases in conductivity. The typical flight record in conductive areas is characterized by in-phase and quadrature channels that are continuously active. Local EM peaks reflect either increases in conductivity of the earth or decreases in survey altitude. For such conductive areas, apparent resistivity profiles and contour maps are necessary for the correct interpretation of the airborne data. The advantage of the resistivity parameter is that anomalies caused by altitude changes are virtually eliminated, so the resistivity data reflect only those anomalies caused by conductivity changes. The resistivity analysis also helps the interpreter to differentiate between conductive bedrock and conductive overburden. For example, discrete conductors will generally appear as narrow lows on the contour map and broad conductors (e.g., overburden) will appear as wide lows.

The apparent resistivity is calculated using the pseudo-layer (or buried) half-space model defined by Fraser (1978)[6]. This model consists of a resistive layer overlying a conductive half-space. The depth channels give the apparent depth below surface of the conductive material. The apparent depth is simply the apparent thickness of the overlying resistive layer. The apparent depth (or thickness) parameter will be positive when the upper layer is more resistive than the underlying material, in which case the apparent depth may be quite close to the true depth.

The apparent depth will be negative when the upper layer is more conductive than the underlying material, and will be zero when a homogeneous half-space exists. The apparent depth parameter must be interpreted cautiously because it will contain any errors that might exist in the measured altitude of the EM bird (e.g., as caused by a dense tree cover). The inputs to the resistivity algorithm are the in-phase and quadrature components of the coplanar coil-pair. The outputs are the apparent resistivity of the conductive half-space (the source) and the sensor-source distance. The flying height is not an input variable, and the output resistivity and sensor-source distance are independent of the flying height when the conductivity of the measured material is sufficient to yield significant in-phase as well as quadrature responses. The apparent depth, discussed above, is simply the sensor-source distance minus the measured altitude or flying height. Consequently, errors in the measured altitude will affect the apparent depth parameter but not the apparent resistivity parameter.

The apparent depth parameter is a useful indicator of simple layering in areas lacking a heavy tree cover. Depth information has been used for permafrost mapping, where positive apparent depths were used as a measure of permafrost thickness. However, little

[6] Resistivity mapping with an airborne multicoil electromagnetic system: Geophysics, v. 43, p.144-172

quantitative use has been made of negative apparent depths because the absolute value of the negative depth is not a measure of the thickness of the conductive upper layer and, therefore, is not meaningful physically. Qualitatively, a negative apparent depth estimate usually shows that the EM anomaly is caused by conductive overburden. Consequently, the apparent depth channel can be of significant help in distinguishing between overburden and bedrock conductors.

Interpretation in Conductive Environments

Environments having low background resistivities (e.g., below 30 ohm-m for a 900 Hz system) yield very large responses from the conductive ground. This usually prohibits the recognition of discrete bedrock conductors. However, Fugro data processing techniques produce three parameters that contribute significantly to the recognition of bedrock conductors in conductive environments. These are the in-phase and quadrature difference channels (DIFI and DIFQ, which are available only on systems with “common” frequencies on orthogonal coil pairs), and the resistivity and depth channels (RES and DEP) for each coplanar frequency.

The EM difference channels (DIFI and DIFQ) eliminate most of the responses from conductive ground, leaving responses from bedrock conductors, cultural features (e.g., telephone lines, fences, etc.) and edge effects. Edge effects often occur near the perimeter of broad conductive zones. This can be a source of geologic noise. While edge effects yield anomalies on the EM difference channels, they do not produce resistivity anomalies. Consequently, the resistivity channel aids in eliminating anomalies due to edge effects. On the other hand, resistivity anomalies will coincide with the most highly conductive sections of conductive ground, and this is another source of geologic noise. The recognition of a bedrock conductor in a conductive environment therefore is based on the anomalous responses of the two difference channels (DIFI and DIFQ) and the resistivity channels (RES). The most favourable situation is where anomalies coincide on all channels.

The DEP channels, which give the apparent depth to the conductive material, also help to determine whether a conductive response arises from surficial material or from a conductive zone in the bedrock. When these channels ride above the zero level on the depth profiles (i.e., depth is negative), it implies that the EM and resistivity profiles are responding primarily to a conductive upper layer, i.e., conductive overburden. If the DEP channels are below the zero level, it indicates that a resistive upper layer exists, and this usually implies the existence of a bedrock conductor. If the low frequency DEP channel is below the zero level and the high frequency DEP is above, this suggests that a bedrock conductor occurs beneath conductive cover.

Reduction of Geologic Noise

Geologic noise refers to unwanted geophysical responses. For purposes of airborne EM surveying, geologic noise refers to EM responses caused by conductive overburden and magnetic permeability. It was mentioned previously that the EM difference channels (i.e., channel DIFI for in-phase and DIFQ for quadrature) tend to eliminate the response of conductive overburden.

Magnetite produces a form of geological noise on the in-phase channels. Rocks containing less than 1% magnetite can yield negative in-phase anomalies caused by magnetic permeability. When magnetite is widely distributed throughout a survey area, the in-phase EM channels may continuously rise and fall, reflecting variations in the magnetite percentage, flying height, and overburden thickness. This can lead to difficulties in recognizing deeply buried bedrock conductors, particularly if conductive overburden also exists. However, the response of broadly distributed magnetite generally vanishes on the in-phase difference channel DIFI. This feature can be a significant aid in the recognition of conductors that occur in rocks containing accessory magnetite.

EM Magnetite Mapping

The information content of HEM data consists of a combination of conductive eddy current responses and magnetic permeability responses. The secondary field resulting from conductive eddy current flow is frequency-dependent and consists of both in-phase and quadrature components, which are positive in sign. On the other hand, the secondary field resulting from magnetic permeability is independent of frequency and consists of only an in-phase component which is negative in sign. When magnetic permeability manifests itself by decreasing the measured amount of positive in-phase, its presence may be difficult to recognize. However, when it manifests itself by yielding a negative in-phase anomaly (e.g., in the absence of eddy current flow), its presence is assured. In this latter case, the negative component can be used to estimate the percent magnetite content.

A magnetite mapping technique, based on the low frequency coplanar data, can be complementary to magnetometer mapping in certain cases. Compared to magnetometry, it is far less sensitive but is more able to resolve closely spaced magnetite zones, as well as providing an estimate of the amount of magnetite in the rock. The method is sensitive to 1/4% magnetite by weight when the EM sensor is at a height of 30 m above a magnetitic half-space. It can individually resolve steep dipping narrow magnetite-rich bands which are separated by 60 m. Unlike magnetometry, the EM magnetite method is unaffected by remanent magnetism or magnetic latitude.

The EM magnetite mapping technique provides estimates of magnetite content which are usually correct within a factor of 2 when the magnetite is fairly uniformly distributed. EM magnetite maps can be generated when magnetic permeability is evident as negative in-phase responses on the data profiles.

Like magnetometry, the EM magnetite method maps only bedrock features, provided that the overburden is characterized by a general lack of magnetite. This contrasts with resistivity mapping which portrays the combined effect of bedrock and overburden.

The Susceptibility Effect

When the host rock is conductive, the positive conductivity response will usually dominate the secondary field, and the susceptibility effect[7] will appear as a reduction in the in-phase, rather than as a negative value. The in-phase response will be lower than would be predicted by a model using zero susceptibility. At higher frequencies the in-phase conductivity response also gets larger, so a negative magnetite effect observed on the low frequency might not be observable on the higher frequencies, over the same body. The susceptibility effect is most obvious over discrete magnetite-rich zones, but also occurs over uniform geology such as a homogeneous half-space.

High magnetic susceptibility will affect the calculated apparent resistivity, if only conductivity is considered. Standard apparent resistivity algorithms use a homogeneous half-space model, with zero susceptibility. For these algorithms, the reduced in-phase response will, in most cases, make the apparent resistivity higher than it should be. It is important to note that there is nothing wrong with the data, nor is there anything wrong with the processing algorithms. The apparent difference results from the fact that the simple geological model used in processing does not match the complex geology.

Measuring and Correcting the Magnetite Effect

Theoretically, it is possible to calculate (forward model) the combined effect of electrical conductivity and magnetic susceptibility on an EM response in all environments. The difficulty lies, however, in separating out the susceptibility effect from other geological effects when deriving resistivity and susceptibility from EM data.

Over a homogeneous half-space, there is a precise relationship between in-phase, quadrature, and altitude. These are often resolved as phase angle, amplitude, and altitude. Within a reasonable range, any two of these three parameters can be used to calculate the half space resistivity. If the rock has a positive magnetic susceptibility, the in-phase component will be reduced and this departure can be recognized by comparison to the other parameters.

The algorithm used to calculate apparent susceptibility and apparent resistivity from HEM data, uses a homogeneous half-space geological model. Non half-space geology, such as horizontal layers or dipping sources, can also distort the perfect half-space relationship of the three data parameters. While it may be possible to use more

---

[7] Magnetic susceptibility and permeability are two measures of the same physical property. Permeability is generally given as relative permeability, μ_r, which is the permeability of the substance divided by the permeability of free space ($4 \pi \times 10^{-7}$). Magnetic susceptibility k is related to permeability by $k=\mu^r-1$. Susceptibility is a unitless measurement, and is usually reported in units of 10^{-6}. The typical range of susceptibilities is –1 for quartz, 130 for pyrite, and up to 5×10^5 for magnetite, in 10^{-6} units (Telford et al, 1986).

complex models to calculate both rock parameters, this procedure becomes very complex and time-consuming. For basic HEM data processing, it is most practical to stick to the simplest geological model.

Magnetite reversals (reversed in-phase anomalies) have been used for many years to calculate an “FeO” or magnetite response from HEM data (Fraser, 1981). However, this technique could only be applied to data where the in-phase was observed to be negative, which happens when susceptibility is high and conductivity is low.

Applying Susceptibility Corrections

Resistivity calculations done with susceptibility correction may change the apparent resistivity. High-susceptibility conductors, that were previously masked by the susceptibility effect in standard resistivity algorithms, may become evident. In this case the susceptibility corrected apparent resistivity is a better measure of the actual resistivity of the earth. However, other geological variations, such as a deep resistive layer, can also reduce the in-phase by the same amount. In this case, susceptibility correction would not be the best method. Different geological models can apply in different areas of the same data set. The effects of susceptibility, and other effects that can create a similar response, must be considered when selecting the resistivity algorithm.

Susceptibility from EM vs Magnetic Field Data

The response of the EM system to magnetite may not match that from a magnetometer survey. First, HEM-derived susceptibility is a rock property measurement, like resistivity. Magnetic data show the total magnetic field, a measure of the potential field, not the rock property. Secondly, the shape of an anomaly depends on the shape and direction of the source magnetic field. The electromagnetic field of HEM is much different in shape from the earth’s magnetic field. Total field magnetic anomalies are different at different magnetic latitudes; HEM susceptibility anomalies have the same shape regardless of their location on the earth.

In far northern latitudes, where the magnetic field is nearly vertical, the total magnetic field measurement over a thin vertical dike is very similar in shape to the anomaly from the HEM-derived susceptibility (a sharp peak over the body). The same vertical dike at the magnetic equator would yield a negative magnetic anomaly, but the HEM susceptibility anomaly would show a positive susceptibility peak.

Effects of Permeability and Dielectric Permittivity

Resistivity algorithms that assume free-space magnetic permeability and dielectric permittivity, do not yield reliable values in highly magnetic or highly resistive areas. Both magnetic polarization and displacement currents cause a decrease in the in-phase component, often resulting in negative values that yield erroneously high apparent resistivities. The effects of magnetite occur at all frequencies, but are most evident at the lowest frequency. Conversely, the negative effects of dielectric permittivity are most evident at the higher frequencies, in resistive areas.

The table below shows the effects of varying permittivity over a resistive (10,000 ohm-m) half space, at frequencies of 56,000 Hz (DIGHEM^{V}) and 140,000 Hz (RESOLVE).

Apparent Resistivity Calculations
Effects of Permittivity on In-phase/Quadrature/Resistivity

Freq (Hz)	Coil	Sep (m)	Thres (ppm)	Alt (m)	In Phase	Quad Phase	App Res	App Depth (m)	Permittivity
56,000	CP	6.3	0.1	30	7.3	35.3	10118	-1.0	1 Air
56,000	CP	6.3	0.1	30	3.6	36.6	19838	-13.2	5 Quartz
56,000	CP	6.3	0.1	30	-1.1	38.3	81832	-25.7	10 Epidote
56,000	CP	6.3	0.1	30	-10.4	42.3	76620	-25.8	20 Granite
56,000	CP	6.3	0.1	30	-19.7	46.9	71550	-26.0	30 Diabase
56,000	CP	6.3	0.1	30	-28.7	52.0	66787	-26.1	40 Gabbro
102,000	CP	7.86	0.1	30	32.5	117.2	9409	-0.3	1 Air
102,000	CP	7.86	0.1	30	11.7	127.2	25956	-16.8	5 Quartz
102,000	CP	7.86	0.1	30	-14.0	141.6	97064	-26.5	10 Epidote
102,000	CP	7.86	0.1	30	-62.9	176.0	83995	-26.8	20 Granite
102,000	CP	7.86	0.1	30	-107.5	215.8	73320	-27.0	30 Diabase
102,000	CP	7.86	0.1	30	-147.1	259.2	64875	-27.2	40 Gabbro

Methods have been developed (Huang and Fraser, 2000, 2001) to correct apparent resistivities for the effects of permittivity and permeability. The corrected resistivities yield more credible values than if the effects of permittivity and permeability are disregarded.

Recognition of Culture

Cultural responses include all EM anomalies caused by man-made metallic objects. Such anomalies may be caused by inductive coupling or current gathering. The concern of the interpreter is to recognize when an EM response is due to culture. Points of consideration used by the interpreter, when coaxial and coplanar coil-pairs are operated at a common frequency, are as follows:

1. Channels CXPL and CPPL monitor 60 Hz radiation. An anomaly on these channels shows that the conductor is radiating power. Such an indication is normally a guarantee that the conductor is cultural. However, care must be taken to ensure that the conductor is not a geologic body that strikes across a power line, carrying leakage currents.

2. A flight that crosses a "line" (e.g., fence, telephone line, etc.) yields a centre-peaked coaxial anomaly and an m-shaped coplanar anomaly.[8] When the flight crosses the cultural line at a high angle of intersection, the amplitude ratio of coaxial/coplanar response is 2. Such an EM anomaly can only be caused by a line. The geologic body that yields anomalies most closely resembling a line is the vertically dipping thin dike. Such a body, however, yields an amplitude ratio of 1 rather than 2. Consequently, an m-shaped coplanar anomaly with a CXI/CPI amplitude ratio of 2 is virtually a guarantee that the source is a cultural line.

3. A flight that crosses a sphere or horizontal disk yields centre-peaked coaxial and coplanar anomalies with a CXI/CPI amplitude ratio (i.e., coaxial/coplanar) of 1/8. In the absence of geologic bodies of this geometry, the most likely conductor is a metal roof or small fenced yard.[9] Anomalies of this type are virtually certain to be cultural if they occur in an area of culture.

4. A flight that crosses a horizontal rectangular body or wide ribbon yields an m-shaped coaxial anomaly and a centre-peaked coplanar anomaly. In the absence of geologic bodies of this geometry, the most likely conductor is a large fenced area.[5] Anomalies of this type are virtually certain to be cultural if they occur in an area of culture.

5. EM anomalies that coincide with culture, as seen on the camera film or video display, are usually caused by culture. However, care is taken with such coincidences because a geologic conductor could occur beneath a fence, for example. In this example, the fence would be expected to yield an m-shaped coplanar anomaly as in case #2 above. If, instead, a centre-peaked coplanar anomaly occurred, there would be concern that a thick geologic conductor coincided with the cultural line.

---

[8] See Figure C-1 presented earlier.

[9] It is a characteristic of EM that geometrically similar anomalies are obtained from: (1) a planar conductor, and (2) a wire which forms a loop having dimensions identical to the perimeter of the equivalent planar conductor.

6. The above description of anomaly shapes is valid when the culture is not conductively coupled to the environment. In this case, the anomalies arise from inductive coupling to the EM transmitter. However, when the environment is quite conductive (e.g., less than 100 ohm-m at 900 Hz), the cultural conductor may be conductively coupled to the environment. In this latter case, the anomaly shapes tend to be governed by current gathering. Current gathering can completely distort the anomaly shapes, thereby complicating the identification of cultural anomalies. In such circumstances, the interpreter can only rely on the radiation channels and on the camera film or video records.

Magnetic Responses

The measured total magnetic field provides information on the magnetic properties of the earth materials in the survey area. The information can be used to locate magnetic bodies of direct interest for exploration, and for structural and lithological mapping.

The total magnetic field response reflects the abundance of magnetic material in the source. Magnetite is the most common magnetic mineral. Other minerals such as ilmenite, pyrrhotite, franklinite, chromite, hematite, arsenopyrite, limonite and pyrite are also magnetic, but to a lesser extent than magnetite on average.

In some geological environments, an EM anomaly with magnetic correlation has a greater likelihood of being produced by sulphides than one which is non-magnetic. However, sulphide ore bodies may be non-magnetic (e.g., the Kidd Creek deposit near Timmins, Canada) as well as magnetic (e.g., the Mattabi deposit near Sturgeon Lake, Canada).

Iron ore deposits will be anomalously magnetic in comparison to surrounding rock due to the concentration of iron minerals such as magnetite, ilmenite and hematite.

Changes in magnetic susceptibility often allow rock units to be differentiated based on the total field magnetic response. Geophysical classifications may differ from geological classifications if various magnetite levels exist within one general geological classification. Geometric considerations of the source such as shape, dip and depth, inclination of the earth's field and remanent magnetization will complicate such an analysis.

In general, mafic lithologies contain more magnetite and are therefore more magnetic than many sediments which tend to be weakly magnetic. Metamorphism and alteration can also increase or decrease the magnetization of a rock unit.

Textural differences on a total field magnetic contour, colour or shadow map due to the frequency of activity of the magnetic parameter resulting from inhomogeneities in the distribution of magnetite within the rock, may define certain lithologies. For example, near surface volcanics may display highly complex contour patterns with little line-to-line correlation.

Rock units may be differentiated based on the plan shapes of their total field magnetic responses. Mafic intrusive plugs can appear as isolated "bulls-eye" anomalies. Granitic intrusives appear as sub-circular zones, and may have contrasting rings due to contact metamorphism. Generally, granitic terrain will lack a pronounced strike direction, although granite gneiss may display strike.

Linear north-south units are theoretically not well-defined on total field magnetic maps in equatorial regions due to the low inclination of the earth's magnetic field. However, most stratigraphic units will have variations in composition along strike that will cause the units to appear as a series of alternating magnetic highs and lows.

Faults and shear zones may be characterized by alteration that causes destruction of magnetite (e.g., weathering) that produces a contrast with surrounding rock. Structural breaks may be filled by magnetite-rich, fracture filling material as is the case with diabase dikes, or by non-magnetic felsic material.

Faulting can also be identified by patterns in the magnetic total field contours or colours. Faults and dikes tend to appear as lineaments and often have strike lengths of several kilometres. Offsets in narrow, magnetic, stratigraphic trends also delineate structure. Sharp contrasts in magnetic lithologies may arise due to large displacements along strike-slip or dip-slip faults.

Gamma Ray Spectrometry

Radioelement concentrations are measures of the abundance of radioactive elements in the rock. The original abundance of the radioelements in any rock can be altered by the subsequent processes of metamorphism and weathering.

Gamma radiation in the range that is measured in the thorium, potassium, uranium and total count windows is strongly attenuated by rock, overburden and water. Almost all of the total radiation measured from rock and overburden originates in the upper .5 metres. Moisture in soil and bodies of water will mask the radioactivity from underlying rock. Weathered rock materials that have been displaced by glacial, water or wind action will not reflect the general composition of the underlying bedrock. Where residual soils exist, they may reflect the composition of underlying rock except where equilibrium does not exist between the original radioelement and the products in its decay series.

Radioelement counts (expressed as counts per second) are the rates of detection of the gamma radiation from specific decaying particles corresponding to products in each radioelements decay series. The radiation source for uranium is bismuth (Bi-214), for thorium it is thallium (Tl-208) and for potassium it is potassium (K-40).

The uranium and thorium radioelement concentrations are dependent on a state of equilibrium between the parent and daughter products in the decay series. Some daughter products in the uranium decay are long lived and could be removed by processes such as leaching. One product in the series, radon (Rn-222), is a gas which can easily escape. Both of these factors can affect the degree to which the calculated uranium concentrations reflect the actual composition of the source rock. Because the daughter products of thorium are relatively short lived, there is more likelihood that the thorium decay series is in equilibrium.

Lithological discrimination can be based on the measured relative concentrations and total, combined, radioactivity of the radioelements. Feldspar and mica contain potassium. Zircon, sphene and apatite are accessory minerals in igneous rocks that are sources of uranium and thorium. Monazite, thorianite, thorite, uraninite and uranothorite are also sources of uranium and thorium which are found in granites and pegmatites.

In general, the abundance of uranium, thorium and potassium in igneous rock increases with acidity. Pegmatites commonly have elevated concentrations of uranium relative to thorium. Sedimentary rocks derived from igneous rocks may have characteristic signatures that are influenced by their parent rocks, but these will have been altered by subsequent weathering and alteration.

Metamorphism and alteration will cause variations in the abundance of certain radioelements relative to each other. For example, alterative processes may cause uranium enrichment to the extent that a rock will be of economic interest. Uranium anomalies are more likely to be economically significant if they consist of an increase in the uranium relative to thorium and potassium, rather than a sympathetic increase in all three radioelements.

Faults can exhibit radioactive highs due to increased permeability which allows radon migration, or as lows due to structural control of drainage and fluvial sediments which attenuate gamma radiation from the underlying rocks. Faults can also be recognized by sharp contrasts in radiometric lithologies due to large strike-slip or dip-slip displacements. Changes in relative radioelement concentrations due to alteration will also define faults.

Similar to magnetics, certain rock types can be identified by their plan shapes if they also produce a radiometric contrast with surrounding rock. For example, granite intrusions will appear as sub-circular bodies, and may display concentric zonations. They will tend to lack a prominent strike direction. Offsets of narrow, continuous, stratigraphic units with contrasting radiometric signatures can identify faulting, and folding of stratigraphic trends will also be apparent.

APPENDIX D

DATA ARCHIVE DESCRIPTION

APPENDIX D

ARCHIVE DESCRIPTION

This archive contains FINAL data, grids and maps of an airborne Dighem V electromagnetic and spectrometry geophysical survey over the New Hazelton, BC conducted by FUGRO AIRBORNE SURVEYS CORP. on behalf of Duncasatle Gold Corp. flown from July 7 to 17, 2010

Fugro Job # 10037

This Archive contains 4 directories

\GRIDS

Grids in Geosoft format (with associated GI files)

CVG_PorphyryCreek.grd	- Calculated Vertical Magnetic Gradient nT/m
MAG_PorphyryCreek.grd	- Residual Magnetic Intensity nT
RES900_PorphyryCreek.grd	- Apparent Resistivity 900 Hz ohm•m
RES7200_PorphyryCreek.grd	- Apparent Resistivity 7200 Hz ohm•m
RES56K_PorphyryCreek.grd	- Apparent Resistivity 56k Hz ohm•m
TC_PorphyryCreek.grd	- Total Counts cps
TH_PorphyryCreek.grd	- Thorium Counts cps
K_PorphyryCreek.grd	- Potassium Counts cps
U_PorphyryCreek.grd	- Uranium Counts cps
DoseRate_PorphyryCreek.grd	- Air Absorbed Dose Rate nGy/Hr
eU_PorphyryCreek.grd	- Equivalent Uranium ppm
eTh_PorphyryCreek.grd	- Equivalent Thorium ppm
eK_PorphyryCreek.grd	- Equivalent Potassium ppm
eUeTh_PorphyryCreek.grd	- Equivalent Uranium/Thorium Ratio
eUeK_PorphyryCreek.grd	- Equivalent Uranium/ Potassium Ratio
eTheK_PorphyryCreek.grd	- Equivalent Thorium/Potassium Ratio

\LINEDATA

PorphyryCreek.GDB	- Data archive in Geosoft GDB format
PorphyryCreek.XYZ	- Data archive in Geosoft ASCII format
PorphyryCreek_AEM.XYZ	- Anomaly archive in ASCII format

\MAPS

Final colour maps in PDF format

AEM_PorphyryCreek.pdf	- Electromagnetic Anomalies
CVG_PorphyryCreek.pdf	- Calculated Vertical Magnetic Gradient
MAG_PorphyryCreek.pdf	- Residual Magnetic Intensity
RES900_PorphyryCreek.pdf	- Apparent Resistivity 900 Hz
RES7200_PorphyryCreek.pdf	- Apparent Resistivity 7200 Hz
RES56K_PorphyryCreek.pdf	- Apparent Resistivity 56k Hz
TC_PorphyryCreek.pdf	- Total Counts

TH_PorphyryCreek.pdf	- Thorium Counts
K_PorphyryCreek.pdf	- Potassium Counts
U_PorphyryCreek.pdf	- Uranium Counts
DoseRate_PorphyryCreek.pdf	- Air Absorbed Dose Rate nGy/Hr
eU_PorphyryCreek.pdf	- Equivalent Uranium ppm
eTh_PorphyryCreek.pdf	- Equivalent Thorium ppm
eK_PorphyryCreek.pdf	- Equivalent Potassium ppm

\REPORT

10037_Report.PDF	- Logistics and Interpretation Report

****

GEOSOFT GDB and XYZ ARCHIVE SUMMARY

#	Channel	Time	Units	Description
1	X	0.1	m	easting NAD 83 (UTM Zone 9N)
2	Y	0.1	m	northing NAD 83 (UTM Zone 9N)
3	FID	0.1		fiducial increment
4	LATITUDE	0.1		degrees latitude WGS 84
5	LONGITUDE	0.1		degrees longitude WGS 84
6	FLIGHT	0.1		flight number
7	DATE	0.1		flight date (yyyy/mm/dd)
8	ALTRAD_HELI	0.1	m	helicopter height above surface from radar altimeter
9	ALTBAD_BIRD	0.1	m	calculated bird height above surface from radar altimeter
10	GPSZ	0.1	m	bird height above spheroid
11	DTM	0.1	m	digital terrain model (above WGS 84 datum)
12	DIURNAL_FILT	1.0	nT	measured diurnal ground magnetic intensity
13	DIURNAL_COR	0.1	nT	diurnal correction - base removed
14	MAG_RAW	0.1	nT	total magnetic field - spike rejected
15	MAG_LAG	0.1	nT	total magnetic field - corrected for lag
16	MAG_DIU	0.1	nT	total magnetic field - diurnal variation removed
17	IGRF	0.1	nT	international geomagnetic reference field
18	MAG_RMI	0.1	nT	residual magnetic intensity - final
19	CPI900_FILT	0.1	ppm	coplanar inphase 900 Hz - unlevelled
20	CPQ900_FILT	0.1	ppm	coplanar quadrature 900 Hz - unlevelled
21	CXI1000_FILT	0.1	ppm	coaxial inphase 1000 Hz - unlevelled
22	CXQ1000_FILT	0.1	ppm	coaxial quadrature 1000 Hz - unlevelled
23	CXI5500_FILT	0.1	ppm	coaxial inphase 5500 Hz - unlevelled
24	CXQ5500_FILT	0.1	ppm	coaxial quadrature 5500 Hz -unlevelled
25	CPI7200_FILT	0.1	ppm	coplanar inphase 7200 Hz - unlevelled
26	CPQ7200_FILT	0.1	ppm	coplanar quadrature 7200 Hz -unlevelled
27	CPI56K_FILT	0.1	ppm	coplanar inphase 56 kHz - unlevelled
28	CPQ56K_FILT	0.1	ppm	coplanar quadrature 56 kHz - unlevelled
29	CPI900	0.1	ppm	coplanar inphase 900 Hz

30	CPQ900	0.1	ppm	coplanar quadrature 900 Hz
31	CXI1000	0.1	ppm	coaxial inphase 1000 Hz
32	CXQ1000	0.1	ppm	coaxial quadrature 1000 Hz
33	CXI5500	0.1	ppm	coaxial inphase 5500 Hz
34	CXQ5500	0.1	ppm	coaxial quadrature 5500 Hz
35	CPI7200	0.1	ppm	coplanar inphase 7200 Hz
36	CPQ7200	0.1	ppm	coplanar quadrature 7200 Hz
37	CPI56K	0.1	ppm	coplanar inphase 56 kHz
38	CPQ56K	0.1	ppm	coplanar quadrature 56 kHz
39	RES900	0.1	ohm·m	apparent resistivity - 900 Hz
40	RES7200	0.1	ohm·m	apparent resistivity - 7200 Hz
41	RES56K	0.1	ohm·m	apparent resistivity - 56 kHz
42	DEP900	0.1	m	apparent depth - 900 Hz
43	DEP7200	0.1	m	apparent depth - 7200 Hz
44	DEP56K	0.1	m	apparent depth - 56 kHz
45	DIFI	0.1		difference channel based on cxi5500/cpi7200
46	DIFQ	0.1		difference channel based on cxq5500/cpq7200
47	CPPL	0.1		coplanar powerline monitor
48	CXSP	0.1		coaxial spherics monitor
49	CPSP	0.1		coplanar spherics monitor
50	TC_RAW	1.0	counts	total counts, uncorrected
51	Th_RAW	1.0	counts	thorium counts, uncorrected
52	U_RAW	1.0	counts	uranium counts, uncorrected
53	K_RAW	1.0	counts	potassium counts, uncorrected
54	U_UP	1.0	counts	upward looking uranium, uncorrected
55	COSMIC	1.0	counts	cosmic counts
56	LIVETIME	1.0	ms	livetime
57	EFFECTIVEHEIGHT	0.1	m	height at standard temperature and pressure
58	KPA	0.1	kPa	pressure
59	TEMP_EXT	0.1	ºC	external temperature in Celcius
60	TC	1.0	cps	total counts, corrected
61	TH	1.0	cps	thorium counts, corrected
62	U	1.0	cps	uranium counts, corrected
63	K	1.0	cps	potassium counts, corrected
64	Doserate	1.0	cps	air absorbed dose rate
65	eTh	1.0	cps	equivalent thorium concentration
66	eU	1.0	cps	equivalent uranium concentration
67	eK	1.0	cps	equivalent potassium concentration
68	eUeTh	1.0	cps	equivalent thorium concentration
69	eUeK	1.0	cps	equivalent uranium concentration
70	eTheK	1.0	cps	equivalent potassium concentration
71	GR820_DOWN	1.0		downward spectrum array (gdb only)
72	GR820_DOWN_NASVD	1.0		downward spectrum array after NASVD correction (gdb only)

****

FUGRO ANOMALY SUMMARY

#	CHANNEL NAME	TIME	UNITS	DESCRIPTION

1 Easting	0.10	m	easting NAD83 (Zone 10N)
2 Northing	0.10	m	northing NAD83 (Zone 10N)
3 FID	1.00		Synchronization Counter
4 FLT	0.10		Flight
5 MHOS	0.10	siemens	Conductance (see report for model used)
6 DEPTH	0.10	m	Depth (see report for model used)
7 MAG	0.10	nT	Mag Correlation, local amplitude
8 CXI1	0.10	ppm	Inphase Coaxial 1000 Hz, local amplitude
9 CXQ1	0.10	ppm	Quadrature Coaxial 1000 Hz, local amplitude
10 CPI1	0.10	ppm	Inphase Coplanar 900 Hz, absolute amplitude
11 CPQ1	0.10	ppm	Quadrature Coplanar 900 Hz, absolute amplitude
12 CPI2	0.10	ppm	Inphase Coplanar 7200 Hz, absolute amplitude
13 CPQ2	0.10	ppm	Quadrature Coplanar 7200 Hz, absolute amplitude
14 LET	0.10		Anomaly Identifier
15 SYM	0.10		Anomaly Interpretation Symbol
16 GRD	0.10		Anomaly Grade

The coordinate system for all grids and the data archive is projected as follows

Datum	NAD83
Spheroid	GRS80
Central meridian	129 degrees West (Z9N)
False easting	0
False northing	0
Scale factor	0
Northern parallel	N/A
Base parallel	N/A
Delta X shift	0
Delta Y shift	0
Delta Z shift	0

APPENDIX E

EM ANOMALY LIST

EM Anomaly List : JOB 10037, New Hazelton, BC

CX=COAXIAL,CP=COPLANAR			Note: EM amplitudes are local for types B,D,T and are absolute for all others		Estimated depth may be unreliable because the strongest part of the conductor may be deeper or to one side of the flight line, or because of a shallow dip or magnetite/overburden effects							
Label	Fid	Interp	XUTM (m), YUTM (m)	CXI5500_LLEVHz Real (ppm)	CXQ5500_LLEVHz Quad (ppm)	CPI7200_LLEVHz Real (ppm)	CPQ7200_LLEVHz Quad (ppm)	CPI900_LLEVHz Real (ppm)	CPQ900_LLEVHz Quad (ppm)	Conductance (siemens)	Depth (metres)	Magnetic Corr. (nT)
LINE 10060		**FLIGHT 29030**										
A	1353.9	B?	592181.6,6113171.9	0.0	11.1	0.0	62.5	0.0	10.0	0.0	0.0	272.9
LINE 10090		**FLIGHT 29030**										
A	2798.1	H	593417.6,6112596.4	11.7	12.0	39.0	31.4	12.3	20.3	2.3	40.7	---
LINE 10100		**FLIGHT 29030**										
A	3200.3	B?	587143.8,6112248.5	5.6	5.5	16.8	5.8	2.1	7.2	1.1	15.8	---
B	3188.2	H	587333.5,6112265.4	12.3	20.2	34.0	47.4	4.4	18.6	1.2	23.3	27.0
C	2853.3	H	593467.1,6112390.0	12.0	13.2	45.4	43.0	9.7	24.1	1.8	17.3	---
LINE 10110		**FLIGHT 29027**										
A	1556.6	B?	586979.2,6112045.5	1.0	0.1	0.5	15.5	0.1	5.0	---	---	32.2
B	1692.9	D	588136.9,6112046.2	1.4	2.1	0.0	0.0	0.0	0.1	---	---	7.1
C	1711.4	D	588356.0,6112079.1	4.9	7.1	4.3	18.3	0.0	0.5	0.7	28.8	---
LINE 10113		**FLIGHT 29030**										
A	3662.5	S?	592936.5,6112201.3	3.9	11.4	9.7	28.5	-0.7	7.5	1.0	17.5	---
B	3684.4	H	593436.3,6112238.6	12.6	12.9	42.5	30.3	11.4	22.1	2.1	22.5	---
LINE 10120		**FLIGHT 29027**										
A	3739.7	B?	587333.4,6111854.5	0.2	0.0	31.8	56.6	0.8	16.2	---	---	20.6
B	3761.5	H	587584.3,6111867.8	20.6	28.0	80.4	109.4	17.9	46.4	2.0	21.9	---
LINE 10124		**FLIGHT 29030**										
A	4034.0	B?	589801.2,6111907.5	8.5	2.4	6.1	5.7	6.8	4.1	3.3	16.4	85.4

EM Anomaly List : JOB 10037, New Hazelton, BC

CX=COAXIAL,CP=COPLANAR			Note: EM amplitudes are local for types B,D,T and are absolute for all others		Estimated depth may be unreliable because the strongest part of the conductor may be deeper or to one side of the flight line, or because of a shallow dip or magnetite/overburden effects							
Label Fid		**Interp**	**XUTM (m), YUTM (m)**	**CXI5500_LLEVHz Real (ppm)**	**CXQ5500_LLEVHz Quad (ppm)**	**CPI7200_LLEVHz Real (ppm)**	**CPQ7200_LLEVHz Quad (ppm)**	**CPI900_LLEVHz Real (ppm)**	**CPQ900_LLEVHz Quad (ppm)**	**Conductance (siemens)**	**Depth (metres)**	**Magnetic Corr. (nT)**
LINE 10130		**FLIGHT 29027**										
A	1346.3	H	586929.7,6111659.0	23.2	16.2	58.8	39.1	24.0	27.8	3.5	12.8	47.5
LINE 10134		**FLIGHT 29030**										
A	4230.8	B?	589802.2,6111724.6	1.4	2.7	5.3	5.6	1.0	1.4	---	---	69.7
LINE 10140		**FLIGHT 29027**										
A	3597.9	B?	586899.9,6111484.9	2.6	0.5	22.0	4.3	33.9	6.1	---	---	16.8
B	3588.0	H	587151.4,6111471.9	31.4	11.3	83.7	30.8	68.9	38.5	8.8	6.5	---
C	3552.7	B	588207.6,6111475.5	12.7	9.0	31.1	40.0	8.2	18.0	2.0	24.2	---
LINE 10143		**FLIGHT 29031**										
A	710.8	B?	589780.7,6111520.6	6.4	3.0	16.4	24.6	14.9	9.6	2.7	30.6	15.6
LINE 10150		**FLIGHT 29027**										
A	1060.8	B?	586877.1,6111261.5	2.1	2.2	7.3	21.3	26.2	5.1	---	---	---
B	1081.5	B?	587012.7,6111264.8	0.6	1.7	54.2	26.1	33.7	26.2	---	---	32.5
C	1102.0	B	587210.6,6111259.4	31.7	14.7	57.7	18.9	47.8	69.3	4.8	15.4	11.4
D	1118.9	E	587563.6,6111281.0	56.0	43.3	137.7	104.0	57.9	73.4	1.5	11.5	---
E	1125.8	D	587728.3,6111288.8	29.7	21.1	236.2	42.1	221.7	119.7	2.7	12.0	---
F	1129.9	D	587820.0,6111294.0	16.6	0.0	254.4	29.1	235.9	161.8	19.9	31.8	9.4
G	1136.5	E	587951.9,6111300.6	95.5	71.3	257.9	216.9	53.2	126.6	1.6	7.9	---
H	1150.3	S?	588192.2,6111305.2	50.8	97.1	173.6	322.0	13.2	96.9	1.0	3.6	53.5
I	1169.1	S?	588547.9,6111312.9	28.0	38.8	79.0	102.7	4.8	39.2	1.0	13.8	27.7

EM Anomaly List : JOB 10037, New Hazelton, BC

CX=COAXIAL,CP=COPLANAR			Note: EM amplitudes are local for types B,D,T and are absolute for all others	Estimated depth may be unreliable because the strongest part of the conductor may be deeper or to one side of the flight line, or because of a shallow dip or magnetite/overburden effects								
Label	Fid	Interp	XUTM (m), YUTM (m)	CXI5500_LLEVHz Real (ppm)	CXQ5500_LLEVHz Quad (ppm)	CPI7200_LLEVHz Real (ppm)	CPQ7200_LLEVHz Quad (ppm)	CPI900_LLEVHz Real (ppm)	CPQ900_LLEVHz Quad (ppm)	Conductance (siemens)	Depth (metres)	Magnetic Corr. (nT)
LINE 10154		**FLIGHT 29031**										
A	1189.3	D	589823.6,6111303.5	8.3	4.4	43.4	2.6	54.1	22.6	2.6	23.7	46.1
B	1186.3	D	589904.6,6111309.1	10.8	3.1	48.8	2.6	48.4	22.6	6.4	17.9	---
LINE 10160		**FLIGHT 29023**										
A	4517.7	B	592671.6,6111192.6	0.3	6.9	2.4	61.3	2.7	17.9	0.3	7.8	---
B	4512.8	B	592795.7,6111186.5	5.5	14.5	2.4	61.3	2.7	17.9	0.4	4.9	28.0
C	4484.6	H	593459.1,6111185.0	3.4	7.2	20.5	16.1	11.8	11.7	3.2	62.2	---
LINE 10162		**FLIGHT 29027**										
A	3273.0	H	586432.1,6111031.4	19.9	5.7	59.6	13.0	63.3	18.9	16.8	15.2	---
B	3285.5	H	586784.3,6111054.2	28.0	15.2	110.6	38.0	92.6	42.2	11.8	21.6	---
C	3337.3	S?	587594.8,6111105.2	17.4	17.4	68.0	45.4	20.3	32.9	1.4	23.6	---
D	3347.8	D	587736.5,6111115.4	9.4	38.1	326.7	216.8	39.8	151.3	0.3	1.9	23.1
E	3351.4	D	587799.7,6111119.9	29.2	12.8	326.7	216.0	39.8	151.3	5.0	24.8	7.5
F	3361.3	B	587982.1,6111121.5	54.3	20.7	165.2	62.5	84.1	98.0	7.5	8.9	22.6
G	3372.9	B?	588231.8,6111120.5	49.7	48.4	98.7	157.8	2.7	42.9	2.2	0.0	---
LINE 10170		**FLIGHT 29023**										
A	4370.3	B	592880.9,6110987.6	16.8	2.0	31.9	3.5	1.3	4.5	9.6	24.4	77.2
B	4397.5	H	593544.5,6110991.6	6.0	6.8	24.1	14.9	13.1	11.8	3.5	23.2	---
LINE 10172		**FLIGHT 29027**										
A	968.3	B	586604.0,6110856.3	2.5	0.0	26.1	3.1	41.0	7.5	---	---	---
B	891.4	B?	587969.8,6110908.3	8.5	3.2	13.9	3.2	6.9	4.9	4.1	31.3	34.2
C	880.5	B	588173.6,6110900.5	12.0	11.0	31.3	14.1	40.2	22.9	1.5	20.9	11.8

EM Anomaly List : JOB 10037, New Hazelton, BC

CX=COAXIAL,CP=COPLANAR			Note: EM amplitudes are local for types B,D,T and are absolute for all others	Estimated depth may be unreliable because the strongest part of the conductor may be deeper or to one side of the flight line, or because of a shallow dip or magnetite/overburden effects								
Label	Fid	Interp	XUTM (m), YUTM (m)	CXI5500_LLEVHz Real (ppm)	CXQ5500_LLEVHz Quad (ppm)	CPI7200_LLEVHz Real (ppm)	CPQ7200_LLEVHz Quad (ppm)	CPI900_LLEVHz Real (ppm)	CPQ900_LLEVHz Quad (ppm)	Conductance (siemens)	Depth (metres)	Magnetic Corr. (nT)
D	874.0	D	588309.7,6110898.6	10.5	24.2	0.0	6.9	4.5	19.7	0.6	2.1	---
E	867.3	B	588447.8,6110889.8	5.9	3.7	192.5	155.1	5.0	29.5	1.9	40.4	---
LINE 10180		**FLIGHT 29023**										
A	4200.9	H	592971.2,6110798.7	28.7	42.6	67.6	117.2	2.5	30.1	1.1	12.4	---
LINE 10182		**FLIGHT 29027**										
A	3191.2	B	586769.5,6110655.6	9.7	1.9	47.4	1.1	51.3	4.7	4.6	21.1	---
B	3178.6	B	587154.6,6110665.3	0.4	0.0	3.8	0.2	5.8	0.2	---	---	---
C	3146.4	/	587945.2,6110696.2	21.0	7.6	28.1	21.7	26.3	14.5	5.9	21.4	---
D	3133.3	S?	588271.4,6110681.8	19.6	38.3	88.2	134.7	7.1	42.6	1.0	1.8	47.1
LINE 10183		**FLIGHT 29031**										
A	1701.9	H	589331.4,6110729.5	3.2	4.3	7.5	10.5	5.4	4.3	3.1	88.3	---
B	1802.1	S?	590576.9,6110722.2	7.7	31.6	48.0	143.0	-0.1	30.5	1.0	1.6	---
LINE 10190		**FLIGHT 29023**										
A	4095.3	E	592948.8,6110592.3	9.4	25.9	2.9	58.2	-9.8	10.5	1.0	0.0	75.2
B	4098.7	S?	593039.8,6110587.9	7.6	24.0	36.2	85.8	-1.7	22.8	1.0	4.4	---
C	4108.3	B?	593294.9,6110590.7	8.9	5.1	34.5	27.3	19.1	23.8	2.3	39.2	---
D	4118.9	B	593588.3,6110605.5	37.0	36.4	246.0	86.4	58.7	135.3	2.0	0.0	---
LINE 10192		**FLIGHT 29027**										
A	500.9	H	586721.8,6110464.6	37.8	19.5	131.1	61.3	113.5	40.9	16.3	26.1	---
B	517.1	H	587166.8,6110473.4	49.7	12.2	145.4	21.7	159.7	39.1	28.5	6.9	---
C	532.3	B?	587640.8,6110478.9	1.5	1.1	31.8	8.5	43.0	11.5	---	---	---
D	551.5	B?	588067.9,6110486.3	8.5	17.1	23.2	25.7	1.5	11.3	0.6	7.4	---

EM Anomaly List : JOB 10037, New Hazelton, BC

CX=COAXIAL,CP=COPLANAR			Note: EM amplitudes are local for types B,D,T and are absolute for all others	Estimated depth may be unreliable because the strongest part of the conductor may be deeper or to one side of the flight line, or because of a shallow dip or magnetite/overburden effects								
Label	Fid	Interp	XUTM (m), YUTM (m)	CXI5500_LLEVHz Real (ppm)	CXQ5500_LLEVHz Quad (ppm)	CPI7200_LLEVHz Real (ppm)	CPQ7200_LLEVHz Quad (ppm)	CPI900_LLEVHz Real (ppm)	CPQ900_LLEVHz Quad (ppm)	Conductance (siemens)	Depth (metres)	Magnetic Corr. (nT)
E	628.2	B	589378.2,6110532.7	7.1	2.3	48.7	40.5	12.4	21.8	2.8	35.8	---
LINE 10200		**FLIGHT 29023**										
A	3867.8	B	593182.6,6110392.5	8.1	10.7	47.6	24.1	14.5	26.1	0.9	14.6	---
LINE 10202		**FLIGHT 29027**										
A	2888.4	B	587252.3,6110268.1	9.2	2.3	42.7	4.3	53.8	13.5	3.8	28.9	---
B	2895.5	B	587461.7,6110286.8	22.1	5.9	18.4	29.2	104.0	32.3	9.1	23.6	---
C	2899.7	E	587597.6,6110300.5	59.2	20.9	133.6	68.3	85.2	58.8	1.9	13.2	---
D	2917.3	\	588146.0,6110306.5	13.9	0.7	31.2	10.6	25.6	9.5	11.3	28.3	---
LINE 10210		**FLIGHT 29023**										
A	2968.5	S	593118.0,6110182.7	2.9	5.7	5.1	15.1	-0.3	4.0	1.0	1.4	---
LINE 10212		**FLIGHT 29027**										
A	1964.2	H	586962.6,6110067.1	75.6	30.6	257.6	85.8	270.7	76.5	28.7	10.5	---
B	1983.8	B	587438.6,6110090.3	16.3	0.0	25.4	10.1	48.2	6.3	19.5	0.0	12.5
C	2004.3	B	587881.7,6110117.9	13.8	3.3	31.9	21.7	34.9	10.6	9.2	34.4	---
D	2014.7	B?	588119.4,6110130.1	15.3	4.6	20.8	31.7	7.0	1.4	6.8	28.8	61.7
LINE 10213		**FLIGHT 29031**										
A	2186.3	H	590583.3,6110066.6	7.7	5.7	28.8	17.0	6.6	15.8	1.7	0.0	163.6
LINE 10220		**FLIGHT 29023**										
A	3258.2	S?	592960.3,6110013.7	4.3	18.7	4.5	34.1	-2.8	6.4	1.0	0.0	18.0
LINE 10222		**FLIGHT 29027**										
A	2707.7	B	587099.8,6109865.6	7.4	3.9	30.0	0.2	43.3	7.9	2.5	33.3	15.7

EM Anomaly List : JOB 10037, New Hazelton, BC

CX=COAXIAL,CP=COPLANAR			Note: EM amplitudes are local for types B,D,T and are absolute for all others		Estimated depth may be unreliable because the strongest part of the conductor may be deeper or to one side of the flight line, or because of a shallow dip or magnetite/overburden effects							
Label	Fid	Interp	XUTM (m), YUTM (m)	CXI5500_LLEVHz Real (ppm)	CXQ5500_LLEVHz Quad (ppm)	CPI7200_LLEVHz Real (ppm)	CPQ7200_LLEVHz Quad (ppm)	CPI900_LLEVHz Real (ppm)	CPQ900_LLEVHz Quad (ppm)	Conductance (siemens)	Depth (metres)	Magnetic Corr. (nT)
B	2696.7	B	587326.2,6109885.6	13.0	4.7	0.4	14.0	19.6	7.7	5.1	27.2	10.2
LINE 10223		**FLIGHT 29031**										
A	2345.6	H	590560.8,6109915.6	10.8	10.2	35.3	22.7	8.6	22.2	1.7	0.0	---
LINE 10232		**FLIGHT 29027**										
A	2277.1	H	587094.8,6109683.4	22.1	8.9	68.3	23.2	64.4	23.8	13.2	0.0	19.1
B	2256.0	H	587657.8,6109659.7	11.1	5.2	27.4	14.4	12.9	15.0	2.9	0.0	10.4
LINE 10233		**FLIGHT 29031**										
A	2526.7	H	590747.3,6109752.9	8.7	9.6	12.9	17.0	4.7	9.6	1.7	43.4	77.0
LINE 10243		**FLIGHT 29031**										
A	2823.7	B?	586101.4,6109465.4	2.0	0.5	0.5	1.0	27.4	0.3	---	---	---
B	2914.1	H	587563.5,6109483.6	30.8	18.1	99.4	57.8	36.0	51.2	3.4	9.1	185.7
C	2966.6	H	588331.0,6109519.9	9.1	9.9	41.7	34.0	13.4	24.1	2.3	6.6	---
LINE 10250		**FLIGHT 29027**										
A	2381.3	H	586120.6,6109273.9	13.6	8.4	47.7	28.1	38.5	18.7	8.4	44.3	---
B	2397.6	S?	586422.7,6109264.2	14.8	18.5	67.3	57.7	28.1	33.6	1.2	28.4	---
C	2434.9	H	587029.7,6109267.7	15.1	34.8	56.9	126.7	13.3	35.2	1.9	24.0	14.5
D	2466.8	B?	587636.0,6109290.6	33.7	22.6	34.3	58.3	32.5	50.3	3.0	2.9	168.8
LINE 10260		**FLIGHT 29031**										
A	3495.2	H	586048.0,6109045.0	5.2	3.3	22.0	11.1	20.5	8.7	8.0	0.0	---
B	3546.1	B	586937.6,6109059.9	10.7	11.3	79.8	68.8	15.7	20.6	1.2	11.5	---
C	3552.7	D	587043.7,6109061.1	8.7	5.0	6.7	16.5	11.1	23.8	2.4	26.1	49.7

EM Anomaly List : JOB 10037, New Hazelton, BC

CX=COAXIAL,CP=COPLANAR		Note: EM amplitudes are local for types B,D,T and are absolute for all others	Estimated depth may be unreliable because the strongest part of the conductor may be deeper or to one side of the flight line, or because of a shallow dip or magnetite/overburden effects									
Label	Fid	Interp	XUTM (m), YUTM (m)	CXI5500_LLEVHz Real (ppm)	CXQ5500_LLEVHz Quad (ppm)	CPI7200_LLEVHz Real (ppm)	CPQ7200_LLEVHz Quad (ppm)	CPI900_LLEVHz Real (ppm)	CPQ900_LLEVHz Quad (ppm)	Conductance (siemens)	Depth (metres)	Magnetic Corr. (nT)
D	3611.6	H	588060.4,6109096.8	10.6	4.8	32.3	11.0	27.5	16.4	6.2	0.0	---
LINE 10271		**FLIGHT 29032**										
A	1536.0	S?	586918.9,6108862.8	19.1	14.2	44.5	31.1	21.0	21.6	1.2	0.0	23.2
B	1481.2	B?	587912.8,6108889.2	7.8	6.8	5.7	9.0	0.9	3.3	1.4	15.3	22.5
LINE 10282		**FLIGHT 29032**										
A	1952.4	H	587878.7,6108665.7	8.2	7.3	32.2	23.0	13.0	17.6	2.7	6.8	8.8
LINE 10293		**FLIGHT 29013**										
A	1264.3	E	588426.6,6108455.4	21.2	16.7	34.2	31.7	16.3	17.3	1.0	18.1	---
B	1258.2	B	588528.1,6108458.3	7.7	1.5	51.4	23.0	35.1	3.6	3.8	11.5	---
LINE 10301		**FLIGHT 29011**										
A	4614.4	H	586158.4,6108207.1	5.7	5.8	20.5	9.6	14.1	11.9	3.8	9.6	---
B	4526.4	D	588033.5,6108300.8	11.0	12.1	0.0	17.5	1.3	1.6	1.2	6.2	54.9
C	4509.1	/	588420.8,6108281.3	21.6	14.6	46.5	37.2	0.0	22.4	2.6	5.6	11.0
LINE 10311		**FLIGHT 29012**										
A	1885.1	H	588013.6,6108106.2	29.0	21.9	82.0	68.7	43.0	40.1	4.9	33.8	60.4
B	1870.8	D	588285.1,6108100.5	6.5	20.3	26.5	110.1	0.0	12.2	0.4	3.6	---
C	1861.1	B	588452.8,6108091.2	37.6	45.9	264.4	114.3	124.8	157.3	1.6	0.0	7.9
D	1857.1	D	588526.9,6108088.1	14.3	0.0	83.2	0.0	87.9	86.5	16.0	14.5	---
LINE 10321		**FLIGHT 29012**										
A	3267.5	H	587116.5,6107886.8	8.5	16.8	21.2	42.6	7.6	12.8	2.0	42.4	---
B	3244.7	B	587607.2,6107867.7	1.5	0.6	22.3	1.0	24.4	10.0	---	---	---

EM Anomaly List : JOB 10037, New Hazelton, BC

CX=COAXIAL,CP=COPLANAR			Note: EM amplitudes are local for types B,D,T and are absolute for all others		Estimated depth may be unreliable because the strongest part of the conductor may be deeper or to one side of the flight line, or because of a shallow dip or magnetite/overburden effects							
Label	**Fid**	**Interp**	**XUTM (m), YUTM (m)**	**CXI5500_LLEVHz Real (ppm)**	**CXQ5500_LLEVHz Quad (ppm)**	**CPI7200_LLEVHz Real (ppm)**	**CPQ7200_LLEVHz Quad (ppm)**	**CPI900_LLEVHz Real (ppm)**	**CPQ900_LLEVHz Quad (ppm)**	**Conductance (siemens)**	**Depth (metres)**	**Magnetic Corr. (nT)**
C	3229.6	H	587901.1,6107886.3	37.6	13.0	80.6	38.2	50.5	36.9	6.2	8.9	21.3
D	3207.1	B	588298.4,6107872.8	58.1	20.1	260.8	80.6	121.5	153.3	8.7	0.0	---
E	3198.6	D	588464.7,6107871.3	5.4	10.3	104.4	13.8	65.9	48.1	0.5	11.3	---
F	3195.1	D	588544.1,6107875.0	31.0	10.5	94.4	48.0	65.9	43.0	7.3	7.2	---
LINE 10330		**FLIGHT 29011**										
A	4734.6	B	586977.7,6107685.0	3.9	11.1	1.2	24.8	1.3	0.9	0.3	11.2	---
B	4750.3	H	587147.4,6107675.2	21.8	27.9	107.4	98.8	53.7	59.0	4.6	27.4	---
C	4814.4	H	588420.0,6107701.8	17.9	3.7	41.6	6.7	45.7	11.8	17.9	0.0	---
LINE 10340		**FLIGHT 29012**										
A	3521.8	H	586946.6,6107480.4	14.3	11.0	52.7	29.4	33.8	30.0	4.7	12.8	---
B	3572.0	B	587964.5,6107515.9	14.9	1.9	41.1	1.3	44.8	1.6	8.2	0.0	13.0
C	3589.0	B	588373.5,6107505.1	12.8	1.4	44.4	0.8	51.2	12.9	7.6	6.6	---
D	3627.4	D	589194.6,6107511.8	29.2	11.5	6.8	48.6	9.1	6.3	5.8	11.6	---
LINE 10350		**FLIGHT 29012**										
A	4437.7	D	587483.9,6107253.4	4.6	0.8	3.2	0.7	0.0	0.0	2.7	25.3	---
B	4430.1	B	587606.8,6107267.7	34.2	20.1	141.4	65.6	96.5	80.8	3.6	0.0	---
C	4421.8	H	587796.8,6107277.0	44.6	11.4	127.8	30.2	110.9	49.4	12.9	7.7	---
D	4405.4	H	588235.8,6107277.0	34.0	10.9	92.2	29.3	71.3	40.5	8.7	5.7	5.9
E	4360.9	H	589276.9,6107325.9	20.9	12.4	65.0	31.4	31.3	33.1	4.0	1.0	---
LINE 10360		**FLIGHT 29012**										
A	4596.8	H	586818.4,6107057.9	11.7	15.2	26.4	41.1	6.4	15.1	1.7	28.5	30.4
B	4637.6	H	587919.5,6107083.1	5.9	2.6	18.0	5.9	18.3	6.0	10.2	0.0	---

EM Anomaly List : JOB 10037, New Hazelton, BC

CX=COAXIAL,CP=COPLANAR			Note: EM amplitudes are local for types B,D,T and are absolute for all others	Estimated depth may be unreliable because the strongest part of the conductor may be deeper or to one side of the flight line, or because of a shallow dip or magnetite/overburden effects								
Label	Fid	Interp	XUTM (m), YUTM (m)	CXI5500_LLEVHz Real (ppm)	CXQ5500_LLEVHz Quad (ppm)	CPI7200_LLEVHz Real (ppm)	CPQ7200_LLEVHz Quad (ppm)	CPI900_LLEVHz Real (ppm)	CPQ900_LLEVHz Quad (ppm)	Conductance (siemens)	Depth (metres)	Magnetic Corr. (nT)
LINE 10370		**FLIGHT 29013**										
A	1553.8	H	586428.2,6106860.0	19.0	9.7	54.8	22.9	32.5	29.2	4.6	15.7	---
B	1623.3	H	587668.4,6106906.7	8.7	2.9	24.7	6.5	24.8	9.1	9.9	0.0	---
LINE 10371		**FLIGHT 29013**										
A	1965.9	S	592951.8,6106997.0	8.1	21.3	24.3	67.1	-9.3	18.7	1.0	0.0	---
LINE 10380		**FLIGHT 29013**										
A	2173.8	S?	593136.1,6106805.1	4.8	9.4	19.8	34.7	-2.8	13.1	1.0	1.1	31.1
LINE 10381		**FLIGHT 29013**										
A	2515.4	H	586123.9,6106636.4	10.1	7.1	33.7	19.4	19.3	14.4	4.6	27.4	---
B	2504.0	H	586424.0,6106646.7	24.7	16.3	65.9	46.2	30.4	32.0	4.0	29.6	---
C	2472.2	H	587260.8,6106662.4	5.8	3.9	21.7	8.3	16.5	9.2	5.7	3.5	25.6
LINE 10394		**FLIGHT 29017**										
A	2211.0	H	586255.6,6106444.3	9.2	6.2	28.2	17.7	17.6	17.4	3.6	17.7	---
B	2187.0	H	586975.7,6106458.2	5.0	2.4	13.2	5.3	12.3	9.8	3.8	0.0	24.4
LINE 10400		**FLIGHT 29016**										
A	3027.2	S	592958.9,6106390.0	1.1	2.3	5.2	5.9	-0.2	2.8	1.0	0.0	---
LINE 10403		**FLIGHT 29029**										
A	2645.3	H	586278.1,6106242.8	10.7	5.5	28.4	15.8	9.9	15.0	2.3	15.4	---
LINE 10414		**FLIGHT 29017**										
A	3114.8	H	586355.2,6106071.4	12.6	12.5	39.4	30.5	8.8	21.1	1.8	13.9	16.7

EM Anomaly List : JOB 10037, New Hazelton, BC

CX=COAXIAL,CP=COPLANAR			Note: EM amplitudes are local for types B,D,T and are absolute for all others	Estimated depth may be unreliable because the strongest part of the conductor may be deeper or to one side of the flight line, or because of a shallow dip or magnetite/overburden effects								
Label	Fid	Interp	XUTM (m), YUTM (m)	CXI5500_LLEVHz Real (ppm)	CXQ5500_LLEVHz Quad (ppm)	CPI7200_LLEVHz Real (ppm)	CPQ7200_LLEVHz Quad (ppm)	CPI900_LLEVHz Real (ppm)	CPQ900_LLEVHz Quad (ppm)	Conductance (siemens)	Depth (metres)	Magnetic Corr. (nT)
B	3007.2	H?	588469.7,6106122.4	7.4	12.6	22.2	40.4	3.1	13.1	1.1	12.2	7.7
LINE 10425		**FLIGHT 29017**										
A	3425.4	H	588596.6,6105889.2	6.1	8.2	19.8	19.5	8.7	9.9	2.7	43.2	8.0
B	3481.2	H	589816.8,6105953.6	3.8	4.4	12.0	4.1	7.0	8.4	2.4	0.0	---
LINE 10434		**FLIGHT 29017**										
A	3928.6	/	587370.7,6105685.3	15.0	5.1	19.7	7.3	0.5	9.8	5.8	17.0	14.7
B	3878.1	H	588648.9,6105708.7	15.7	15.7	33.4	36.9	16.8	19.4	3.2	25.1	---
LINE 10440		**FLIGHT 29016**										
A	3872.7	H	595691.0,6105629.0	7.8	13.9	30.8	45.8	2.9	16.2	1.4	10.5	---
LINE 10444		**FLIGHT 29017**										
A	4014.7	H	587444.6,6105477.4	26.1	15.6	64.6	31.7	36.8	35.4	4.5	19.0	6.7
B	4042.4	H	587912.8,6105487.4	13.1	17.1	40.1	39.4	23.2	19.5	4.4	43.3	---
C	4091.2	H	588666.2,6105501.6	17.3	17.2	46.3	42.0	30.9	25.5	4.9	38.0	---
D	4145.3	B	589794.7,6105515.4	13.5	3.3	32.6	8.9	36.8	23.7	9.0	6.5	8.1
LINE 10450		**FLIGHT 29016**										
A	4199.8	S	592851.1,6105377.1	0.2	5.4	-5.7	18.6	-0.7	4.2	1.0	0.0	---
B	4139.6	S	594542.7,6105411.0	3.0	12.0	6.7	36.9	-2.6	8.5	1.0	0.0	---
LINE 10455		**FLIGHT 29023**										
A	1428.3	B	587793.7,6105314.5	13.6	2.1	14.8	8.6	15.5	12.5	6.8	19.2	---
B	1409.4	D	588354.3,6105296.3	9.7	7.5	16.5	10.0	0.0	6.8	1.7	28.0	---
C	1397.1	H	588699.1,6105311.0	41.9	28.8	110.9	73.7	62.9	57.2	5.6	25.5	---

EM Anomaly List : JOB 10037, New Hazelton, BC

CX=COAXIAL,CP=COPLANAR			Note: EM amplitudes are local for types B,D,T and are absolute for all others	Estimated depth may be unreliable because the strongest part of the conductor may be deeper or to one side of the flight line, or because of a shallow dip or magnetite/overburden effects								
Label	Fid	Interp	XUTM (m), YUTM (m)	CXI5500_LLEVHz Real (ppm)	CXQ5500_LLEVHz Quad (ppm)	CPI7200_LLEVHz Real (ppm)	CPQ7200_LLEVHz Quad (ppm)	CPI900_LLEVHz Real (ppm)	CPQ900_LLEVHz Quad (ppm)	Conductance (siemens)	Depth (metres)	Magnetic Corr. (nT)
LINE 10460		**FLIGHT 29016**										
A	4436.9	H	595693.0,6105239.6	4.7	6.6	18.1	21.4	4.1	9.4	1.5	11.4	---
LINE 10465		**FLIGHT 29023**										
A	1660.4	H	588190.9,6105111.5	27.7	17.2	77.9	35.9	50.3	38.6	6.0	23.1	---
B	1684.5	H	588678.9,6105121.6	33.2	18.9	94.0	42.6	54.4	47.9	5.5	11.5	---
C	1740.2	E	589670.3,6105125.2	28.6	39.0	113.3	119.2	24.6	46.4	1.2	0.0	---
LINE 10472		**FLIGHT 29017**										
A	1331.3	H?	593288.7,6104997.1	4.8	5.7	10.1	13.0	3.2	6.3	1.6	44.6	---
LINE 10474		**FLIGHT 29023**										
A	1920.1	H	588333.2,6104910.9	21.9	14.9	60.3	36.9	30.9	29.2	4.4	5.1	---
LINE 10485		**FLIGHT 29023**										
A	2125.9	H	588351.2,6104729.5	4.4	7.9	16.4	19.8	7.9	8.4	2.7	59.3	---
B	2199.3	H	589984.3,6104725.4	7.8	14.5	24.6	40.7	8.6	11.9	2.4	43.6	---
LINE 10500		**FLIGHT 29014**										
A	1108.3	H	588287.1,6104294.8	11.5	34.7	40.7	113.5	2.1	27.0	1.1	10.3	5.1
LINE 10510		**FLIGHT 29013**										
A	4682.2	S?	588406.7,6104083.7	12.2	30.6	61.1	103.6	4.4	28.8	1.0	0.0	---
LINE 10530		**FLIGHT 29013**										
A	4191.6	S	587799.1,6103709.0	11.2	23.9	45.1	71.8	5.7	21.7	1.0	0.0	---
B	4297.4	H?	589598.1,6103734.8	10.7	27.7	29.8	64.3	1.1	17.0	1.2	20.8	18.7

EM Anomaly List : JOB 10037, New Hazelton, BC

CX=COAXIAL,CP=COPLANAR		Note: EM amplitudes are local for types B,D,T and are absolute for all others	Estimated depth may be unreliable because the strongest part of the conductor may be deeper or to one side of the flight line, or because of a shallow dip or magnetite/overburden effects								
Label	Fid	Interp	XUTM (m), YUTM (m)	CXI5500_LLEVHz Real (ppm)	CXQ5500_LLEVHz Quad (ppm)	CPI7200_LLEVHz Real (ppm)	CPQ7200_LLEVHz Quad (ppm)	CPI900_LLEVHz Real (ppm)	CPQ900_LLEVHz Quad (ppm)	Conductance (siemens)	Depth (metres)	Magnetic Corr. (nT)
LINE 10540		**FLIGHT 29013**										
A	3841.5	H	586847.9,6103472.1	8.8	18.0	35.8	51.7	3.7	16.6	1.2	5.0	---
LINE 10542		**FLIGHT 29032**										
A	2935.5	H?	589571.0,6103496.0	3.9	5.0	13.4	11.1	5.0	7.7	1.9	12.4	5.1
LINE 10551		**FLIGHT 29013**										
A	3436.6	S	588114.9,6103311.3	11.3	30.8	47.9	99.7	4.3	26.8	1.0	0.0	---
LINE 10553		**FLIGHT 29013**										
A	3573.8	H?	589440.7,6103340.5	4.9	3.2	10.6	8.4	5.0	5.7	2.3	20.2	20.7
LINE 19010		**FLIGHT 29011**										
A	1855.3	H	586304.6,6107363.1	16.4	12.3	54.9	34.1	27.8	26.5	4.2	18.5	20.0
B	1879.9	H?	586298.3,6108126.5	11.8	17.0	52.6	56.5	18.5	26.3	2.8	32.1	43.7
C	1920.4	H	586276.2,6109506.2	8.5	7.5	29.3	20.9	29.2	10.4	10.7	58.0	---
LINE 19020		**FLIGHT 29011**										
A	2296.0	H	587345.9,6105265.5	2.9	5.1	12.8	8.8	7.3	6.2	3.1	17.6	---
B	2203.8	B?	587314.2,6107565.7	5.5	3.8	4.6	11.5	1.1	0.9	1.6	23.1	25.6
C	2118.9	B	587240.5,6109969.6	2.8	1.3	22.4	4.4	19.5	8.6	---	---	9.2
D	2077.4	H	587218.8,6111292.9	7.2	3.2	14.8	7.0	10.6	9.0	3.5	16.0	21.5
LINE 19030		**FLIGHT 29011**										
A	2580.8	S	588372.7,6104148.2	13.5	32.6	60.5	114.2	4.0	32.5	1.0	0.0	---
B	2692.4	H	588334.7,6106685.0	5.4	11.2	28.7	15.1	23.4	16.5	5.1	19.6	17.5

EM Anomaly List : JOB 10037, New Hazelton, BC

CX=COAXIAL,CP=COPLANAR			Note: EM amplitudes are local for types B,D,T and are absolute for all others	Estimated depth may be unreliable because the strongest part of the conductor may be deeper or to one side of the flight line, or because of a shallow dip or magnetite/overburden effects								
Label	Fid	Interp	XUTM (m), YUTM (m)	CXI5500_LLEVHz Real (ppm)	CXQ5500_LLEVHz Quad (ppm)	CPI7200_LLEVHz Real (ppm)	CPQ7200_LLEVHz Quad (ppm)	CPI900_LLEVHz Real (ppm)	CPQ900_LLEVHz Quad (ppm)	Conductance (siemens)	Depth (metres)	Magnetic Corr. (nT)
LINE 19031		**FLIGHT 29011**										
A	2859.6	H	588110.5,6108601.7	1.1	1.9	3.9	8.0	4.0	3.5	2.6	66.5	26.9
B	2932.7	H?	588253.9,6110947.5	6.5	5.6	21.4	11.2	9.0	12.4	2.4	6.1	27.5
C	2986.2	H	588151.8,6112132.2	2.7	2.8	13.6	10.4	4.6	6.3	2.0	50.6	---
LINE 19040		**FLIGHT 29011**										
A	3275.8	H	589336.4,6106960.1	8.6	3.9	27.4	6.5	23.9	11.6	7.3	16.7	---
B	3212.7	B?	589278.7,6108888.2	5.0	12.6	11.8	23.5	0.3	6.5	0.4	0.0	24.0
LINE 19041		**FLIGHT 29011**										
A	3503.8	H?	589390.2,6103359.3	4.2	5.4	15.6	14.2	5.2	10.3	1.7	14.9	19.3
LINE 19070		**FLIGHT 29016**										
A	2069.0	S?	592196.1,6113259.0	0.4	15.8	-1.5	34.9	-11.3	8.2	1.0	0.0	69.9
B	2058.9	S?	592220.8,6113455.7	0.6	13.9	3.4	36.4	-9.6	7.9	1.0	0.0	86.5
LINE 19075		**FLIGHT 29022**										
A	1474.4	S?	592951.6,6107102.1	4.8	33.5	25.4	113.4	-25.6	26.3	1.0	0.0	95.5
LINE 19090		**FLIGHT 29012**										
A	1328.7	S?	594337.9,6105696.4	0.3	8.7	9.2	42.4	-5.6	10.1	1.0	0.0	20.2
LINE 19100		**FLIGHT 29011**										
A	5273.4	S	595347.6,6106043.7	0.9	2.7	5.1	7.5	1.0	3.1	1.0	0.0	---

Anomalies Summary

Conductor Grade	No. of Responses
7	0
6	0
5	2
4	12
3	30
2	118
1	11
0	14
Total	187

Conductor Model	No. of Responses
L	0
D	18
/	3
\	1
T	0
B	53
H	81
S	25
E	6
M	0
Total	187

APPENDIX F

TESTS AND CALIBRATIONS

COSMIC CORRECTION COEFFICENTS

Job Number:	10037	**Crystal Pack Volume:**	One Crystal Pack 16.8 L Down, 4.2 L Up	**Spec Pack(s) Serial Number:**	5522
Date Flown:	8-Jul-10	**Helicopter Registration:**	C-FIDA	**Spec Console Type:**	RS500
Flight Number:	29015	**Database Name:**	cosmic_jul07.gdb	**Spec Console Serial Number:**	5522

LINE	AVERAGE TC_DOWN	Use Data Point	AVERAGE K_DOWN	Use Data Point	AVERAGE U_DOWN	Use Data Point	AVERAGE TH_DOWN	Use Data Point	AVERAGE U_UP	Use Data Point	AVERAGE COSMIC
7500	242.17200	☐	19.92308	☑	10.60615	☑	10.87692	☐	2.86769	☐	183.23000
8000	257.35125	☑	20.90323	☑	11.26523	☐	12.26523	☑	2.85305	☑	197.72641
8500	275.00403	☑	21.87903	☑	11.87097	☑	12.76613	☐	3.15726	☑	213.83272
9000	290.17241	☐	22.86590	☐	12.39464	☐	14.39080	☐	3.30268	☑	229.63983
9500	310.00733	☑	23.35165	☐	13.58242	☑	15.27106	☑	3.63004	☑	251.32843
10000	330.25000	☑	24.56597	☐	14.40972	☑	16.31250	☑	3.87500	☑	270.02139
10500	352.66667	☑	26.43590	☑	15.52747	☑	17.49451	☑	4.17582	☑	287.25091

Summary of Cosmic Correction Coefficents

	Cosmic Stripping (Slope)	Aircraft Background (Intercept)
TC	1.03757	51.85602
K	0.06231	8.54505
U	0.04644	2.00149
Th	0.05770	0.81925
U Up	0.01425	0.05469

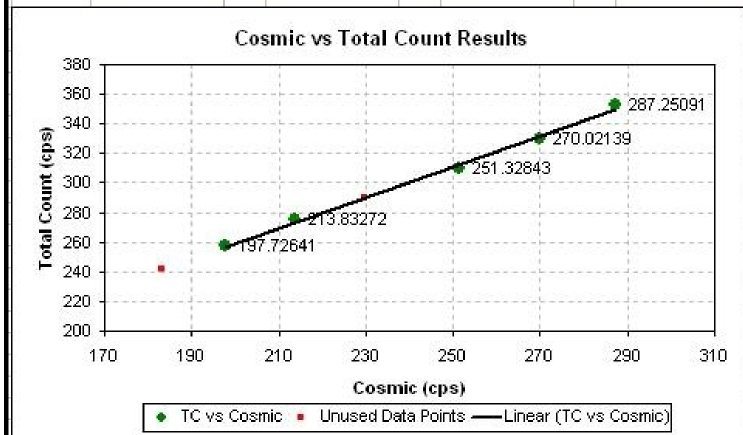

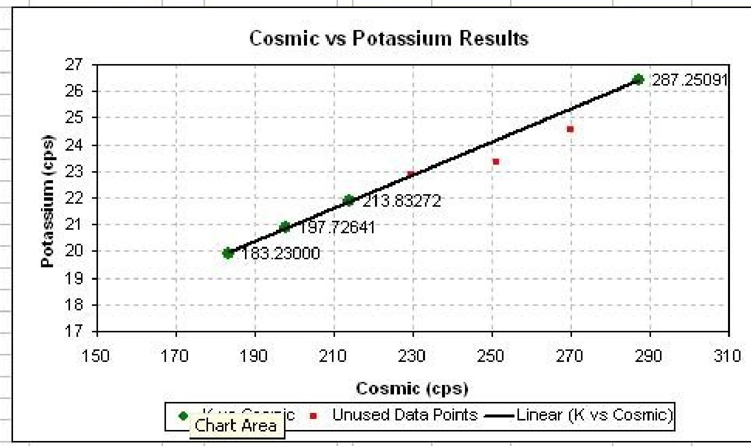

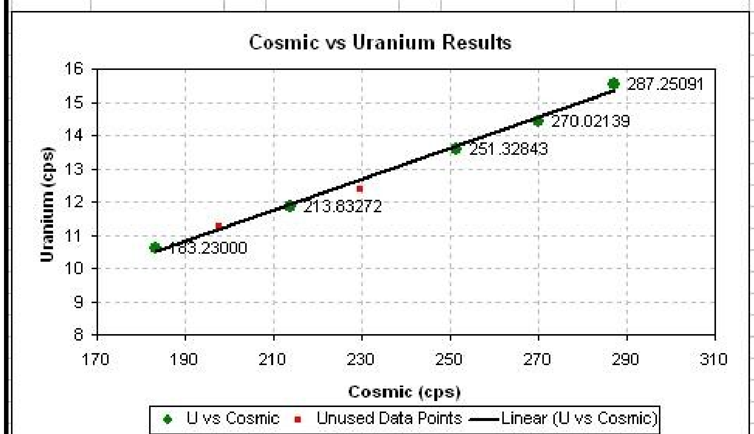

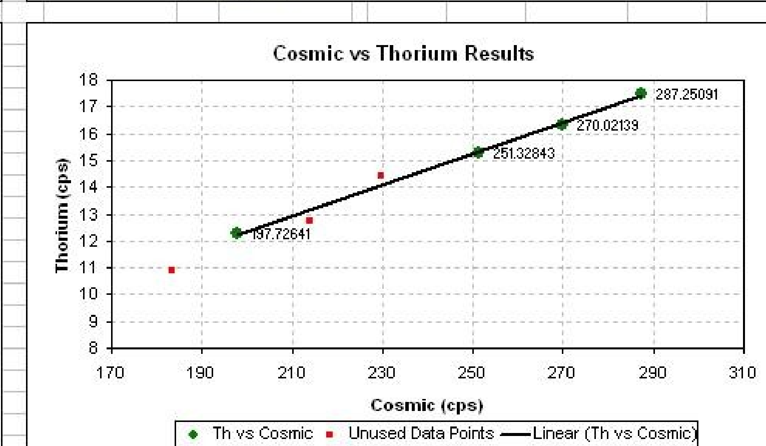

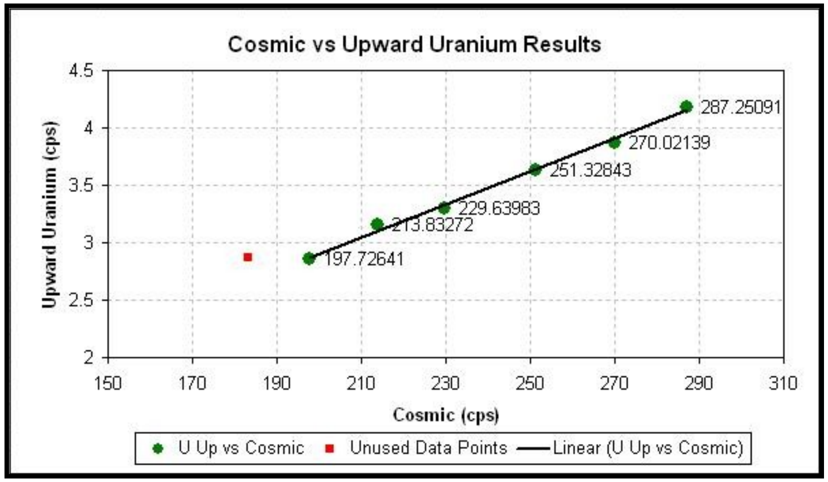

Cosmic vs Upward Uranium Results
Upward Uranium (cps)
4.5
4
3.5
3
2.5
2
150
170
190
210
230
250
270
290
310
Cosmic (cps)
287.25091
270.02139
251.32843
229.63983
213.83272
197.72641
U Up vs Cosmic
Unused Data Points
Linear (U Up vs Cosmic)

ALTITUDE ATTENUATION COEFFICENTS

Job Number:	10037	**Crystal Pack Volume:**	One Crystal Pack 16.8 L Down, 4.2 L Up	**pec Pack(s) Serial Number:**	
Date Flown:	8-Jul-10	**Helicopter Registration:**		**Spec Console Type:**	RS500
Flight Number:	29015	**Database Name:**		**pec Console Serial Number:**	

LINE	AVERAGE TC_DOWN_ ATTENCOR	Use Data Point	AVERAGE K_DOWN_ ATTENCOR	Use Data Point	AVERAGE U_DOWN_ ATTENCOR	Use Data Point	AVERAGE TH_DOWN_ ATTENCOR	Use Data Point	AVERAGE EFFECTIVE HEIGHT
100	540.53000	☐	52.88000	☑	9.98825	☑	8.20500	☑	43.67060
200	468.46000	☑	43.56000	☐	9.70400	☑	6.61980	☐	55.54040
300	368.40300	☑	31.96000	☑	7.44320	☐	5.63760	☑	82.95915
400	226.40000	☐	29.73000	☐	6.44220	☐	4.84010	☑	104.03770
500	274.30000	☑	20.44800	☑	6.46200	☑	3.63900	☑	138.27053
1000		☐		☐		☐		☐	
		☐		☐		☐		☐	
		☐		☐		☐		☐	
		☐		☐		☐		☐	

Summary of Altitude Attenuation Coefficents (Must Be Negative)	
TC	-0.00630
K	-0.00991
U	-0.00472
Th	-0.00854

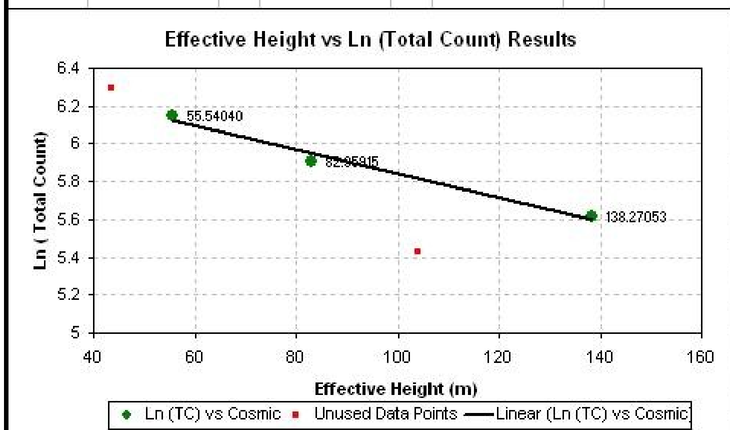

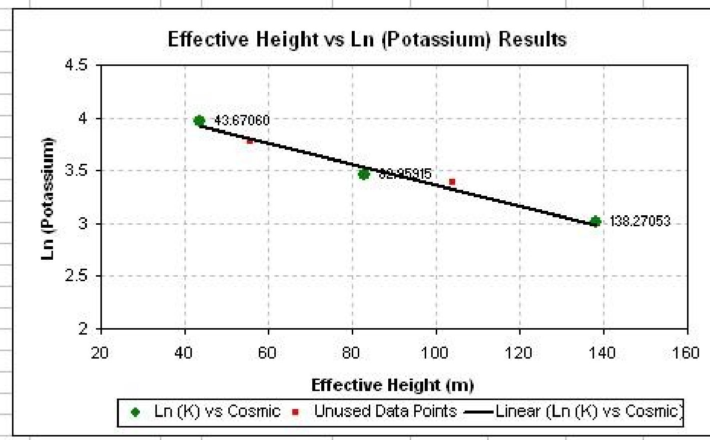

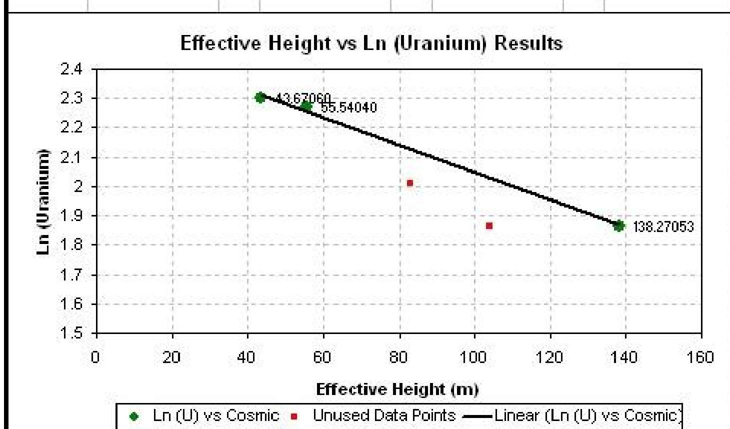

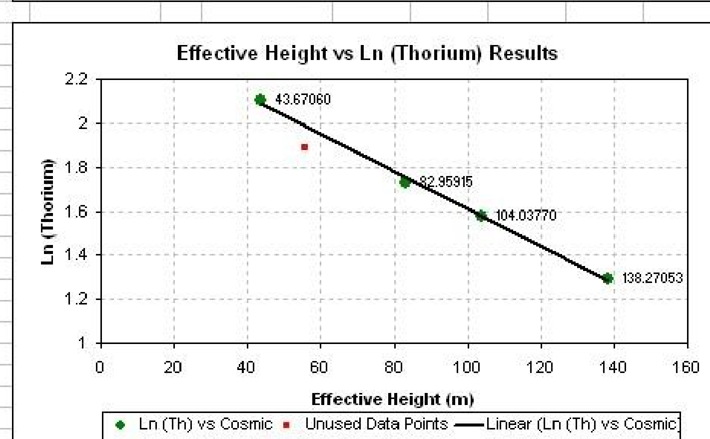

APPENDIX G

RADIOMETRIC PROCESSING CONTROL FILE

```
//////////////////////////////////////////////////
// Atlas Control/Workspace File
// # or // for commment
//////////////////////////////////////////////////

CONTROL_BEGIN

 PROGRAM  = AGSCorrection
 VERSION  = 1.4.0

  ### Process or Calibration? ###
    WhatToDo = Process Survey Line

  ### Corrections to apply ###
    CorrectionType = Yes  Filtering
    CorrectionType = Yes  LiveTimeCorrection
    CorrectionType = Yes  CosmicAircraftBGRemove
    CorrectionType = Yes  CalcEffectiveHeight
    CorrectionType = No   RadonBGRemove
    CorrectionType = Yes  ComptonStripping
    CorrectionType = Yes  HeightCorrection
    CorrectionType = Yes  ConvertToConcentration


  ### Main I/O settings ###
    MainChannelIO|TC       = TC_NASVD   --> TC_NASVD_Cor
    MainChannelIO|K        = K_NASVD    --> K_NASVD_Cor
    MainChannelIO|U        = U_NASVD    --> U_NASVD_Cor
    MainChannelIO|Th       = TH_NASVD   --> TH_NASVD_Cor
    MainChannelIO|UpU      = U_UP       --> U_UP_Cor
    MainChannelIO|Cosmic   = COSMIC     --> COSMIC_Cor
    MainChannelIO|Spectrum =            -->

  ### Control Channel I/O settings ###
    ControlChannel|RadarAltimeter     = ALTRAD_HELI  [metres]
    ControlChannel|Pressure/Barometer = KPA          [kPa]
    ControlChannel|Temperature        = TEMP_EXT


  ### Input for correction ###
    InputForCorrection    = ROIs


  ### Negative count handling ###
    NegativeCountHandlingROI          = 0    //-1: Allow negative  0:Replace with zero
1:Replace with dummy
    NegativeCountHandlingFullSpectrum = 0    //-1: Allow negative  0:Replace with zero
```

```
### Pre-filtering settings ###
   Filtering|TC      = 0
   Filtering|K       = 0
   Filtering|U       = 0
   Filtering|Th      = 0
   Filtering|UpU     = 0
   Filtering|Cosmic  = 9
   Filtering|RadarAltimeter     = 3
   Filtering|Pressure/Barometer = 3
   Filtering|Temperature        = 3

### Live-time correction settings ###
   LiveTimeChannel            = LIVE_TIME
   LiveTimeUnits              = milli-seconds
   ApplyLiveTimeCorrToUpU     = Yes

### Cosmic correction settings ###
   CosmicCorrParam|TC      = 1.036390,  52.166861
   CosmicCorrParam|K       = 0.062325,  8.544426
   CosmicCorrParam|U       = 0.047416,  1.904960
   CosmicCorrParam|Th      = 0.057701,  0.819269
   CosmicCorrParam|UpU     = 0.014254,  0.054672
   CosmicCorrParam|SpectrumBackgroundFile    =

### Effective-Height settings ###
   EffectiveHeightOutputChannel = EffectiveHeight
   EffectiveHeightOutputUnits   = metres

### Special Stripping (Compton Stripping) ###
   ComptonCorrParam_Stripping_Alpha     = 0.276000
   ComptonCorrParam_Stripping_Beta      = 0.417000
   ComptonCorrParam_Stripping_Gamma     = 0.754000
   ComptonCorrParam_AlphaPerMetre       = 0.000001
   ComptonCorrParam_BetaPerMetre        = 0.000001
   ComptonCorrParam_GammaPerMetre       = 0.000001
   ComptonCorrParam_GrastyBackscatter_a = 0.043000
   ComptonCorrParam_GrastyBackscatter_b = 0.000000
   ComptonCorrParam_GrastyBackscatter_g = 0.000000

### Height Correction settings ###
   SurveyHeightDatum     = 60.000000
   AttenuationCorrControl = 1
   AttenuationForNegROIs  = Yes
   HeightCorrParam|TC      = -0.006485, 300.000000
   HeightCorrParam|K       = -0.009986, 300.000000
   HeightCorrParam|U       = -0.004718, 300.000000
   HeightCorrParam|Th      = -0.008543, 300.000000
```

```
  ### Concentration settings ###
    ConcentrationParam|K       = Concentration_K,  58.200000
    ConcentrationParam|U       = Concentration_U,  6.480000
    ConcentrationParam|Th      = Concentration_Th,  3.780000
    AirAbsorbedDoseRateParam   = DoseRate,  19.600000
    NaturalAirAbsorbedDoseRateParam = NaturalDoseRate,  13.078000, 5.675000,
2.494000

CONTROL_END
```

APPENDIX H

GLOSSARY

GLOSSARY OF AIRBORNE GEOPHYSICAL TERMS

Note: The definitions given in this glossary refer to the common terminology as used in airborne geophysics.

altitude attenuation: the absorption of gamma rays by the atmosphere between the earth and the detector. The number of gamma rays detected by a system decreases as the altitude increases.

apparent- : the ***physical parameters*** of the earth measured by a geophysical system are normally expressed as apparent, as in “apparent ***resistivity*****”**. This means that the measurement is limited by assumptions made about the geology in calculating the response measured by the geophysical system. Apparent resistivity calculated with ***HEM***, for example, generally assumes that the earth is a ***homogeneous half-space*** – not layered.

amplitude: The strength of the total electromagnetic field. In ***frequency domain*** it is most often the sum of the squares of ***in-phase*** and ***quadrature*** components. In multi-component electromagnetic surveys it is generally the sum of the squares of all three directional components.

analytic signal: The total amplitude of all the directions of magnetic ***gradient***. Calculated as the sum of the squares.

anisotropy: Having different ***physical parameters*** in different directions. This can be caused by layering or fabric in the geology. Note that a unit can be anisotropic, but still **homogeneous**.

anomaly: A localized change in the geophysical data characteristic of a discrete source, such as a conductive or magnetic body. Something locally different from the **background**.

B-field: In time-domain **electromagnetic** surveys, the magnetic field component of the (electromagnetic) **field**. This can be measured directly, although more commonly it is calculated by integrating the time rate of change of the magnetic field **dB/dt**, as measured with a receiver coil.

background: The “normal” response in the geophysical data – that response observed over most of the survey area. **Anomalies** are usually measured relative to the background. In airborne gamma-ray spectrometric surveys the term defines the **cosmic**, radon, and aircraft responses in the absence of a signal from the ground.

base-level: The measured values in a geophysical system in the absence of any outside signal. All geophysical data are measured relative to the system base level.

base frequency: The frequency of the pulse repetition for a ***time-domain electromagnetic*** system. Measured between subsequent positive pulses.

bird: A common name for the pod towed beneath or behind an aircraft, carrying the geophysical sensor array.

calibration coil: A wire coil of known size and dipole moment, which is used to generate a field of known ***amplitude*** and ***phase*** in the receiver, for system calibration. Calibration coils can be external, or internal to the system. Internal coils may be called Q-coils.

coaxial coils: **[CX]** Coaxial coils are in the vertical plane, with their axes horizontal and collinear in the flight direction. These are most sensitive to vertical conductive objects in the ground, such as thin, steeply dipping conductors perpendicular to the flight direction. Coaxial coils generally give the sharpest anomalies over localized conductors. (See also ***coplanar coils***)

coil: A multi-turn wire loop used to transmit or detect electromagnetic fields. Time varying ***electromagnetic*** fields through a coil induce a voltage proportional to the strength of the field and the rate of change over time.

compensation: Correction of airborne geophysical data for the changing effect of the aircraft. This process is generally used to correct data in ***fixed-wing time-domain electromagnetic*** surveys (where the transmitter is on the aircraft and the receiver is moving), and magnetic surveys (where the sensor is on the aircraft, turning in the earth's magnetic field.

component: In ***frequency domain electromagnetic*** surveys this is one of the two **phase** measurements – ***in-phase or quadrature***. In "multi-component" electromagnetic surveys it is also used to define the measurement in one geometric direction (vertical, horizontal in-line and horizontal transverse – the Z, X and Y components).

Compton scattering: gamma ray photons will bounce off the nuclei of atoms they pass through (earth and atmosphere), reducing their energy and then being detected by ***radiometric*** sensors at lower energy levels. See also ***stripping***.

conductance: See ***conductivity thickness***

conductivity: [σ] The facility with which the earth or a geological formation conducts electricity. Conductivity is usually measured in milli-Siemens per metre (mS/m). It is the reciprocal of ***resistivity***.

conductivity-depth imaging: see ***conductivity-depth transform***.

conductivity-depth transform: A process for converting electromagnetic measurements to an approximation of the conductivity distribution vertically in the earth, assuming a ***layered earth***. (Macnae and Lamontagne, 1987; Wolfgram and Karlik, 1995)

conductivity thickness: [**σt**] The product of the ***conductivity***, and thickness of a large, tabular body. (It is also called the "conductivity-thickness product") In electromagnetic geophysics, the response of a thin plate-like conductor is proportional to the conductivity multiplied by thickness. For example a 10 metre thickness of 20 Siemens/m mineralization will be equivalent to 5 metres of 40 S/m; both have 200 S conductivity thickness. Sometimes referred to as conductance.

conductor: Used to describe anything in the ground more conductive than the surrounding geology. Conductors are most often clays or graphite, or hopefully some type of mineralization, but may also be man-made objects, such as fences or pipelines.

coplanar coils: **[CP]** The coplanar coils lie in the horizontal plane with their axes vertical, and parallel. These coils are most sensitive to massive conductive bodies, horizontal layers, and the ***halfspace***.

cosmic ray: High energy sub-atomic particles from outer space that collide with the earth's atmosphere to produce a shower of gamma rays (and other particles) at high energies.

counts (per second): The number of ***gamma-rays*** detected by a gamma-ray ***spectrometer*.** The rate depends on the geology, but also on the size and sensitivity of the detector.

culture: A term commonly used to denote any man-made object that creates a geophysical anomaly. Includes, but not limited to, power lines, pipelines, fences, and buildings.

current gathering: The tendency of electrical currents in the ground to channel into a conductive formation. This is particularly noticeable at higher frequencies or early time channels when the formation is long and parallel to the direction of current flow. This tends to enhance anomalies relative to inductive currents (see also ***induction***). Also known as current channelling.

current channelling: See current gathering.

daughter products: The radioactive natural sources of gamma-rays decay from the original element (commonly potassium, uranium, and thorium) to one or more lower-energy elements. Some of these lower energy elements are also radioactive and decay further. ***Gamma-ray spectrometry*** surveys may measure the gamma rays given off by the original element or by the decay of the daughter products.

dB/dt: As the ***secondary electromagnetic field*** changes with time, the magnetic field [**B**] component induces a voltage in the receiving ***coil***, which is proportional to the rate of change of the magnetic field over time.

decay: In ***time-domain electromagnetic*** theory, the weakening over time of the ***eddy currents*** in the ground, and hence the ***secondary field*** after the ***primary field*** electromagnetic pulse is turned off. In ***gamma-ray spectrometry***, the radioactive breakdown of an element, generally potassium, uranium, thorium, or one of their ***daughter*** products.

decay series: In ***gamma-ray spectrometry***, a series of progressively lower energy ***daughter products*** produced by the radioactive breakdown of uranium or thorium.

decay constant: see time constant.

depth of exploration: The maximum depth at which the geophysical system can detect the target. The depth of exploration depends very strongly on the type and size of the target, the contrast of the target with the surrounding geology, the homogeneity of the surrounding geology, and the type of geophysical system. One measure of the maximum depth of exploration for an electromagnetic system is the depth at which it can detect the strongest conductive target – generally a highly conductive horizontal layer.

differential resistivity: A process of transforming ***apparent resistivity*** to an approximation of layer resistivity at each depth. The method uses multi-frequency HEM data and approximates the effect of shallow layer ***conductance*** determined from higher frequencies to estimate the deeper conductivities (Huang and Fraser, 1996)

dipole moment: [NIA] For a transmitter, the product of the area of a ***coil***, the number of turns of wire, and the current flowing in the coil. At a distance significantly larger than the size of the coil, the magnetic field from a coil will be the same if the dipole moment product is the same. For a receiver coil, this is the product of the area and the number of turns. The sensitivity to a magnetic field (assuming the source is far away) will be the same if the dipole moment is the same.

diurnal: The daily variation in a natural field, normally used to describe the natural fluctuations (over hours and days) of the earth's magnetic field.

dielectric permittivity: **[ε]** The capacity of a material to store electrical charge, this is most often measured as the relative permittivity [ε_r], or ratio of the material dielectric to that of free space. The effect of high permittivity may be seen in HEM data at high frequencies over highly resistive geology as a reduced or negative ***in-phase***, and higher ***quadrature*** data.

drift: Long-time variations in the base-level or calibration of an instrument.

eddy currents: The electrical currents induced in the ground, or other conductors, by a time-varying ***electromagnetic field*** (usually the ***primary field***). Eddy currents are also induced in the aircraft's metal frame and skin; a source of ***noise*** in EM surveys.

electromagnetic: **[EM]** Comprised of a time-varying electrical and magnetic field. Radio waves are common electromagnetic fields. In geophysics, an electromagnetic system is one which transmits a time-varying ***primary field*** to induce ***eddy currents*** in the ground, and then measures the ***secondary field*** emitted by those eddy currents.

energy window: A broad spectrum of ***gamma-ray*** energies measured by a spectrometric survey. The energy of each gamma-ray is measured and divided up into numerous discrete energy levels, called windows.

equivalent (thorium or uranium): The amount of radioelement calculated to be present, based on the gamma-rays measured from a **daughter** element. This assumes that the ***decay series*** is in equilibrium – progressing normally.

fiducial, or fid: Timing mark on a survey record. Originally these were timing marks on a profile or film; now the term is generally used to describe 1-second interval timing records in digital data, and on maps or profiles.

fixed-wing: Aircraft with wings, as opposed to “rotary wing” helicopters.

footprint: This is a measure of the area of sensitivity under the aircraft of an airborne geophysical system. The footprint of an ***electromagnetic*** system is dependent on the altitude of the system, the orientation of the transmitter and receiver and the separation between the receiver and transmitter, and the conductivity of the ground. The footprint of a ***gamma-ray spectrometer*** depends mostly on the altitude. For all geophysical systems, the footprint also depends on the strength of the contrasting ***anomaly***.

frequency domain: An ***electromagnetic*** system which transmits a ***primary field*** that oscillates smoothly over time (sinusoidal), inducing a similarly varying electrical current in the ground. These systems generally measure the changes in the ***amplitude*** and ***phase*** of the ***secondary field*** from the ground at different frequencies by measuring the **in-phase** and **quadrature** phase components. See also ***time-domain***.

full-stream data: Data collected and recorded continuously at the highest possible sampling rate. Normal data are stacked (see ***stacking***) over some time interval before recording.

gamma-ray: A very high-energy photon, emitted from the nucleus of an atom as it undergoes a change in energy levels.

gamma-ray spectrometry: Measurement of the number and energy of natural (and sometimes man-made) gamma-rays across a range of photon energies.

gradient: In magnetic surveys, the gradient is the change of the magnetic field over a distance, either vertically or horizontally in either of two directions. Gradient data is often measured, or calculated from the total magnetic field data because it changes more quickly over distance than the ***total magnetic field***, and so may provide a more precise measure of the location of a source. See also ***analytic signal***.

ground effect: The response from the earth. A common calibration procedure in many geophysical surveys is to fly to altitude high enough to be beyond any measurable response from the ground, and there establish ***base levels*** or ***backgrounds***.

half-space: A mathematical model used to describe the earth – as infinite in width, length, and depth below the surface. The most common halfspace models are ***homogeneous*** and ***layered earth***.

heading error: A slight change in the magnetic field measured when flying in opposite directions.

HEM: Helicopter ElectroMagnetic, This designation is most commonly used to helicopter-borne, ***frequency-domain*** electromagnetic systems. At present, the transmitter and receivers are normally mounted in a ***bird*** carried on a sling line beneath the helicopter.

herringbone pattern: a pattern created in geophysical data by an asymmetric system, where the **anomaly** may be extended to either side of the source, in the direction of flight. Appears like fish bones, or like the teeth of a comb, extending either side of centre, each tooth an alternate flight line.

homogeneous: This is a geological unit that has the same ***physical parameters*** throughout its volume. This unit will create the same response to an HEM system anywhere, and the HEM system will measure the same apparent ***resistivity*** anywhere. The response may change with system direction (see ***anisotropy***).

in-phase: the component of the measured ***secondary field*** that has the same phase as the transmitter and the ***primary field***. The in-phase component is stronger than the ***quadrature*** phase over relatively higher ***conductivity***.

induction: Any time-varying electromagnetic field will induce (cause) electrical currents to flow in any object with non-zero ***conductivity***. (see ***eddy currents***)

infinite: In geophysical terms, an "infinite' dimension is one much greater than the ***footprint*** of the system, so that the system does not detect changes at the edges of the object.

International Geomagnetic Reference Field: **[IGRF]** An approximation of the smooth magnetic field of the earth, in the absence of variations due to local geology. Once the IGRF is subtracted from the measured magnetic total field data, any remaining variations are assumed to be due to local geology. The IGRF also predicts the slow changes of the field up to five years in the future.

inversion, or **inverse modeling**: A process of converting geophysical data to an earth model, which compares theoretical models of the response of the earth to the data measured, and refines the model until the response closely fits the measured data (Huang and Palacky, 1991)

layered earth: A common geophysical model which assumes that the earth is horizontally layered – the ***physical parameters*** are constant to ***infinite*** distance horizontally, but change vertically.

magnetic permeability: **[μ]** This is defined as the ratio of magnetic induction to the inducing magnetic field. The relative magnetic permeability [μ_r] is often quoted, which is the ratio of the rock permeability to the permeability of free space. In geology and geophysics, the ***magnetic susceptibility*** is more commonly used to describe rocks.

magnetic susceptibility: **[k]** A measure of the degree to which a body is magnetized. In SI units this is related to relative ***magnetic permeability*** by $k=\mu_r-1$, and is a dimensionless unit. For most geological material, susceptibility is influenced primarily by the percentage of magnetite. It is most often quoted in units of 10^{-6}. In HEM data this is most often apparent as a negative ***in-phase*** component over high susceptibility, high ***resistivity*** geology such as diabase dikes.

noise: That part of a geophysical measurement that the user does not want. Typically this includes electronic interference from the system, the atmosphere (***sferics***), and man-made sources. This can be a subjective judgment, as it may include the response from geology other than the target of interest. Commonly the term is used to refer to high frequency (short period) interference. See also ***drift***.

Occam's inversion: an ***inversion*** process that matches the measured ***electromagnetic*** data to a theoretical model of many, thin layers with constant thickness and varying resistivity (Constable et al, 1987).

off-time: In a ***time-domain electromagnetic*** survey, the time after the end of the ***primary field pulse***, and before the start of the next pulse.

on-time: In a ***time-domain electromagnetic*** survey, the time during the ***primary field pulse***.

phase: The angular difference in time between a measured sinusoidal electromagnetic field and a reference – normally the primary field. The phase is calculated from $\tan^{-1}$(***in-phase / quadrature***).

physical parameters: These are the characteristics of a geological unit. For electromagnetic surveys, the important parameters for electromagnetic surveys are ***conductivity, magnetic permeability*** (or ***susceptibility***) and ***dielectric permittivity***; for magnetic surveys the parameter is magnetic susceptibility, and for gamma ray spectrometric surveys it is the concentration of the major radioactive elements: potassium, uranium, and thorium.

permittivity: see ***dielectric permittivity***.

permeability: see ***magnetic permeability***.

primary field: the EM field emitted by a transmitter. This field induces ***eddy currents*** in (energizes) the conductors in the ground, which then create their own ***secondary* fields**.

pulse: In time-domain EM surveys, the short period of intense ***primary*** field transmission. Most measurements (the ***off-time***) are measured after the pulse.

quadrature: that component of the measured ***secondary field*** that is phase-shifted 90° from the ***primary field***. The quadrature component tends to be stronger than the ***in-phase*** over relatively weaker ***conductivity***.

Q-coils: see ***calibration coil***.

radiometric: Commonly used to refer to ***gamma ray*** spectrometry.

radon: A radioactive daughter product of uranium and thorium, radon is a gas which can leak into the atmosphere, adding to the non-geological background of a gamma-ray spectrometric survey.

resistivity: **[ρ]** The strength with which the earth or a geological formation resists the flow of electricity, typically the flow induced by the ***primary field*** of the electromagnetic transmitter. Normally expressed in ohm-metres, it is the reciprocal of ***conductivity***.

resistivity-depth transforms: similar to ***conductivity depth transforms***, but the calculated ***conductivity*** has been converted to ***resistivity***.

resistivity section: an approximate vertical section of the resistivity of the layers in the earth. The resistivities can be derived from the ***apparent resistivity***, the ***differential resistivities***, ***resistivity-depth transforms***, or ***inversions***.

secondary field: The field created by conductors in the ground, as a result of electrical currents induced by the ***primary field*** from the ***electromagnetic*** transmitter. Airborne ***electromagnetic*** systems are designed to create, and measure a secondary field.

Sengpiel section: a ***resistivity section*** derived using the ***apparent resistivity*** and an approximation of the depth of maximum sensitivity for each frequency.

sferic: Lightning, or the ***electromagnetic*** signal from lightning, it is an abbreviation of “atmospheric discharge”. These appear to magnetic and electromagnetic sensors as sharp “spikes” in the data. Under some conditions lightning storms can be detected from hundreds of kilometres away. (see ***noise***)

signal: That component of a measurement that the user wants to see – the response from the targets, from the earth, etc. (See also ***noise***)

skin depth: A measure of the depth of penetration of an electromagnetic field into a material. It is defined as the depth at which the primary field decreases to 1/e of the field at the surface. It is calculated by approximately 503 x √(resistivity/frequency). Note that depth of penetration is greater at higher ***resistivity*** and/or lower ***frequency***.

spectrometry: Measurement across a range of energies, where ***amplitude*** and energy are defined for each measurement. In gamma-ray spectrometry, the number of gamma rays are measured for each energy ***window***, to define the ***spectrum***.

spectrum: In ***gamma ray spectrometry***, the continuous range of energy over which gamma rays are measured. In ***time-domain electromagnetic*** surveys, the spectrum is the energy of the **pulse** distributed across an equivalent, continuous range of frequencies.

spheric: see ***sferic***.

stacking: Summing repeat measurements over time to enhance the repeating ***signal***, and minimize the random ***noise***.

stripping: Estimation and correction for the gamma ray photons of higher and lower energy that are observed in a particular ***energy window***. See also ***Compton scattering***.

susceptibility: See ***magnetic susceptibility***.

tau: [τ] Often used as a name for the ***time constant***.

TDEM: ***time domain electromagnetic***.

thin sheet: A standard model for electromagnetic geophysical theory. It is usually defined as thin, flat-lying, and ***infinite*** in both horizontal directions. (see also ***vertical plate***)

tie-line: A survey line flown across most of the ***traverse lines***, generally perpendicular to them, to assist in measuring ***drift*** and ***diurnal*** variation. In the short time required to fly a tie-line it is assumed that the drift and/or diurnal will be minimal, or at least changing at a constant rate.

time constant: The time required for an ***electromagnetic*** field to decay to a value of 1/e of the original value. In ***time-domain*** electromagnetic data, the time constant is proportional to the size and ***conductance*** of a tabular conductive body. Also called the decay constant.

Time channel: In ***time-domain electromagnetic*** surveys the decaying ***secondary field*** is measured over a period of time, and the divided up into a series of consecutive discrete measurements over that time.

time-domain: ***Electromagnetic*** system which transmits a pulsed, or stepped ***electromagnetic*** field. These systems induce an electrical current (***eddy current***) in the ground that persists after the ***primary field*** is turned off, and measure the change over time of the ***secondary field*** created as the currents ***decay***. See also ***frequency-domain***.

total energy envelope: The sum of the squares of the three ***components*** of the ***time-domain electromagnetic secondary field***. Equivalent to the ***amplitude*** of the secondary field.

transient: Time-varying. Usually used to describe a very short period pulse of ***electromagnetic*** field.

traverse line: A normal geophysical survey line. Normally parallel traverse lines are flown across the property in spacing of 50 m to 500 m, and generally perpendicular to the target geology.

vertical plate: A standard model for electromagnetic geophysical theory. It is usually defined as thin, and ***infinite*** in horizontal dimension and depth extent. (see also ***thin shee***t)

waveform: The shape of the ***electromagnetic pulse*** from a ***time-domain*** electromagnetic transmitter.

window: A discrete portion of a ***gamma-ray spectrum*** or ***time-domain electromagnetic decay***. The continuous energy spectrum or ***full-stream*** data are grouped into windows to reduce the number of samples, and reduce ***noise***.

Version 1.1, March 10, 2003
Greg Hodges,
Chief Geophysicist
Fugro Airborne Surveys, Toronto

Common Symbols and Acronyms

k Magnetic susceptibility
ε Dielectric permittivity
μ, μ_r Magnetic permeability, apparent permeability
ρ, ρ_a Resistivity, apparent resistivity
σ,σ_a Conductivity, apparent conductivity
σt Conductivity thickness
τ Tau, or time constant
Ω.m Ohm-metres, units of resistivity
AGS Airborne gamma ray spectrometry.
CDT Conductivity-depth transform, conductivity-depth imaging (Macnae and Lamontagne, 1987; Wolfgram and Karlik, 1995)
CPI, CPQ Coplanar in-phase, quadrature
CPS Counts per second
CTP Conductivity thickness product
CXI, CXQ Coaxial, in-phase, quadrature
fT femtoteslas, normal unit for measurement of B-Field
EM Electromagnetic
keV kilo electron volts – a measure of gamma-ray energy
MeV mega electron volts – a measure of gamma-ray energy 1MeV = 1000keV
NIA dipole moment: turns x current x Area
nT nano-Tesla, a measure of the strength of a magnetic field
ppm parts per million – a measure of secondary field or noise relative to the primary.
pT/s picoTeslas per second: Units of decay of secondary field, dB/dt
S Siemens – a unit of conductance
x: the horizontal component of an EM field parallel to the direction of flight.
y: the horizontal component of an EM field perpendicular to the direction of flight.
z: the vertical component of an EM field.

References:

Constable, S.C., Parker, R.L., And Constable, C.G., 1987, Occam's inversion: a practical algorithm for generating smooth models from electromagnetic sounding data: Geophysics, 52, 289-300

Huang, H. and Fraser, D.C, 1996. The differential parameter method for muiltifrequency airborne resistivity mapping. Geophysics, 55, 1327-1337

Huang, H. and Palacky, G.J., 1991, Damped least-squares inversion of time-domain airborne EM data based on singular value decomposition: Geophysical Prospecting, v.39, 827-844

Macnae, J. and Lamontagne, Y., 1987, Imaging quasi-layered conductive structures by simple processing of transient electromagnetic data: Geophysics, v52, 4, 545-554.

Sengpiel, K-P. 1988, Approximate inversion of airborne EM data from a multi-layered ground. Geophysical Prospecting, 36, 446-459

Wolfgram, P. and Karlik, G., 1995, Conductivity-depth transform of GEOTEM data: Exploration Geophysics, 26, 179-185.

Yin, C. and Fraser, D.C. (2002), The effect of the electrical anisotropy on the responses of helicopter-borne frequency domain electromagnetic systems, Submitted to *Geophysical Prospecting*

TECHNICAL SUMMARY

Navigation	Differentially-corrected GPS
Data reduction grid interval	40 metres
Terrain clearance	Helicopter, Spectrometer 60 m Electromagnetic sensor 35 m Magnetometer 35 m
Data sampling interval	0.1 second
Magnetometer / sensitivity	Cesium / 0.01 nT
Electromagnetic system	DIGHEM^{V}
Spectrometer	RS-500
Spectrometer data sampling	1.0 second

Frequency	Sensitivity	Coil Orientation
1000 Hz	.06 ppm	Vertical coaxial
5500 Hz	.12 ppm	Vertical coaxial
900 Hz	.12 ppm	Horizontal coplanar
7200 Hz	.24 ppm	Horizontal coplanar
56000 Hz	.60 ppm	Horizontal coplanar

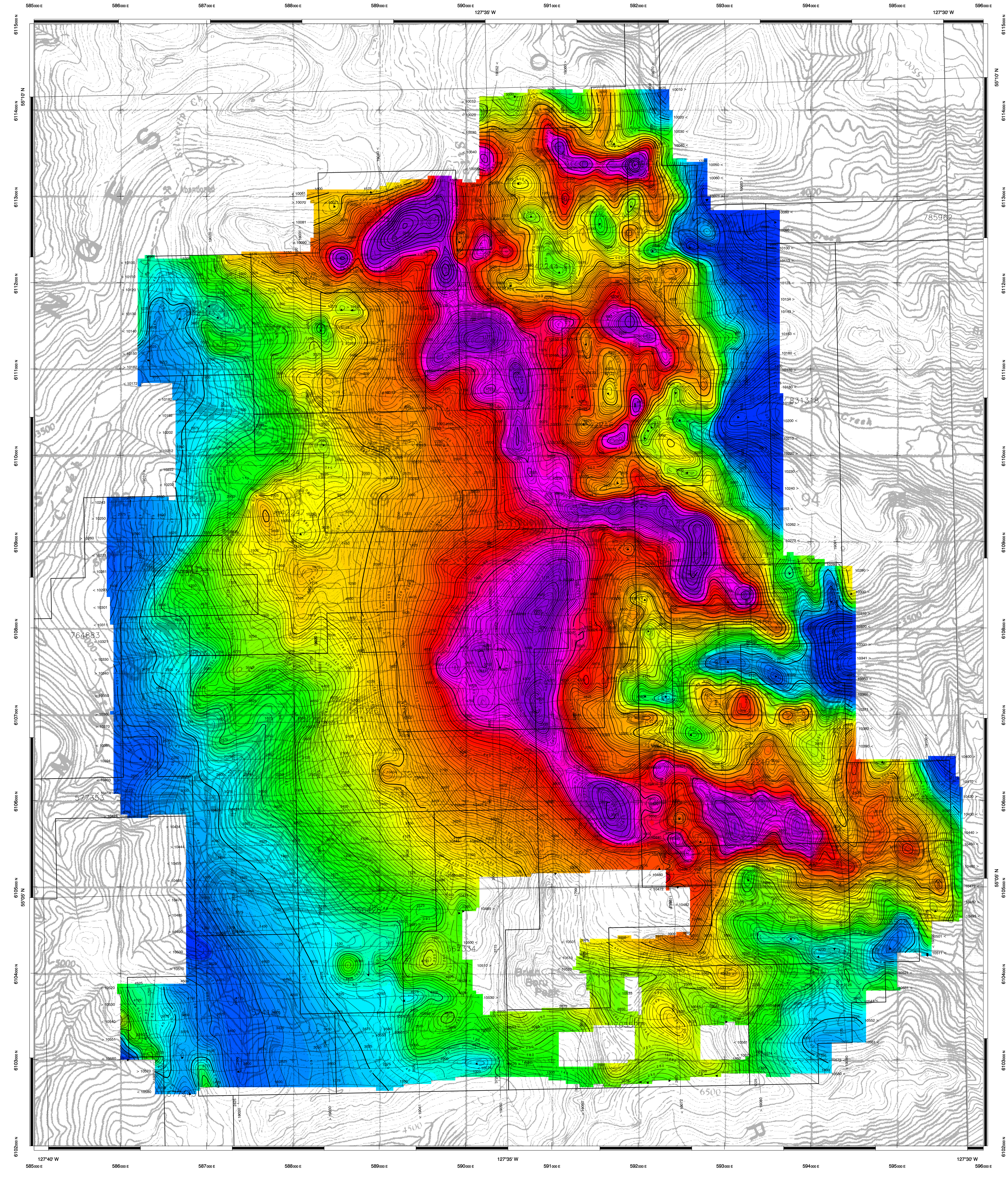

nT

1231, 1166, 1119, 1084, 1050, 1019, 988, 959, 928, 897, 868, 842, 815, 787, 760, 731, 701, 674, 648, 622, 597, 574, 550, 526, 504, 483, 464, 446, 427, 407, 389, 372, 354, 337, 320, 304, 287, 269, 252, 236, 217, 196, 177, 160, 143, 129, 115, 100, 85, 71, 57, 44, 29, 14, -1, -15, -28, -43, -62, -80, -101, -126, -165

FLIGHT LINES

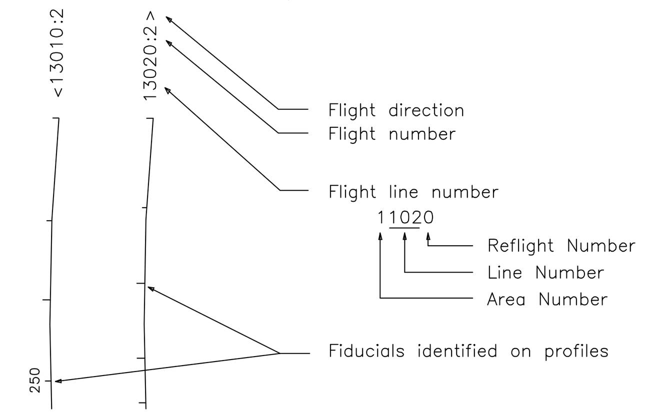

RESIDUAL MAGNETIC FIELD CONTOURS

. . . . 500 nT
. . . . 100 nT
. . . . 20 nT
. . . . 10 nT
. . . . magnetic low

Magnetic inclination within the survey area: 74 degrees N
Magnetic declination within the survey area: 20 degrees E

LOCATION MAP

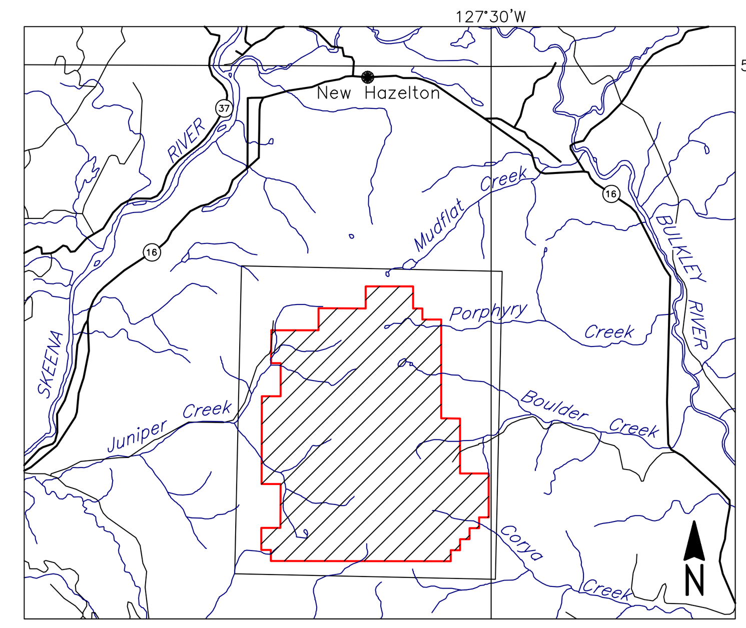

NTS: 93M/4 UTM ZONE: 9 NAD83 SCALE: 1:250,000

DUNCASTLE GOLD CORP.
PORPHYRY CREEK PROPERTY, BC

RESIDUAL MAGNETIC FIELD
IGRF Removed

FUGRO DIGHEM^{V}/RAD SURVEY	NTS: 93M/4	GEOPHYSICIST:
DATE: AUGUST, 2010	JOB: 10037	SHEET: 1

Fugro Airborne Surveys

0 1 2 Km
0 1 Mi
Scale 1:20 000

FUGRO AIRBORNE SURVEYS

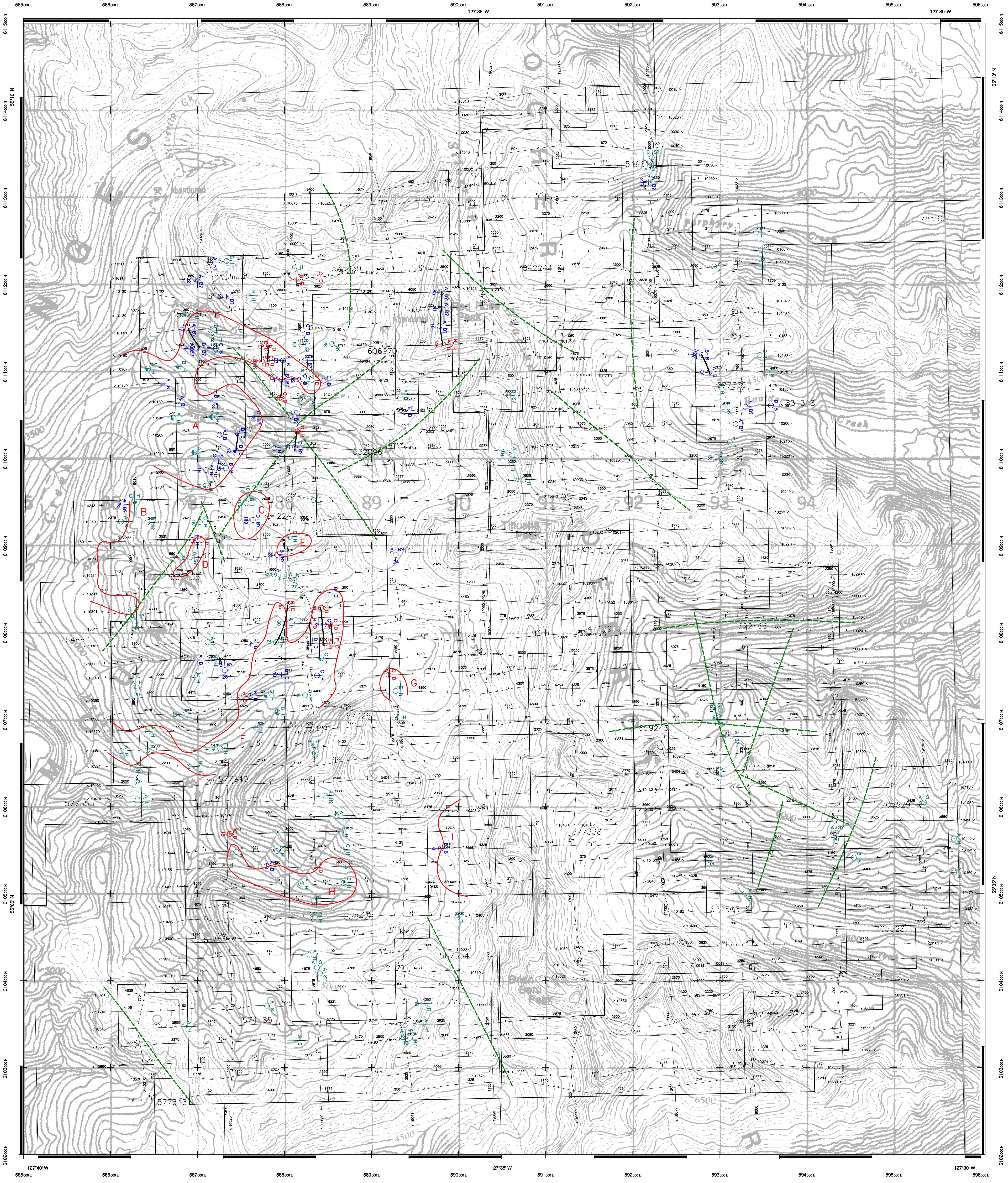

TECHNICAL SUMMARY

Navigation	Differentially–corrected GPS
Data reduction grid interval	40 metres
Terrain clearance	Helicopter, Spectrometer 60 m Electromagnetic sensor 35 m Magnetometer 35 m
Data sampling interval	0.1 second
Magnetometer / sensitivity	Cesium / 0.01 nT
Electromagnetic system	DIGHEM[V]
Spectrometer	RS–500
Spectrometer data sampling	1.0 second

Frequency	Sensitivity	Coil Orientation
1000 Hz	.06 ppm	Vertical coaxial
5500 Hz	.12 ppm	Vertical coaxial
900 Hz	.12 ppm	Horizontal coplanar
7200 Hz	.24 ppm	Horizontal coplanar
56000 Hz	.60 ppm	Horizontal coplanar

N

ELECTROMAGNETIC ANOMALIES

Grade	Anomaly	Conductance
7	●	>100 siemens
6	◕	50–100 siemens
5	◒	20–50 siemens
4	⊕	10–20 siemens
3	⊕	5–10 siemens
2	○	1–5 siemens
1	◌	< 1 siemens
–	✳	Questionable anomaly

Anomaly identifier
Interpretive symbol
C H
Depth is greater than
· 15 m
: 30 m
⋮ 45 m
⋮ 60 m

Inphase and Quadrature of coaxial coil is greater than
. 5 ppm
.. 10 ppm
... 15 ppm
.... 20 ppm

Interpretive symbol	Conductor ("model")
B	Bedrock conductor
D	Narrow bedrock conductor ("thin dike")
S	Conductive cover ("horizontal thin sheet")
H	Broad conductive rock unit, deep conductive weathering, thick conductive cover ("half space")
E	Edge of broad conductor ("edge of half space")
L	Culture, e.g. power line, metal building or fence

FLIGHT LINES WITH EM ANOMALIES

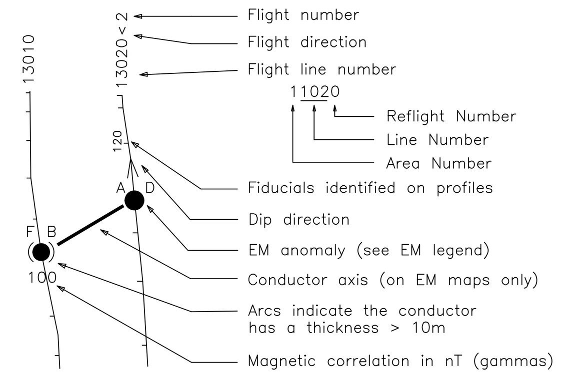

INTERPRETATION LEGEND

EM conductor

Inferred magnetic linears

Conductive zone

LOCATION MAP

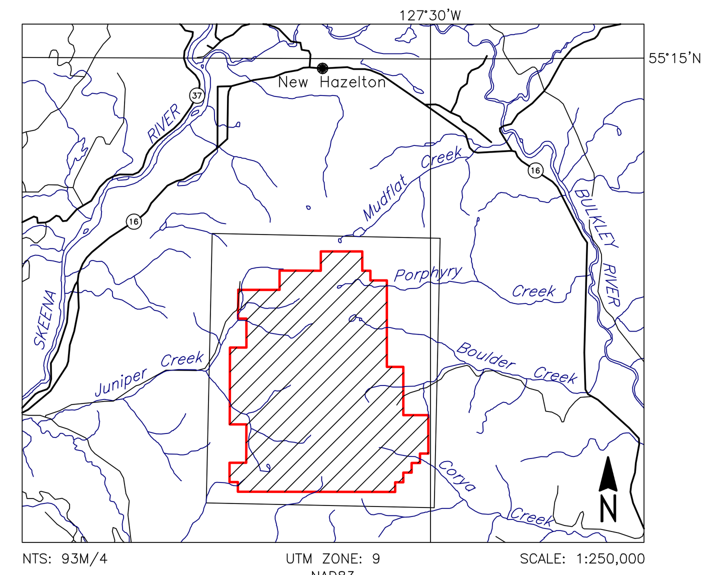

NTS: 93M/4
UTM ZONE: 9
NAD83
SCALE: 1:250,000

DUNCASTLE GOLD CORP.
PORPHYRY CREEK PROPERTY, BC

ELECTROMAGNETIC ANOMALIES

FUGRO DIGHEM[V]/RAD SURVEY	NTS: 93M/4	GEOPHYSICIST:
DATE: AUGUST, 2010	JOB: 10037	SHEET: 1

Fugro Airborne Surveys

0 1 2 Km
0 1 Mi
Scale 1:20 000

FUGRO AIRBORNE SURVEYS

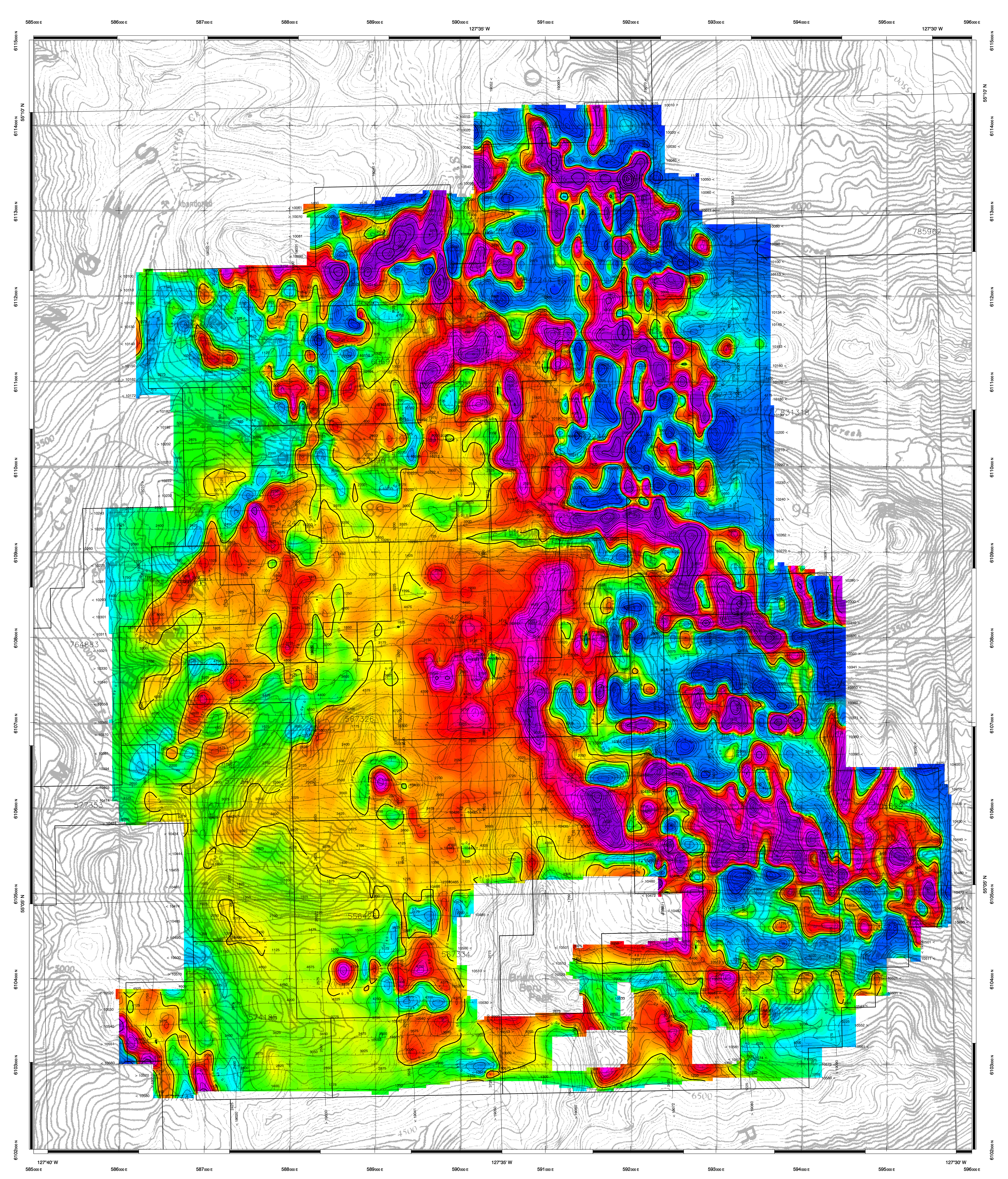

TECHNICAL SUMMARY

Navigation . . . . Differentially-corrected GPS
Data reduction grid interval . . . . 40 metres
Terrain clearance . . . . Helicopter, Spectrometer 60 m
Electromagnetic sensor 35 m
Magnetometer 35 m
Data sampling interval . . . . 0.1 second
Magnetometer / sensitivity . . . . . Cesium / 0.01 nT
Electromagnetic system . . . . . . DIGHEM^V
Spectrometer RS-500
Spectrometer data sampling . . . . 1.0 second

Frequency	Sensitivity	Coil Orientation
1000 Hz	.06 ppm	Vertical coaxial
5500 Hz	.12 ppm	Vertical coaxial
900 Hz	.12 ppm	Horizontal coplanar
7200 Hz	.24 ppm	Horizontal coplanar
56000 Hz	.60 ppm	Horizontal coplanar

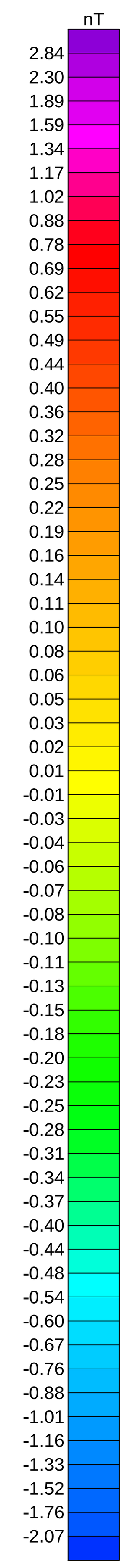

FLIGHT LINES

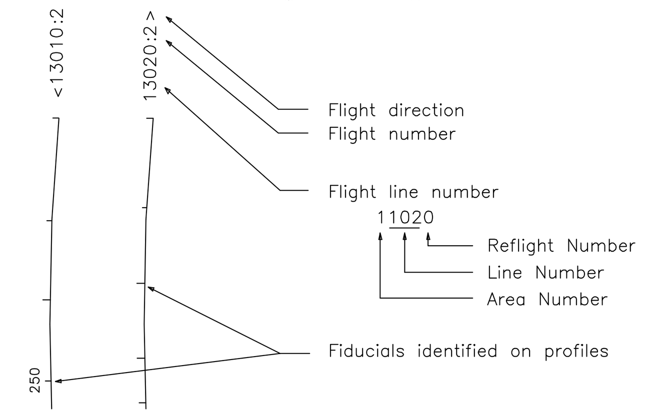

CALCULATED VERTICAL GRADIENT CONTOURS

....	10.0 nT/metre
....	2.0 nT/metre
....	0.4 nT/metre
....	0.2 nT/metre

LOCATION MAP

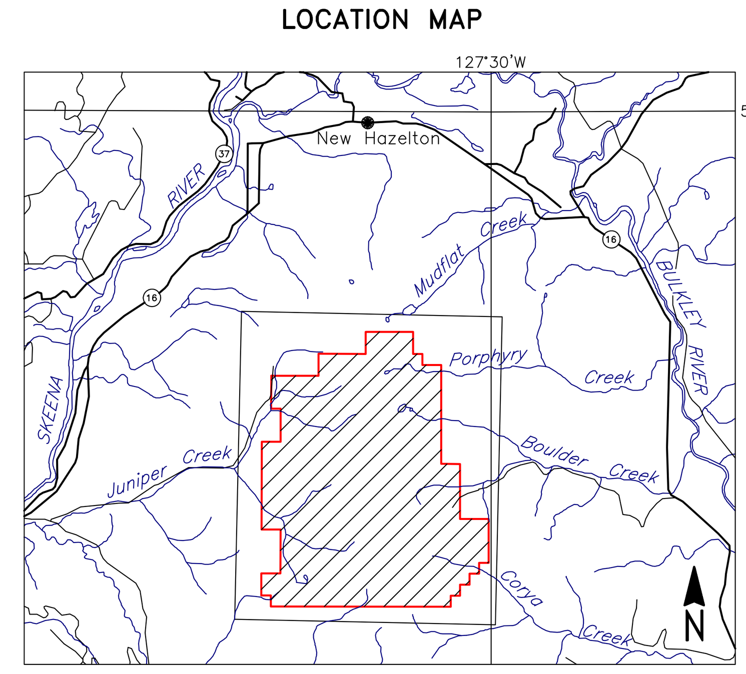

NTS: 93M/4   UTM ZONE: 9 NAD83   SCALE: 1:250,000

DUNCASTLE GOLD CORP.
PORPHYRY CREEK PROPERTY, BC

CALCULATED VERTICAL MAGNETIC GRADIENT

FUGRO DIGHEM^V/RAD SURVEY	NTS: 93M/4	GEOPHYSICIST:
DATE: AUGUST, 2010	JOB: 10037	SHEET: 1

Fugro Airborne Surveys

0 1 2 Km
0 1 Mi
Scale 1:20 000

FUGRO AIRBORNE SURVEYS

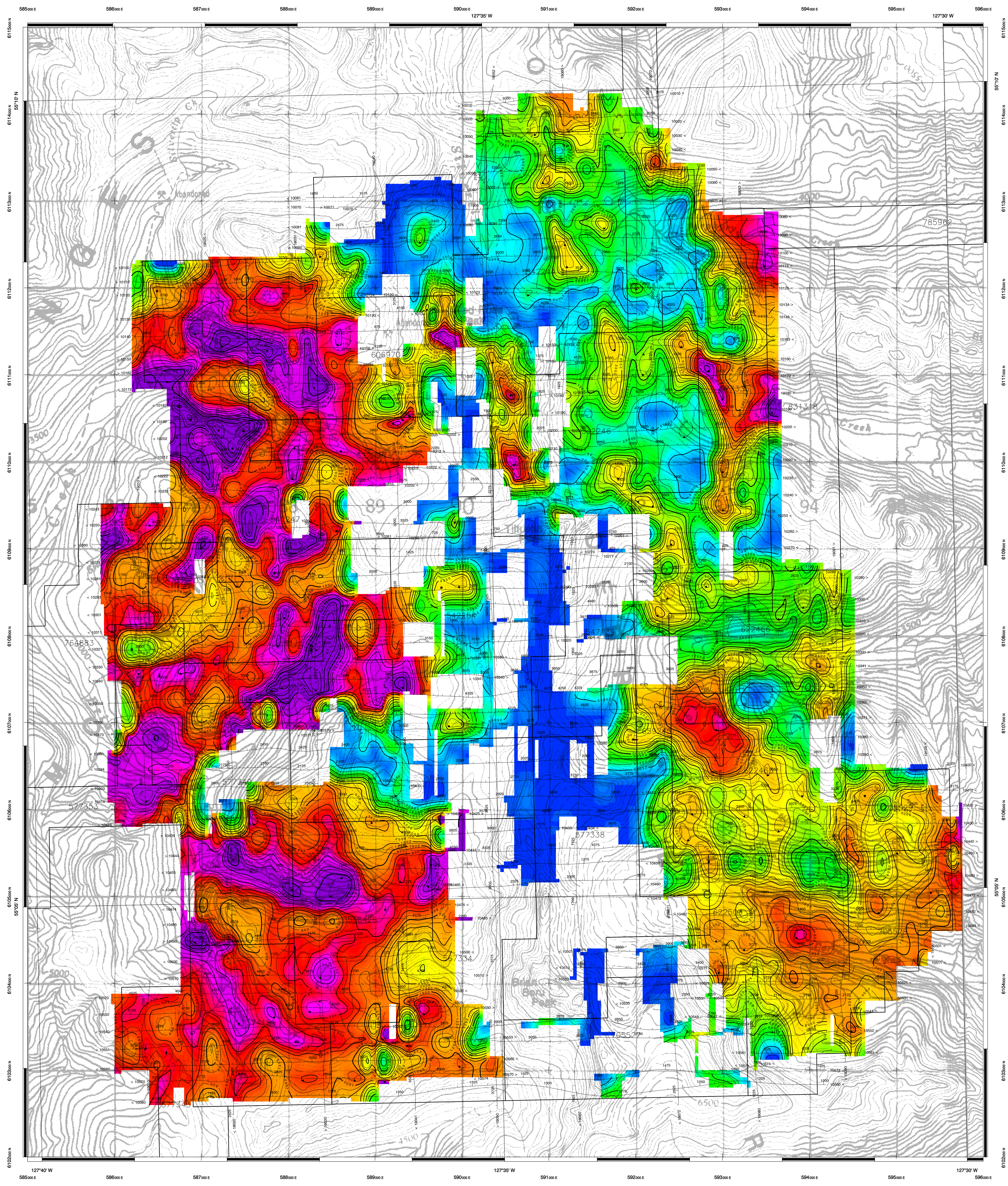

TECHNICAL SUMMARY

Navigation . . . . Differentially-corrected GPS
Data reduction grid interval . . . . 40 metres
Terrain clearance . . . . Helicopter, Spectrometer 60 m
Electromagnetic sensor 35 m
Magnetometer 35 m
Data sampling interval . . . . 0.1 second
Magnetometer / sensitivity . . . . . Cesium / 0.01 nT
Electromagnetic system . . . . . . DIGHEM[V]
Spectrometer RS-500
Spectrometer data sampling . . . . 1.0 second

Frequency	Sensitivity	Coil Orientation
1000 Hz	.06 ppm	Vertical coaxial
5500 Hz	.12 ppm	Vertical coaxial
900 Hz	.12 ppm	Horizontal coplanar
7200 Hz	.24 ppm	Horizontal coplanar
56000 Hz	.60 ppm	Horizontal coplanar

ohm·m

30000
29992
29890
29621
29128
28439
27603
26649
25669
24598
23521
22529
21593
20602
19546
18576
17364
16319
15192
14103
13011
11942
10891
9942
9038
8131
7277
6465
5697
4910
4351
3854
3463
3102
2768
2455
2177
1933
1710
1524
1383
1257
1148
1048
959
875
807
744
686
628
575
530
489
450
416
383
347
311
275
239
197
151
106

FLIGHT LINES

<13010:2
13020:2>
Flight direction
Flight number
Flight line number
11020
Reflight Number
Line Number
Area Number
Fiducials identified on profiles
250

RESISTIVITY CONTOURS

1000
800
600
500
400
300
250
200
150
125
100

Contours in ohm-m at 10 intervals per decade. Apparent resistivity calculated using a pseudo-layer half-space model (Fraser 1978).

LOCATION MAP

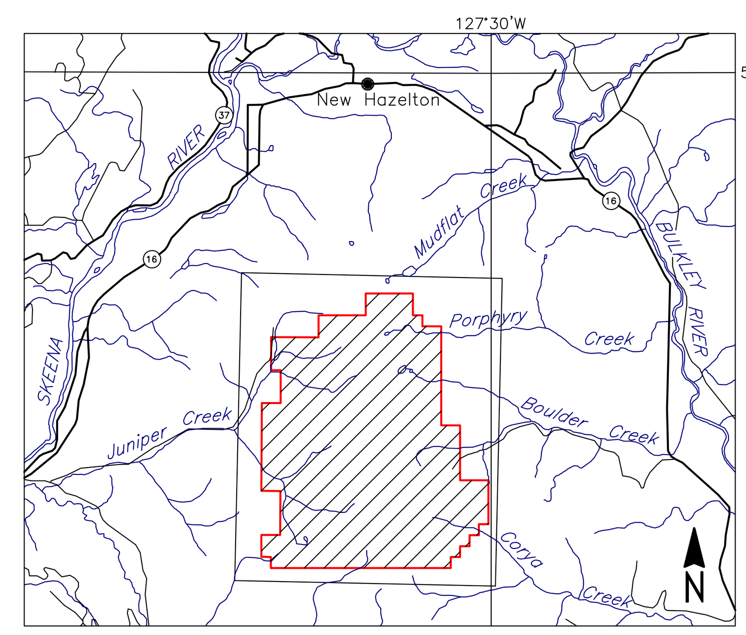

NTS: 93M/4 UTM ZONE: 9 NAD83 SCALE: 1:250,000

DUNCASTLE GOLD CORP.
PORPHYRY CREEK PROPERTY, BC

APPARENT RESISTIVITY 56,000 Hz COPLANAR

FUGRO DIGHEM[V]/RAD SURVEY	NTS: 93M/4	GEOPHYSICIST:
DATE: AUGUST, 2010	JOB: 10037	SHEET: 1

Fugro Airborne Surveys

0 1 2 Km
0 1 Mi
Scale 1:20 000

FUGRO AIRBORNE SURVEYS

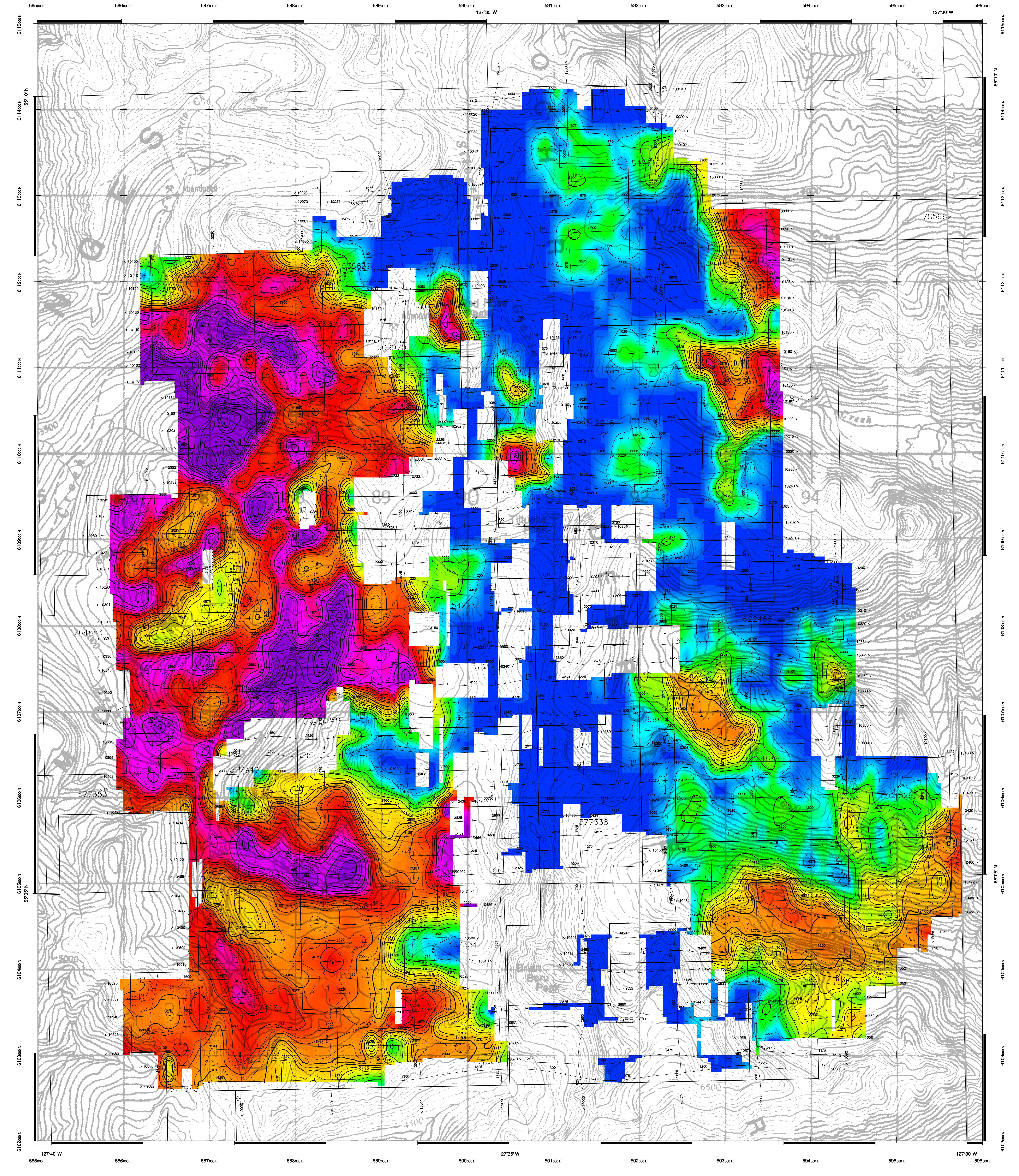

TECHNICAL SUMMARY

Navigation . . . . Differentially-corrected GPS
Data reduction grid interval . . . . 40 metres
Terrain clearance . . . . Helicopter, Spectrometer 60 m
Electromagnetic sensor 35 m
Magnetometer 35 m
Data sampling interval . . . . 0.1 second
Magnetometer / sensitivity . . . . . Cesium / 0.01 nT
Electromagnetic system . . . . . . DIGHEM[V]
Spectrometer RS-500
Spectrometer data sampling . . . . 1.0 second

Frequency	Sensitivity	Coil Orientation
1000 Hz	.06 ppm	Vertical coaxial
5500 Hz	.12 ppm	Vertical coaxial
900 Hz	.12 ppm	Horizontal coplanar
7200 Hz	.24 ppm	Horizontal coplanar
56000 Hz	.60 ppm	Horizontal coplanar

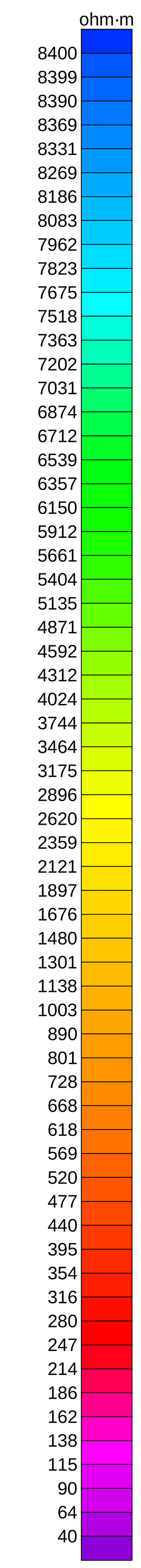

FLIGHT LINES

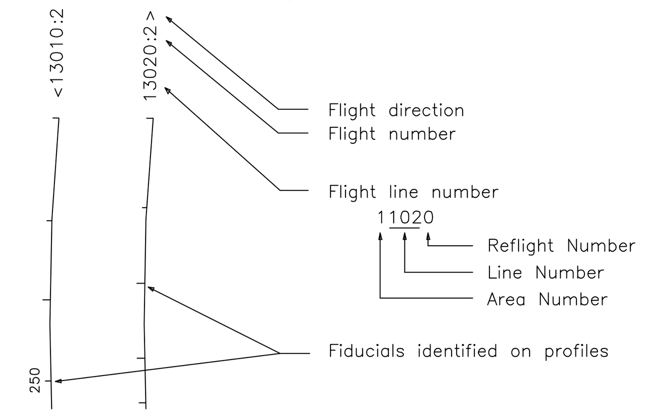

RESISTIVITY CONTOURS

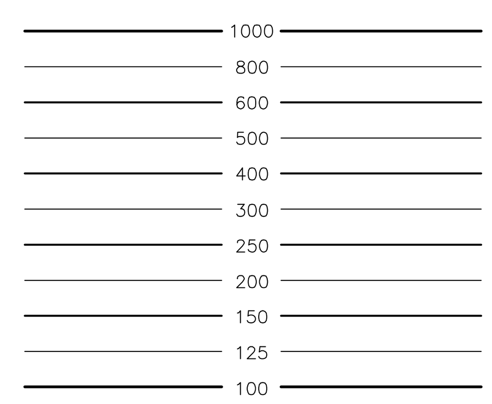

Contours in ohm-m at 10 intervals per decade. Apparent resistivity calculated using a pseudo-layer half-space model (Fraser 1978).

LOCATION MAP

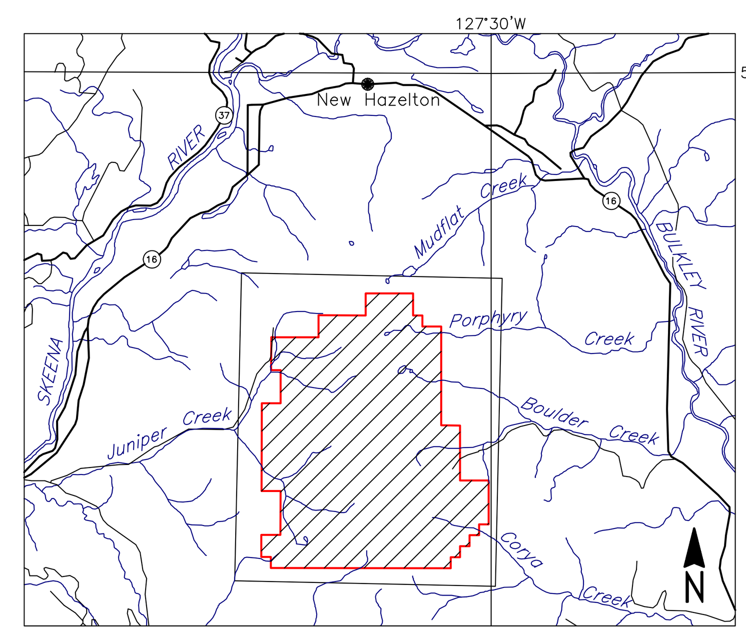

NTS: 93M/4 UTM ZONE: 9 NAD83 SCALE: 1:250,000

DUNCASTLE GOLD CORP.
PORPHYRY CREEK PROPERTY, BC

APPARENT RESISTIVITY 7200 Hz COPLANAR

FUGRO DIGHEM[V]/RAD SURVEY	NTS: 93M/4	GEOPHYSICIST:
DATE: AUGUST, 2010	JOB: 10037	SHEET: 1

Fugro Airborne Surveys

0 1 2 Km
0 1 Mi
Scale 1:20 000

FUGRO AIRBORNE SURVEYS

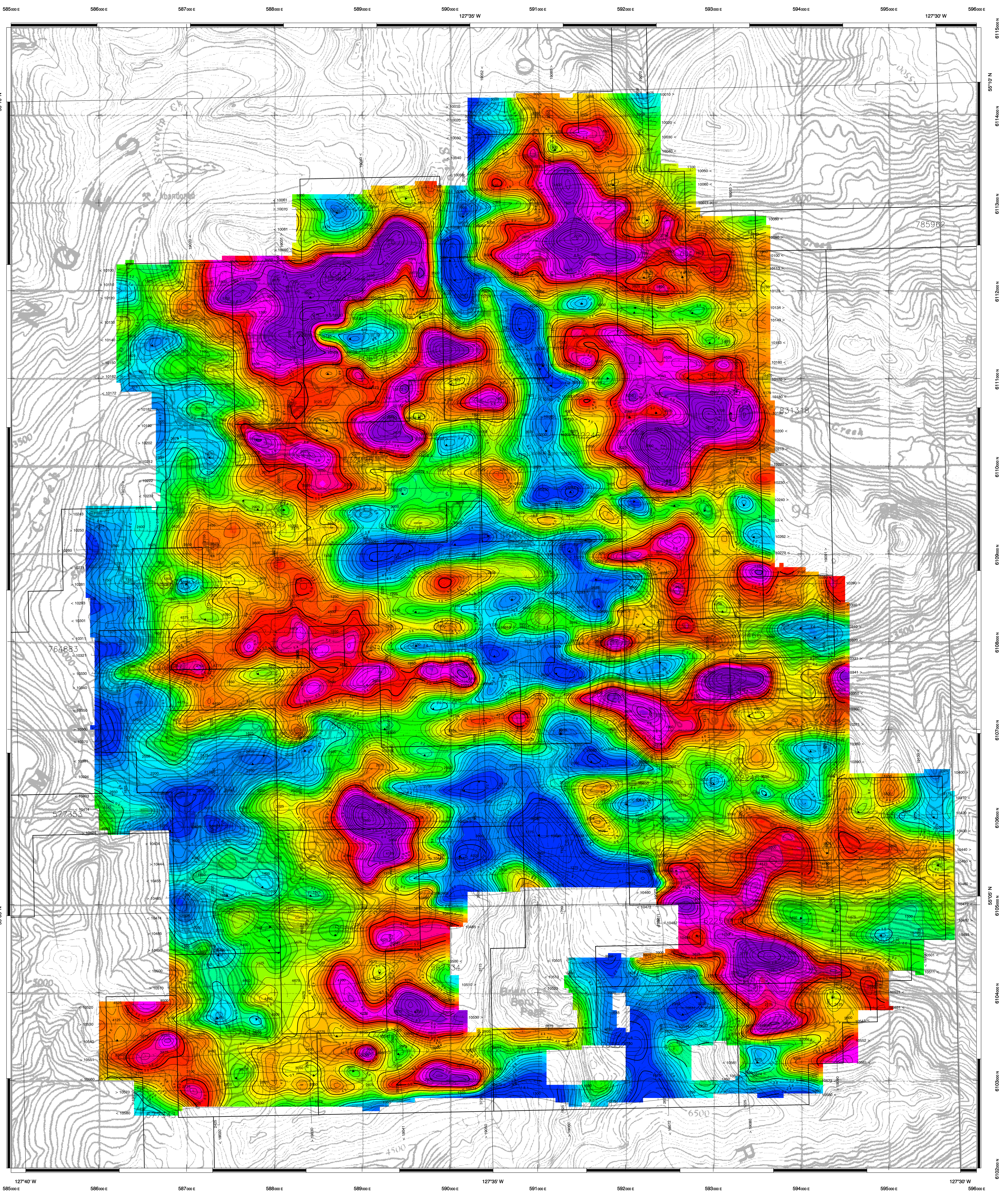

TECHNICAL SUMMARY

Navigation	Differentially-corrected GPS
Data reduction grid interval	50 metres
Terrain clearance	Helicopter, Spectrometer 60 m Electromagnetic sensor 35 m Magnetometer 35 m
Data sampling interval	0.1 second
Magnetometer / sensitivity	Cesium / 0.01 nT
Electromagnetic system	DIGHEM^V
Spectrometer	RS-500
Spectrometer data sampling	1.0 second

Frequency	Sensitivity	Coil Orientation
1000 Hz	.06 ppm	Vertical coaxial
5500 Hz	.12 ppm	Vertical coaxial
900 Hz	.12 ppm	Horizontal coplanar
7200 Hz	.24 ppm	Horizontal coplanar
56000 Hz	.60 ppm	Horizontal coplanar

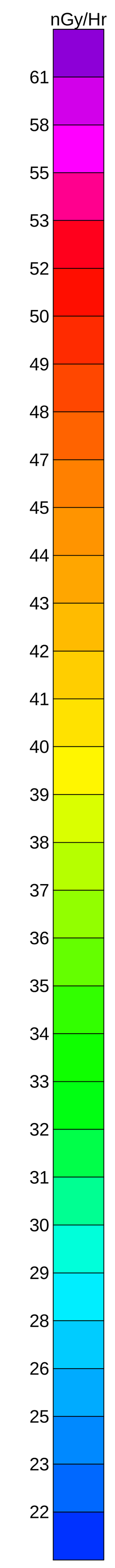

FLIGHT LINES

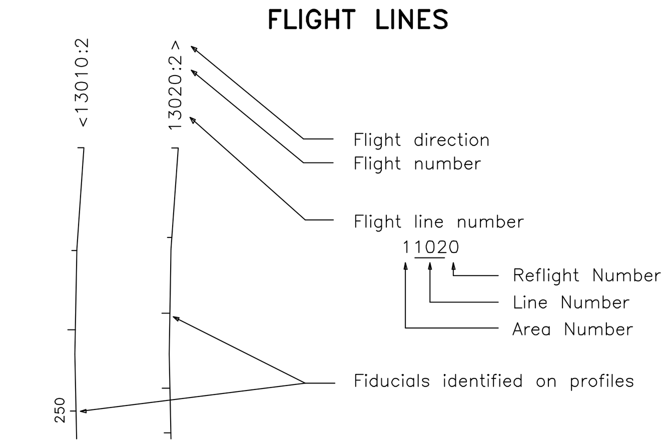

CONTOUR INTERVALS

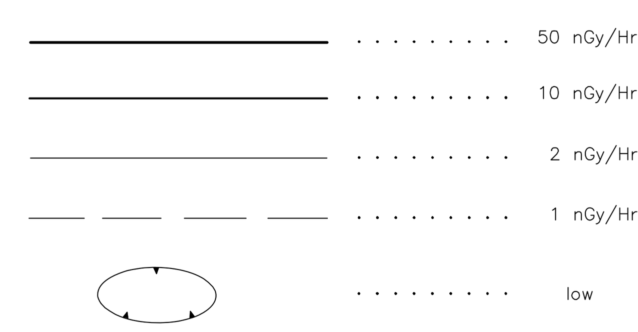

LOCATION MAP

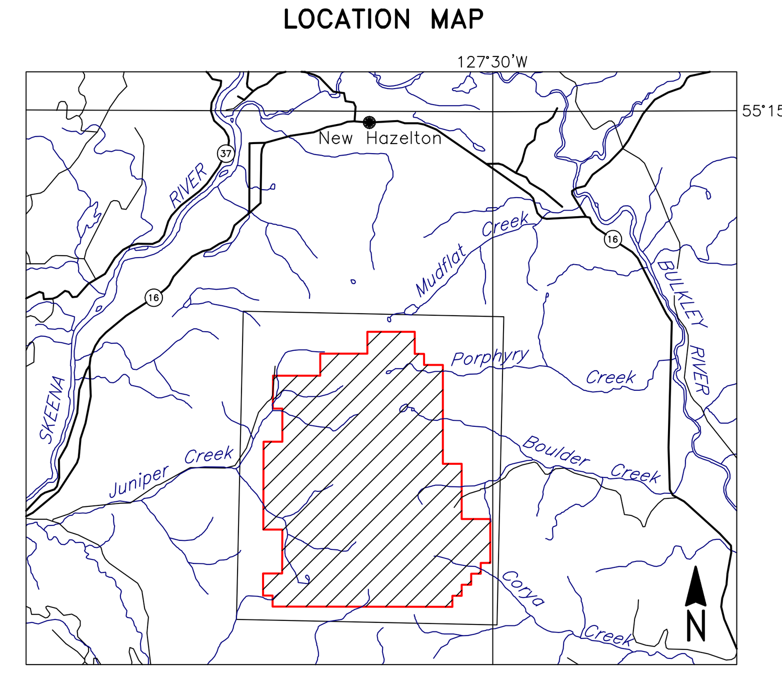

NTS: 93M/4 — UTM ZONE: 9 NAD83 — SCALE: 1:250,000

DUNCASTLE GOLD CORP.

PORPHYRY CREEK PROPERTY, BC

AIR ABSORBED DOSE RATE

FUGRO DIGHEM^V/RAD SURVEY	NTS: 93M/4	GEOPHYSICIST:
DATE: AUGUST, 2010	JOB: 10037	SHEET: 1

Fugro Airborne Surveys

0 1 2 Km
0 1 Mi
Scale 1:20 000

FUGRO AIRBORNE SURVEYS

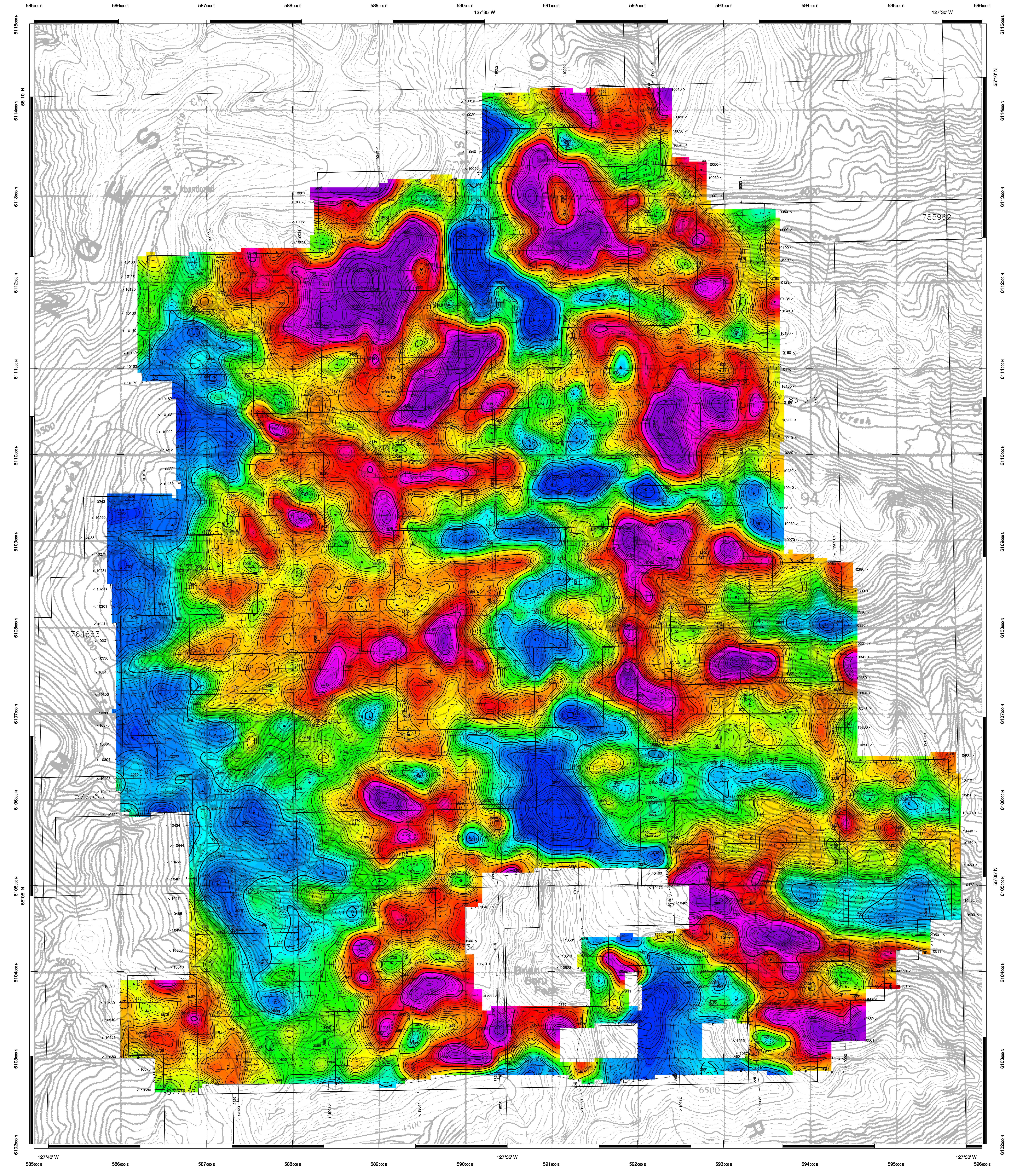

TECHNICAL SUMMARY

Navigation	Differentially-corrected GPS
Data reduction grid interval	50 metres
Terrain clearance	Helicopter, Spectrometer 60 m Electromagnetic sensor 35 m Magnetometer 35 m
Data sampling interval	0.1 second
Magnetometer / sensitivity	Cesium / 0.01 nT
Electromagnetic system	DIGHEM[V]
Spectrometer	RS-500
Spectrometer data sampling	1.0 second

Frequency	Sensitivity	Coil Orientation
1000 Hz	.06 ppm	Vertical coaxial
5500 Hz	.12 ppm	Vertical coaxial
900 Hz	.12 ppm	Horizontal coplanar
7200 Hz	.24 ppm	Horizontal coplanar
56000 Hz	.60 ppm	Horizontal coplanar

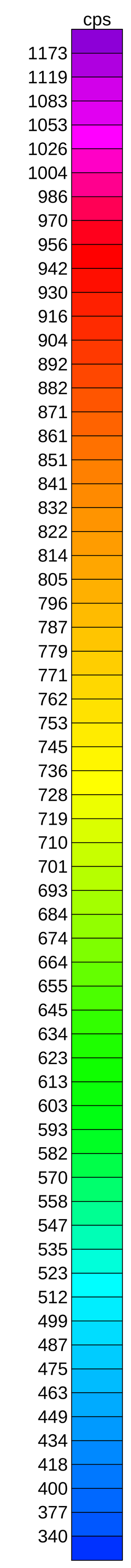

FLIGHT LINES

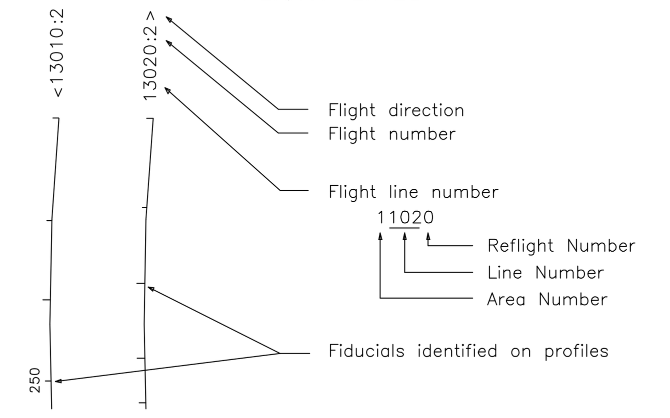

CONTOUR INTERVALS

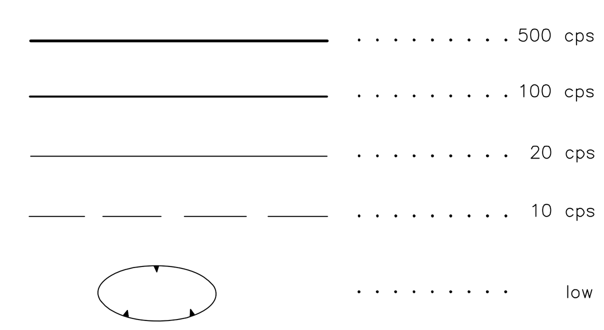

LOCATION MAP

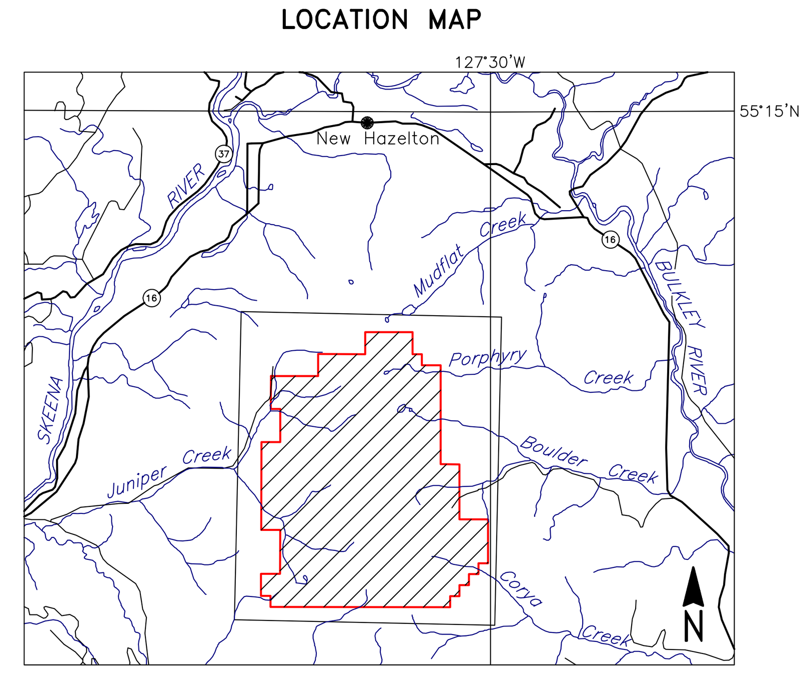

NTS: 93M/4 | UTM ZONE: 9 NAD83 | SCALE: 1:250,000

DUNCASTLE GOLD CORP.
PORPHYRY CREEK PROPERTY, BC

RADIOMETRIC TOTAL COUNT

FUGRO DIGHEM[V]/RAD SURVEY	NTS: 93M/4	GEOPHYSICIST:
DATE: AUGUST, 2010	JOB: 10037	SHEET: 1

Fugro Airborne Surveys

0 1 2 Km
0 1 Mi
Scale 1:20 000

FUGRO AIRBORNE SURVEYS

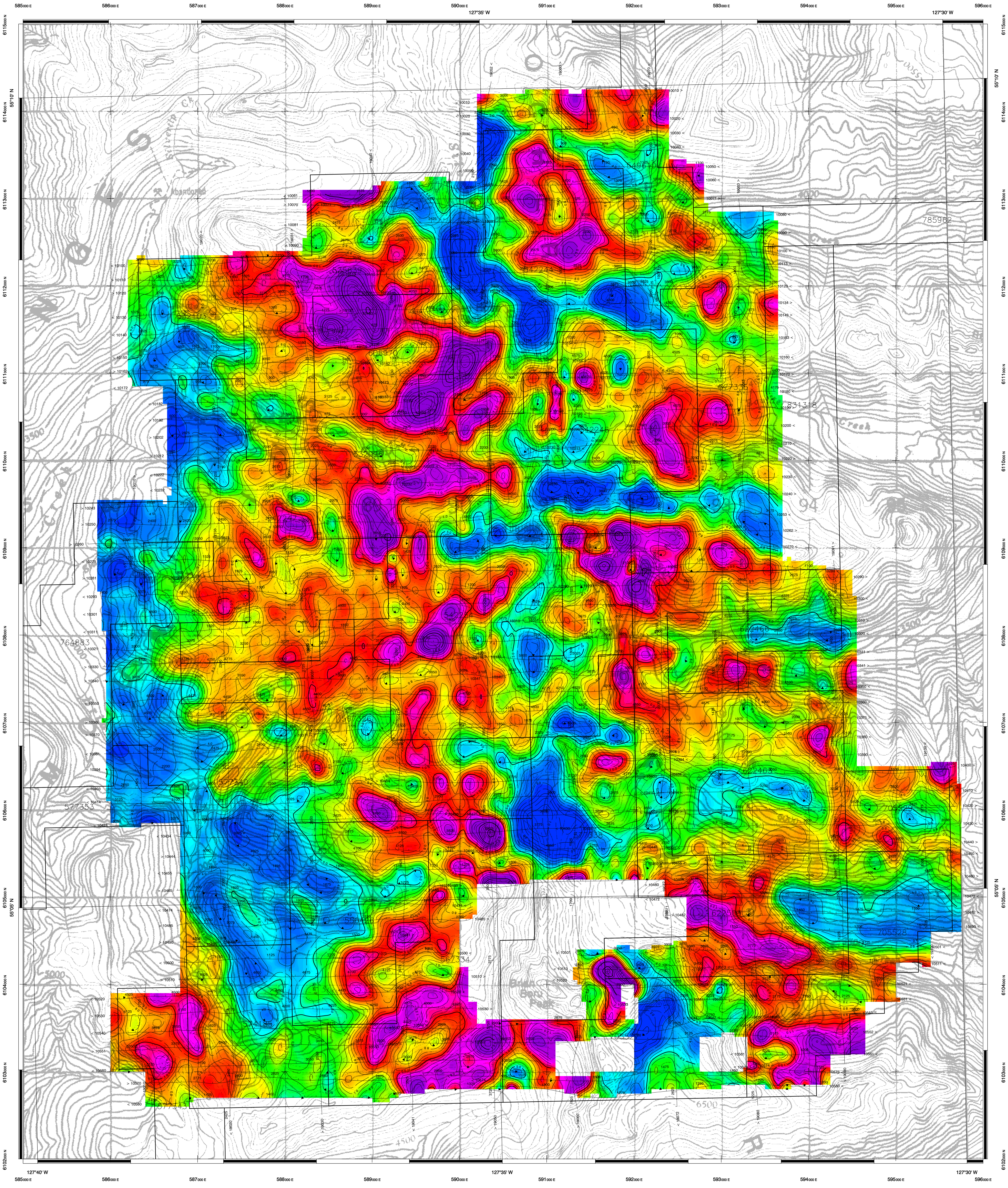

TECHNICAL SUMMARY

Navigation . . . . Differentially-corrected GPS
Data reduction grid interval . . . . 50 metres
Terrain clearance . . . . Helicopter, Spectrometer 60 m
Electromagnetic sensor 35 m
Magnetometer 35 m
Data sampling interval . . . . 0.1 second
Magnetometer / sensitivity . . . . . Cesium / 0.01 nT
Electromagnetic system . . . . DIGHEM^V
Spectrometer RS-500
Spectrometer data sampling . . . . 1.0 second

Frequency	Sensitivity	Coil Orientation
1000 Hz	.06 ppm	Vertical coaxial
5500 Hz	.12 ppm	Vertical coaxial
900 Hz	.12 ppm	Horizontal coplanar
7200 Hz	.24 ppm	Horizontal coplanar
56000 Hz	.60 ppm	Horizontal coplanar

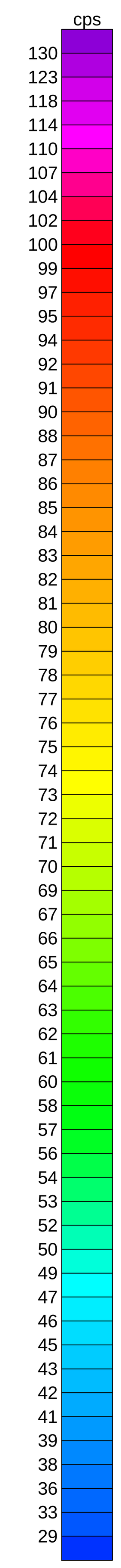

FLIGHT LINES

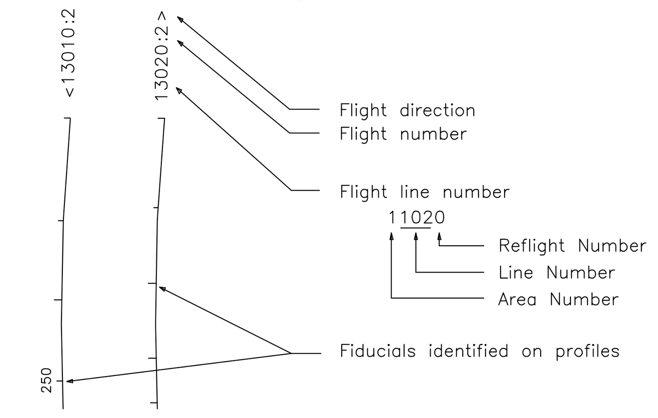

CONTOUR INTERVALS

. . . . 250 cps
. . . . 50 cps
. . . . 10 cps
. . . . 5 cps
. . . . low

LOCATION MAP

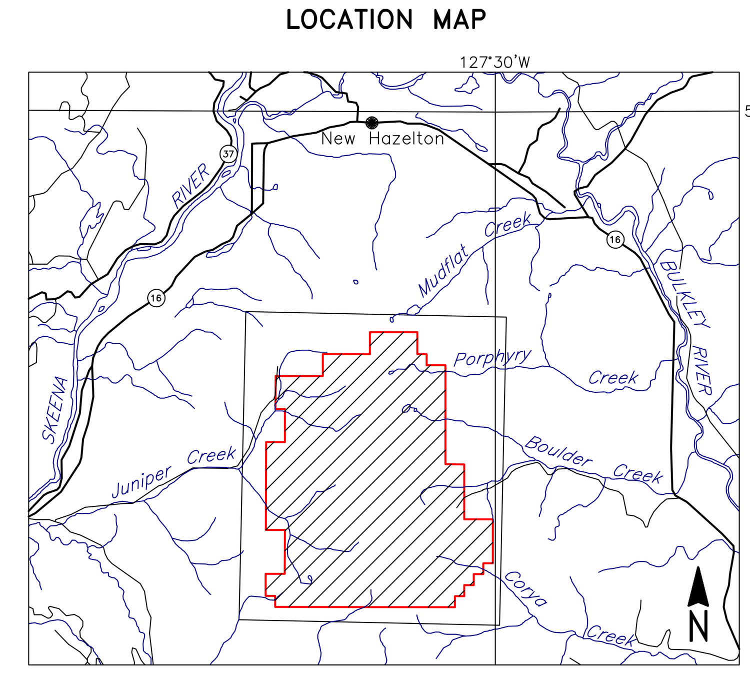

NTS: 93M/4
UTM ZONE: 9
NAD83
SCALE: 1:250,000

DUNCASTLE GOLD CORP.
PORPHYRY CREEK PROPERTY, BC

RADIOMETRIC POTASSIUM COUNTS

FUGRO DIGHEM^V/RAD SURVEY	NTS: 93M/4	GEOPHYSICIST:
DATE: AUGUST, 2010	JOB: 10037	SHEET: 1

Fugro Airborne Surveys

0 1 2 Km
0 1 Mi
Scale 1:20 000

FUGRO AIRBORNE SURVEYS

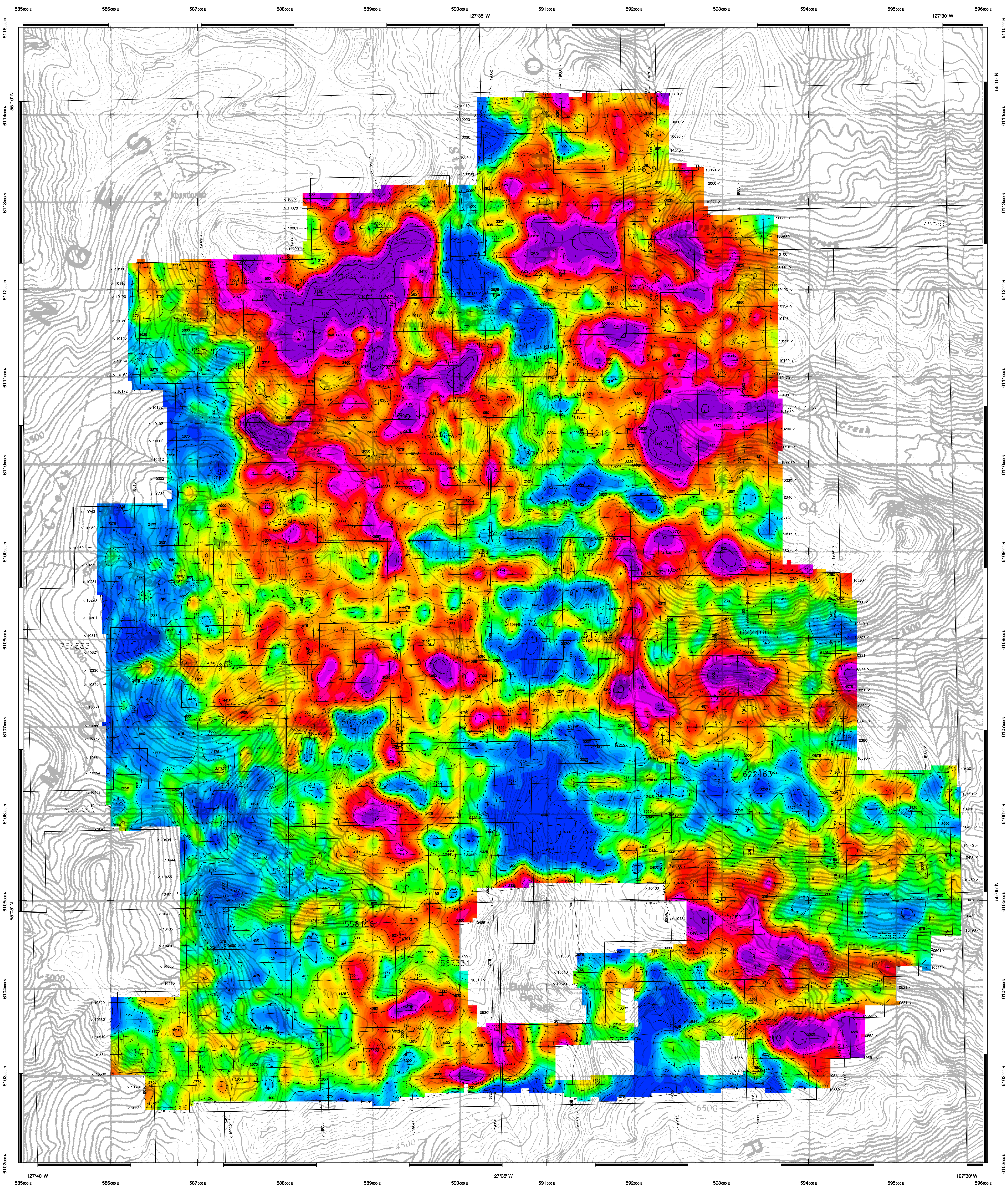

TECHNICAL SUMMARY

Navigation . . . . Differentially-corrected GPS
Data reduction grid interval . . . . 50 metres
Terrain clearance . . . . Helicopter, Spectrometer 60 m
Electromagnetic sensor 35 m
Magnetometer 35 m
Data sampling interval . . . . 0.1 second
Magnetometer / sensitivity . . . . . Cesium / 0.01 nT
Electromagnetic system . . . . . . DIGHEM^V
Spectrometer RS-500
Spectrometer data sampling . . . . 1.0 second

Frequency	Sensitivity	Coil Orientation
1000 Hz	.06 ppm	Vertical coaxial
5500 Hz	.12 ppm	Vertical coaxial
900 Hz	.12 ppm	Horizontal coplanar
7200 Hz	.24 ppm	Horizontal coplanar
56000 Hz	.60 ppm	Horizontal coplanar

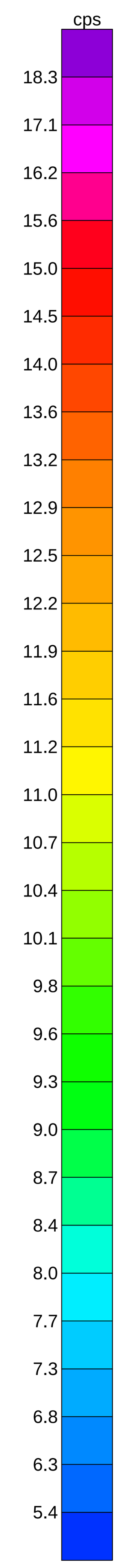

FLIGHT LINES

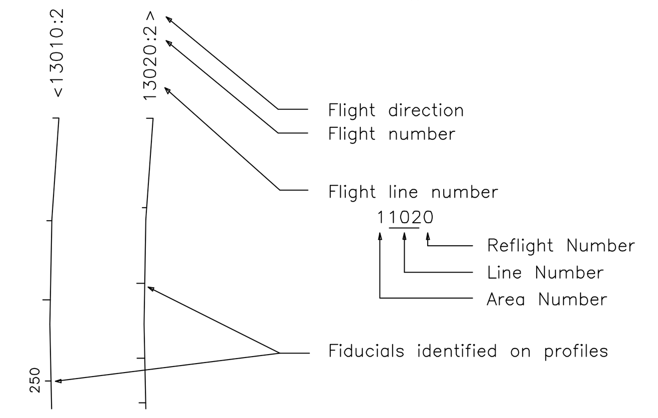

CONTOUR INTERVALS

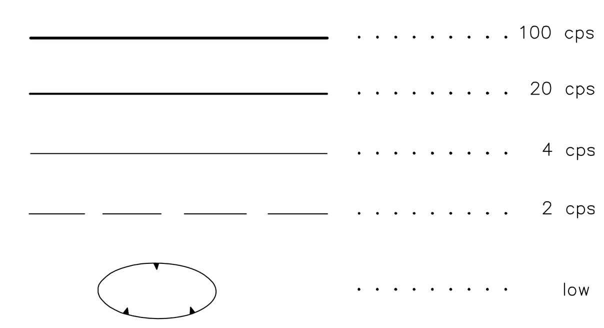

LOCATION MAP

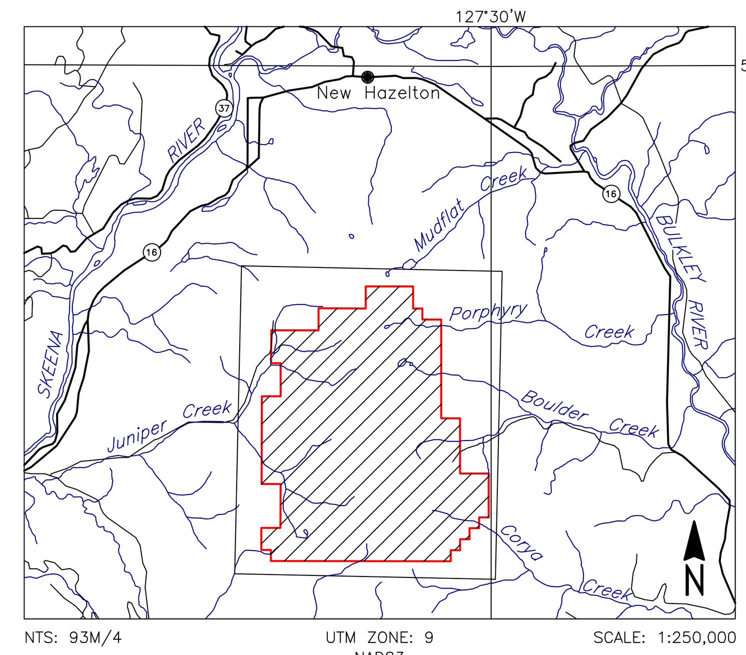

NTS: 93M/4 UTM ZONE: 9 NAD83 SCALE: 1:250,000

DUNCASTLE GOLD CORP.
PORPHYRY CREEK PROPERTY, BC

RADIOMETRIC URANIUM COUNTS

FUGRO DIGHEM^V/RAD SURVEY	NTS: 93M/4	GEOPHYSICIST:
DATE: AUGUST, 2010	JOB: 10037	SHEET: 1

Fugro Airborne Surveys

0 1 2 Km
0 1 Mi
Scale 1:20 000

FUGRO AIRBORNE SURVEYS

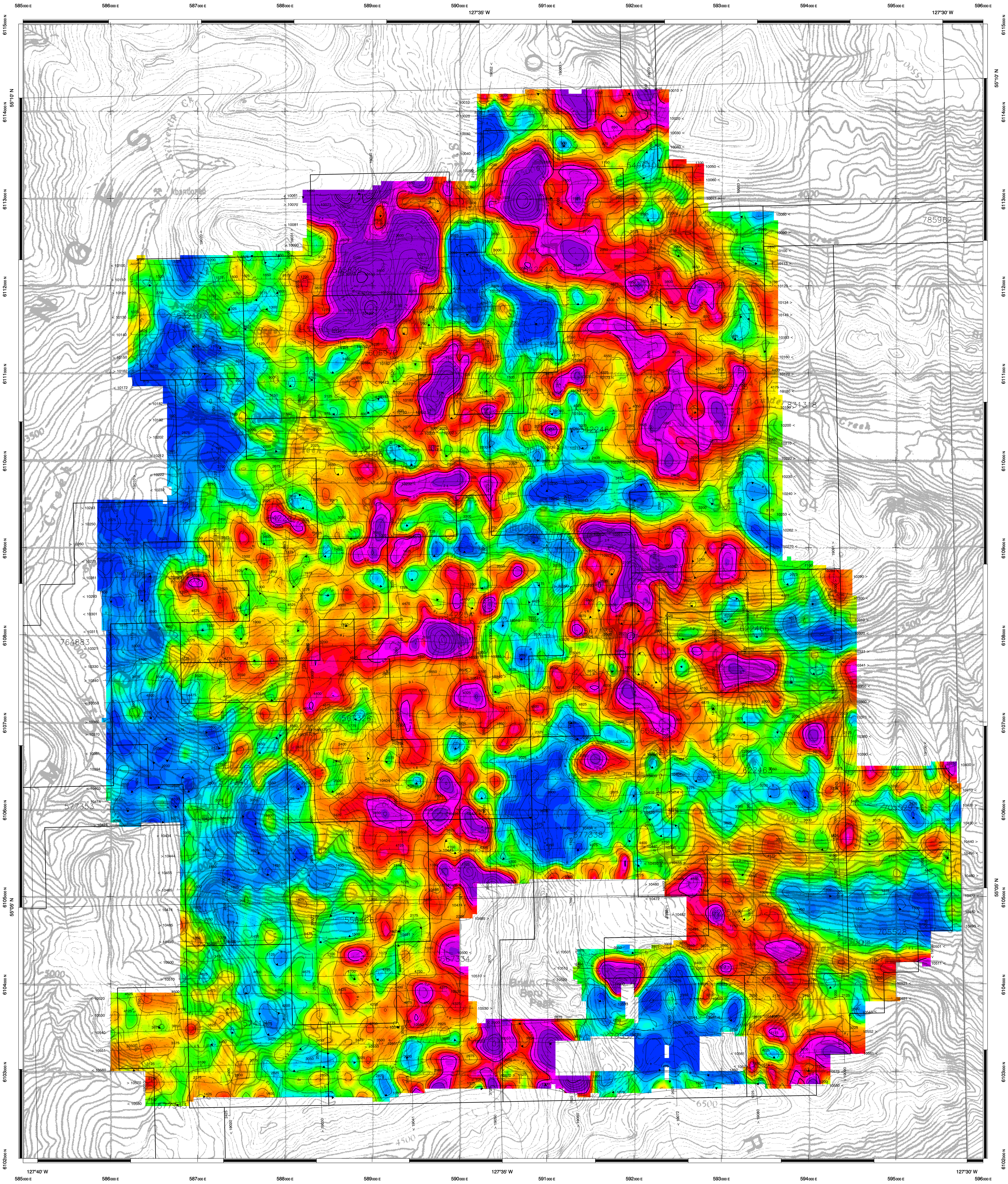

TECHNICAL SUMMARY

Navigation	Differentially-corrected GPS
Data reduction grid interval	50 metres
Terrain clearance	Helicopter, Spectrometer 60 m Electromagnetic sensor 35 m Magnetometer 35 m
Data sampling interval	0.1 second
Magnetometer / sensitivity	Cesium / 0.01 nT
Electromagnetic system	DIGHEM^{V}
Spectrometer	RS-500
Spectrometer data sampling	1.0 second

Frequency	Sensitivity	Coil Orientation
1000 Hz	.06 ppm	Vertical coaxial
5500 Hz	.12 ppm	Vertical coaxial
900 Hz	.12 ppm	Horizontal coplanar
7200 Hz	.24 ppm	Horizontal coplanar
56000 Hz	.60 ppm	Horizontal coplanar

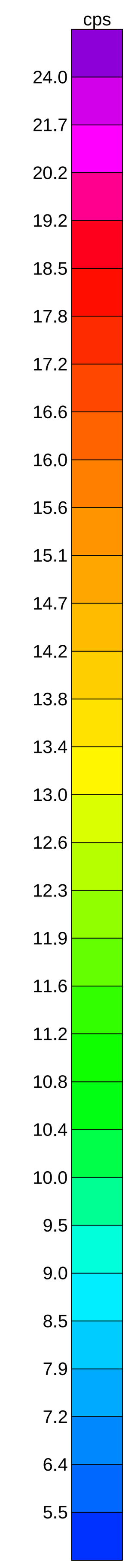

FLIGHT LINES

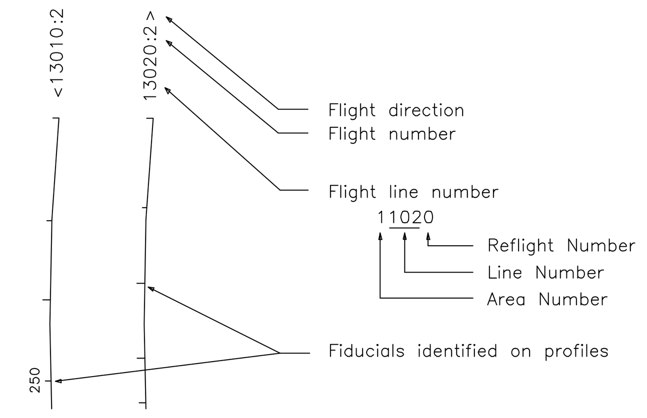

CONTOUR INTERVALS

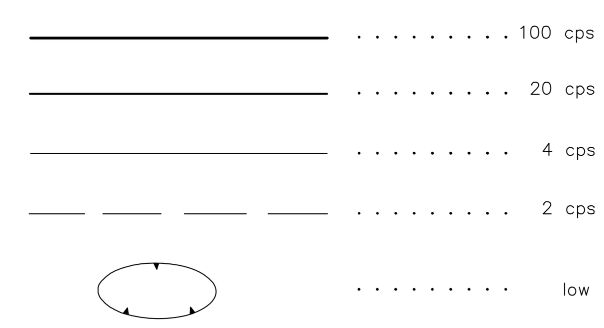

LOCATION MAP

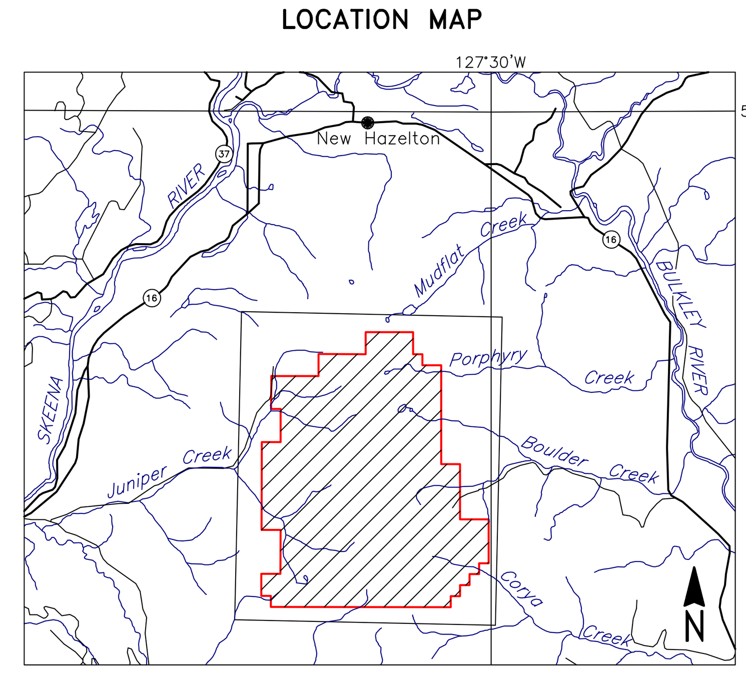

NTS: 93M/4 UTM ZONE: 9 NAD83 SCALE: 1:250,000

DUNCASTLE GOLD CORP.

PORPHYRY CREEK PROPERTY, BC

RADIOMETRIC THORIUM COUNTS

FUGRO DIGHEM^{V}/RAD SURVEY	NTS: 93M/4	GEOPHYSICIST:
DATE: AUGUST, 2010	JOB: 10037	SHEET: 1

Fugro Airborne Surveys

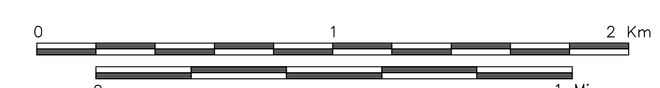

Scale 1:20 000

FUGRO AIRBORNE SURVEYS

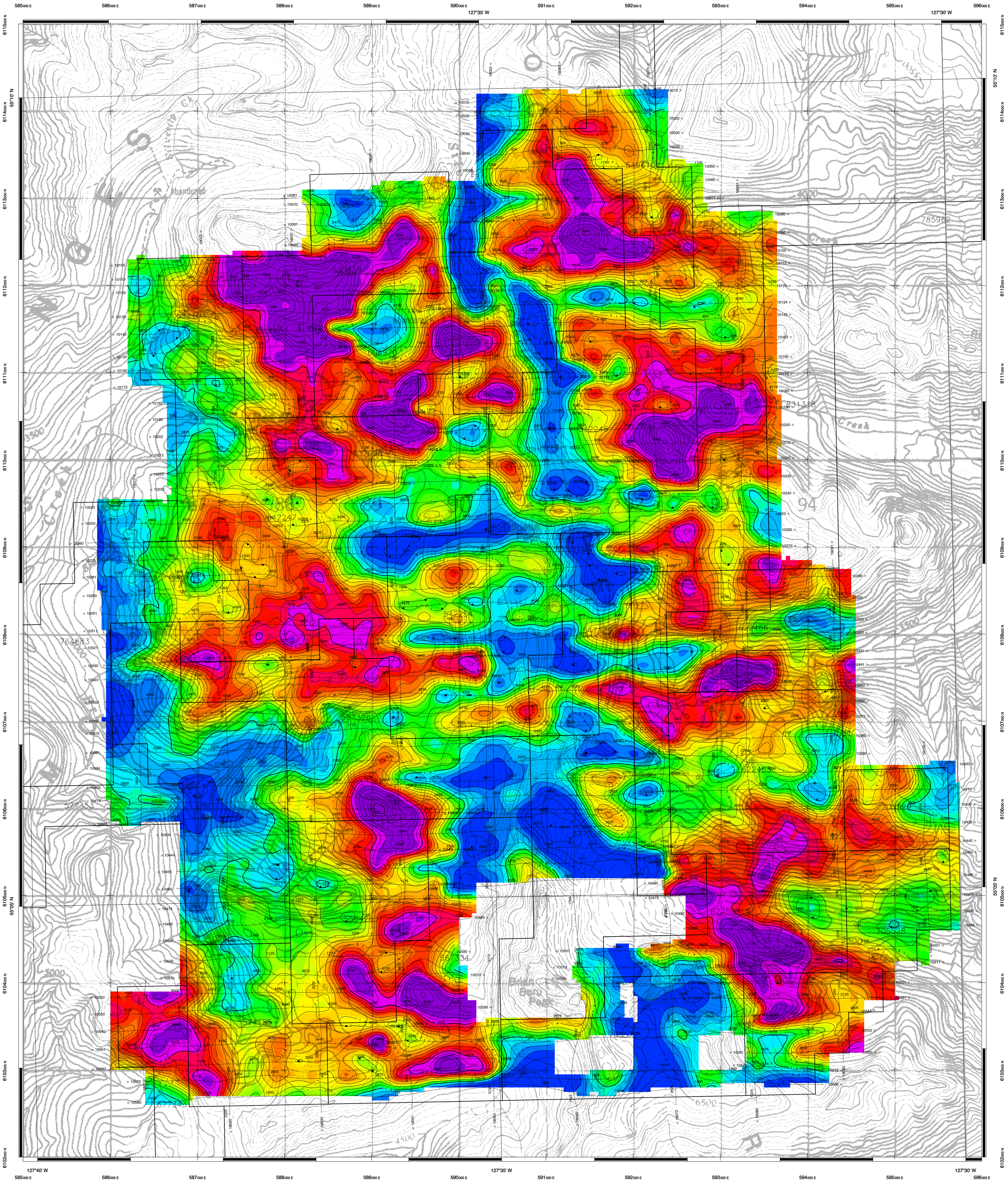

TECHNICAL SUMMARY

Navigation	Differentially-corrected GPS
Data reduction grid interval	50 metres
Terrain clearance	Helicopter, Spectrometer 60 m Electromagnetic sensor 35 m Magnetometer 35 m
Data sampling interval	0.1 second
Magnetometer / sensitivity	Cesium / 0.01 nT
Electromagnetic system	DIGHEM[V]
Spectrometer	RS-500
Spectrometer data sampling	1.0 second

Frequency	Sensitivity	Coil Orientation
1000 Hz	.06 ppm	Vertical coaxial
5500 Hz	.12 ppm	Vertical coaxial
900 Hz	.12 ppm	Horizontal coplanar
7200 Hz	.24 ppm	Horizontal coplanar
56000 Hz	.60 ppm	Horizontal coplanar

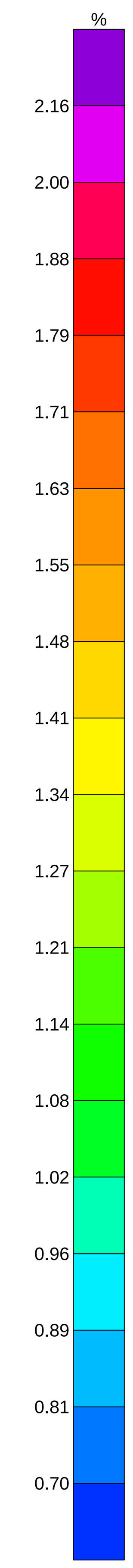

FLIGHT LINES

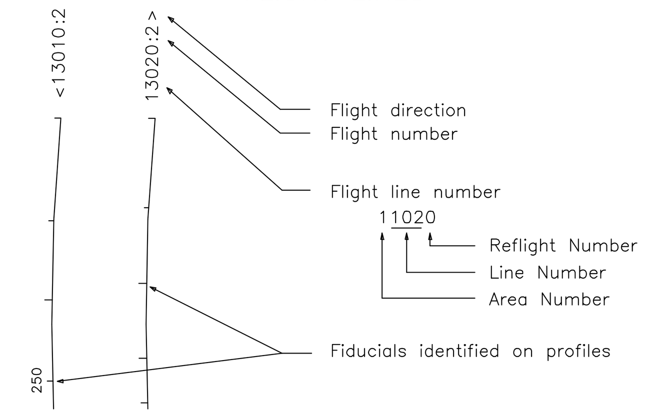

CONTOUR INTERVALS

(solid heavy line)	5.0 %
(solid line)	1.0 %
(thin line)	0.2 %
(dashed line)	0.1 %
(ellipse with ticks)	low

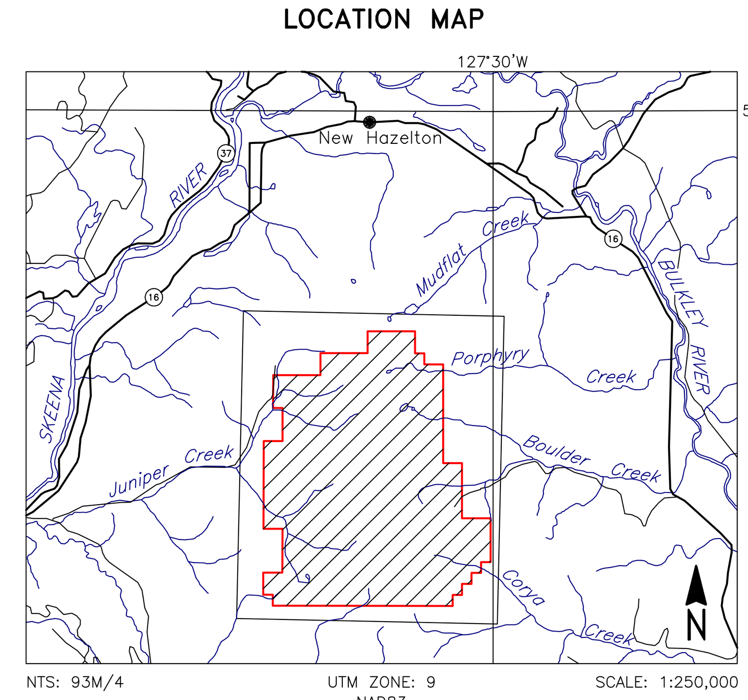

DUNCASTLE GOLD CORP.
PORPHYRY CREEK PROPERTY, BC

RADIOMETRIC POTASSIUM CONCENTRATION

FUGRO DIGHEM[V]/RAD SURVEY	NTS: 93M/4	GEOPHYSICIST:
DATE: AUGUST, 2010	JOB: 10037	SHEET: 1

Fugro Airborne Surveys

0 1 2 Km
0 1 Mi
Scale 1:20 000

FUGRO AIRBORNE SURVEYS

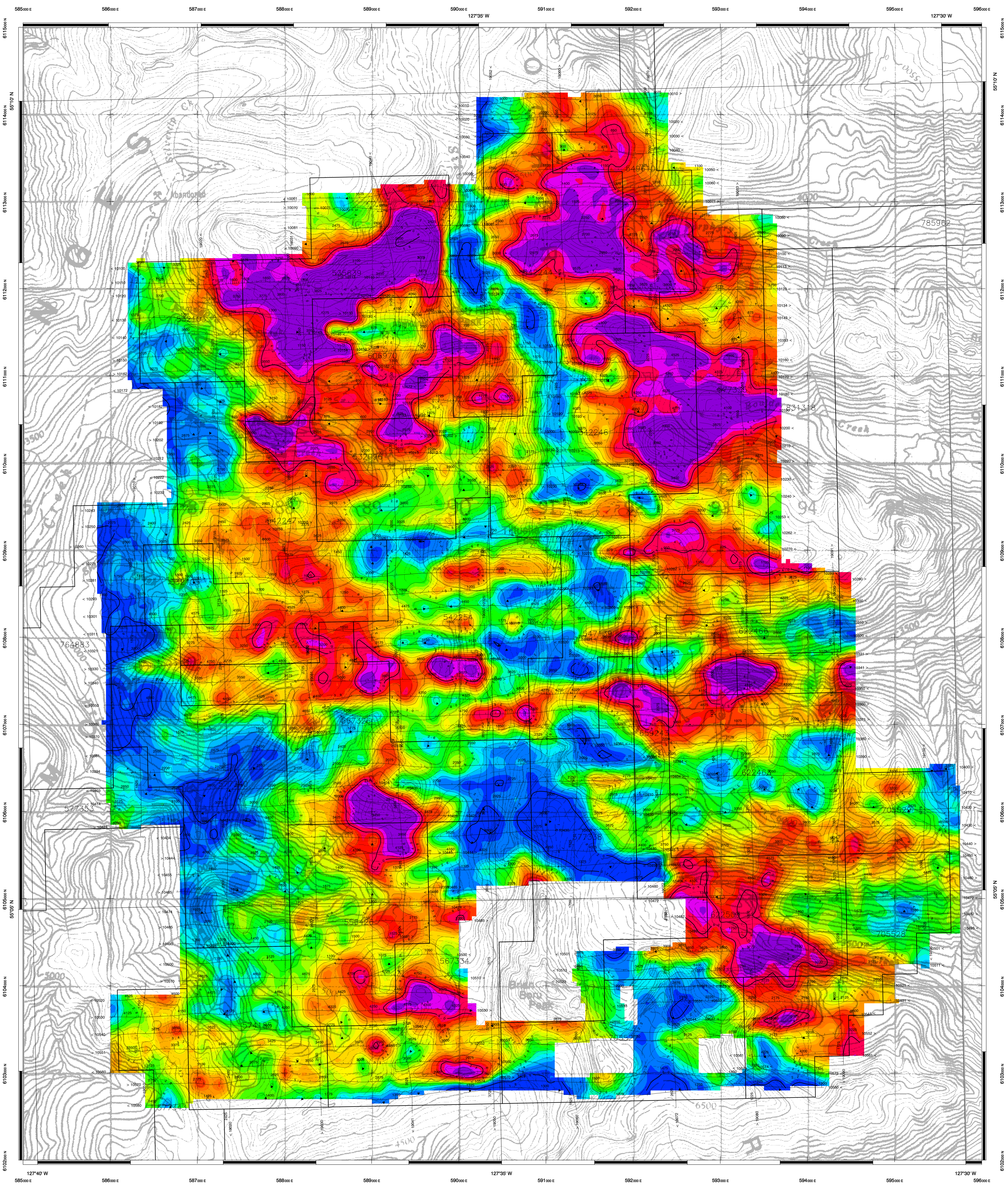

TECHNICAL SUMMARY

Navigation . . . . Differentially–corrected GPS
Data reduction grid interval . . . . 50 metres
Terrain clearance . . . . Helicopter, Spectrometer 60 m
Electromagnetic sensor 35 m
Magnetometer 35 m
Data sampling interval . . . . 0.1 second
Magnetometer / sensitivity . . . . . Cesium / 0.01 nT
Electromagnetic system . . . . DIGHEM^{V}
Spectrometer RS–500
Spectrometer data sampling . . . . 1.0 second

Frequency	Sensitivity	Coil Orientation
1000 Hz	.06 ppm	Vertical coaxial
5500 Hz	.12 ppm	Vertical coaxial
900 Hz	.12 ppm	Horizontal coplanar
7200 Hz	.24 ppm	Horizontal coplanar
56000 Hz	.60 ppm	Horizontal coplanar

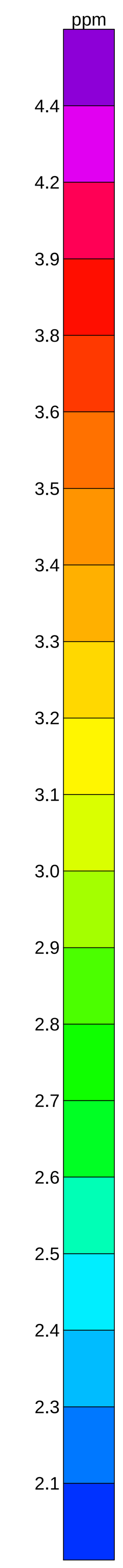

FLIGHT LINES

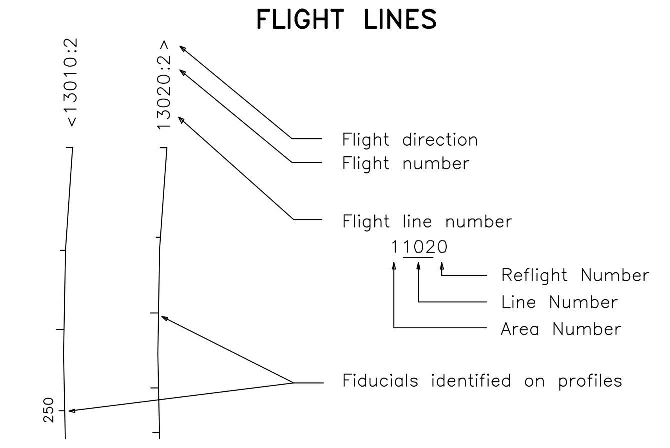

CONTOUR INTERVALS

. . . . 10.0 ppm
. . . . 2.0 ppm
. . . . 0.4 ppm
. . . . 0.2 ppm
. . . . low

LOCATION MAP

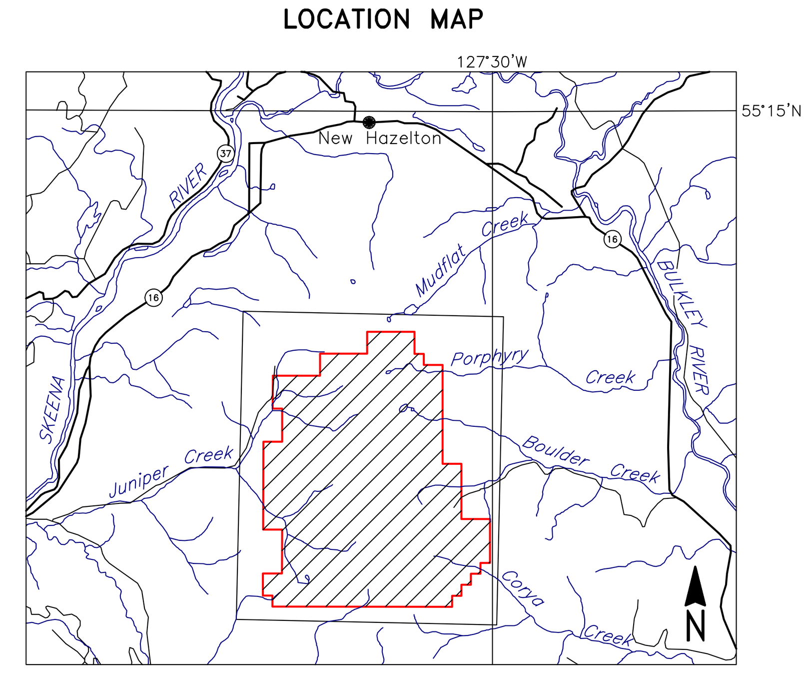

NTS: 93M/4 UTM ZONE: 9 NAD83 SCALE: 1:250,000

DUNCASTLE GOLD CORP.
PORPHYRY CREEK PROPERTY, BC

RADIOMETRIC EQUIVALENT URANIUM CONCENTRATION

FUGRO DIGHEM^{V}/RAD SURVEY	NTS: 93M/4	GEOPHYSICIST:
DATE: AUGUST, 2010	JOB: 10037	SHEET: 1

Fugro Airborne Surveys

0 1 2 Km
0 1 Mi
Scale 1:20 000

FUGRO AIRBORNE SURVEYS

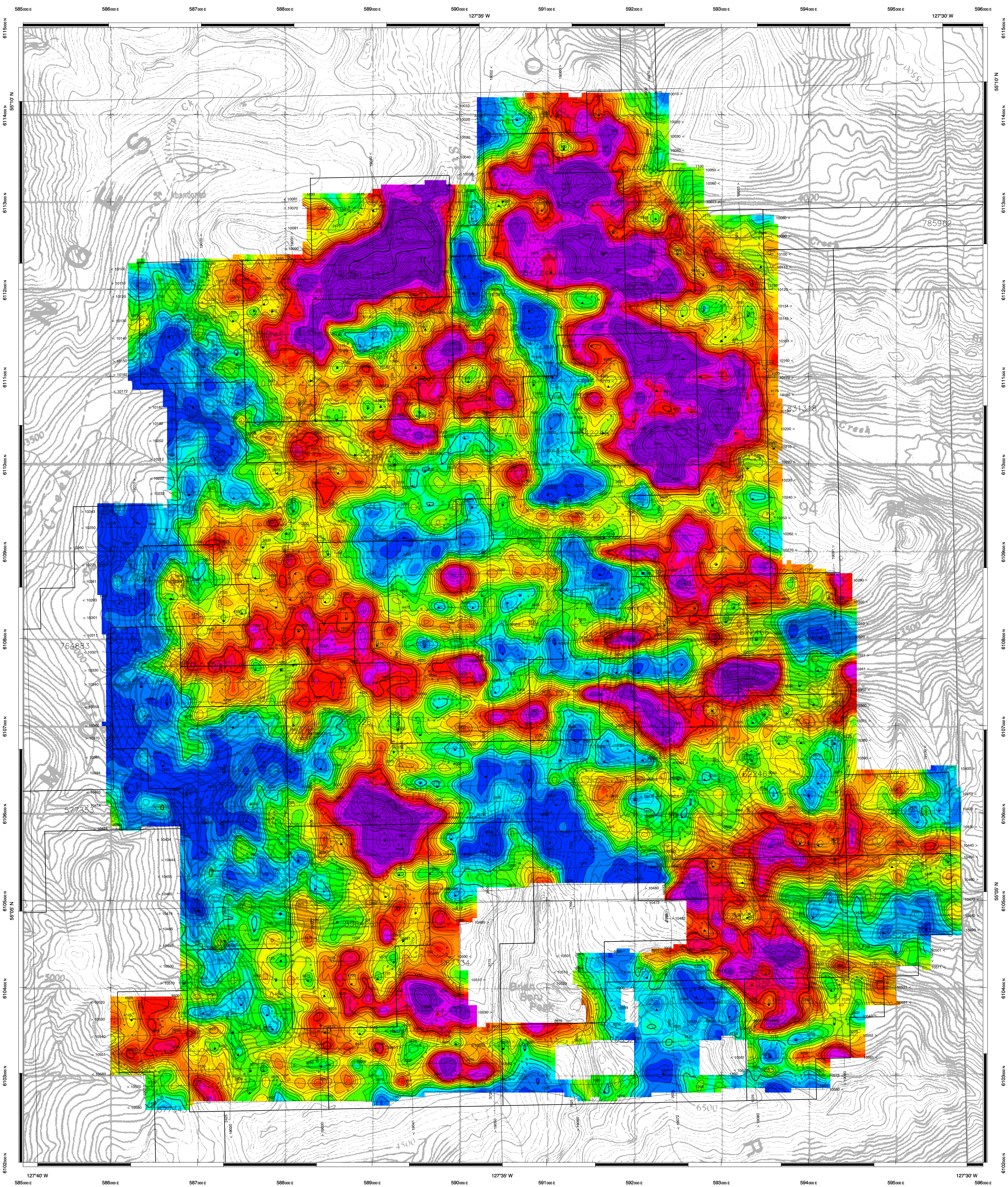

TECHNICAL SUMMARY

Navigation . . . . Differentially-corrected GPS
Data reduction grid interval . . . . 50 metres
Terrain clearance . . . . Helicopter, Spectrometer 60 m
Electromagnetic sensor 35 m
Magnetometer 35 m
Data sampling interval . . . . 0.1 second
Magnetometer / sensitivity . . . . . Cesium / 0.01 nT
Electromagnetic system . . . . DIGHEM^{V}
Spectrometer RS-500
Spectrometer data sampling . . . . 1.0 second

Frequency	Sensitivity	Coil Orientation
1000 Hz	.06 ppm	Vertical coaxial
5500 Hz	.12 ppm	Vertical coaxial
900 Hz	.12 ppm	Horizontal coplanar
7200 Hz	.24 ppm	Horizontal coplanar
56000 Hz	.60 ppm	Horizontal coplanar

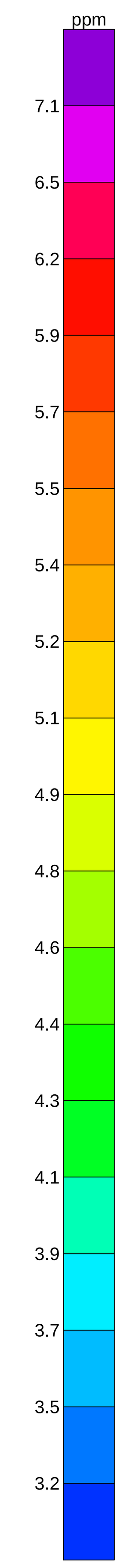

FLIGHT LINES

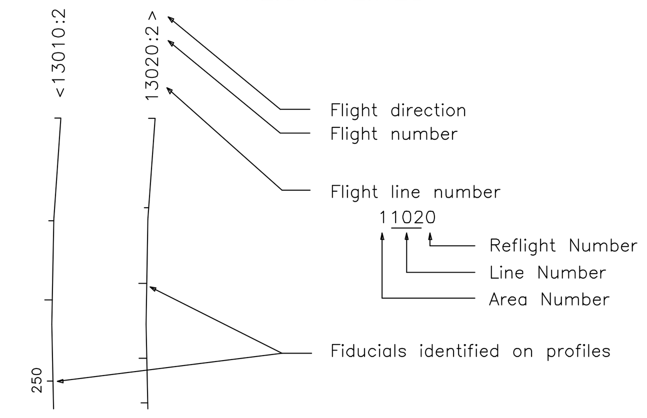

CONTOUR INTERVALS

. . . . 10.0 ppm
. . . . 2.0 ppm
. . . . 0.4 ppm
. . . . 0.2 ppm
. . . . low

LOCATION MAP

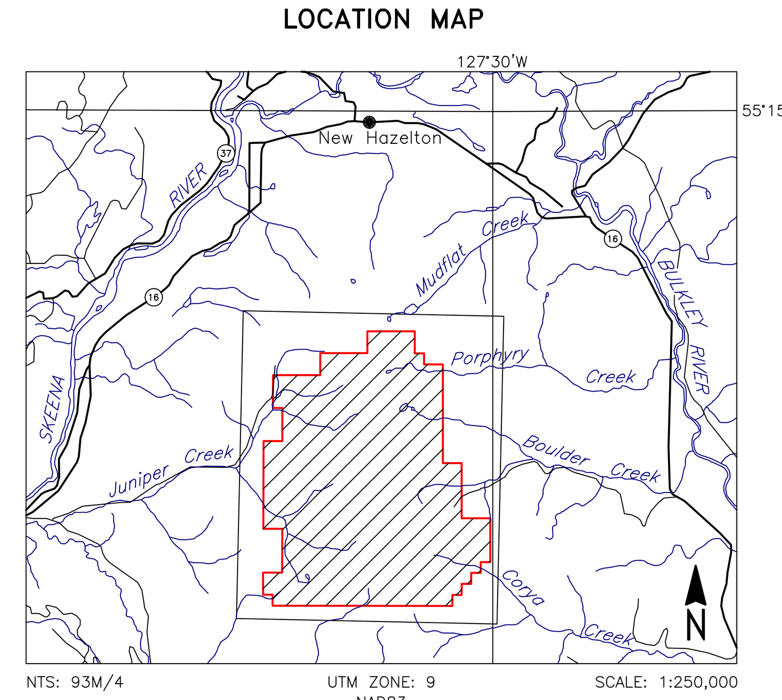

NTS: 93M/4 UTM ZONE: 9 NAD83 SCALE: 1:250,000

DUNCASTLE GOLD CORP.
PORPHYRY CREEK PROPERTY, BC

RADIOMETRIC EQUIVALENT THORIUM CONCENTRATION

FUGRO DIGHEM^{V}/RAD SURVEY	NTS: 93M/4	GEOPHYSICIST:
DATE: AUGUST, 2010	JOB: 10037	SHEET: 1

Fugro Airborne Surveys

0 1 2 Km
0 1 Mi
Scale 1:20 000

FUGRO AIRBORNE SURVEYS